Physiol Rev
83: 475–579, 2003; 10.1152/physrev.00028.2002.

Voltage-Gated Proton Channels and Other Proton Transfer Pathways

THOMAS E. DECOURSEY

Department of Molecular Biophysics and Physiology, Rush Presbyterian St. Luke's Medical Center, Chicago, Illinois

DeCoursey, Thomas E. Voltage-Gated Proton Channels and Other Proton Transfer Pathways. *Physiol Rev* 83: 475–579, 2003; 10.1152/physrev.00028.2002.—Proton channels exist in a wide variety of membrane proteins where they transport protons rapidly and efficiently. Usually the proton pathway is formed mainly by water molecules present in the protein, but its function is regulated by titratable groups on critical amino acid residues in the pathway. All proton channels conduct protons by a hydrogen-bonded chain mechanism in which the proton hops from one water or titratable group to the next. Voltage-gated proton channels represent a specific subset of proton channels that have voltage- and time-dependent gating like other ion channels. However, they differ from most ion channels in their extraordinarily high selectivity, tiny conductance, strong temperature and deuterium isotope effects on conductance and gating kinetics, and insensitivity to block by steric occlusion. Gating of H^+ channels is regulated tightly by pH and voltage, ensuring that they open only when the electrochemical gradient is outward. Thus they function to extrude acid from cells. H^+ channels are expressed in many cells. During the respiratory burst in phagocytes, H^+ current compensates for electron extrusion by NADPH oxidase. Most evidence indicates that the H^+ channel is not part of the NADPH oxidase complex, but rather is a distinct and as yet unidentified molecule.

I. INTRODUCTION

Voltage-gated proton channels are unique ion channels in several respects. They are called proton channels because they behave like ion channels and are highly selective for protons. Although protons exist in solution almost entirely in the form of hydronium ions, H_3O^+, all proton-selective channels conduct protons as H^+, rather than H_3O^+. This is true even for water-filled pores like gramicidin. It remains a matter of some contention whether proton channels should be considered to be ion channels at all, although this designation seems more appropriate than any alternative and is becoming accepted (444). Proton channels differ from carriers and unequivocally are not pumps. Protons are unique ions with respect to their behavior in bulk solutions, their interactions with proteins, and the mechanism by which they traverse ion channels and other molecules. The unique chemical properties of protons explain why proton channels hold the records for both the largest and smallest single-channel currents. Thus there is an introductory discussion of selected aspects of proton chemistry. For a detailed discussion of the methods of pH measurement, the reader is referred to the superb review by Roos and Boron (850).

This review includes what I as a student of voltage-gated proton channels consider to be useful and relevant. Although the main focus is voltage-gated proton channels, there is substantial coverage of salient properties of a number of other proton-conducting molecules, for several reasons. First, the structure and even the molecular identity of voltage-gated proton channels is essentially unknown, whereas the structures of a number of other proton-conducting molecules are known to within a few Angstroms. Second, certain features that differentiate proton channels from other ion channels may be shared among molecules whose function involves proton translocation. Once nature discovers a solution to a design problem, this solution tends to recur (245). Proton conduction through the prototypical ion channel, gramicidin, provides a frame of reference with respect to which we interpret many results (deuterium and temperature effects, pH dependence, unitary conductance, etc.). It is possible to distinguish two broad classes of proton-permeable molecules. Some molecules couple the flux of protons to a bioenergetic or enzymatic goal, such as photosynthesis or CO_2 hydrolysis. Other molecules are simple proton channels that apparently exist for the sole purpose of mediating proton flux across membranes. In both cases, proton flux is tightly regulated, either by coupling to events central to the function of the molecule or by a gating mechanism that turns proton flux on and off at appropriate times. A premise of this review is that the molecular details of proton movement through all types of proton-conducting molecules are likely to display similarities with general applicability.

The properties common to all voltage-gated proton

channels are described in detail. Then the properties and proposed functions of H^+ channels in specific cells are discussed. There is a strong emphasis on proton channel function in phagocytes, because much more is known about function in these cells than in any other. Evidence for and against the proposal that part of the phagocyte NADPH oxidase complex functions as a proton channel (427) is summarized.

I do not expect more than a handful of people to read the entire review. For those who study any of the numerous molecules with proton pathways, I hope to present a synopsis of their molecule from the vantage point of an electrophysiologist interested in proton conduction. I feel that it is useful to have information specifically regarding proton conduction in various channels/molecules assembled in one place. Those who study "normal" ion channels and are curious about H^+ channels will want to know their biophysical properties, which will appear esoteric and tedious to others. Phagocyte biologists will be interested mainly in the section on H^+ channels in phagocytes. For everyone else, the review should be a resource enabling a particular bit of information to be located in the table of contents.

II. CHEMISTRY OF PROTONS

A. Protons in Solution: Hydrogen Bonds

Protons in aqueous solution almost always exist in hydrated form as hydronium ions, H_3O^+ (or $H_3O^+ \cdot nH_2O$, including waters of hydration), also called oxonium (605) or hydroxonium ions (1070). Protons exist as H^+ <1% of the time during transfer from one water to another (184). The three protons in H_3O^+ are equivalent, and each is equally likely to jump to a neighboring water molecule (84). The proton is unique among cations in being interchangeable with the protons that form water molecules. This capability is significant in light of the tiny concentration of "free protons" (H_3O^+) in physiological solutions, ~40 nM, and the enormous total concentration of H in water, 110 M. Only one proton in a billion is part of H_3O^+ at any moment. The average lifetime of the H_3O^+ ion is ~1 ps in liquid water at room temperature: estimates in chronological order include 0.65 ps (84), 0.24 ps (184), 3.0 ps (287), 1.7 ps (636), 1.1 ps (11), 1.3 ps (1095), 0.95 ps (1050), and 0.5–0.79 ps (890). The proton is also unique as a monovalent cation in having no electrons, giving it a radius 10^5 smaller than other ions, which greatly facilitates proton transfer reactions (80) and electrostatic interactions with nearby molecules (696).

The quintessential feature of water and other proton conduction pathways is the hydrogen bond (80, 84, 287, 361, 380, 469, 470, 592, 605, 799, 800, 967, 1101). Huggins appears to have originated the concept of the hydrogen bond while in the laboratory of Latimer and Rodebush. Huggins conceived the idea of a hydrogen "kernel" held between two atoms in organic compounds, which he did not publish until 1922 (468); several earlier investigators discussed interactions that in retrospect could be considered examples of hydrogen bonds (490). In 1920, Latimer and Rodebush (592) adopted this idea and applied it to water, foreseeing the existence of networks of water molecules, and used hydrogen bonding to explain the high mobility of protons in water as "a sort of Grotthuss chain effect, rather than . . . a rapid motion of any one H_3O^+ ion."

> "Water . . . shows tendencies both to add and give up hydrogen, which are nearly balanced. Then, in terms of the Lewis theory, a free pair of electrons on one water molecule might be able to exert sufficient force on a hydrogen held by a pair of electrons on another water molecule to bind the two molecules together. Structurally this may be represented as

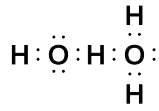

> Such combination need not be limited to the formation of double or triple molecules. Indeed, the liquid may be made up of large aggregates of molecules, continually breaking and reforming under the influence of thermal agitation. Such an explanation amounts to saying that the hydrogen nucleus held between 2 octets constitutes a weak 'bond' [1] " (592).

Linus Pauling coined the term *hydrogen bond* in a general paper on chemical bonds (798) and developed and popularized the idea in a chapter of his book, *The Nature of the Chemical Bond* (800).

Water molecules tend to form tetrahedral hydrogen bonded structures, at least ideally (84). In ice the tetrahedral structure exists (799) and is evidently so rigid at very low temperature (i.e., the dielectric constant drops drastically) that proton conduction is limited (188, 261, 313). In liquid water, however, the tetrahedral ideal is not achieved, and the actual coordination number decreases with increasing temperature (300, 366), which likely accounts for the greater decrease in activation energy at higher temperatures for proton transport than for other ions (319, 605, 784, 786). Water can be considered a "broken down ice structure" with continual formation and breaking of hydrogen bonds (707). Although protons in

[1] "M. Huggins of this laboratory, in some work as yet unpublished, has used the idea of a hydrogen kernel held between two atoms as a theory in regard to certain organic compounds" (592).

water are formally considered to exist as H_3O^+ molecules, it has long been recognized that larger molecular groupings exist and are central to the understanding of proton conduction. As early as 1936, Huggins (470) explicitly postulated the existence of $H_5O_2^+$, showed that proton conduction can occur by shifts in the identities of the water molecules that comprise the cation, and suggested that the rapidity of such shifts accounts for the high mobility of protons in water. The two main larger species are the so-called "Zundel cation," two waters sharing an excess proton as $H_5O_2^+$ (470, 1102, 1103), and the "Eigen cation," four waters sharing an excess proton as $H_9O_4^+$ (80, 287, 1070), although a transitional $H_{13}O_6^+$ structure has also been proposed (1049). These quasi-molecules are in a sense fictitious, in that they are idealizations that exist only transiently along with many undefined intermediate or alternative states (664, 890). Quantum molecular dynamics simulations show that a proton in water sometimes shuttles back and forth between two neighboring water molecules many times per picosecond, behavior that defines a Zundel (or Huggins) cation, but also spends time associated with a single water (which is hydrogen bonded to three first shell waters) as an Eigen cation (890, 1050). Eigen thought that the proton in $H_9O_4^+$ was essentially delocalized (288) and shared among three of the waters surrounding the H_3O^+ molecule; the fourth water is oriented incorrectly for rapid proton transfer (605). Ab initio molecular dynamics calculations indicate that a proton in water is affiliated with one oxygen atom as H_3O^+ ($H_9O_4^+$, including the primary hydration shell) 60% of the time, and 40% of the time it is intermediate between two oxygens as $H_5O_2^+$ (1025). Although the proton spends blocks of time as $H_9O_4^+$ (i.e., associated with a single oxygen), these events occur within bursts of oscillations between the same pair of oxygens as though the proton remembers its former partner (1050), and hence, appearances to the contrary, was never truly delocalized.

B. Proton Conductance in Water by the Grotthuss Mechanism

That there is a fundamental difference between protons and other cations is clear from the fivefold higher conductivity of H^+ in water than other cations like K^+ (84, 217). In fact, considering its degree of hydration (based on solution density) H^+ might be expected to have a low mobility like Li^+ (84, 845) but has nine times higher mobility (845). It has long been appreciated that protons are conducted by a special mechanism in which they hop from one water molecule to the next, which is often called the Grotthuss mechanism, although de Grotthuss' proposal (254a) differs from current views. The Grotthuss mechanism is also called "prototropic" transfer (605), to distinguish it from ordinary "hydrodynamic" diffusion of H_3O^+ as an intact cation. Danneel (217) suggested that a proton in an electric field might bind to one side of a water molecule and that another proton could leave the far side of the molecule, thus saving the time it would have taken to diffuse that distance. A key distinction from other ions is that during proton conduction the identity of the conducted proton changes (84). Except for Hückel's theory (467a), the equivalence of the three protons in H_3O^+ is generally considered to be essential to the special prototropic conduction mechanism. Danneel further proposed in 1905 (217) that proton conduction by a Grotthuss mechanism requires two processes: proton hopping from one water molecule to the next, and also a reorientation of water molecules. Glasstone, Laidler, and Eyring (366) concluded that proton transfer was rate-limiting and that water rotation was rapid. Conway, Bockris, and Linton (184) concluded that the proton transfer step was rapid and proposed that the rate-determining step was the reorientation of the recipient water molecule in the electrical field of the donor H_3O^+ (184, 448). More recent theories growing out of Eigen and co-workers' views agree that the proton transfer step is rapid, but ascribe the rate-limiting step to reorganization of the hydrogen-bonded network through which H^+ conduction occurs (10a, 11, 221, 479, 664, 1024, 1025, 1050).

The special prototropic conduction mechanism appears to require a hydrogen-bonded structure (361, 469, 605). Water is an ideal medium for prototropic conduction because of its propensity to form hydrogen bonds; water has a higher viscosity compared with other solvents due to hydrogen bonding (300). Proton conduction occurs essentially by means of changes in the identity of the water molecules that participate in the hydrogen-bonded network that includes the excess proton. The mechanism of proton conduction in water has been described as "structural diffusion," which was felt to reflect the delocalized nature of the solvated proton within a hydrogen-bonded network (287, 319, 1070). The concept of structural diffusion of protons in water is supported by ab initio molecular dynamics simulation (1024). Proton conduction occurs as a result of isomerization between Zundel and Eigen cations (10a, 11, 1024). The rate-determining step appears to be the breaking of a second shell hydrogen bond, which allows the replacement of one of the waters by a different one (10a, 287, 288, 664). This process has been called the "Moses mechanism," with second shell hydrogen bonds breaking in the path of the proton and reforming behind (10a, 11a), just as the Red Sea parted to allow Moses and his companions to cross (Exodus 14:21–27). At this point the modern view (10a) diverges from most earlier models in which the water molecule immediately adjacent to H_3O^+ is required to rotate into an appropriate configuration to accept the proton (80, 184, 448, 467a). The three first shell hydrogen bonds are too strong to be easily broken (10a), whereas

the second shell hydrogen bonds are expected to be of normal strength, 2.6 kcal/mol, consistent with empirical measurements of proton mobility (636, 678). In Agmon's view, the widely used traditional method of estimating the "abnormal" component of H^+ mobility by subtracting the mobility of a "normal" cation such as Na^+ or K^+ from the total H^+ mobility (319, 361, 366, 467a, 605, 628, 636, 678, 845) is incorrect. Because the H_3O^+ ion is tightly hydrogen bonded to its first shell neighbors, it is effectively immobilized. Consequently, essentially all of the mobility of protons in solution is of the abnormal (Grotthuss type) variety (11). Another difference is that in contrast to Eigen's delocalized proton that could move freely within the $H_9O_4^+$ complex (287, 319, 1070), in the current view the proton is mainly associated with a single oxygen or vascillates rapidly between two oxygens, and eventually transfers successfully as a result of second shell hydrogen bond rearrangement (10a, 890, 1024, 1025, 1095).

Because waters inside proton channels may be bound or constrained in some way, proton movement through water-filled channels is often considered to be more analogous to proton transport in ice than in water (732, 733). Proton conduction in ice is fundamentally different from that in liquid water (288, 552, 771, 783). The extensive hydrogen bond rearrangement that characterizes proton transfer in water cannot occur in ice (552, 771). Liquid water is mainly three-coordinated, but the ice structure enforces four-coordination. Repulsion from the fourth water pushes the H_3O^+ closer to its neighbors, decreasing the energy barrier for proton transfer (552, 771). Historically, the question of proton conduction in ice has proven to be difficult and controversial (42, 44, 96, 157, 188, 288, 294, 380, 500, 808). Eigen and colleagues reported that the mobility of H^+ in ice was extremely high (289), 1–2 orders of magnitude higher than in water (288), and differing "from that of conduction band electrons in metals by only about 2 orders of magnitude" (287). Subsequently, the general consensus has been that these measurements were contaminated by conduction through melted water at the surface and that the true mobility is much lower, 3×10^{-4} to 6.4×10^{-3} $cm^2 \cdot V^{-1} \cdot s^{-1}$, typically $\sim 10^{-3}$ $cm^2 \cdot V^{-1} \cdot s^{-1}$ (142, 157, 294, 575, 734, 782, 808, 809). The mobility of H^+ in water is 3.6×10^{-3} $cm^2 \cdot V^{-1} \cdot s^{-1}$ (845). It is a major problem to determine the number of defects (ionic or bonding) in ice, which must be known to calculate mobility. "Pure" ice almost invariably contains enough impurities to dominate attempts to measure the mobility of ionic defects, which are present at only ~ 1 per 10^{13} H_2O molecules at $-20°C$ (808). This problem can be overcome by "doping" the ice with carriers so that their concentration is known and the signal is larger and thus more accurately measurable (380). In ice studies, it is important to distinguish events at the surface from events occurring within the bulk phase, although the former can be useful in dissecting elementary processes that contribute to proton mobility (260, 356, 357, 1028, 1083).

The only ions that carry current in ice are H^+ and OH^-, and both move as a consequence of proton or proton defect movement (783). Both protons and Bjerrum defects (see sect. III*D*) must move for sustained current (380); movement of L defects (or protons) alone simply produces (or eliminates) polarization (782). In pure ice at moderate temperatures, the dominant charge carrier is the Bjerrum L defect (the conduction of which occurs by rotation of water molecules), and thus for DC conduction the motion of the ionic defect (H_3O^+) is rate determining (809). Protons tend to become shallowly "trapped" by the more abundant Bjerrum L defects, but above 110 K they escape at a significant rate and are mobile until they encounter the next trap (1083). Data on H_3O^+ "soft-landed" onto the surface of ice were interpreted to mean that at temperatures below 190 K proton conductance in ice is essentially absent (188). One danger that must be considered in such studies is that protons can be trapped at the ice surface (1028), probably because the 4-coordinated state that is enforced inside ice is less favorable than the less stringent coordination at the surface (552). Earlier studies of isotope exchange in pure and in doped ice had indicated that Bjerrum defect and proton migration occurred to a similar extent in ice in the 135–150 K range, although OH^- lacked mobility (181). A recent study of isotope exchange in pure ice nanocrystals at 145 K revealed clear evidence of mobility of both Bjerrum L defects and protons, based on the distinctive infrared spectra of D_2O, coupled HDO molecules, and isolated HDO (1028). Most evidence indicates that protons are mobile in ice at least down to 110 K (1083), and possibly as low as 72 K (808), that proton mobility in ice is practically temperature independent (782, 808), and that the mobility of H_3O^+ at ~ 100 K is within an order of magnitude of that in liquid water (808).

The hydroxide anion (OH^-) also has anomalously high conductivity compared with other anions, ~ 198 $cm^2 \cdot S/eq$ (218, 845, 943), although not quite so extreme as H^+ at ~ 350 $cm^2 \cdot S/eq$ (786, 845, 921). In addition, the activation energy for OH^- conductivity is higher than for H^+ (288, 623, 636). The high mobility is believed to reflect OH^- migration by a Grotthuss-like mechanism in which the OH^- moves from one water to the next by virtue of a proton hopping in the opposite direction (80, 84, 184, 217, 469, 605, 845). Protons move via prototropic transfers between H_3O^+ and H_2O, whereas OH^- migrates by prototropic transfers between H_2O and OH^-. The rate-determining step in OH^- mobility may be the same as for H^+ mobility, the breaking of a second shell hydrogen bond (11b), although a recent proposal invokes the crucial breaking of a first-shell hydrogen bond (1026). That OH^- mobility is less than H^+ mobility in spite of the similarity of mechanism has been explained in several ways. Bernal

and Fowler (84) proposed that the two protons in the donor H_2O are held more tightly than the three protons in the donor H_3O^+ molecule, thus reducing the likelihood of the former proton transfer. Conway et al. (184) felt the critical difference was the electrostatic facilitation by the extra proton in H_3O^+ of the prerequisite and rate-limiting water rotation that precedes proton transfer. Gierer and Wirtz (361) suggested a charge mechanism: for H^+ transfer the proton hops between neutral H_2O molecules, whereas for OH^- the proton hops between two residual negative charges (288, 361). Agmon (11b) proposed that contraction of the O-O bond distance adds an extra 0.5 kcal/mol to OH^- transfer. Onsager proposed that H^+ mobility is higher because the additional kinetic energy of the excess proton increases the energy of H_3O^+ and favors subsequent proton transfer, whereas in OH^- conduction the energy of the proton is transferred from OH^- to H_2O and thus does not contribute to the next transfer (J. F. Nagle, personal communication).

C. Proton Transfer Reactions

Eigen (287) studied proton transfer reactions extensively and formulated general rules that govern such reactions. Proton transfer reactions tend to be very rapid and are described as "diffusion controlled" because the rate of the reaction is determined by the frequency of molecular encounters resulting from diffusion (287). The rate of proton transfer in normal proton transfer reactions depends on the pK_a difference between donor and acceptor, as illustrated in Figure 1.[2] When $pK_{acceptor} > pK_{donor}$, the forward reaction is rapid and independent of the pK_a difference. Protonation of various bases occurs with a rate constant $>10^{10}$ $M^{-1} \cdot s^{-1}$, with the electrostatically favorable recombination of H^+ and OH^- clocking in at 1.4×10^{11} $M^{-1} \cdot s^{-1}$ (287). When the forward reaction is diffusion controlled, the reverse reaction will occur at a rate that is linearly related to the pK difference (Fig. 1*A*). By definition, $\log k_f - \log k_r \rightleftharpoons pK_{acceptor} - pK_{donor} = \Delta pK$ (290). If the reaction is asymmetrical with respect to charge (e.g., $HX + Y = X^- + HY^+$), then the diffusion-controlled limit will be different for the forward and backward reactions (Fig. 1*B*). A Brönsted plot (123a) provides similar information (787). A more thorough theoretical development of the kinetics of proton transfer invokes Marcus rate theory (654), as has been applied successfully to carbonic anhydrase (931).

In terms of a proton conduction pathway that is composed of a series of protonation sites, proton hops may not obey the same rules as proton transfer reactions in diffusion-controlled reactions, due to steric constraints, etc. However, the general principles of the ΔpK dependence of transfer rates are likely to apply. Continuous prototropic transfer is most efficient when the donor and acceptor are symmetrical, as in water to water transfer (605). In solvent mixtures, the solvent with higher affinity traps the proton (605). Ab initio molecular orbital method calculations indicate that in a long water wire, multiple proton transfers (hops) can occur simultaneously (i.e., energetically coupled to each other) using the energy cost associated with a single transfer event (882). An example of coherent proton tunneling has been observed directly in a network of four coupled hydrogen bonds (465).

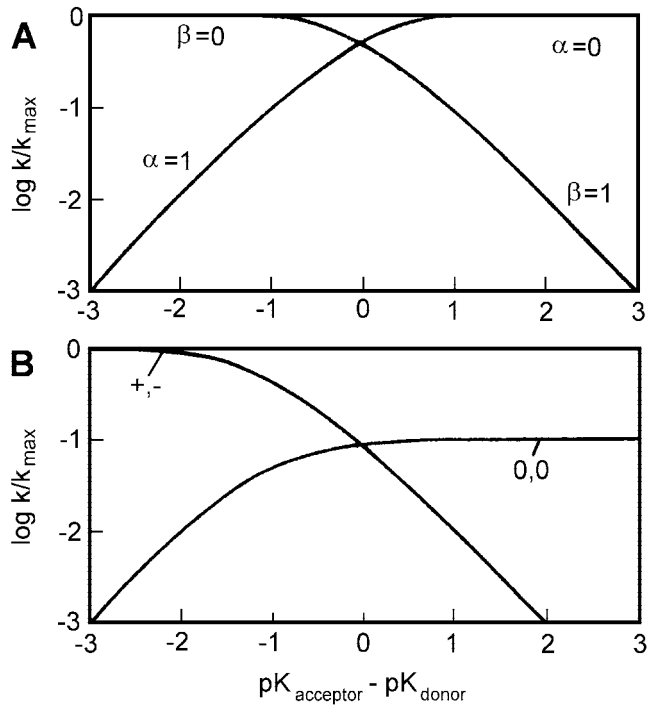

FIG. 1. Idealized dependence of the normalized rates of proton transfer reactions on the pK_a difference between donor and acceptor molecules participating in the reaction. In *A*, the transfer is symmetrical with respect to charge (e.g., $HX^+ + Y = X + HY^+$), whereas in *B*, the reaction results in charge neutralization. The slopes of the forward reaction (α) and backward reaction (β) limit at 0 or 1 at large ΔpK. The limiting rate constant (k_{max}) is 10^9 to 10^{10} $M^{-1} \cdot s^{-1}$ for a diffusion-controlled reaction. [From Eigen and Hammes (290), copyright 1963 John Wiley & Sons, Inc. Reprinted by permission of John Wiley & Sons.]

D. Proton Transfer in the Plane of the Membrane: The "Antenna Effect"

There is long-standing debate over the suggestion that protons may diffuse laterally at the surface of the membrane at a higher rate than they diffuse in bulk solution. The question has been discussed extensively in

[2] The concept of p*K*a was introduced by Hasselbalch (415) acting on a suggestion by N. Bjerrum.

the context of bioenergetic membranes (404, 418, 527, 530, 706, 724, 731, 820, 821, 1002, 1079). This question has arisen in several instances in which the apparent single proton channel current is larger than the maximum rate at which protons can diffuse to the channel, as predicted by simple diffusion models. To some extent, surface enhancement may be ascribed to geometric factors, i.e., the difference between diffusion in two and three dimensions (353) without specifying the mechanism by which protons would bind to the surface. A proton trapped at the membrane surface will diffuse into a proton channel if it does not first desorb, whereas a proton in three-dimensional bulk solution has a low probability of diffusing into the channel. In unbuffered solutions, surface conduction dominates; in buffered solutions, the dominant pathway depends on protonated buffer concentration and the effective size of the proton collecting antenna (353) (see below).

One general way that surface conduction could enhance proton fluxes through a channel is by the "antenna effect" (400, 867). Rather than requiring a proton to diffuse directly to the channel entrance, the entire membrane surface, by virtue of its many negatively charged groups, might collect protons, which then travel in the plane of the membrane surface to the channel. Detailed experimental and computational studies have been done on this question (155, 353, 400, 653, 867). Protonation reactions are often extremely rapid and limited only by diffusion, with rate constants typically $1–6 \times 10^{10}$ $M^{-1} \cdot s^{-1}$ (287, 290, 400, 653, 867). One of the most rapid reactions known is the recombination of H^+ and OH^- with a rate constant 1.4×10^{11} $M^{-1} \cdot s^{-1}$ (287). However, occasionally higher rate constants are observed. An anomalously high protonation rate measured for a site on a Ca^{2+} channel, 4×10^{11} $M^{-1} \cdot s^{-1}$, was explained by proposing the site to be negatively charged and located in the channel vestibule, which would funnel the electric field lines and enhance the electrostatic attraction (823). If two negatively charged groups (e.g., at the surface of a membrane) are close enough together that their Coulomb cages overlap, the "virtual second-order" rate constant governing the transfer of a proton from one group to the other can be 10^{12} $M^{-1} \cdot s^{-1}$ or greater (400), with the current record being 6×10^{12} $M^{-1} \cdot s^{-1}$ (867). The probability that a proton that is bound to a site with -1 charge at the interface between membrane and aqueous solution will transfer to a neighboring site, also with -1 charge, rather than entering bulk phase, calculated with the Debye-Smoluchowski equation, is close to 100% for a 12-Å separation, decreasing with distance to ~40% for a 60-Å separation (867). It seems clear that rapid proton transfer in the plane of the membrane is possible.

On the other hand, the extent to which rapid surface conduction might play a significant role must be established in each specific situation. In a study on proton transfer rates between superficial amino acid groups on tuna cytochrome *c* oxidase, all of the virtual second-order rate constants were $<10^9$ except for one that was as large as 10^{11}, which was between groups within 10 Å of each other (652). A cluster of three carboxylates on bacteriorhodopsin acts as a proton-collecting antenna, each with a high protonation rate of 5.8×10^{10} $M^{-1} \cdot s^{-1}$, but the dimensions of the antenna are smaller than those of the molecule. Long-range proton migration occurs along a protein monolayer, but depends critically on molecular packing, and is abolished at low or high protein densities (331). Molecular dynamics simulation indicates that proton transport near the surface of a dipalmitoylphosphatidylcholine membrane is inhibited rather than enhanced (953). Finally, de Godoy and Cukierman (253a) explored the effects of bilayer composition on H^+ currents through gramicidin channels. The limiting H^+ conductance at low pH was the same in bilayers formed from protonatable phospholipids that presumably should be capable of mediating lateral H^+ conduction and bilayers formed from covalently modified phospholipids that cannot be protonated. Furthermore, differences in the H^+ conductance at higher pH were fully accounted for by electrostatically induced changes in local H^+ concentration near the membrane, providing no evidence of significant lateral H^+ conduction (253a). In summary, it appears that rapid proton transfer at the membrane surface may occur under specialized conditions but cannot be assumed to occur generally.

E. Control of pH

The usual way to control pH is with buffered solutions. Because the control of pH is never perfect, recognizing systematic sources of error is useful. Voltage-gated proton channels appear to be perfectly selective for protons over all other ions besides deuterium, as discussed in section v*E*, and hence act as local pH meters (237). Selectivity is evaluated by measuring the reversal potential (V_{rev}) in solutions of various pH, and comparing the result with the Nernst potential for H^+ (E_H)

$$E_H = \frac{RT}{F} \log \frac{[H^+]_o}{[H^+]_i} \quad (1)$$

Although reasonable agreement between the measured V_{rev} and E_H is often obtainable, the agreement is rarely perfect. If we tentatively accept the conclusion that voltage-gated proton channels are perfectly H^+ selective (see sect. v*E*), then any deviation of V_{rev} from E_H indicates that the true pH differs from the nominal pH. The primary cause of this deviation in patch-clamp experiments is

imbalance between the rate that proton equivalents cross the cell membrane and the rate the buffer from the pipette replenishes the cytoplasmic compartment. The intracellular compartment is a large unstirred volume, and proton efflux such as that occurring during H^+ currents will deplete protonated buffer from the cell. For example, a 10-μm-diameter cell has a volume of 524 fl, and if it is filled with a pipette solution that has 100 mM buffer at its pK_a, the entire cell will contain 1.6×10^{10} protonated buffer molecules. During a modest sustained outward H^+ current of 100-pA amplitude, 6.25×10^8 H^+ leave the cell each second, deprotonating 4% of the total protonated buffer. Even at intracellular pH (pH_i) 6 there are only 315,000 free protons in the entire cell, all of which would be consumed during 0.5 ms of H^+ current. Thus, essentially the entire H^+ current is carried by protons that immediately previously were bound to buffer molecules. Replenishment of buffer occurs by diffusion from the pipette solution and requires the diffusion of these rather large molecules through a small <1-μm-diameter pipette tip into the cell.

Calculations based on Pusch and Neher's empirical determination of diffusion rates (827) predict a time constant of 19 s for the equilibration of 250-Da buffer molecules from a pipette with 5-MΩ tip resistance into a 15-μm-diameter cell. This time constant is proportional to cell volume (776). The rate of equilibration of pH_i will be slower than that for simple buffer diffusion, due to the effective slowing of H^+ diffusion by fixed (immobile) intracellular buffers (514). Direct estimates of the time constant of equilibration of pH_i in HL-60 cells and macrophages of unspecified size were 11 s (258) and 58 s or 97 s (519), respectively, representing at least qualitative agreement.

The presence and action of any membrane transporter that moves proton equivalents across the cell membrane will alter V_{rev}. Thus, when Na^+ is present only in the external solution and pH_i is low, the inward Na^+ gradient and outward H^+ gradient both conspire to activate Na^+/H^+ antiport. H^+ extrusion by the antiporter is rapid enough to raise pH_i substantially (i.e., by 0.5 unit or more) in alveolar epithelial cells studied in whole cell patch-clamp configuration, in spite of the presence of 119 mM buffer in the pipette solution (237). H^+ is extruded by the antiporter faster than the supply is replenished by diffusion of protonated buffer from the pipette. Geometrical factors influence this balance, with smaller cells or larger pipette openings attenuating the change in pH_i due to antiport activity. Thus manifestations of Na^+/H^+ antiport were less pronounced in human neutrophils (237) or murine microglia (546) than in the larger rat alveolar epithelial cells, but obviously differences in the expression of Na^+/H^+ antiport molecules could also play a role. Any other mechanism that results in net movement of H^+ equivalents across the membrane will alter pH_i. Several mechanisms of membrane H^+ flux are discussed in section III*A*, of which the shuttle mechanism in particular could cause attenuation of the pH gradient across the membrane (see sect. III*A3*).

A systematic deviation arises when V_{rev} is measured by the conventional tail current protocol. A depolarizing prepulse activates the H^+ conductance (g_H) and then the voltage is repolarized to various levels, and the direction of the tail current (the decaying current waveform that reflects the progressive closing of H^+ channels) is observed. The necessity to activate a substantial g_H during the prepulse to elicit an interpretable tail current, combined with the extremely slow activation kinetics of voltage-gated proton channels in mammalian cells, inevitably causes significant depletion of intracellular protonated buffer during the prepulse. If a comparable H^+ current is elicited during the prepulse in solutions of varying pH, the error will be a relatively constant addition of a few millivolts to the measured V_{rev}. This systematic error may explain why the vast majority of V_{rev} measurements in the literature are more positive than E_H. On the other hand, V_{rev} measurements that encompass negative ΔpH [$pH_i >$ extracellular pH (pH_o)] indicate deviation in the opposite direction in this range (166, 519, 886), suggesting that an element of dissipation of any pH gradient may also play a role. As a result, measurement of the change in V_{rev} at several pH rather than the absolute V_{rev} often provides a cleaner estimate, which explains the fondness that many experimentalists have for this way of expressing their data. Direct measurements of V_{rev} using prepulses that elicit smaller or larger currents have been shown to raise pH_i and hence shift V_{rev} positively roughly in proportion to the integral of the outward H^+ current during the prepulse (70, 232, 372, 473, 519, 709), although this effect is not apparent in large cells (134). It is important to recognize that the deviation of V_{rev} from E_H is not an error, but instead accurately reflects the effects of the pulse protocol on pH_i. We consider voltage-gated proton channels to be perfect pH meters (see sect. V*E*).

An expedient way to estimate V_{rev} is to activate the g_H and then ramp the membrane voltage "downward" from positive to negative (372). If enough channels open at positive voltages and the ramp is rapid enough that the channels remain open, then V_{rev} can be taken as the zero current voltage, although any leak conductance and capacity current must be either negligibly small or corrected. The problem remains that it is first necessary to activate the g_H to observe V_{rev}, so this approach does not avoid the problem of depletion. Another clever way to estimate V_{rev} is simply to interpolate between the H^+ current at the end of a depolarizing pulse and that at the start of the subsequent tail current (473). One required assumption is that the instantaneous current-voltage re-

lationship be approximately linear. This method is useful in certain situations, particularly if one suspects that significant depletion has occurred. The advantage is that both required data points are obtained by applying a single pulse, and they are measured at nearly the same time. Again, this approach does not avoid the effects of depletion. In fact, its originators used this approach to demonstrate that H^+ efflux during large depolarizing pulses alkalinized the cytoplasm significantly.

H^+ currents increase pH_i in proportion to the amount of H^+ extruded. For small currents, the change in pH_i may be negligible, but for large currents, depletion of protonated buffer will noticeably increase pH_i. These effects are less pronounced in large cells (134) because they reflect the area-to-volume ratio. Restoration of pH_i is determined by the geometrical factors already discussed, and typically requires tens of seconds up to several minutes. A useful rule of thumb is that because voltage-gated proton channels do not inactivate, when the H^+ current peaks and then droops during a sustained depolarization, this always reflects an increase in pH_i. Experimentally, this phenomenon can be annoying, but it is simply a manifestation of the ability of the H^+ conductance to do its job, namely, to extrude acid at a rate adequate to alkalinize the cytoplasm rapidly.

Perhaps not surprisingly, variations in extracellular buffer from 1 to 100 mM had very little effect on voltage-gated proton currents (241). The bath solution represents an effectively infinite sink for protons. The situation for intracellular buffer is more complicated. Several whole cell patch-clamp studies in which pH_i was determined have revealed that including 5–10 mM buffer in the pipette solution does not control pH_i as well as higher buffer concentrations, e.g., 100–120 mM (232, 258, 519, 574). In addition, the time course of the H^+ current during a single depolarizing pulse was shown to depend strongly on "internal" buffer concentration in excised inside-out patches of membrane (241). The initial turn on of H^+ current was similar, but the longer the pulse, the more the current with 1 mM buffer drooped relative to that with 10 mM buffer. Nevertheless, decreasing internal buffer from 100 to 1 mM attenuated the H^+ current by only ~50%; thus this effect is attributable to H^+ current-associated pH changes, rather than a limitation of the conductance of the channel by buffer (241) (cf. sect. v*J*).

In addition to buffers, application of an NH_4^+ gradient has proven to be a useful way to control pH_i in patch-clamped cells (242, 248, 387) (see also sect. iii*D*). Control over pH_i is excellent and rapid when the NH_4^+ gradient is symmetrical, becoming less effective for large NH_4^+ (hence pH) gradients (248, 387). An advantage of this technique is that pH_i can be changed in a cell simply by altering the bathing solution.

F. Selected Properties of Buffers

Several issues related to buffers are relevant to the study of proton channels. Experimental control of pH requires adequate buffering, as just discussed in section ii*E*. Buffering power (or buffering capacity) is defined as dB/dpH (1036), i.e., the concentration of strong base required to change the pH of a solution by one unit. A more rigorous discussion of this and other definitions can be found elsewhere (849, 850). The reported buffering power of the cytoplasm in mammalian cells ranges from 18 to 77 mmol · pH^{-1} · $liter^{-1}$ (850). The measured buffering power of most cells increases substantially at lower pH, typically three- to fivefold between pH_i 7.5 and pH_i 6.5 (24, 41, 92, 324, 603, 630, 840, 850, 1067). A similar observation has been made for the Golgi (153). The buffering power is maximal at the pK_a of the buffer (425, 1064), where it is $(\ln 10)[B]/4 \sim 0.58[B]$, where [B] is the total buffer concentration (559, 849, 1036). Thus a cytoplasmic buffering power of 58 mmol · pH^{-1} · $liter^{-1}$ would reflect the presence of the equivalent of at least 100 mM simple buffer in cytoplasm. To control pH experimentally, many investigators use solutions with 100 mM exogenous buffer near its pK_a. Under normal conditions, this is adequate to prevent pH changes large enough to alter H^+ currents noticeably (240) (but see cautionary tales in sect. ii*E*).

When a cell is dialyzed with a pipette solution containing inadequate buffer, intrinsic cytoplasmic buffers override the attempts of the pipette solution to control pH_i. The larger the cell, the more difficult is the control of pH_i. Byerly and Moody (135) compared the rate of equilibration of pipette solutions containing K^+ or highly buffered H^+ with cytoplasm in large neurons (90–120 μm in diameter) studied with suction pipettes one-third the cell diameter. The effective equilibration of H^+ even with high buffer concentrations (50–100 mM) was three to five times slower than that of K^+, and with 20 mM buffer, little control over pH_i was achieved (135). Similarly, the effective diffusion coefficient of H^+ in cytoplasm is five times slower than that of mobile buffers (15). In small cells studied with patch pipettes containing pH 5.5 solutions, pH_i deduced from the V_{rev} of H^+ currents was ~5.7 for 119 mM MES buffer and ~6.3 for 5 mM MES (232). A pipette solution with 1 mM buffer appeared to have essentially no effect on pH_i (240).

Buffers have variable tendencies to chelate metal ions (805). Because we could not find much information on this property for normal pH buffers beyond the initial description of the Good buffers (370), we measured the binding constants of several buffers for Zn^{2+}, Cd^{2+}, Ni^{2+}, and Ca^{2+} (163). Certain buffers bind Zn^{2+} avidly, including tricine and *N*-(2-acetamido)-2-iminodiacetic acid (ADA). The latter has been used to establish free Zn^{2+} concentrations in the nanomolar range (22, 792).

III. MECHANISMS OF PROTON PERMEATION THROUGH MEMBRANES

A. Proton Permeation Through Membranes Without Transport Proteins

In addition to the plethora of membrane proteins whose function is to transport protons or acid equivalents across cell membranes, there are several mechanisms by which protons can permeate phospholipid membranes in the absence of proteins. These mechanisms will be considered in part in the context of deciding whether voltage-gated proton channels really exist or if they might simply reflect one of the several nonprotein mechanisms of conduction. A large literature exists on the proton permeability of the cell membrane itself (see sect. III*A1*), largely with respect to the important bioenergetic systems in which large proton gradients are created. Thus, in mitochondria, chemical energy is stored as a proton gradient that drives ATP generation. In chloroplasts, light energy is transduced into a proton gradient to create ATP. Energy transduction thus requires the generation of large proton gradients. Nevertheless, many studies indicate that the proton permeability of cell membranes is much higher than that of other cations.

The Born self-energy cost of an ion permeating a pure lipid bilayer is prohibitive (794), ~58.6 kcal/mol for the H_3O^+ (243). Therefore, a mechanism subtler than brute force is required to translocate protons across membranes. Four mechanisms that have been proposed to explain proton permeation through biological membranes are as follows: transient water wires (sect. III*A2*), weak base or acid shuttles (sect. III*A3*), phospholipid flip-flop (sect. III*A4*), and specific proteins (channels, carriers, and pumps) whose function is to transport protons. High "intrinsic" proton permeability must be explained by one of these mechanisms. As will become apparent however, the proton permeability of cell membranes that contain voltage-gated proton channels is several orders of magnitude higher than the highest estimate for simple phospholipid bilayers. In most cells with H^+ channels, any proton permeability of the membrane itself is negligible in comparison (242).

1. Intrinsic proton permeability

It has been maintained widely and for some time that membrane proton permeability (P_H) is anomalous in two respects. First, P_H is many orders of magnitude higher (10^{-4} to 10^{-2} cm/s) than the permeability of other cations (10^{-12} to 10^{-10} cm/s) (227, 228, 390, 755, 797). Second, the proton conductance (G_H) is practically independent of pH (226, 395, 396, 755). These observations have been challenged on various counts, and some of the complications will be mentioned here.

P_H is difficult to measure, and reported values vary over many orders of magnitude, ranging from $<10^{-9}$ to 10^{-1} cm/s (153, 396, 585, 688, 755, 764, 766, 797, 804). Although various studies report no (124), moderate (585), or strong (i.e., up to ~100-fold) (228, 390, 396, 755, 764, 804, 1033) dependence of P_H on the composition of the membrane, this dependence does not come close to resolving the vast disparity in reported values. The idea that P_H is anomalously high was challenged by Nozaki and Tanford (766), who measured P_H 10^{-9} cm/s in phospholipid vesicles and estimated the true value to be $\leq 5 \times 10^{-12}$ cm/s. Deamer and Nichols (227) argued that these measurements were limited by development of a diffusion potential. Diffusion potentials can be avoided by allowing counterion flux (114). The finding that several cells have undetectably small P_H (185, 1054) suggests that proton permeability is not a general property of cell membranes.

Another source of variability may be differences between conductance and permeability measurements. Radioactive tracers reveal unidirectional flux, whereas electrical currents reflect only net flux, i.e., the difference between the unidirectional fluxes. For example, at E_H there is no net H^+ current, but there still can be large bidirectional fluxes. Hence, permeability estimates based on fluxes may be higher than electrical estimates made near E_H. On the other hand, if H^+ current is measured during a large driving voltage, fluxes will be practically unidirectional, so the two estimates should be reasonably consistent.

It has been suggested that both the high apparent P_H and the pH independence of G_H might be the result of proton accumulation near the negatively charged phospholipid head groups at the membrane-solution interface (342). In this view, P_H is high because its calculation assumes the bulk solution concentration and neglects the possibility that the local concentration of protons at the membrane surface may be proportionally much higher than other cations, due to the closer approach of H_3O^+ than a hydrated cation to the negatively charged membrane. It has been known at least since 1937 that negative surface charges tend to lower the surface pH, by up to 2 pH units in physiological solutions (215, 378, 988). Numerous studies indicate that negative surface charges can concentrate protons and other cations near membranes, resulting in higher conductance than expected from bulk concentrations (32, 214, 531, 716). Higher P_H is measured in negatively charged phospholipid membranes (764). Furthermore, because the negative charges at the surface are essentially fully screened by protons, the local proton concentration is relatively independent of bulk pH, and thus the apparent insensitivity of proton flux to bulk pH is also explained (342).

A fundamental difficulty with measuring P_H is that in the physiological pH range, the $[H^+]$ is up to 10^6 smaller than that of other cations. Because the calculation of P_H

effectively normalizes the measured flux according to the nominal $[H^+]$, any error is magnified, and the error is amplified at higher pH. At least in electrical measurements, most errors tend to increase the apparent P_H. In alveolar epithelial cells studied by voltage clamp in solutions lacking small ions, $P_H < 10^{-4}$ cm/s, even assuming that the entire leak is carried by H^+ (242). In fact, the "leak" current was insensitive to pH and the leak reversal potential did not change in a direction consistent with H^+ selectivity, thus $P_H \ll 10^{-4}$ cm/s by direct electrical measurement and any proton permeability was too small to detect (242). Similar observations were made in myelinated nerve (440). Also consistent with a low P_H, large changes in apical pH_o do not change pH_i in alveolar epithelial monolayers (510). From the viewpoint of a cell trying to maintain homeostasis, any proton leak is undesirable. In light of the $>10^4$ increase in P_H that occurs when the cell membrane is depolarized and H^+ channels open, the background level of proton leak is negligible for most purposes.

It is questionable whether the traditional permeability coefficient P_H is useful for H^+ flux through either membranes or most channels. The Goldman-Hodgkin-Katz (GHK) model (368, 444, 456) assumes that permeation is a simple process that occurs at a rate proportional to the rate that the permeant ion species encounters the membrane, which in turn is proportional to the bulk concentration. P_H is thus predicted to be a constant that is independent of pH, and lowering the pH by one unit should increase the H^+ flux (or g_H) 10-fold. In fact, deviations from this prediction are more the rule than the exception. To the extent that simple membrane H^+ conductance is independent of $[H^+]$ (226, 395, 396, 755), the parameter P_H, far from being constant, increases 10-fold/unit increase in pH. The P_H of Golgi membranes increases 3.4-fold/unit increase in pH (153). P_H calculated in alveolar epithelial cells during maximal activation of H^+ currents increases ~5-fold/unit increase in pH (166, 242). This type of behavior demonstrates that these systems do not operate within the assumptions built into the GHK permeability equations, and hence, permeability calculations have little meaning. In contrast, for gramicidin P_H is constant over a wide pH range; i.e., the single-channel H^+ conductance increases 10-fold/unit decrease in pH (Fig. 13). This counter-example suggests that the pH dependence of P_H in other systems does not reflect something peculiar about the diffusion of protons to membranes, at least at pH <5. Instead, it more likely indicates that a rate-limiting step in the permeability process is slower than the diffusional approach of protons to the membrane. In the case of voltage-gated proton channels, permeation through the channels is thought to be rate determining (166, 234, 238–240, 242–245). The GHK equations provide a valuable frame of reference by predicting the behavior of a simple system. However, in the frequently occurring situations in which P_H depends strongly on pH, the parameter P_H is not a meaningful way to evaluate or compare proton fluxes.

2. Transient water wires

A transient water wire might occur if, due to thermal fluctuations, a chain of water molecules happened to align across the membrane (225, 228, 755). Although fatty acid monolayers and cell membranes present a significant barrier that slows water diffusion by ~10^4 (34, 147), water can permeate most cell membranes, and several waters might follow the same path once a trailblazer has led the way. A hydrogen-bonded chain of water molecules intercalated between membrane phospholipids might be imagined to conduct protons. A membrane-spanning chain would need to be ~20 water molecules long, and the Born energy cost of forcing a proton into the bilayer might be reduced by virtue of partial hydration by nearby waters (730). The proton flux could be independent of pH if the rate-determining step were the breaking of hydrogen bonds between neutral waters, which might initiate the turning step of the hop-turn mechanism (730) (see sect. III*D*). A recent modification of this idea is the translocation of protons by small clusters of water molecules in the membrane (405).

There are some difficulties with the transient water wire proposal. Although water permeability varies 27-fold in different synthetic membranes (309), and P_H varies ~100-fold in different membranes, there is no correlation between P_H and water permeability (396). Molecular dynamics simulations indicate that the free energy barrier to formation of a water wire in a membrane is 108 kJ/mol, and thus the likelihood of a membrane-spanning pore forming is very low (658). The lifetime of such a water wire was <10 ps in this study (long enough to transport no more than one proton) and averaged 36 ps in a later simulation study (1038). The H^+ flux calculated for this mechanism could be made to agree with experimental estimates only by assuming that a proton permeates instantaneously and that the entry rate of protons into the water wire is 10^8 faster than provided by diffusion (658). Furthermore, simulations of H^+ permeation through optimal water wires indicate that ~100 ps is required for H^+ to permeate a 30-Å channel (120), which is longer than the predicted lifetimes of the transient water wires (658, 1038). The mean interval between H^+ permeation events through gramicidin during the largest H^+ currents recorded through any ion channel (2.2×10^9 H^+/s in gramicidin at +160 mV and 5 M HCl) (207) is 455 ps, which may or may not represent the maximum conduction rate (see sect. IV*A4*). A spontaneous water wire would have to be narrow and transient, because otherwise other ions might permeate (730), violating the observation that P_H is 10^6 greater than that of other ions (755). Paula et al. (797)

reported that P_H decreased from $\sim 10^{-2}$ to $\sim 10^{-4}$ cm/s as the bilayer thickness was increased from 20 to 38 Å, and concluded that protons were conducted via transient water wires in thin membranes and by a solubility-diffusion mechanism in thicker membranes. As pointed out by Deamer (225), if P_H measured in biological membranes was found to be lower than in model (5) membranes, then the latter would be poor models, because biological membranes may have a variety of additional transport mechanisms that would, if anything, increase H^+ flux. If water wires conduct protons across ordinary cell membranes, then they do so at a rate that is negligibly low compared with the proton fluxes that occur when voltage-gated proton channels are active (242).

3. Weak acid or base shuttles

Protons can cross membranes via weak acids or weak bases that act as proton carriers (106, 169, 671). It has been suggested that contaminant weak acids might account for the high P_H reported in phospholipid bilayer membranes (396). The weak acid mechanism has long been recognized (486) and is illustrated in Figure 2. When a weak acid is added to the extracellular solution, the protonated form (HA) will be present at a concentration determined by its pK_a and the pH as described by the Henderson-Hasselbalch equation (415, 425). The protonated form can permeate the membrane far more readily than the anionic form (A^-), and thus the predominant result will be entry of HA down its gradient into the cell. Once inside, HA will dissociate into A^- and H^+, to an extent determined by pH_i. The net result is that protons have been transported into the cell and released there, thus increasing pH_o and decreasing pH_i. The addition of a weak base will have the opposite effect. Again, the neutral form is far more permeant, but when B, a weak base, enters the cell, it leaves its proton behind, lowering pH_o, and once inside the cell it will tend to bind H^+ thus increasing pH_i. The neutral form of the acid or base will continue to diffuse across the membrane until its concentration is the same inside and outside the cell.

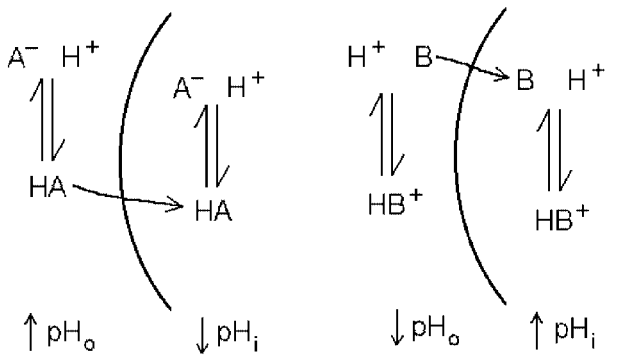

FIG. 2. Diagram illustrating the effects on local pH when weak acids (A) or weak bases (B) are present. The neutral form of each molecule typically is many orders of magnitude more permeant than the charged form. If the acid or base is present on one side of the membrane, the neutral form will permeate and change the pH on both sides of the membrane. The protonated weak acid, HA, carries its proton across the membrane and then may dissociate inside the cell, lowering intracellular pH (pH_i) and increasing extracellular pH (pH_o). These pH changes will be buffered, and the extent of the change will depend on geometrical considerations. The deprotonated weak base will permeate, in effect leaving a proton behind, and will tend to pick up a proton inside the cell, increasing pH_i and lowering pH_o.

A corollary to this mechanism is that weak acids and bases tend to equilibrate across membranes according to the pH on each side, which is important for determining intracellular drug concentrations (e.g., Refs. 233, 443, 744). This mechanism has been exploited as a way to estimate the pH inside cells or organelles (e.g., Refs. 152, 703, 1045). Another application of this phenomenon is the NH_4^+ prepulse technique (850), which is a standard method to study pH_i recovery from an acid load. This principle has been exploited to regulate pH_i in cells under whole cell voltage clamp (242, 248, 387). One can establish a known NH_4^+ (or triethylammonium$^+$, for example) gradient by including a known concentration in the pipette solution, and then adjusting the NH_4^+ in the bathing solution. Ideally, the NH_4^+ gradient will establish an equivalent H^+ gradient. For example, 5 mM NH_4^+ in the bath and 50 mM NH_4^+ in the pipette (and thus in the cell) will lower pH_i by 1 unit relative to pH_o.

Because of their exquisite sensitivity to pH, voltage-gated proton channels are effective pH meters that can be used to report pH changes (237). Adding NH_4^+ to the bath produces intracellular alkalinization, which greatly diminishes H^+ currents (473). Conversely, addition of sodium lactate or sodium acetate to the external solution rapidly and effectively acidifies the cytoplasm, enhancing voltage-gated proton currents (473, 710).

As a practical consideration, if one wants strict control over pH_i, one must worry about the presence of weak acids or bases in the solutions. Obviously, small molecules with pK_a near ambient pH (e.g., HCO_3^-, NH_4^+, etc.) are perilous, but even larger molecules with pK_a >2 units from ambient may produce significant changes in pH_i by the proton shuttle mechanism. For example, *N*-methyl-D-glucamine (NMDG), a commonly used large "impermeant" cation with pK_a 9.6, can cause significant shunting of the pH gradient by the shuttle mechanism (938). Whether it does so quickly enough to affect H^+ currents in a patch-clamped cell has not been reported, but deviations of V_{rev} from E_H appear somewhat greater in a study using NMDG solutions (232) than tetramethylammonium$^+$ solutions in the same cells (166). Tetrabutylammonium$^+$ is sufficiently lipophilic to permeate cell membranes (233) and has been shown to enhance proton flux (764).

4. Phospholipid flip-flop

Another mechanism that might allow net proton flux across a membrane is phospholipid flip-flop (396). This is a subset of the weak-acid mechanism just discussed, but does not require any molecules exogenous to the membrane. Membrane phospholipids might transport protons, acting effectively as carriers. The negatively charged phosphate groups may become protonated, neutralizing their charge, and then the molecule could flip-flop across the membrane, releasing the proton on the other side. Long-chain fatty acids can also transport protons across membranes by this mechanism (397). Biological long-chain fatty acids may transport protons across the membrane by a weak acid mechanism, although their slow intrinsic flip-flop rate makes them relatively inefficient (397). Although it seems likely that this mechanism can occur under some conditions (397, 547), it has been argued that it does occur only at relatively high concentrations of fatty acids, such as 300 μM oleic acid (327).

B. Being and Nothingness: Do Proton Channels Exist?

How do we know that voltage-gated proton currents are mediated by specific membrane proteins, rather than simple flux through the membrane itself or other mechanisms discussed in section III*A*? Several strong arguments resolve this existential question.

H^+ currents have well-defined time- and voltage-dependent gating. It is difficult to imagine that such behavior could occur in the absence of specific membrane proteins.

Direct evidence of gating is provided by current fluctuations (see sect. V*G*) as well as direct single-channel currents (168). Gating is a defining characteristic of ion channels.

The result of time- and voltage-dependent gating is that over a span of ~40 mV, the membrane permeability to H^+ increases reversibly by at least three to four orders of magnitude (242). Again, it is difficult to imagine how a simple membrane, even if perforated by "water wires," could manifest such a remarkable transition.

As a result of voltage-dependent gating, the steady-state g_H rectifies strongly. Outward H^+ flux is at least three to four orders of magnitude greater than inward H^+ flux, which is undetectably small. How could this kind of rectification (asymmetry of flux) be accomplished across a simple membrane?

The H^+ current through voltage-gated proton channels is 1.9 times larger than D^+ currents (242), substantially larger than the isotope effect for simple membrane permeation (226, 804) (see sect. V*I*).

H^+ currents are inhibited by Zn^{2+} and other polyvalent cations, selectively, with high affinity, and in a complex manner, by metal ions binding to a site with an apparent pK_a 6.2–7.0 (163). Such effects are readily explained by interaction with a membrane protein but difficult to explain otherwise.

If protons permeated the membrane itself, H^+ flux ought to be governed by simple diffusion theory, i.e., the Fick equation applied to membranes (368). H^+ flux should be proportional to concentration, and nonsaturable, limited only by diffusion of buffer across the unstirred layer near the membrane (399, 527). As will be discussed further in sections IV*O* and V*F*, over a range of 4 pH units, the $g_{H,max}$ increases only ~2-fold/unit decrease in pH.

Substances such as phloretin or sodium dodecyl sulfate that alter the internal dipole potential of membranes and thereby profoundly affect ion conductances mediated by carriers (29, 955) have no effect on proton currents (V. Cherny and T. DeCoursey, unpublished observations). One can imagine that ions inside a channel protein might be shielded, but if protons permeated the bilayer itself, one would expect sensitivity to the internal dipole potential.

In conclusion, proton channels do exist and are almost certainly membrane proteins.

C. Are Proton Channels "Real" Ion Channels?

This question is ultimately one of semantics and depends on one's definition of ion channels. In my view there is no question that proton channels are ion channels. Proton channels are unique in many respects, but they nevertheless possess all of the fundamental characteristics of ion channels. The first three properties are shared by uniporters.

Ion channels are membrane proteins that provide a low-resistance pathway across cell membranes. That voltage-gated proton channels facilitate H^+ efflux across membrane is evident from the observation that opening H^+ channels by depolarization of the membrane potential increases P_H by >4 orders of magnitude (242).

Voltage-gated proton channels are entirely passive. An open H^+ channel permits passive H^+ conduction down the electrochemical gradient. H^+ channels cannot be considered to be "pumps" in any sense of the word. Removal of ATP prevents neither H^+ channel opening nor H^+ conduction. ATP has subtle effects (574, 710), but these are unrelated to phosphorylation (710) (Cherny and DeCoursey, unpublished data) (see sect. VI*B3*).

In distinction from many carriers, symporters, and antiporters, no co-ion or counterion is required (238).

A fundamental distinction between carriers and channels is that carriers must undergo a conformational change during each ion translocation cycle. The argument becomes semantic at this point. If H^+ conduction occurs

by a HBC mechanism (see sect. III*D*), the turning step of the hop-turn mechanism arguably might be considered a conformational change. However, ions probably interact with normal ion channels during permeation, and it is possible that conformational changes in the protein (induced by the presence of the ion) must occur before conduction can proceed. Second, the rearrangement of hydrogen bonds required during the turning step may be subtle and hardly qualifies as a conformational change. Finally, the distinction of carriers from channels based on the conformational change criterion is invoked to explain the lower turnover rate of carriers. In fact, the participation of a protonatable residue at the entrance to several proton channels has been shown to increase the efficiency of proton conduction (see sect. IV*N*). In summary, the term *channel* is appropriate.

Voltage-gated proton channels exhibit gating: reproducible time- and voltage-dependent activation and deactivation of H^+ current. Excess current fluctuations that reflect stochastic opening and closing transitions, i.e., gating, have been observed (168, 236, 720). Demonstration of the existence of gating is often presented as "proving" an ion channel mechanism. Whether carriers might exhibit behavior interpretable as gating is unclear. By this criterion, voltage-gated proton channels are ion channels.

As the defining property of voltage-gated channels, including proton channels, gating is a major feature that distinguishes channels from other types of transporters. A channel without gating is simply a pernicious hole in a cell membrane. In contrast, the activity of carriers (porters and pumps) is mainly regulated by substrate availability, and secondarily by biochemical modulation. Carriers can perform their physiological functions without a clear requirement for gating. Specifically, porters and pumps have no correlate of the full open state of ion channels, in that at no time in their reaction cycle is there a continuous pathway for the ion across the membrane. The open state enables channels to have high turnover rates, whereas carriers must undergo conformational changes during each transport cycle.

Voltage-dependent gating must be distinguished from voltage-sensitive flux. Any process that results in net charge translocation across a cell membrane must in principle be voltage sensitive. The ion flux will depend on the driving force (596), which includes the electrical potential difference (voltage) across the membrane. Simple diffusion of ions across membranes is voltage sensitive, and so must be ionic flux through porters and pumps whose stoichiometry of ion movement is unbalanced, so that net charge translocation occurs. Well-known examples include the Na^+-K^+ pump (833), the Na^+/Ca^{2+} exchanger (540), a Na^+/HCO_3^- cotransporter (848), the H^+-dependent glucose transporter (947), and many H^+/amino acid transporters (103, 875). The ion transport rate varies with voltage because each cycle of the carrier delivers net charge across the membrane's electric field. Even if the charge-transferring steps are not rate limiting, the overall process must still be voltage sensitive because voltage will affect the probability that the transporter exists in states immediately adjacent to the rate-limiting step (596). However, the voltage sensitivity may not be very obvious for a particular measurement. For example, the current generated by the H^+-ATPase in *Neurospora* changed less than twofold over 300 mV (377). The translocation of electrons across the membrane by NADPH oxidase is nearly voltage independent over a 150-mV range (252). In a model of pump currents, Hansen et al. (410) showed that the current-voltage relationship could be flat or nearly so over a wide voltage range, but steep at other voltages. Voltage gating, in contrast, implies a discontinuous process: a clear difference in the mode of operation of the transporter protein at different voltages. In the case of voltage-gated ion channels, the probability of being open or closed (conducting or not) depends on membrane voltage. Channel gating may reflect a conformational change in the protein or, in some cases, occlusion of the conducting pathway. For all voltage-gated channels, gating is stochastic: the probability of being open or closed depends on voltage. The current through an open ion channel is voltage sensitive, generally increasing as the voltage is increased relative to the reversal potential.

It can be argued that carriers and pumps must function to a variable degree of effectiveness and that this is equivalent to the gating of ion channels; that is, carriers may also exist in states of low functional probability, which are incapable of reacting with the substrate. This circumstance is obvious when a noncompetitive inhibitor is present, but can in principle occur under less well-defined conditions, for which the term *lazy-state* behavior has been coined (411), corresponding to the "closed" ion channel. If we could look at individual carriers, as we can at individual channel molecules, we should see these noncycling intervals (C. L. Slayman, personal communication). However, thus far it has been impossible to measure transport through individual carrier molecules (whose maximal currents would be in the attoampere range), so direct demonstration of this phenomenon is lacking. It has been proposed for the F_o proton channel of H^+-ATPase (1046), that the interaction between Trp^{241} and His^{245} comprises a "gate." Protonation of His^{245} at low pH allows interaction with Trp^{241}, which by conformational changes or pK_a shifts, as speculated, allows protons to enter the channel and access the crucial Asp^{61} (see sect. IV*F*). The term *gate* has also been applied to bacteriorhodopsin (the best understood "active" transporter) in a similar sense, to describe the conformational change in the Schiff base that causes proton flux to be unidirectional (969). In both of these cases, however, the distinction from channels remains, because an open H^+ channel allows continuous H^+ flux across the membrane down its

electrochemical gradient, which does not occur during the normal functioning of bacteriorhodopsin, F-ATPases, or any other carrier-type protein.

The only conceivable alternative descriptor, carrier, is inappropriate (see sect. III*C*). Ion carriers (uniporters) must be voltage sensitive, because at least one form (ion-bound or ion-unbound) must carry net charge across the membrane. As a result, a large applied voltage may trap the carrier at one side of the membrane, and hence transport will not be sustained. The resulting transient current has been described for mutant forms of voltage-gated K^+ channels (R365H and R368H) in which His shuttles protons across the membrane (960, 961). The elegant analysis of possible outcomes of histidine scanning studies of the voltage sensor of K^+ channels by Starace and Bezanilla (960) distinguishes between carriers and channels. A protonatable His acting as a carrier binds a proton at one membrane surface, moves during voltage-dependent gating to a new position in which the protonated His is exposed to the other membrane face, and then releases the proton. The result is sustained H^+ current that is maximal near voltages where P_{open} is 0.5, i.e., where the probability of gating transitions is maximal (Fig. 3*C*). In contrast, mutants in which His becomes accessible simultaneously to both membrane surfaces act as H^+ channels, providing a continuous pathway for protons to cross the membrane. This proton channel turns out to be gated because only in one conformation, whose probability of occurrence is voltage dependent, is the His accessible to both sides of the membrane. In this case, the g_H has a normal sigmoid voltage dependence like other voltage-gated channels. As shown in Figure 3, *A* and *B*, the H^+ current increases monotonically with voltage over a range of 400 mV in native voltage-gated proton channels. This behavior is channel-like.

One objection to the term *channel* is based on the miniscule single-channel conductance. Traditionally (444, 596), channels, carriers, and pumps are characterized as having distinctive maximum turnover rates: 10^5–10^8, 10^2–10^4, and 10^1–10^3 s^{-1}, respectively. Although it is reasonable to argue that finding a turnover rate much higher than the typical range suggests an erroneous classification, the same logic does not apply to a smaller-than-typical turnover rate. If a putative carrier translocated 10^7 ions/s, one might suspect that it was in fact a channel. However, if a channel conducts only 10^4 ions/s, this just means it is a channel with a low conductance. In the case of H^+ channels, the permeant ion normally is present at concentrations $<10^{-7}$ M. The H^+ conductance of the gramicidin channel is the largest of any ion channel at very low pH (see sect. IV*A*), but extrapolated to pH 7 (see sect. IV*P*) is smaller than that estimated for voltage-gated proton channels.

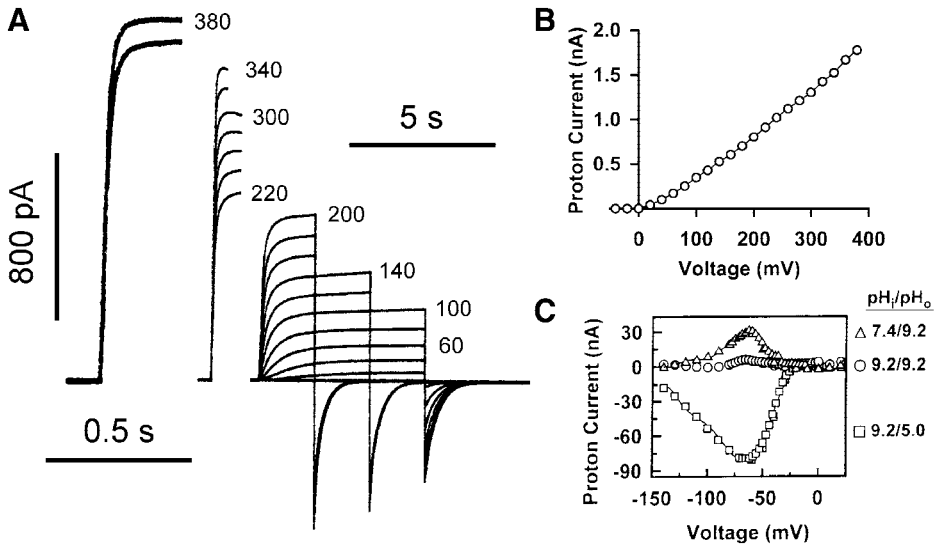

FIG. 3. Absence of saturation of voltage-gated H^+ currents contrasted with nonmonotonic voltage dependence of carrier-mediated H^+ currents. *A*: H^+ currents are illustrated for pulses from a holding potential (V_{hold}) of −60 mV, in 20-mV increments up to +380 mV, at pH_o = pH_i = 7.0 in a human eosinophil studied in permeabilized-patch configuration, as generally described in Ref. 246. The pulse duration was reduced at larger depolarizations to avoid depletion of cytoplasmic protonated buffer, which nevertheless occurred during some pulses as evident from the droop of the current. The records with heavier lines were recorded at a faster time base (calibration bar on *left*). This cell had been stimulated with PMA (phorbol ester) and then treated with diphenylene iodonium. *B*: H^+ current-voltage relationship from the data in *A* indicates no hint of saturation (V. V. Cherny and T. E. DeCoursey, unpublished data). *C*: nonmonotonic current-voltage relationships at three pH_i in a K^+ channel mutant (R365H) that acts as a proton carrier. The current disappears at large positive or negative voltages because a form of the carrier is pinned at one side of the membrane. [From Starace et al. (961). Copyright 1997, with permission from Elsevier Science.]

D. Hydrogen-Bonded Chain Conduction

Proton permeation through a narrow channel or through a protein is generally considered to occur by a mechanism different from the permeation of other cations, just as proton conductance in bulk water differs from that of other cations. Myers and Haydon (723) explained the anomalously large proton conductance through the gramicidin channel by a Grotthuss mechanism of protons hopping across the row of water molecules inside the channel. The gramicidin channel is known to be a narrow pore occupied by a dozen or so water molecules in single file (611). Protons can also permeate channels that do not contain a continuous row of water molecules.

Lars Onsager explicitly proposed what has become known as the hydrogen-bonded chain (HBC) mechanism in 1967 (778, 779). He proposed that ions (778), including protons (779–781), might cross biological membranes through networks of hydrogen bonds formed between side chains of amino acids in membrane proteins. This mechanism was abandoned as a means of cation permeation except for the special case of protons (276, 471, 733, 734). The unique properties of protons make it possible to devise a pathway through a membrane protein that is not a water-filled pore like traditional ion channels (276, 733, 900). Nagle and Morowitz (733) considered in detail the properties and nature of proton conduction via a HBC. The HBC may comprise water molecules, side groups of amino acids capable of forming hydrogen bonds, or a combination of the two. Amino acids suggested as potential HBC elements include Ser, Thr, Tyr, Glu, Asp, Gln, Asn, Lys, Arg, and His (734). Zundel (1102) has measured large proton polarizability, which he considers to indicate facilitation of proton transfer, in Tyr-Arg, Cys-Lys, Tyr-Lys, Glu-His and Asp-His hydrogen bonds. Conduction across a HBC occurs by migration of defects or faults. Bjerrum (96) described two classes of defects in ice: orientational and ionic. Two main types of orientational faults can occur as a result of rotation of one water molecule through 120° (Fig. 4). A Bjerrum D (doppelt = double) defect occurs when two neighboring water molecules are oriented with two protons between them. A Bjerrum L (leer = vacant or empty) defect occurs when the oxygens of two adjacent waters point toward each other. These orientational defects can propagate through the ice crystal (Fig. 4*C*). Two types of ionic defects occur in ice when H_3O^+ and OH^- are formed. These ionic defects migrate by means of proton jumps. Various other defects in ice have been proposed (490).

The general features of HBC conduction are illustrated in the diagram in Figure 5. Proton conduction occurs in two obligate steps, called the "hop-turn" mechanism. The hopping step reflects the movement of the ionic defect, whereas the turning step reflects the propagation of a Bjerrum L fault from the right (distal) side of the channel back to the left side. In Figure 5*A*, a proton enters the HBC from the left, and through a series of jumps, all of the protons in the chain advance, and the terminal proton exits into the solution at the distal end of the channel. The proton that exits is not the same one that entered, but the net result is that one proton disappears from the proximal solution and one proton emerges into the distal solution. A distinctive feature of HBC conduction illustrated in Figure 5*B* is that after the "hopping" step depicted in Figure 5*A*, the chain is oriented differently than before, such that another proton cannot enter the chain from the left. First, it is necessary to reorient the entire chain, which in the example shown is accomplished by rotation of each hydroxyl group. Presumably, the hopping and "turning" steps of this hop-turn mechanism occur sequentially. A consequence of the hop-turn mechanism is that an empty proton channel has a "memory" of the last proton to permeate, which persists until the turning step is complete. Another consequence is that in the absence of a membrane potential or other orienting factor, an approaching proton has only a 50% chance that the HBC will be oriented correctly.

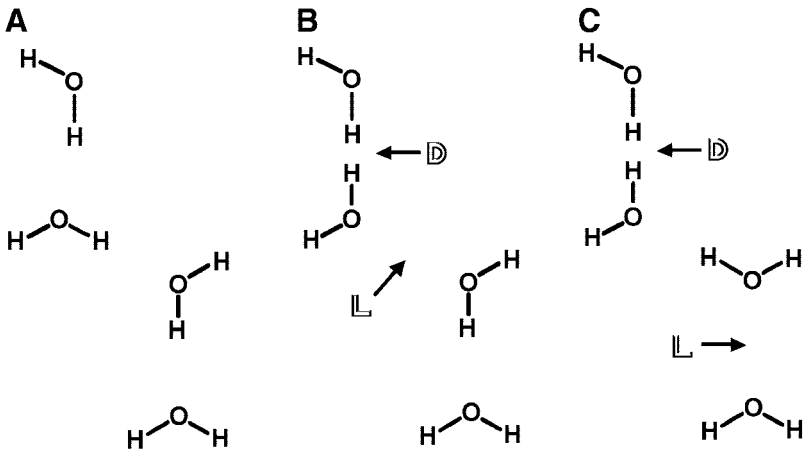

FIG. 4. Formation of Bjerrum orientational faults in ice. *A*: normal orientation of water molecules with hydrogen bonds (implicit) between each oxygen and a hydrogen of a neighboring molecule. *B*: rotation of one water molecule results in two types of orientational faults: the D defect where two hydrogens point toward each other, and the L defect where there is no hydrogen between two oxygens. *C*: illustrates the infrequent occasion when these orientational defects separate and then migrate through the ice crystal. [Redrawn from Bjerrum (96).]

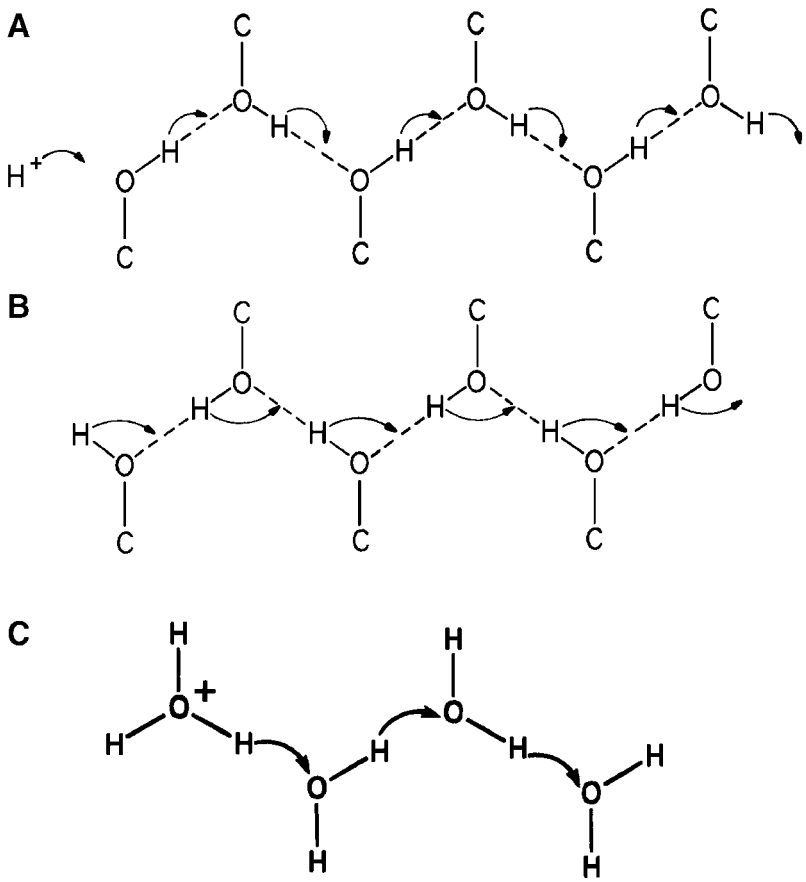

FIG. 5. Diagram illustrating the hydrogen bonded chain (HBC) mechanism for proton conduction. In this example, the HBC is formed by hydroxyl groups (e.g., from serine residues). *A*: a proton enters the chain on the left side and then as a result of the series of proton hops indicated by the arrows, a proton exits the chain on the right. *B*: after the hopping process is complete, the orientation of the HBC is different, and another proton cannot enter the chain from the left. First, it is necessary for the chain to reorient, in this example by rotation of all of the hydroxyl groups as indicated by the arrows. This turning process must be complete before another proton can enter the chain in the same direction. [From Nagle and Morowitz (733), copyright 1978 National Academy of Sciences, USA.] *C*: proton conduction along a simple water wire. [From Hammes-Schiffer (408), copyright 1998 American Chemical Society.]

An intriguing aspect of the HBC conduction mechanism is that the net translocation of one proton across the membrane does not result in the translocation of one full elementary charge. Part of the charge is translocated during the turning step (781). In ice, the hopping step translocates 0.64*e*, and the remaining 0.36*e* is translocated during the turning step (782, 885); in gramicidin the corresponding values are 0.69*e* and 0.31*e* (901). The reorientation of hydrogen bonds within the HBC results in a net charge movement within the membrane, acting as a capacitive load. Both processes are favored by an appropriate electrical driving force (i.e., positive on the side from which proton flux originates). It would be intriguing to devise an experiment to demonstrate that H^+ conduction occurs in these two steps.

For various reasons, it generally has been believed that in HBC conduction the hopping step is faster than the turning step, by an order of magnitude or more (733, 734, 810, 814, 816, 818, 819, 900). With a few notable early exceptions (84, 366), the rate-determining step in H^+ conduction in water is considered to be the reorientation of water molecules rather than proton hopping (184, 448, 535, 818). If the turning step were also rate determining for H^+ current through voltage-gated proton channels, then it would be more reasonable to consider H^+ conduction in terms of the voltage-driven HBC reorientation rather than proton hopping.

Although the idea that protons permeate channels via a HBC mechanism has become widely accepted, some have questioned whether the concept is overused. Citing the example of ATP synthases that are driven by translocation of Na^+ instead of H^+, Boyer (112) suggested that the hydronium ion, H_3O^+, may be the transported species. The HBC concept was proposed before any proton channel structure was known. Over the past two decades, specific proposed proton pathways have generally progressed from being mostly amino acids side groups (e.g., Refs. 189, 392, 483, 969) to including more and more water molecules (803). Many amino acids can be demonstrated by mutagenesis to play important roles in creating proton pathways, but it is very difficult to distinguish whether a particular amino acid comprises a direct element in the HBC or simply is required to preserve structure or to constrain water molecules in an appropriate position (458, 633, 693, 765). It may be that nontitratable amino acids contribute to proton conduction not as direct elements in the HBC but rather by providing the correct microenvironment for water molecules that actually conduct the protons. It seems clear that titratable amino acids with low enough pK_a not to hold protons too tightly

(Asp, Glu, and His) do relay protons in several channels, including M_2, mutant K^+ channels, H^+-ATPase, carbonic anhydrase, the bacterial reaction center, and bacteriorhodopsin (Table 2). P. A. Loach (personal communication) has suggested that a prototypical transmembrane proton channel may consist of water microchannels, pockets that contain a small number of water molecules. Protons or solvated hydroxide ions could move freely within a microchannel by a hop-turn mechanism, principally via water molecules stabilized by ligands (e.g., carbonyl groups) from the protein. Gating in this context is viewed as the establishment or breaking of proton pathways that interconnect neighboring microchannels, and the microchannels with the aqueous interfaces. Single, titratable acid-base groups, such as the side chains of Asp and Glu, may play a critical role in interfacing and gating between microchannels. In addition, the water content may change drastically during conformational changes that occur in the protein, thus providing another mechanism for "gating," i.e., completing or disrupting the continuity of the proton pathway.

E. Proton Transfer in Water Wires

Because of the importance of proton pathways in various proteins, much effort has gone into studying simple systems. A favorite model ion channel that has been studied exhaustively is the gramicidin channel, in which H^+ is conducted along a simple single-file water wire (see sect. IV*A*). In addition to experimental studies, molecular dynamics simulations have been done on proton transfer along water wires inside gramicidin or imaginary channels, or even in simple chains of water molecules (Fig. 5*C*). In general, the more detailed and exhaustive the calculation, the simpler the system is in terms of numbers of molecules, by computational necessity. Several themes emerge from these studies. The (reversible) transfer of a proton from one water to the next is very rapid (270, 868), with a mean rate of 1.2 ps^{-1} (817). Proton transfer is activationless in a simple water wire, suggesting that propagation of the bonding defect is rate determining (814, 818). The hydrogen bond length and angle are critically important (882); linear or angular deformation of the hydrogen bond results in higher energy barriers to proton transfer both in water wires (882) and other types of HBC (883, 948). The longer the hydrogen bond, the higher the energy barrier to proton transfer (884). This feature is relevant to the finding that electrostriction (shortening of the distance between waters) can occur in ion-occupied channels (271). Quantum effects play a significant role (231, 408, 817). The intriguing idea of concerted transfer, i.e., nearly simultaneous hopping of multiple protons along the chain (as elements in the net transfer of a single proton) as a semicollective process has been discussed and may occur to some extent (231, 816–819, 868, 882, 890, 948). Concerted transfer is facilitated when the hydrogen bonds are equivalent (948). Further results of molecular dynamics calculations specific to gramicidin channels are discussed below (see sect. IV*A*).

Nagle and Morowitz (733) considered the possibility that water inside a confined geometry such as a narrow ion channel might be constrained, and that proton conduction in such a water-filled pore might behave more like proton conduction in ice than in liquid water. This prediction has been supported strongly by an assortment of molecular dynamics calculations, which conclude that water inside confined spaces like narrow ion channels diffuses or reorients much more slowly than in bulk water, i.e., the water inside channels is to some extent "frozen" (118, 120, 173, 174, 295, 317, 402, 414, 509, 726, 834, 856, 877). Obviously, structural details matter: in large-diameter pores with smooth nonpolar walls, calculated water self-diffusion can actually increase beyond bulk values due to a molecular-level capillary action-like effect related to a paucity of hydrogen bonds near the walls (414), but nevertheless, structures like real biological channels exhibit distinctly reduced water mobility. In various microcavities and confined structures, both the apparent dielectric constant of water and the diffusion coefficient of protons increased with the diameter of the confined space (117). A complication arising from the analogy with ice is that we do not understand proton conduction in ice very well (see sect. II*B*). Eigen (287) suggested that the very rapid proton conduction in ice reflected proton delocalization due to the rigidly ordered (by hydrogen bonds) ice structure; ironically, present proponents of the idea that proton movement in ice is greatly inhibited at low temperature use a similar argument, namely, that the rigid structure prevents the water rotation required for HBC conduction (188). In any case, the general consensus seems to be that any restriction of water mobility will tend to reduce proton mobility. Bernal and Fowler (84) considered the low dielectric constant of ice to indicate that most of the water molecules were not free to rotate, consequently decreasing proton conductance. Proton diffusion inside the phoE channel is reduced to 50% its value in bulk water (402); a similar reduction has been calculated for gramicidin channels (14, 207). A cleft in lactose permease exhibits reduced water activity and a threefold reduction in the H^+ diffusion coefficient (726). Despite these general considerations, there is evidence in several systems that amino acids that line proton channels may function by constraining or orienting water molecules to facilitate proton transfer (458, 633, 693, 765). In fact, hydrogen bonding between the waters inside gramicidin and the channel wall facilitates proton transfer (819), and the diffusion coefficient for protons inside gramicidin channels, calculated from

molecular dynamics simulations, is 40 times larger than that in bulk water (901). Finally, a recent molecular dynamics study of proton conduction in smooth, cylindrical, hydrophobic, water-filled pores indicated that although the water diffusion constant decreased with pore radius, proton mobility increased sharply at 2-Å radius compared with larger pores, providing evidence of water-wire behavior when waters are in single file (120). Ultimately, although kinetic competence is a prerequisite, the speed of proton transfer may be less critical biologically than the establishment of conditions that allow it to take place in a controlled and predictable manner.

IV. CLASSES OF PROTON-PERMEABLE ION CHANNELS

A number of molecules that conduct protons during their normal operation, or have at one time or another been thought to do so, are discussed here briefly, roughly in order of increasing complexity. The list is arbitrary and not meant to be complete. Many other molecules could have been included, such as Photosystem II used by green plants during photosynthesis (266, 1014), proton-translocating transhydrogenases (95, 865), fumarate reductase (583), the flavoprotein *p*-hydroxybenzoate hydroxylase (897), ferridoxin I from *Azotobacter vinelandii* in which electron transfer is controlled by coupling with the more discriminating process of proton transfer (156), etc. A number of proton-conducting molecules were reviewed recently in a special issue of *Biochimica et Biophysica Acta* (Vol. 1458, No. 1, 12 May, 2000).

A. Gramicidin

1. Gramicidin is a water-filled pore

The gramicidin channel, a peptide antibiotic composed of 15 amino acid residues formed by *Bacillus brevis*, has been studied extensively as a simple prototypical ion channel. Gramicidin is in some ways reminiscent of a synthetic channel discussed in section IV*C* in that it is a small polypeptide with no formal charges, yet it is cation selective and can conduct protons. The gramicidin channel is a dimer formed when two hemi-channels assemble together head-to-head in the membrane (310, 1029). It is readily incorporated into artificial phospholipid bilayer membranes, permitting control over the solutions on both sides of the membrane, and it tolerates extreme voltages and ionic conditions that would destroy ordinary biological ion channels in situ. There is strong experimental evidence that the gramicidin channel is a water-filled pore. Streaming potential and electro-osmotic flux measurements, both of which reflect the enforced concerted motion of water molecules and ions in a long, single-file pore, indicate that gramicidin channels contain ~12 water molecules (310, 611). Molecular dynamics simulations are consistent with the presence of ~7–10 water molecules inside the pore (173, 316, 509, 816, 819, 856, 859, 944) and suggest that the number of waters may vary with permeant ion species (271, 944). Electro-osmosis measurements detect the flux of water pushed through the channel by ions as they permeate driven by voltage, whereas streaming potential measurements detect the electrical consequences of ions pushed through the channel by water molecules as they are driven to permeate by an osmotic gradient. Movement of H^+ through gramicidin did not generate a streaming potential (611), indicating that protons permeate without the need to move water through the channel, precisely as expected for a water-wire mechanism (723).

2. Protons permeate gramicidin by a Grotthuss-type mechanism

Gramicidin channels can conduct protons at a higher rate than any other ion channel conducts any other ion species, $>2 \times 10^9$ H^+/s (207). This statement refers to normal ion-selective channels through which ions permeate in single file; poorly selective wide-pore channels such as the mitochondrial voltage-dependent anion channel (VDAC) that are permeable to molecules up to 1,000 Da may have higher conductances (318). The proton permeability of gramicidin channels (calculated from bi-ionic reversal potential measurements and the GHK voltage equation) is 43–55 times that of Na^+ (723). Similarly, the proton conductance is 14-fold higher than the Na^+ conductance when the conductances are normalized according to permeant ion concentrations (453). The proton conductance of a ethylenediamine analog of gramicidin was 19–25 times that of the next most permeant ion, NH_4^+, and 150–200 times that of Na^+ (1085). The H^+ conductance of dioxolane-linked gramicidin dimers was >40 times that of K^+ (959). The explanation for the relatively high proton conductance is that protons permeate a water-filled gramicidin channel by a Grotthuss-type mechanism, hopping across the water chain without displacing the water molecules (723). One would expect that the presence of a normal cation might interfere with H^+ conduction by preventing Grotthuss-type H^+ hopping through the channel; however, the dwell time of Na^+ is evidently so brief (~10 ns) that such interactions were barely detectable (421). Indirect confirmation that protons permeate gramicidin by a Grotthuss-like mechanism rather than as hydronium ions was provided by the effects of changing the dipole potential either by fluorination of Trp residues or by mutational replacement of Trp with Phe at the entrance to the pore. Both interventions affected H^+ conductance and the conductance of other monovalent cations in opposite directions (132, 810). Sim-

ilarly, agents like phloretin that change the internal dipole potential of membranes (29) reportedly also affect proton and alkali cation conductances through gramicidin channels in opposite directions (847), although other investigators see no effect (253a).

3. *Proton diffusion to the channel is rate determining at most pH values*

Examination of the concentration dependence of H^+ conduction through gramicidin channels (Fig. 13) indicates several distinct regions (244). At pH >2, the unitary H^+ current is directly proportional to $[H^+]$, which has been interpreted as indicating that the rate-determining step is the diffusional approach of H^+ to the channel mouth (14, 230, 610). The implication is that each proton permeates independently of other protons and that permeation is so rapid that each proton enters the channel long after the previous one has left. Between pH 2 and 1 the slope of the $[H^+]$ versus H^+ conductance relationship decreases, but at lower pH, the slope again approaches unity (292, 374). The "shoulder" region was ascribed to multiple occupancy of the channel by protons (292), as can be predicted to occur in rate theory simulations of ion permeation (445). Some subsequent studies have supported the existence of a shoulder region in native gramicidin A (14, 374), gramicidin B (374), and in the RR stereoisomer of covalently linked gramicidin dimers (207). However, no shoulder was evident in gramicidin A between pH 2.6 and 0.5 (421), and in gramicidin M, the H^+ conductance was proportional to $[H^+]$ up to pH <0 (374). Finally, in dioxolane-linked SS dimers, the $[H^+]$ versus H^+ conductance relationship was linear over a wide concentration range (1–2,000 mM H^+), with slope 0.75, a finding seemingly inconsistent with diffusion being rate determining (207). H^+ conduction through gramicidin can be simulated in a combined molecular dynamics and diffusion model by assuming single proton occupancy, but only at pH >1.7 (901). Above this concentration (i.e., at lower pH), the model conductance decreases, reminiscent of the decrease at high permeant ion concentration predicted by some Eyring-type models for multiply-occupied single-file channels (445, 874). However, the actual H^+ current continues to increase at lower pH (14, 208, 292). It is generally accepted that normal ion channels can be occupied by multiple permeant ions, and this conclusion is supported for the bacterial KcsA channel by X-ray crystallographic evidence (268, 496). Nevertheless, in general, the entrance of a second ion would tend to be hindered by the presence of an ion in the pore, due to both electrostatic repulsion and the unfavorable orientation of waters near each ion (487, 609). The difficulty of forcing two protons into the same relatively short water wire might be even greater than for ordinary ions. The simultaneous presence of two protons in a water wire would create a Bjerrum D defect that would interrupt the HBC and block conduction, and the defect would have to be conducted through the channel (244). H^+ conduction in a doubly occupied channel would likely be slower than in a singly occupied channel, because it would be limited by the rate of defect permeation. The proportionality between $[H^+]$ and current in gramicidin at pH <1 could reflect this slower defect permeability. Alternatively (244), the "shoulder region" might reflect *1*) a shift in the rate-determining step from proton entry to water reorientation, *2*) saturation of titratable groups on the membrane exterior that contribute to the supply of protons to the channel so that lateral conduction cannot occur at very low pH, or *3*) a shift from a Grotthuss-type to a hydrodynamic conduction mechanism (molecular H_3O^+ permeation).

4. *H^+ current saturation at very low pH may reflect bulk diffusion limitation, not permeation*

The H^+ conductances of both gramicidin (14) and two synthetic channels, LSLLLSL and LSLBLSL (254), saturate at pH <0 (Fig. 13). One possibility is that this saturation reflects the upper limit of the rate that H^+ can permeate the channel (14). In a simple Michaelis-Menten (684) single binding site model of permeation (186, 595), occupancy of the site by protons would increase with concentration until it approached 100%, at which point no further increase could occur. However, because the bulk conductivity drops precipitously in the same extremely concentrated HCl solutions (+ in Fig. 13), we proposed that the apparent saturation reflects bulk diffusion limitation rather than an upper limit of H^+ flux through these channels (244). In this view, water-filled channels could conduct $>2 \times 10^9$ H^+/s if the proton supply were adequate.

It has been noted that single-channel current-voltage relationships can be sublinear, or saturating, at low permeant ion concentrations, whereas the current-voltage relationship is superlinear at higher permeant ion concentrations (27, 30, 453). Similar observations have been made for H^+ permeation through gramicidin (14, 292, 810, 847). A widely held view is that sublinear behavior reflects diffusion-limited entry of ions, whereas superlinear behavior reflects permeation, and more specifically, ion exit from the pore as being rate-determining (27, 28, 30, 132, 292, 374, 810, 847, 901). The evidence presented by Andersen (27, 28) that the saturation phenomenon reflects a diffusion limited approach is substantial. However, the conventional interpretation of superlinearity is less well established. At high [HCl], many studies describe superlinearity (14, 207, 292, 374, 847). However, in phosphatidylethanolamine-phosphatidylcholine (PEPC) bilayers, the gramicidin single-channel current-voltage relationship was sublinear up to 400 mV even at 7 M HCl

(208). The RR stereoisomer of covalently linked gramicidin dimers exhibits a sigmoid current-voltage characteristic, being superlinear up to 200 mV, but sublinear at higher voltage (36, 831). The interpretation of these data would become more complicated if one accepted the suggestion that proton conduction through gramicidin in fact occurs by OH^- flux in the opposite direction (847), an idea that is difficult to reconcile with the near proportionality between g_H and $[H^+]$ over ~5 pH units (Fig. 13).

5. Proton mobility inside the gramicidin channel

If the rate-determining step in permeation is the diffusional approach of protons to the channel entrance, then permeation must be relatively rapid. To the extent that a shoulder occurs, the rate-limiting step must shift to some other process at lower pH. Akeson and Deamer (14) reported that the current ratio in H_2O/D_2O was 1.34 at 10 mM HCl, dropped to 1.20 at 1 M HCl, and returned to 1.35 at 5 M HCl, concluding that the rate-determining step at these concentrations was access, permeation through the channel, and exit, respectively. However, Chernyshev et al. (172) found that the H_2O/D_2O ratio was 1.22 at 50 mM HCl, increasing to 1.27 at 1 M HCl and to 1.36 at 5 M HCl. Furthermore, in the SS or RR covalently-linked dimers of gramicidin, the current ratios at all three [HCl] were 1.31–1.37, very near the bulk solution conductivity ratios of 1.32–1.35. They concluded that the rate-limiting step was in the channel or at the channel/solution interface at all concentrations. That the two dimers whose g_H displays very different dependence on $[H^+]$ in this range (207) have isotope effects indistinguishable from that for bulk solution suggests that the rate-determining process is similar to that for bulk diffusion.

Several investigators have attempted to calculate the apparent mobility of protons inside gramicidin (or other) channels. These empirical mobility calculations assume that the mean transit time is simply the inverse of the H^+ flux rate. The pore is assumed to be a smooth cylinder with particular dimensions, and it is assumed that there are no interactions between permeating ion and the channel, reminiscent of Pomès and Roux's "greasy pore" (818). As a general rule, ion diffusion inside channels is slower than in bulk solution, which is not too surprising in light of the several steps that must occur (dehydration, interaction with the channel walls, rehydration, etc.). In fact, it is remarkable that the mobility of ions inside channels is as high as it is! The conductance of most ion channels is within an order of magnitude of the conductance expected for unrestricted diffusion through a cylinder 3 Å in diameter and only 5 Å long (444). Part of the modest reduction of cation mobility inside channels is attributable to the relative immobilization of water in the pore. In contrast, because protons permeate by hopping from one water to the next without requiring water permeation, their mobility should be impeded less by water immobilization. Obviously, the calculated mobility of protons inside gramicidin channels will be reduced for measurements at higher $[H^+]$ than the shoulder region. The mobility of protons inside the channel was calculated to be 28% of the value in bulk solution (14), which coincidentally is identical to one estimate of the relative mobility of protons in ice (294). However, this calculation was based on measurements at 4 M HCl, well beyond the "shoulder" region, at a concentration high enough that bulk HCl conductivity is beginning to decrease significantly (206, 207, 267, 606) (+ in Fig. 13). The proton mobility calculated by Cukierman (207) was identical inside the SS gramicidin dimer and in bulk solution at pH 4, and decreased progressively at higher concentrations. Furthermore, the mobility of protons in gramicidin A at 6 M HCl was 75% of the mobility measured in bulk solution at the same concentration (208). The diffusivity of protons in gramicidin at pH 5.3 was estimated by a different approach to be similar to bulk values (725). As discussed in section IV*O*, even in concentrated HCl solutions, the mobility of protons in gramicidin is still within an order of magnitude of its value in bulk solution (207) (Fig. 13). As mentioned in section III*E*, the calculated diffusion coefficient of the proton itself inside gramicidin was 40 times that in bulk water (901), but for continuous proton flux, the slower turning step must also occur. In summary, at pH >2, proton flux through gramicidin is constrained very little by the channel.

6. Molecular dynamics simulations of proton conduction in gramicidin

A number of molecular dynamics simulations have explored the nature of water inside gramicidin or gramicidin-like channels and the phenomenon of proton conduction. In fact, there probably have been more theoretical studies of proton conduction in gramicidin than experimental ones. Several themes emerge from these studies.

Proton transfer in gramicidin was found to be semicollective, i.e., neither concerted nor incoherent (816, 870). The proton did not cross the entire channel in a concerted manner, rather it appeared to fluctuate among a subset of two to five waters within the channel (816). FT-IR spectroscopy indicates large proton polarizability in gramicidin channels, suggestive of collective proton fluctuations (72).

The water inside the gramicidin channel is less mobile than in bulk solution (173, 271, 509, 870, but cf. Ref. 856), which is generally true for water in other confined spaces or channels (see sect. III*E*). Although its mobility may be reduced, water is still highly mobile in the pore; the very idea that gramicidin is a water-filled pore was

established by elegant measurements of water flux through the channel (611).

Water molecules inside the gramicidin channel are probably oriented to some extent. Many molecular dynamics simulations indicate that the waters in a pore containing no ions are essentially entirely oriented (174, 316, 487, 640, 816, 856, 857), although some defects or breaks in the HBC may occur (173, 819, 856, 870). In contrast, Jordan (509) found that water alignment did not persist the entire length of the channel, but extended only over approximately two water molecules (509). Pomès and Roux (819) found that most channels contained a single bonding defect that was located preferentially near one end of the channel and that the remaining waters were polarized.

A proton (or other cation) will tend to orient the waters in the channel on either side of the permeating ion, although the extent to which this occurs varies among studies (316, 487, 640, 816, 819, 856, 856, 870). Calculations that include polarizability indicate that the ordering may extend only over a few water molecules (271, 272, 509, 870). If the flexibility of the channel is increased, the ordering of waters is reduced (271). In this regard, if the waters do not interact with the channel that confines them (a greasy channel), the water wire is uninterrupted (818), whereas when the waters can interact with the walls of the pore, interruptions (i.e., hydrogen bonding defects) often occur (816).

Because proton hopping through gramicidin is extremely rapid, the reorientation of water molecules (the turning step of the hop-turn mechanism) was almost universally believed to be slower, and at low pH, the rate-determining process (810, 814, 816, 818) (see sect. III*D*). At pH >2, proton entry is rate determining, because it occurs infrequently. A recent study of gramicidins A, B, and M (374) and modeling of proton conduction in gramicidin (901) resulted in the surprising proposal that the rate-determining step for gramicidin A at pH <1.5 is not water reorientation, but instead is proton exit from the channel. The modeling also suggested that for gramicidin M, proton entry is rate determining at most pH values, with proton exit and water reorientation becoming rate determining only at pH <0. It will be interesting to see if more direct experiments will support these deductions.

Pomès (814) has emphasized the importance of the water coordination number for proton conduction. In bulk water, the waters ideally are four-coordinated (84, 814). Proton conduction in water is thought to reflect fluctuation between Eigen and Zundel cationic forms (see sect. II*B*), in both of which water is three-coordinated. Gramicidin provides a better medium for rapid proton conduction than a hydrophobic cylinder, because its waters are three-coordinated, with hydrogen bonds with both neighbors and a third with the channel wall (814).

B. "Normal" Ion Channels

Cation-selective ion channels comprise narrow water-filled pores that exclude anions and accomplish cation selectivity by various techniques, including steric or electrostatic constraints, and ion-dependent compensation for removal of the waters of hydration around ions (89, 444, 761). The presence of a row of water molecules in a cation channel provides presumptive evidence that proton conduction by a water-wire mechanism is possible. Admittedly, by use of clever design, aquaporin channels manage to exclude protons, but at the same time, they also exclude other cations (see sect. IV*D*). To detect proton current through normal cation channels, it is usually necessary to remove other permeant ions and lower the pH to maximize the H^+ current. If H^+ and Na^+, for example, were equally likely to enter and permeate Na^+ channels, then at physiological concentrations, 3.5×10^6 Na^+ would permeate for every H^+. In other words, 1 pA of Na^+ current would be "contaminated" by only 1.8 protons. Even if normal ion channels, by virtue of their containing a water wire apparently begging for protons to hop through, conducted protons 100 times better than other cations, the total H^+ flux in physiological solutions would be negligible.

Voltage-gated Na^+ channels conduct protons at low pH in the absence of Na^+ (60, 79, 219, 714, 715). The relative permeability (P_H/P_{Na}) calculated with the GHK voltage equation (368, 444, 456) is 252–274 (714, 715), reminiscent of the high P_H/P_{Na} of gramicidin channels (see sect. IV*A*). Amiloride-sensitive Na^+ channels conduct protons, and this proton current is inhibited by amiloride (363, 364, 637, 638). Evidence has been presented that protons can permeate the Na^+/H^+ antiporter in gastrointestinal apical membrane vesicles from rabbits (1078). It should be emphasized that because of the low concentration of H^+ even at pH 4 (1,000 times smaller than $[Na^+]$), there still was no detectable shift of V_{rev} of Na^+ or K^+ channels in nerve studied at pH 4 (440, 1082). Thus proton permeability of normal ion channels is unlikely to play an important role under physiological conditions.

No reports of H^+ current through K^+ channels exist. Although it may be that no serious attempt at such a measurement has been made, K^+ channels may just conduct H^+ poorly. K^+ channels appear normally to be occupied by several permeant ions (268, 445, 457, 496, 752), and complete removal of K^+ seems to abolish channel function (19). In this context, H^+ might be able to permeate only by sneaking through the channel in between K^+.

Colicin and other bacterial channels have wide pores that conduct ions as large as tetraethylammonium$^+$, yet surprisingly, they have anomalously high proton permeability (537). Based on reversal potential measurements, $P_H/P_K > 1{,}000$ under some conditions. This high P_H was not influenced by DEPC diethylpyrocarbonate (DEPC, a

histidine modifying reagent), amantadine, or changes in buffer concentration. The mechanism responsible for this phenomenon remains obscure.

C. Synthetic Proton Channels

Artificial ion channels have been synthesized with simple, defined amino acid sequences. A 21-amino acid peptide containing no formal charges, $(LSLLLSL)_3$, forms proton-selective channels (599). A similar peptide, $(LSSLLSL)_3$, forms cation-selective channels that conduct protons approximately four times faster than any other cation (599). Energy minimization models of these channels suggest that $(LSLLLSL)_3$ assembles into trimers or tetramers that contain only a few waters, whereas $(LSSLLSL)_3$ assembles into hexamers or larger aggregates that contain a continuous row of waters (13c, 599). Molecular dynamics simulations indicate that the waters in $(LSLLLSL)_3$ are immobile, whereas those in $(LSSLLSL)_3$ are mobile, although less so than in bulk solution (834). Another synthetic proton-selective channel, $(LSLBLSL)_3$, was constructed including Aib, a conformationally constrained amino acid, to confirm that these channels are helical in their functional conformation. The tetrameric nature was established by attaching four helices together with a tetraphenylporphyrin template (13b). These synthetic channels reinforce ideas derived from gramicidin studies, that protons permeate a HBC or water wire without requiring translational movement of the water molecules, and that any cation-selective water-filled ion channel is likely to conduct H^+ more rapidly than any other cation.

Long-chain polyamino acids (polyleucine, polyalanine) incorporated into lipid bilayers increased the proton permeability severalfold but did not form discrete channel-like openings (777). This behavior may reflect induction of a transient leak (between peptide and lipid) rather than the formation of channels.

A novel type of proton channel is formed by mutagenesis of *Shaker* voltage-gated potassium channels. Insertion of a His residue at position 371 (R371H) results in proton channel behavior (960). This channel is gated because His^{371} is part of the channel's voltage sensor, and it happens that when the channel opens, His^{371} becomes simultaneously accessible to solutions on both sides of the membrane. Other mutations in which a His is able to access only one side of the membrane at a time result in proton carrier function (see sect. III*C*).

D. Aquaporins (Water Channels)

Although water permeates cell membranes fairly readily, some cells have specialized channels called aquaporins that conduct water rapidly, 3.9×10^9 H_2O/s (13). Permeation of water through aquaporin requires breaking hydrogen bonds, and the activation energy for water permeation, 3.1 kcal/mol (1096), is near that of hydrogen bond strength in water, 2.6 kcal/mol (1056). Because of the facility with which protons are conducted both in bulk water and in water-filled ion channels like gramicidin, one might expect that aquaporins would conduct protons as well (367, 413). However, no proton permeability is observed (1096). How does this water-filled pore exclude protons? The atomic structure of aquaporin-1 has been determined and the relevant structures identified (718). The channel lining is generally hydrophobic, but at a central constriction the amido groups of two Asn residues project toward the center of the pore. These positively charged groups form hydrogen bonds with one or two water molecules in the pore. During permeation, each water molecule is briefly hydrogen-bonded to both amido groups. The water is then conformationally constrained and prevented from forming the hydrogen bonds with adjacent waters that are necessary for Grotthuss-type proton conduction (718). In addition, the net positive charge in this region would tend to exclude all cations, including protons (12). The nonpolar walls of the pore also disfavor permeation of any ions including H^+ (839). More recent molecular dynamics simulations of the *Escherichia coli* water channel, GlpF, reveal the same crucial two Asn residues at the central constriction but provide a different mechanism (989). The central H_2O molecule forms hydrogen bonds simultaneously with waters on either side, acting exclusively as a hydrogen bond donor. The waters in both half-channels are thus oriented oppositely, with their hydrogens pointing toward the channel mouths.

E. M_2 Viral Proton Channel

A membrane protein of the influenza A virus, M_2 plays a critical role in the infection process. The M_2 channel is believed to allow proton influx into the virion, which enables viral uncoating, i.e., the unpacking of the viral ribonucleoproteins that is necessary for them to enter the host cell's nucleus (661). A second proposed function is to dissipate the low pH of the *trans*-Golgi network, thereby preserving the hemagglutinin molecules from acid inactivation and preventing them from entering the noninfective acidic conformation prematurely (422). Inhibition of M_2 channels with amantadine or rimantadine inhibits viral replication (220, 416). Mutations of the M_2 channel that prevent its proton channel function resulted in an influenza A virus that could replicate through multiple cycles in cell culture, but not in mice (1065). However, viral replication in the M_2 mutant that lacked channel activity was considerably slower (1065), comparable to that of wild-type M_2 after inhibition by amantadine, and the mutant viruses could not compete with wild-type

viruses in cell culture (992). Thus, although M_2 channel function is not absolutely essential for viral survival in cell culture, it promotes efficient viral replication in an infected organism.

The M_2 protein expressed in *Xenopus* oocytes (812), mammalian CV-1 cells (1058), or lipid bilayers (1016) functions as an ion channel when it is activated by acidic pH. Because the M_2 channel is not voltage gated, it can be studied only by inhibiting the currents with amantadine and subtracting to obtain the amantadine-sensitive current. This technical complication made it difficult to establish precisely the selectivity of the M_2 channel. Early studies reported distinct permeability to Na^+ and a variety of cations (812, 923, 1016, 1058). Proton permeability of a 25-amino acid peptide comprising the membrane-spanning region of M_2 was demonstrated at pH 2.3 after its incorporation into bilayers (273). Indirect evidence for proton permeability of intact M_2 channels was provided by measurements of pH changes in lipid vesicles (898) and in *Xenopus* oocytes (923). Finally, direct measurements of H^+ currents through M_2 channels expressed in murine erythroleukemia cells were reported, in which the reversal potentials for the rimantadine-sensitive current indicated nearly perfect proton selectivity (175). It has been demonstrated that much of the deviation of V_{rev} from E_H in *Xenopus* oocytes was the result of local pH changes resulting from proton flux through M_2 channels and that under physiological conditions M_2 is indeed highly H^+ selective (711). Measurement of ion fluxes into vesicles supports the idea that M_2 channels are essentially perfectly proton selective (617).

The M_2 channel is a homotetramer formed by 96-amino acid monomers that span the membrane once. The M_2 mRNA codes for a 97-amino acid polypeptide, but the initiation Met is cleaved in the mature protein (1013). In its membrane-spanning region there are mainly hydrophobic residues, with the exception of Ser^{31} and His^{37}. Amantadine sterically occludes the channel near the center of the transmembrane domain, between Val^{27} and Ser^{31} (274), or perhaps by binding to His^{37} (873). Substantial evidence supports an important role for His^{37} in the activation of M_2 channels by low pH. Deletion of His^{37} or mutation to Ala, Gly, or Glu abolishes activation by low pH (812, 1059). Two types of roles for His^{37} have been proposed: *1*) as a proton shuttle and selectivity filter or *2*) as a gating regulator, the protonation of which results in a conformational change (i.e., channel opening). Pinto et al. (811) proposed a structure for M_2 in which there is a channel large enough to contain a continuous water wire with a single occlusion at the point where the four His^{37} protrude into the lumen of the pore (Fig. 6, yellow). This proposal was supported by cysteine scanning mutagenesis that showed extracellular accessibility of Ala^{30} and Gly^{34}, and intracellular accessibility of Trp^{41} (925). The occlusion formed by His^{37} could prevent cation conduction and would produce H^+ selectivity by allowing H^+ conduction by successive protonation of a His imidazole nitrogen, deprotonation of another nitrogen, and then a ring flip (tautomerization) to complete the cycle (811). A virtually identical His tautomerization mechanism had been proposed to occur at the His^{64} at the entrance to the proton channel in carbonic anhydrase II (735, 932). In this model, His^{37} actively and obligatorily participates in H^+ conduction. This shuttle model was supported by molecular dynamics simulations in which only singly or doubly protonated channels were stable (906).

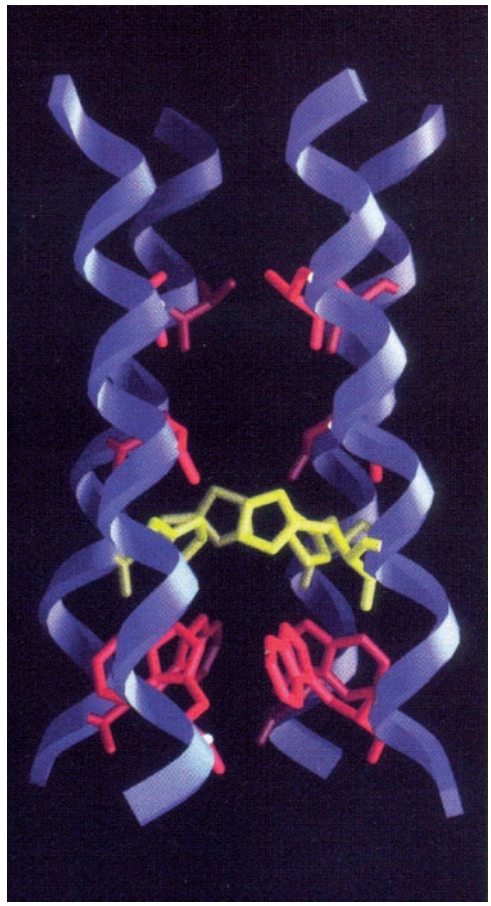

FIG. 6. Side view of the proposed transmembrane section of the M_2 viral proton channel. Every fourth amino acid residue (in colors) is expected to face the pore. Starting at the extracellular end (*top*), the residues identified by cysteine-scanning mutagenesis to be accessible to the external solution are Ala^{30} and Gly^{34}. The crucial His^{37} (yellow) is believed to occlude the pore to cations other than protons. The internally accessible Trp^{41} (red) may play a role in gating the channel (774). [From Shuck et al. (925), copyright 2000 American Society for Microbiology.]

The gating model retains the concept of His^{37} as a regulator of channel activity (878). Molecular dynamics simulations (878) as well as site-directed dichroism studies (573) indicate that when all four His^{37} in the M_2 channel are deprotonated they protrude into the pore, occluding it. When these residues are fully protonated, they retract due at least in part to electrostatic repulsion,

which permits a continuous water wire to span the entire pore (878). This mechanism might require only two of the four His to be protonated at low pH to activate the channel (312). In support of the shuttle mechanism, the conductance of M_2 was reduced by 40–50% in deuterium, suggesting that H^+ does not permeate as H_3O^+ (712), because the isotope effect for proton/deuteron conduction in bulk water is weaker than this (see sect. v*I*) (65, 325, 612, 624, 844). However, this conclusion is compromised by the possibility that water inside the M_2 channel may be to some extent effectively "frozen" (i.e., less mobile) as has been suggested (317) (see also sect. iii*E*). In this event, a larger isotope effect might be predicted by analogy with the larger deuterium isotope effect reported for conduction in ice (289, 575). In support of the "gating" model, Raman spectroscopy indicates that His^{37} is indeed protonated when the channel is activated at low pH, and furthermore that it appears to interact with the indole ring of Trp^{41} (774). On this basis, a model similar to that of Sansom et al. (878) was proposed, in which low pH activation occurs when protonation of the four His^{37} residues results in their retraction (774). A novel feature is that the protonated His^{37} imidazolium in its retracted position is closer to Trp^{41}, and this conformation is stabilized by interaction of the cationic imidazolium with π electrons of the indole ring of Trp^{41} (774). The importance of Trp^{41} in M_2 gating was demonstrated by alteration of the pH dependence of gating in W41A, W41C, W41F, and W41Y mutations (995).

The world record for the smallest unitary conductance of any ion channel was claimed recently for the viral M_2 proton channel (617). At room temperature and pH 7.4, the single-channel current was estimated to be 1.2 aA (2.7–4.1 aA at pH 5.7; △, Fig. 13), corresponding with a conductance of 8–44 aS (aS = attoSiemens = 10^{-18} Siemens). By calculating the net H^+ flux, we find that one M_2 channel transports 12 yM (1 yoctomole = 10^{-24} mol; Ref. 1001) of protons per second at pH 7.4, or 7.5 H^+/s. It should be noted that this conductance estimate was indirect and assumes that every M_2 molecule is functional, and therefore represents a lower limit. Whether this miniscule unitary current is truly a record may depend on comparison with a mammalian serotonin receptor, which can act as a proton channel at low pH (145, 146). The flux through a single transporter is 300 H^+/s at pH 3.5, but only 20 H^+/s at pH 5.5 (146) (▼, Fig. 13), thus when extrapolated to physiological pH the proton flux is even smaller than through M_2. Estimates of the M_2 unitary current based on other considerations are much larger, 0.5 fA at pH 6.2 to an upper limit of 10 fA (712). These latter values fall precisely in the range of estimates for voltage-gated proton channels (85, 136, 168, 236, 244).

An intriguing structural parallel with voltage-gated proton channels is provided by evidence that M_2 channels bind a heavy metal, Cu^{2+}, and that this binding occurs at His^{37} (340). Because His^{37} is believed to regulate M_2 channel function depending on its degree of protonation, this is very similar to the suggestion that Zn^{2+} binds to voltage-gated proton channels at an externally accessible site formed by His residues (163), the protonation of which regulates the gating of these channels (166).

F. F_o, CF_o, or V_o Proton Channels of H^+-ATPases

ATP is generated in plant and animal cells by H^+-ATPases that utilize energy stored in the form of a proton gradient (694, 698). Some of these enzymes can reverse direction and function as proton pumps. H^+-ATPases are divided into F (chloroplast, mitochondria, bacteria), V (vacuolar, in organelles), and P (plants, fungi, bacteria) types, with F and V sharing similar sequences and mechanisms (596). The intricacy and complexity of the operation of this enzyme is astonishing. The F_oF_1 ATP synthase consists of two main parts: a subunit that is embedded in the membrane and contains proton channels, F_o, and the ATP binding subunit, F_1, which is attached via a narrow stalk (Fig. 7).[3] Recent studies in which large fluorescent molecules have been attached to the γ-subunit at the interface between the F_o and F_1 components have demonstrated in spectacular fashion that the oligomeric ring of F_o proton channel molecules spins around during ATP hydrolysis (760, 1089), confirming earlier proposals (4, 113, 275, 384, 697, 866). The whole complex is anchored in the membrane by subunit *b*, which acts as a stator. Rotation of subunit *c* relative to subunit *b* has been confirmed biochemically (503) and is required for proton translocation (978). This rotary engine motif is shared by the Na^+-driven ATP synthase of *Propionigenium modestum* (265, 513) and the flagellar motor (86, 513, 681). The key amino acid in the F_o proton channel is Asp^{61} (or Glu^{65} in Na^+-driven F-ATPases, Ref. 264), one of which is present in each of the 9–14 *c* subunits (20, 495, 958). When the carboxyl group of Asp^{61} is protonated it rotates, and rotation in the correct direction is enforced by electrostatic interactions with Arg^{210} on the stator, which lower the pK_a of Asp^{61} if it rotates incorrectly, with the result that the group becomes deprotonated. The proton gradient across the membrane thus ensures correct rotation by a probabilistic process (293). ATP synthesis is accomplished when protons at the side with high local [H^+] bind to a low pK_a site (Asp^{61}), are translocated, and then released to the side with low [H^+]. Release occurs simultaneously with a conformational change that promotes ATP synthesis and also increases the proton affinity of the

[3] Counterintuitively, despite the apparent logical parallel with F_1, the correct subscript is not zero, but lowercase "oh," reflecting the origin of the name from oligomycin sensitivity. The error is propagated by several prominent biochemistry journals, whose editors refuse to allow the correct spelling.

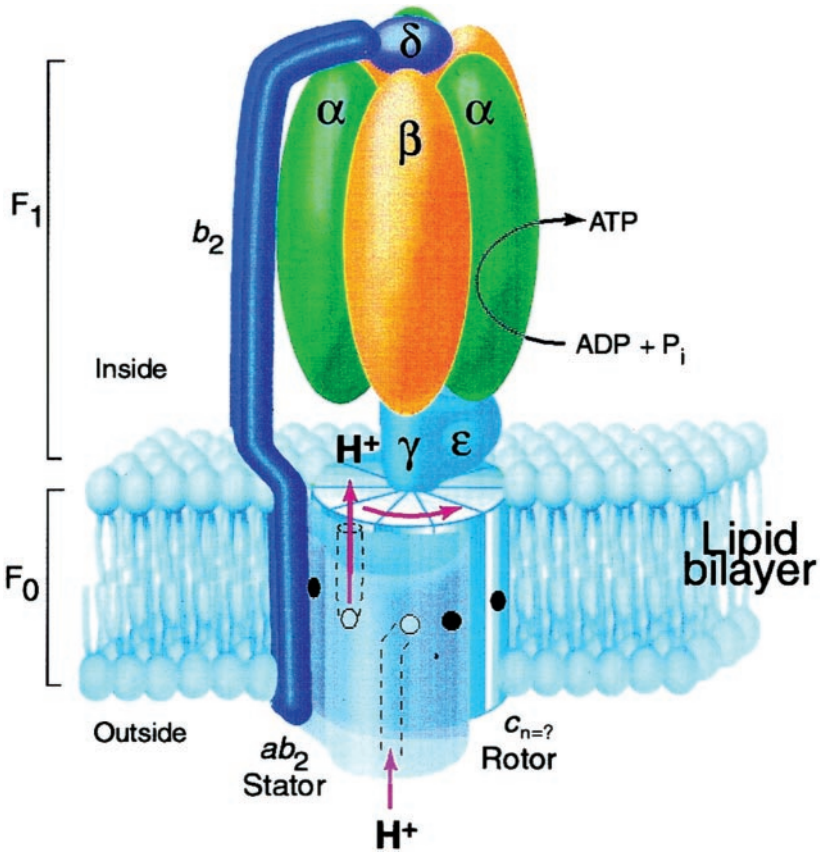

FIG. 7. The components of ATP synthase, a rotary motor. Protons enter the 10 proton channels in the membrane-bound F_o component, where they bind to Asp^{61}, and are subsequently released to the opposite side of the membrane via an outlet channel after F_o rotation (arrow). The $\gamma\epsilon$-subunits are attached to the F_o ring and also rotate relative to the F_1 component, which catalyzes ATP synthesis (or breakdown if the reaction is driven backwards), which is thus driven by the proton-motive force. [From Jiang et al. (495), copyright 2001 National Academy of Sciences, USA.]

site (307). When the H^+-ATPase reverses direction to act as a pump, Asp^{61} changes from high to low pK_a conformation as protons are pumped uphill (307). It appears that V-ATPases function generally like F-ATPases, but with certain differences (375). The V_o rotor has 6 protonation sites compared with 9–14 for the F_o rotor, and V-ATPases can pump against a larger ΔpH but at a lower maximum rate than F-ATPases (375). Only F-ATPases are reversible under in vivo conditions; V-ATPases function exclusively as H^+ pumps (596).

Recent cysteine scanning studies have shown that *N*-ethylmaleimide can access several residues well inside the F_o proton channel and that even more of them are accessible to Ag^+, which is close to H_3O^+ in size (306). These data suggest that the proton pathway through the access channel to Asp^{61} is a water wire. They further indicate that this part of the proton channel is not strictly H^+ selective (Table 1).

Dicyclohexylcarbodiimide (DCCD), a classical inhibitor of H^+-ATPase, inhibits by binding to Asp^{61} in the F_o component at alkaline pH, blocking proton conduction through F_o (148, 308, 392, 449, 464, 512, 1092). At low pH, DCCD also binds covalently to Glu^{199} in the F_1 sector (299, 359, 1091). Despite this evidence of promiscuity, DCCD does not inhibit voltage-gated proton channels (Table 6). V-type H^+-ATPases are inhibited by DCCD, but in addition are inhibited potently by bafilomycin A_1 (110, 269), which binds to the *c* subunit and blocks proton flux (193, 667).

Torque generation by the Na^+-driven ATP synthase of *Propionigenium modestum* requires an electrical potential of $\pm$90 mV, which cannot be substituted by a Na^+ gradient (515). This voltage-dependent switch from idling mode to torque generation may conceptually resemble the voltage-gating mechanism of voltage-gated proton channels. However, a required voltage-sensitive step in the reaction cycle could also account for these data.

Many attempts have been made to demonstrate proton conduction through F_o after removing the F_1 component. Although some data to the contrary have been presented (129, 702, 1098), most studies conclude that F_o in isolation from F_1 (or V_o in the case of vacuolar proton pumps, or CF_o in the case of chloroplast proton pumps) can act as a passive proton conductor (21, 143, 150, 192, 193, 323, 615, 749, 891, 892, 928, 1097). One group found that native V_o did not conduct protons (1098), but that reconstituted V_o did (1097). Another found that F_o by itself conducted protons at a rate too low for kinetic competence during ATP synthesis, but that coexpression with F_1 increased H^+ flux (795). Yoshida et al. (1092) found that F_o proton conduction was prevented by binding of the γ-subunit and suggested that this might com-

prise a gate (1092). Schindler and Nelson (887) reported that proteolipid derived from mitochondrial H^+-ATPase incorporated into lipid bilayers formed H^+-selective channels detectable at pH 2.2 (887). More recent attempts to record H^+ currents electrically through CF_o (1053) have been complicated by evidence that either contaminating protein or the F_o component itself is capable of functioning as a nonselective cation-permeable channel (16, 143) that in some cases is inhibited by the standard F_o inhibitors venturicidin and DCCD (669, 893). Indirect measurements of the unitary conductance of CF_o at first provided estimates of 10 fS (892). Shortly thereafter, it was concluded that because only a small fraction of the CF_o was active, the actual conductance was much higher, 169 fS (616) or even 1 pS (21, 615). Surprisingly, the conductance is independent of pH between pH 5.6 and 8.0 (21, 512), suggesting that proton conduction through the channel, rather than the proton supply, is rate determining. The pH independence of the conductance at high pH appears to contradict the proportionality between $[H^+]$ and conductance at lower pH reported by Schindler and Nelson (887). The very large estimated unitary H^+ conductance is indeed enigmatic (21, 512) and far exceeds the conductance of any other proton-conducting channel in this pH range with the exception of carbonic anhydrase II (see sect. IV*K*) (Fig. 13). An array of mechanisms that might increase the supply of protons to a channel with such prodigious H^+ conductance in the face of such tiny H^+ concentrations is discussed in section IV*O*. A recent estimate of the conductance of F_o reconstituted into liposomes is much lower, 0.1–0.2 fS, which amounts to a unitary flux of ~70 H^+/s (143). In several respects, CF_o behavior strongly resembles that of voltage-gated proton channels (Table 1): the channel is extremely selective for H^+ ($P_H/P_K > 10^7$), the H^+ current is 1.7-fold greater than D^+ current, and the Q_{10} for the conductance is 1.9 (21, 512).

G. Flagellar Motor, MotA, MotB

Bacteria swim by means of rapidly rotating flagella. Flagellar rotation is driven by a motor that is powered by the proton gradient, or protonmotive force (or in some cases by a Na^+ gradient). The membrane-bound part of the flagellar motor (the stator, which anchors the whole complex to the cell wall) consists of two molecular components, MotA and MotB. Proton conduction does not occur when MotA is expressed alone, in the absence of the rest of the flagellar motor components (970). H^+ flux through a proton channel formed by MotA and MotB drives the rotation of the flagellum (97, 98, 344, 970). Because too few of the amino acids that form the proton channel have protonatable side chains to form a HBC that would span the membrane, it has been proposed that water molecules comprise most of the proton pathway (98, 920). Correct operation of this system requires an aspartyl residue in MotB (Asp^{32}) that is believed to comprise a proton binding site; surprisingly, no other individual conserved acidic residue was required for torque generation (1100). When Asp^{32} was replaced with 15 other amino acids, only D32E mutants (conservative replacement of Asp by Glu) exhibited any function (1100).

There are striking similarities between the flagellar motor proton channel (in situ in low-torque mode) and voltage-gated proton channels. Both have strong temperature dependence, large deuterium isotope effects, and weak dependence on pH (159, 160, 682). The flagellar motor speed is directly proportional to applied voltage (proton-motive force), demonstrating tight coupling between proton flux and motor rotation (328).

H. Bacteriorhodopsin

Bacteriorhodopsin is a light-driven proton pump in the purple membrane of *Halobacterium halobium* that creates a proton gradient used for the manufacture of ATP (101, 596). Like F_oF_1-ATPases (695, 698), bacteriorhodopsin contains a "proton channel" that is essential to its function (556, 969). This "channel" probably at no time forms a continuous pathway across the membrane (1009); rather, the proton moves through two partial channels separated by a Schiff base (Fig. 8). The proton pathway in bacteriorhodopsin is one of the first explicitly proposed to comprise HBC elements (969). The entire photocycle can be dissected into at least eight intermediate states. Energy is introduced by absorption of a photon, and as the cycle proceeds, the result is the translocation of one proton from the cytoplasm to the extracellular solution. Proton movement occurs in three main steps (588) that are "backwards" in a sense. First, light-induced isomerization of retinal in the Schiff base alters the local geometry, which results in transfer of a proton from the Schiff base to Asp^{85}, causing the exit of a proton through the extracellular-facing "release" channel (587, 589). Next, the Schiff base is reprotonated from the intracellular-facing (cytoplasmic) channel, receiving the proton from Asp^{96}. A proton then enters the cytoplasmic "uptake" channel to reprotonate Asp^{96}. Finally, the released proton is replaced as Asp^{85} deprotonates. A minimal model requires five separate proton transfer events (436). The "reprotonation switch" serves to ensure directionality to proton transport through bacteriorhodopsin by preventing reprotonation from the exit side (586).

The proton pathway (Table 2) includes several water molecules in addition to titratable amino acid residues. The X-ray structure of bacteriorhodopsin crystals indicates eight or nine water molecules in the putative proton pathway (633, 801). The cytoplasmic pathway is hydrophobic but must acquire enough waters during the pho-

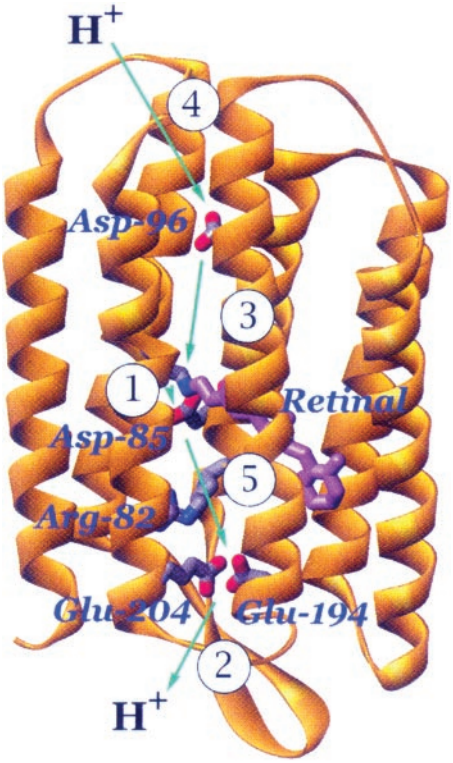

FIG. 8. Proposed proton pathways through bacteriorhodopsin. The proton moves from the cytoplasmic side at the top to the extracellular side at the bottom. The numbered steps indicate the chronology: *1*) a proton is transferred from the Schiff base to Asp^{85}, *2*) the proton is released to the extracellular solution, *3*) a proton is transferred from Asp^{96} to the Schiff base, *4*) Asp^{96} is reprotonated from the cytoplasmic solution, and *5*) transfer of a proton from Asp^{85} to a release site, perhaps comprising waters held in position by the two Glu residues near the extracellular surface. [From Luecke et al. (632), copyright 1999 American Association for the Advancement of Science.]

tocycle (2–4) to bridge the 10- to 12-Å gap between Asp^{96} and the Schiff base (436, 633, 858, 1074). The isotope effect on proton transfer through this channel is weak, 1.3–1.7 (601), similar to that for ordinary hydrogen bond cleavage in water, 1.4 (1056), and for H^+ conductivity in water, 1.4–1.5 (65, 325, 612, 624, 844). This suggests that proton movement through this channel is similar to that in bulk water (601, 1074), in which the rate-determining step is hydrogen bond cleavage (8). The extracellular pathway contains seven bound waters in an extensive three-dimensional hydrogen-bonded network with amino acid residues and the retinal Schiff base (633). The very large isotope effect on proton release (Table 1) may reflect a conformational change in the protein (601). An alternative interpretation that is supported by a highly curved proton inventory plot (127) is that it reflects multiple proton transfers or extensive hydrogen bond rearrangement within the exit channel. The proton release pathway may include several titratable amino acid residues (Table 2).

Any step in the photocycle that involves net charge moving across the membrane potential field should be influenced by membrane potential. The rate of proton pumping by bacteriorhodopsin has been shown to depend linearly on membrane potential (347, 650, 717, 727, 728). However, this does not mean that bacteriorhodopsin is obligatorily voltage gated. The influence of membrane potential on charge movement across the membrane is an unavoidable electrostatic property that is distinct from voltage-dependent gating. Nevertheless, to achieve proton pumping, proton translocation must be vectorial (unidirectional). A conformational change resulting from deprotonation of the Schiff base toward the extracellular side of the membrane, which may switch the accessibility of the active site of bacteriorhodopsin to the cytoplasmic side of the membrane, has been proposed on the basis of electron crystallography (971). The configuration of the retinal, from X-ray crystallography of an early M state (590), indicated a more local change for the switch, which reorients the direction of the N-H bond from the extracellular to the cytoplasmic direction after deprotonation of the Schiff base. The reprotonation switch mechanism closely resembles the proposed mechanism of gating of voltage-gated proton channels (Fig. 20), except that the result of the latter is believed to be an uninterrupted H^+ conduction path across the membrane.

I. Bacterial Reaction Center

In photosynthetic bacteria (e.g., *Rhodobacter sphaeroides*), light induces a series of electron transfer events in the photosynthetic reaction center protein that are coupled to proton transport across the membrane. The catalysis involves the light-driven reduction of quinone to quinol, which involves the uptake of two protons by the reaction center protein ($Q + 2e^- + 2h\nu + 2H^+ \rightarrow QH_2$). Normally electron transfer is rate limiting; proton transfer can be made to be rate limiting by Zn^{2+} or Cd^{2+} binding (789, 790) or by mutations that greatly slow proton transfer (788). One of several proposed proton pathways is illustrated in Figure 9 (43, 775, 788, 790). Two parallel pathways are illustrated which have the following elements

$$BH \rightarrow His^{H126/H128} \rightarrow H_2O \rightarrow Asp^{L210/M17} \rightarrow H_2O \rightarrow Asp^{L213} \rightarrow Ser^{L223} \rightarrow Q_B$$

$$BH \rightarrow His^{H126/128} \rightarrow H_2O \rightarrow Asp^{L210/M17} \rightarrow H_2O \rightarrow Asp^{L213} \rightarrow H_2O \rightarrow Glu^{L212} \rightarrow Q_B$$

where BH is protonated buffer and the amino acid residues are labeled as described in Figure 9. The inner end of both pathways may be accessible to the external solution, because mutations of Glu^{L212} and Asp^{L213} inhibit proton transfer, and function is restored by "chemical rescue"

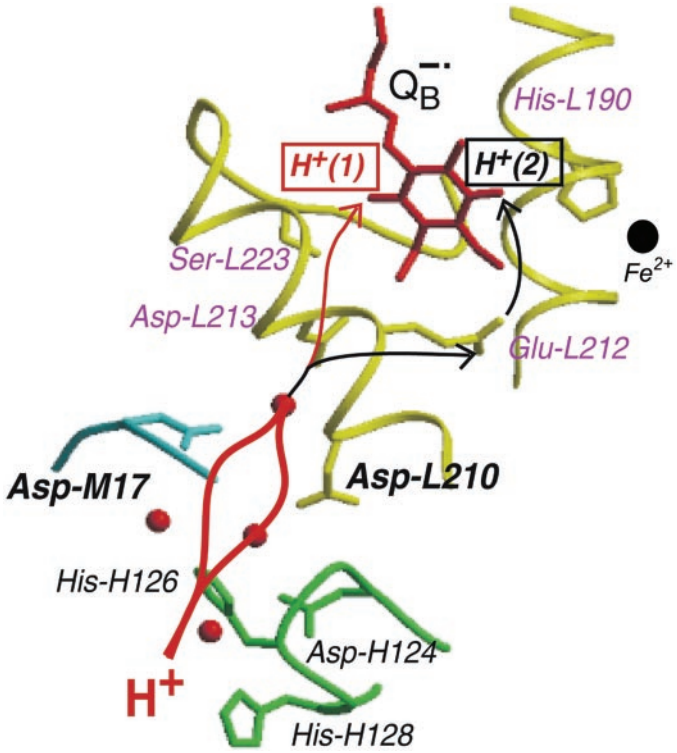

FIG. 9. Proposed proton pathways in the bacterial reaction center. The reaction center consists of three polypeptides (L, M, and H subunits) and nine cofactors. Catalysis involves the light-driven reduction of quinone to quinol, which involves the uptake of two protons by the reaction center ($Q + 2e^- + 2h\nu + 2H^+ \rightarrow QH_2$). Proton entry occurs from a buffer molecule in solution (BH) to a His, either His-H126 and/or His-H128; the subunit and position of the residue is indicated (e.g., His-H128 means His at position 128 of the H subunit). The evidence for the involvement of these His residues is relatively recent (47). Proton transfer proceeds via bridging water molecules (red spheres) to an Asp at either L210 or M17, shown in bold (789). These two Asp provide parallel branches, because the presence of either one is sufficient for function. They also act cooperatively in that the rate of proton transfer is much greater (>10-fold) with both present than with just one present. Proton transfer then proceeds via another water molecule to Asp-L213, which provides a branch point. Here the pathways for the two protons involved in the formation of QH_2 diverge, with one proton proceeding to a carbonyl oxygen of the quinone via Ser-L223 [$H^+(1)$] and the other proceeding to Glu-L212 via at least two water molecules, and then onto the other carbonyl oxygen of the quinone [$H^+(2)$]. Direct transfer from Glu-L212 to Q_B is not likely, because they are separated by ~5 Å. Thus the transfer from Glu-L212 to the quinone may involve Q_B movement or a bridging water molecule that is not seen in the structure. [From Paddock et al. (788), copyright 2001 American Chemical Society.]

with several small weak acids (990). For this reason, the bacterial reaction center (BRC) proton channel is listed as having low proton selectivity in Table 1. Part of the evidence that protons enter via this channel is based on the inhibition of proton uptake by divalent metal ions. Zn^{2+} and Cd^{2+} inhibition occurs when the metal ion is coordinated at the surface of the BRC by two His and one Asp (Asp^{124}) (43). The similarity of this proposed binding site to the external metal receptor (three His residues) proposed for the voltage-gated proton channel (163) is noteworthy. There is strong competition between metal cations and protons in both molecules. As a result of this competition, the apparent metal affinity of the metal binding sites on both BRC and voltage-gated proton channels decreases upon protonation (163, 355, 869). The pH effect observed for the BRC is evidently weaker: lowering pH from 8 to 5 reduced the affinity of Ni^{2+} for BRC by a factor 10^2, and for Cd^{2+} by a smaller amount (355), whereas over the same pH range the apparent affinity of Zn^{2+} for the voltage-gated proton channel decreased by 10^3–10^5 (163). For voltage-gated proton channels, the strong competition between H^+ and Zn^{2+} required assuming that the Zn^{2+} receptor comprises two or three protonation sites (163). The BRC exhibits simple 1:1 competition (869) in spite of the presence of several protonatable groups near the putative metal receptor.

As for voltage-gated proton channels, proton uptake by the BRC appears not to be limited by diffusion of protons or protonated buffer, because it is weakly dependent on pH, has high temperature sensitivity, weak dependence on viscosity, and a large deuterium isotope effect (657). Maróti and Wraight (657) proposed that a conformational change or hydrogen bond rearrangement was required to enable proton transfer into the reaction center.

The proposed role of the two superficial His (His^{126} and His^{128}) as proton donors was confirmed by mutating them to Ala. Surprisingly, replacing either one alone had no effect, but in the double mutant, the two proton-limited rate constants were reduced eight- and fourfold (10). The actual slowing of proton transfer is greater than this but cannot be determined directly because the rate constants include both proton transfer and the coupled electron transfer. In the native BRC electron transfer is rate limiting. This also means that the single mutants might have reduced proton transfer but that any such reduction is not evident because electron transfer is still rate determining. Function was completely restored by chemical rescue with 50 mM imidazole, which has no effect on the native BRC (10). The fact that single mutants retained full function indicates that the two His are redundant; only one is necessary for normal enzyme function. Proton uptake can be restored in the double mutant by chemical rescue with acids with a wide range of pK_a, to generate a Brönsted plot, which revealed that the rate constant for proton transfer across this 20-Å pathway is 10^5 s^{-1} (787). The presence of protonatable groups at the entrance to the channel speeds proton transport by at least two orders of magnitude (787).

J. Cytochrome *c* Oxidase

Cytochrome *c* oxidase is the final enzyme in the respiratory chain in the inner mitochondrial membrane, responsible for pumping protons across the membrane

from the matrix into the intermembrane space, thus creating the proton gradient used to generate ATP (51, 52, 350, 352, 1072, 1075). Widely studied homologous heme-copper oxidases are found in the cell membranes of aerobic bacteria, such as *Escherichia coli*, *Paracoccus denitrificans*, and *Rhodobacter sphaeroides*. In each catalytic cycle, four protons are pumped across the membrane, and four additional protons combine with four electrons and O_2 to form water as a by-product. In some models, the translocated ("pumped" or "vectorial") protons and the substrate ("consumed," "scalar," or "chemical") protons were proposed to travel through different proton channels (483), D and K, respectively (see below). Proton and electron movements are tightly coupled, although the details remain controversial (517, 685, 686, 708, 842, 1041, 1075, 1076). Based on the crystal structure, three proton pathways were proposed, each comprising a number of amino acid side groups and several water molecules in an extensively hydrogen-bonded arrangement (483, 1018, 1093). Of three proposed proton channels, H, D, and K, the latter two have been shown by mutagenesis to be functionally important (305, 341, 352, 602, 689, 1004, 1040, 1074). The D and K channels are named for crucial Asp and Lys residues (D^{132} and K^{362} in Figs. 10 and 11, respectively) that upon mutation prevent proton conduction (558). These two channels appear to function during distinct parts of the catalytic cycle (352, 558, 689, 862, 1051, 1077). In addition, there is another, more recently investigated proton channel, the "exit" channel, that allows pumped protons to reach the external medium (689, 828). Intriguingly, after block of the D channel, but not the K channel, the oxidase still can transfer electrons slowly, but cannot pump protons (305, 691, 1004). To support this activity, protons may be taken up through the exit channel, resulting in a futile cycle (689).

Figure 10 shows one of the proton uptake pathways, the D channel. As was the case in the bacterial photosynthetic reaction center (see sect. IV*I*), the proton pathway comprises a combination of amino acid side groups and water molecules (red dots). Calculations based on the known structure of cytochrome *c* oxidase predict that ~130 water molecules reside within subunits I and II of the enzyme (458). The proton pathway may consist mainly of water molecules that are stabilized within the channel by polar residues that line the channel, such as Ser and Asn (458, 843). Mutation of some of these polar residues reduces the proton-pumping ability of the enzyme only slightly (693), whereas mutation of others pre-

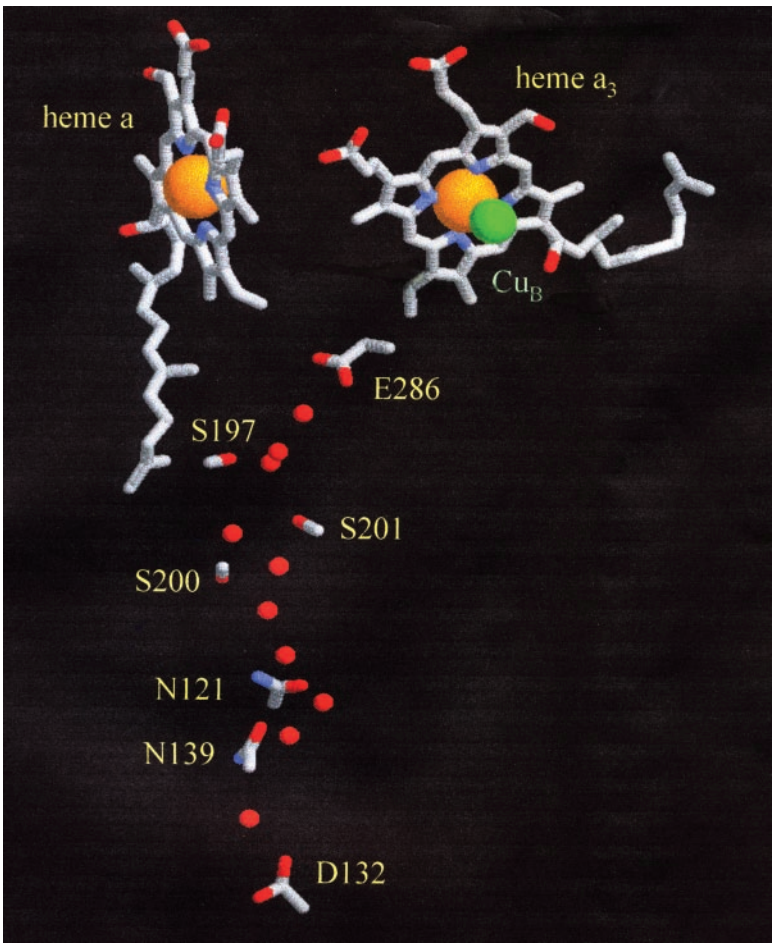

FIG. 10. One of the proton pathways inside cytochrome *c* oxidase, the D channel of *Rhodobacter sphaeroides*. This pathway is used for the transfer of both pumped and substrate protons during the reaction of the reduced enzyme with O_2. Asp^{132} is at the surface and functions as the entrance to the channel from the inside (N side). The red dots illustrate waters that are present in the crystal structure and probably participate in proton conduction. The protons bind to E^{286} and then are somehow transferred to the binuclear center (*top right*, heme a_3/Cu_B). Subsequently, the pumped protons exit through a different channel to the external solution (P side) (690). [From Svensson-Ek et al. (979).]

vents proton translocation (341, 1004). The mutations D132N and E286Q abolish function (689, 1040, 1051). At the entrance to the D channel there is a cluster of negatively charged amino acids and six His, all of which combine to form an effective proton-collecting antenna (523, 653). The proton transport process in the D channel is reminiscent of that in bacteriorhodopsin (1074). First, a proton is transferred from Glu^{286} to the binuclear center or to the outside, and then Glu^{286} is reprotonated from bulk solution (949). The proton transfer via Glu^{286} is rate determining for one of the electron transport steps and displays a kinetic isotope effect of 7 for the *R. sphaeroides* enzyme (525). Thus not only the electron transport, but the proton displacement across 30 Å is rate limited by this single proton transfer step.

The Glu residue (Glu^{286} in *E. coli* and *R. sphaeroides*; Glu^{278} in *P. denitrificans*) deep in the D channel near the heme-copper (Cu_B) bimetallic center is highly conserved and is crucial to proton translocation and O_2 reduction (59, 1040). The Glu side chain may have to move to mediate proton translocation (458, 815, 843). Mutation of Glu to anything but Asp abolishes proton translocation and grossly impairs enzyme function, but if a Tyr is inserted nearby, function and proton translocation are restored (59).

Like voltage-gated proton channels (and many other proton pathways), the D channel is inhibited by Zn^{2+}, and less potently by Cd^{2+} or Cu^{2+} (1). Although the Zn^{2+} affinity is high, K_i ~2.6 μM, inhibition of decay of the peroxy intermediate, which involves proton uptake, saturates at a 56% lower rate of O_2 catalysis by the enzyme (1). However, proton uptake per se into the D channel is slowed >20-fold (2). The D132N mutation abolishes Zn^{2+} effects in the purified enzyme, suggesting that Zn^{2+} binds and exerts its effects near this Asp residue (2).

Figure 11 shows a second important pathway in cytochrome *c* oxidase, the K pathway. This pathway comprises mainly protonatable amino acids with only a few waters interspersed. Although it was considered possible that the K pathway subserves OH^- release rather than H^+ uptake (855), the latter role is supported by mutagenesis studies (862, 929). An alternative proposal is that the K channel is not a proton channel at all, but instead functions as a "dielectric well" in which electron movement within the binuclear center is compensated by movement of charges within the K channel (511).

Based on the principle that an ion that interrupts a water wire should inhibit proton conductivity (421), Kornblatt (564) proposed that the inhibition of cytochrome *c* oxidase by formamide and formaldehyde reflects this mechanism.

The exit pathway in cytochrome *c* oxidase exhibits several intriguing parallels with voltage-gated proton channels. Both are potently inhibited by Zn^{2+} (163, 642, 692, 1008). The only other polyvalent cation with comparable effects was Cd^{2+}, another classical voltage-gated proton channel inhibitor (134, 1008). Another similarity is that Zn^{2+} is strongly competitive with protons in inhibition of the exit channel, with the Zn^{2+} efficacy 10-fold weaker at pH 6 than pH 7; technical limitations prevented extending the measurements to lower pH (692) at which in voltage-gated proton channels protons compete with Zn^{2+} at >1:1 stoichiometry (163). The apparent pK_a for the cytochrome *c* oxidase exit channel was 6.8 (692), identical to the pK_a of 6.2–7.0 for the Zn^{2+} receptor of voltage-gated proton channels (163). Based on this apparent pK_a, the Zn^{2+} receptor in voltage-gated proton channels was speculated to comprise three His (163). Surprisingly, mutation of individual titratable amino acids near the cytochrome *c* oxidase exit channel did not prevent inhibition by Zn^{2+} (692), perhaps indicating redundancy or that multiple groups contribute to the Zn^{2+} receptor. Nevertheless, potent, selective inhibition by Zn^{2+} strongly supports the idea that electron-coupled proton backflow occurs through a specific channel rather than through the phospholipid bilayer. Zn^{2+} inhibition was lost in the presence of valinomycin or uncouplers, suggesting that proton flux through the exit channel is required to sustain electron transfer (692). The loss of Zn^{2+} binding when the membrane potential was removed could indicate that the exit channel is gated by membrane potential, allowing Zn^{2+} entry only when the channel is opened by hyperpolarization (692). In that case, the cytochrome *c* oxidase

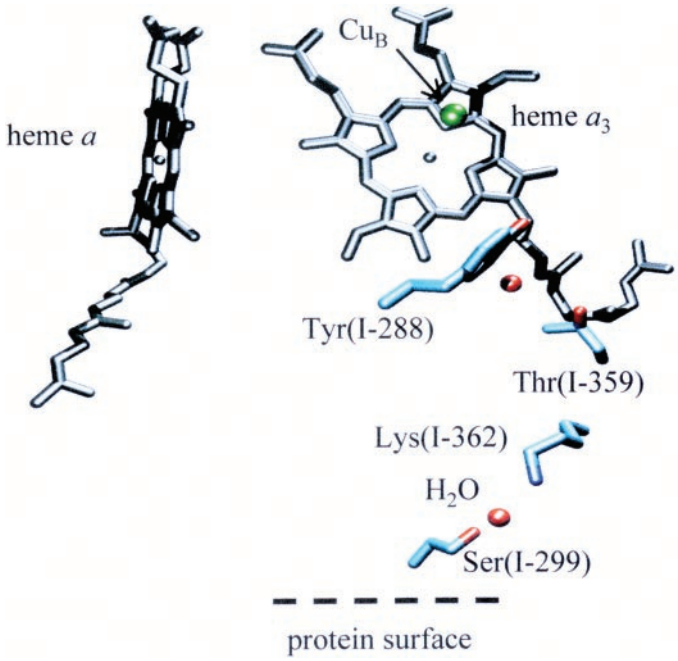

FIG. 11. The K channel is another proton pathway in cytochrome *c* oxidase of *Rhodobacter sphaeroides*. The entrance was first thought to be near Ser^{299} (115), but recent evidence supports Glu^{101} as a more probable entrance (116). Red dots indicate waters. [From Brändén et al. (116), copyright 2002 American Chemical Society.]

exit channel might belong to the rarified class of proton channels gated by voltage (Table 1). Alternatively, the loss of Zn^{2+} binding from the external solution when the normally large negative membrane potential is uncoupled could indicate that the Zn^{2+} binding site is within the membrane electrical field and that block is voltage dependent.

K. Carbonic Anhydrase

Carbonic anhydrase (CA), which comes in seven isoforms in mammals, catalyzes the following hydration/dehydration reaction: $CO_2 + H_2O \rightarrow HCO_3^- + H^+$ (620). The maximal turnover rate for human CA II is $\sim 10^6$/s in either direction at 25°C, making it one of the fastest enzymes known (533, 621). The rapidity of this reaction can be appreciated when one considers that the conversion of CO_2 to HCO_3^- almost reaches equilibrium during the passage of blood through systemic capillaries, and the reverse reaction (including diffusion and other in vivo complications) in alveolar capillaries equilibrates within ~300 ms (1052). The catalytic center (active site) of the molecule (Fig. 12) is formed by a zinc atom coordinated to three His and to one solvent ligand and is located in a deep funnel-shaped pocket within the molecule (298). During hydration of CO_2, a zinc-bound hydroxide reacts with CO_2 and releases HCO_3^-, which is replaced at the zinc by a water molecule. In a separate stage of catalysis, H^+ is transferred from zinc-bound water out to His^{64} along a chain of two or more water molecules, and then H^+ is transferred from His^{64} to buffer in solution (1023). The position of His^{64} differs substantially in crystals formed at low or high pH (735), suggesting that perhaps the imidazole ring of His^{64} shuttles the proton by flipping its conformation into or out of the active site cavity, although this has not been shown definitively. In support of this idea, catalysis by the slower isozyme, CA V, is not enhanced by introducing His at position 64 (Y64H) unless the F65A mutation is simultaneously introduced; the bulky side chain of Phe^{65} evidently prevents the requisite motion of His^{64} (419) or disrupts water structure in the active site cavity (485).

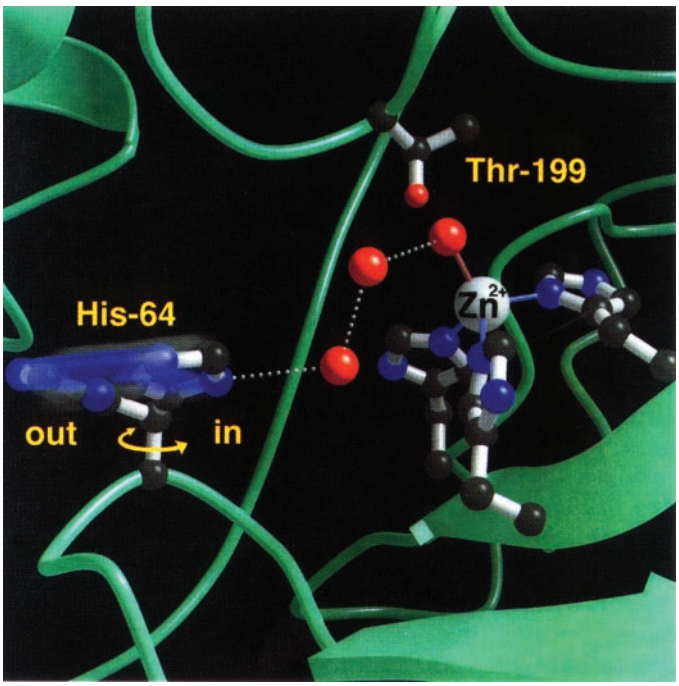

FIG. 12. The proton pathway inside human carbonic anhydrase II. The active site is formed by a zinc atom coordinated between three His residues (blue). A chain of three (or more) waters (red spheres) relays a proton from the zinc-bound hydroxyl to His^{64}. At high pH, the His^{64} is in the "in" conformation, but upon protonation (or at low pH), the imidazole ring flips to the "out" conformation to allow the proton to be transferred to a buffer for transport to the outside world. [From Christianson and Fierke (176), copyright 1996 American Chemical Society.]

The catalytic rate of CA II is limited by an intramolecular proton transfer at high buffer concentrations, but is buffer-limited at low buffer concentrations (620). When the buffer concentration is decreased below 10 mM, the catalytic rate of hydration at steady state decreases greatly because the supply of external protons is compromised (507, 621, 860, 933, 934, 1022). This result indicates that the proton is transferred from His^{64} to a buffer molecule in the bulk solution. Rate constants are consistent with a diffusion-limited bimolecular proton transfer between enzyme and buffer (cf. Fig. 1) that depends only on the pK_a difference between buffer and the binding site, now known to be His^{64} (860). When His^{64} is replaced by Ala in human CA II, the maximum rate of CO_2 hydration is reduced 20-fold in the absence of buffers, and this can be overcome by chemical rescue by certain exogenous buffers (1023).

Intriguingly, the presence of His^{64} appears to facilitate proton transfer, rather than slowing it. Two isoforms that lack any equivalent of His^{64}, CA III and CA V, are slower enzymes (104, 1020). Human CA III does not have His^{64} or any comparable proton shuttle, and its catalytic rate is only 10^3 s^{-1} (491). The absence of His^{64} does not account for all of this effect, however. In the mutant K64H HCA III in which a His is introduced at position 64, the activity is enhanced only ~10-fold (491), leaving K64H HCA III still ~100-fold slower than HCA II. Evidently, there are other differences in the active-site cavity of HCA III that slow catalysis. Replacing Lys^{64} in CA III with Asp or Glu (K64E and K64D mutations) increases the proton transfer rate 20-fold (829). It appears that the presence of a titratable residue (His, Asp, or Glu) at the entrance to the proton channel in carbonic anhydrases enhances proton conduction by enabling direct Eigen-type proton transfer between buffer and the enzyme.

Like voltage-gated proton channels, the proton pathway in CA II is inhibited by divalent cations (Table 1).

L. Uncoupling Protein of Brown Fat

The fundamental mechanism of energy transduction in animal cells is the electron transfer chain in mitochondrial membranes, which generates a proton gradient that is used to synthesize ATP. There is a measurable proton conductance in some mitochondrial inner membranes, which results in "slippage" or dissipation of the proton gradient (125, 342, 572, 753, 759). Brown fat cells also have an inducible proton leak mediated by a 32-kDa uncoupling protein (UCP), formerly called thermogenin, in the inner mitochondrial membrane (754). The UCP-mediated proton leak is activated by fatty acids and suppressed by purine nucleotides (ATP, GDP) or serum albumin, at least in isolated mitochondria, and functions to dissipate the mitochondrial proton gradient, which forces the mitochondria to work harder and generate heat metabolically. Substantial interest in UCPs is based on the hope that these molecules can be exploited to combat obesity by dissipating energy. There are now three isoforms of UCP, with the one in brown fat being UCP1. The sequences of UCP2 and UCP3 are 55–59% identical with UCP1, but 71–73% identical with each other (109, 314, 1042), and their contribution to physiological uncoupling is less well established. UCP3 is highly expressed in skeletal muscle (109, 369, 1043). However, UCP3 knock-out mice are not obese (369, 1043). Although some evidence suggests an uncoupling function of UCP3 (369, 484, 1043), Cadenas and co-workers (138, 277) found no change in mitochondrial proton conductance in UCP3 knock-outs and concluded that UCP3 does not form a basal proton conductance pathway. The thermogenic response to norepinephrine or fatty acids was abolished in UCP1 knockout mice in spite of high expression of UCP2 and UCP3, indicating that UCP1 alone is responsible for thermogenesis in brown fat cells (665, 666).

It is not clear that UCP1 is a proton channel. A recent novel proposal is that the thermogenic function of UCP1 is secondary and that its main role is to protect mitochondria from reactive oxygen species when stimulated by superoxide anion (277). In light of other examples of H^+ channels with low conductance (Fig. 13), the low turnover rate of UCP1 (50–600 H^+/min at 11°C) (549) does not preclude its being a channel. The proton conductance increases with the proton-motive force (549) and is greatly and nonlinearly enhanced at large values (e.g., >100 mV) of proton-motive force (373). Similar observations were made in skeletal muscle mitochondria, although it was not clear whether UCP3 was involved (137). Two His residues in UCP1 appear to facilitate proton transport; H^+ flux was reduced 90% by mutation of either and abolished by the double mutation (94). Neutralization by mutation of either of two Asp residues reduced proton flux by >75% (278). Replacement of Asp with Glu preserved almost normal proton transport (278). These results are suggestive of a HBC conduction mechanism, as explored in detail by Klingenberg and Echtay (548). A novel feature is the inclusion of carboxyl groups from fatty acids in the HBC (Table 2).

UCP1 appears also to mediate Cl^- conductance (754), leading to the suggestion that the anion channel also binds fatty acids that activate proton transport (492). Skulachev (946) proposed that although the fatty acids that activate UCP1 do not mediate proton transport by a simple weak acid mechanism (see sect. III*A3*), UCP1 completes a weak acid circuit by facilitating the flip-flop of the anionic form $RCOO^-$. In this view, UCP1 does not mediate proton permeation per se; instead, protons are transported in the form of protonated fatty acids, RCOOH. More recent studies support this conclusion (343, 484, 493). In conclusion, although the primary sequences of the UCPs are known, it is unclear whether they directly translocate protons, much less whether they might do so as channels or as carriers.

M. Proton Conductance Associated With Expression of Various Proteins With Other Jobs

There are several reports of proton conductance associated with expression of various membrane proteins that are not yet sufficiently characterized to speculate on the mechanism involved. In *Xenopus* oocytes expressing the excitatory amino acid transporter EAAT4, arachidonic acid substantially enhances the substrate-gated (not voltage-gated) current by eliciting a proton-selective conductance (301). The rat serotonin receptor expressed in *Xenopus* oocytes mediates a proton-selective conductance at low pH, with exceedingly small unitary currents (~20 protons $\cdot$ s^{-1} $\cdot$ transporter^{-1} at pH 5.5) (145, 146). A non-voltage-gated conductance in *Rana catesbeiana* taste receptor cells is reportedly permeable to K^+ and H^+ (555). One conformation of the Na^+-K^+-ATPase appears to be capable of proton conduction (1060). However, the reversal potential varied 82.7 mV/unit pH, suggesting that the Na^+-K^+-ATPase can transport protons in a manner like the H^+-K^+-ATPase, rather than as a passive channel (841). Envelope proteins of Semliki Forest virus can function as proton channels, possibly as a triple helical structure (888). Sarcoplasmic reticulum membranes appear to contain pathways permeable to protons that may serve to compensate for Ca^{2+} flux (679, 680). Renal cortex membranes may contain proton pathways that dissipate pH gradients (836). A light-induced H^+ current is mediated by Channelrhodopsin-1 in the alga *Chlamydomonas reinhardtii* (285, 729). A H^+-coupled oligopeptide transporter from *Caenorhabditis elegans* may function mainly as a proton channel (302). Uncoupled H^+ leak occurs through a H^+-coupled amino acid transporter in *Arabidopsis thaliana* (103). Diphtheria toxin induced nonselective cation channels are permeable to protons (876).

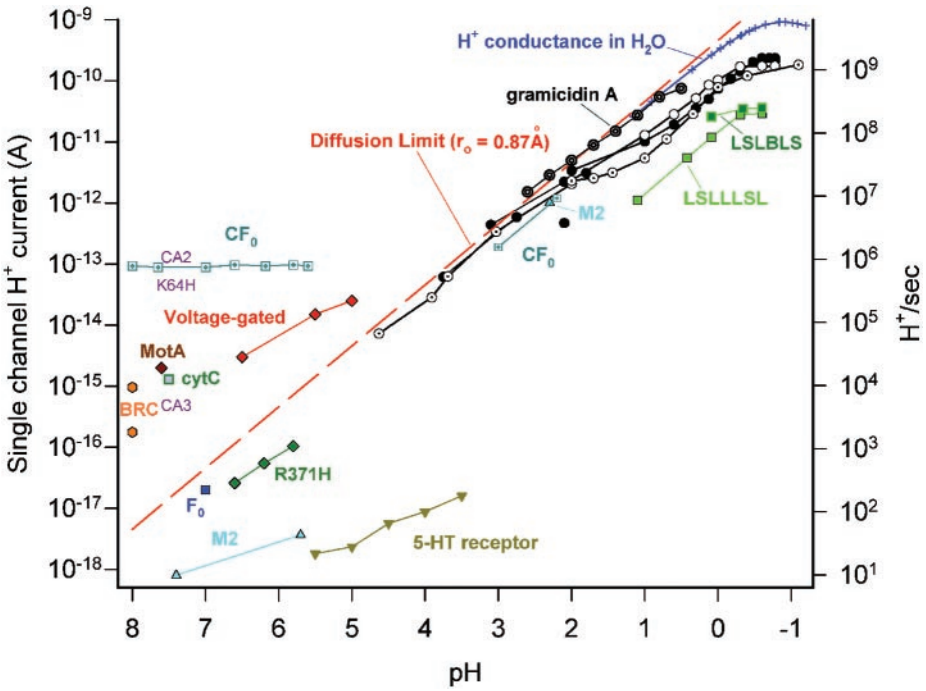

FIG. 13 Compilation of data in the literature for single-channel H^+ currents through various proton-conducting channels, mostly obtained at symmetrical pH. Lines connect data from each source. All values have been scaled linearly with voltage to 100 mV. The pH is simply taken as the bulk value; the local pH near a membrane made of charged phospholipids can differ substantially from bulk pH (215, 554), and the H^+ conductance of gramicidin channels has been shown to reflect the local pH (253a). The dashed line shows the maximum H^+ current if diffusion of H^+ to the channel were rate limiting (*Eq. 2*), assuming a capture radius r_o of 0.87 Å as found for gramicidin (230). Note that the H^+ conductance is proportional to $[H^+]$ over a wide range for several channels that are believed to be water-filled pores. The product of the conductivity of concentrated HCl at 25°C (786) and its concentration is plotted for comparison (+), after arbitrary scaling. The parallel behavior of this parameter and the conductance of ion channels studied at high [HCl] suggests that the apparent saturation of single-channel H^+ current may simply reflect bulk properties of HCl (244). If so, then the apparent saturation of H^+ conductance of the gramicidin water wire reflects diffusion limitation external to the channel, and the maximum H^+ flux that a water wire can sustain has not been attained experimentally. Possible explanations of the "shoulder" in the gramicidin data between pH 2 and pH 1 are discussed in Reference 244. Sources of data for the channels are as follows: (●) gramicidin A (14, 208, 230, 453, 748); (○) covalently linked gramicidin dimer in GMO membranes (206, 208); (small dot within a circle) gramicidin A (292); (large dot within a circle) gramicidin A (421); (blue ▲) M_2 proton channel of the influenza A virus (low pH, Ref. 273; high pH, Ref. 617); (gold ▼) "5-HT" serotonin receptor H^+ selective "leakage" current (146); (brown ♦) "MotA" flagellar motor torque generator (682); (aqua □) CF_o the proton channel component of H^+-ATPase (low pH, Ref. 887; high pH, Ref. 21); (orange hexagons) electron-coupled proton transfer rates for both proton transfer steps in the *Rhodobacter sphaeroides* bacterial reaction center (788); (blue ■) H^+ flux through the F_o proton channel of H^+-ATPase in vesicles (143); (green ♦), H^+ flux through the R371H K^+ channel voltage sensor (960); (green □) cytochrome *c* oxidase proton uptake rate (526); and (green ■) $(LSLLLSL)_3$ and (green ■) $(LSLBLSL)_3$ are 21-amino acid synthetic channels (254). For carbonic anhydrase (1020), the turnover rate is plotted in purple letters without symbols for carbonic anhydrase II (CA2), carbonic anhydrase III (CA3), which lacks His^{64}, and K64H, a CA III mutant into which the His^{64} that guards the entrance to the channel in CA II has been inserted. The voltage-gated H^+ channel estimates (red ♦) are based on noise measurements in inside-out patches of human eosinophils (168, 720). The value given for MotA is based on H^+ flux/torque generator (1,200 H^+/revolution, 8 torque generators/motor) during flagellar rotation at 100 Hz (682), with the proton-motive force scaled linearly with voltage (328) to 100 mV; the passive H^+ flux through MotA incorporated into bilayers is substantially less (97, 970). The 5-HT receptor current appears to be an acid-induced "leak" mode of the serotonin receptor, induced by 5-HT addition, but not part of the normal transport cycle (146). [Modified from DeCoursey and Cherny (245).]

N. Summary of Insights Gained From Other Proton Pathways

In Table 1, selected properties of a number of proton-conducting molecules are compared. Most channels listed are highly proton selective, a few are nonselective but can conduct protons, and aquaporins are impermeable to protons and other cations. Selectivity is determined by the nature of the proton-conducting pathway. The nonselective proton-permeable channels, gramicidin and voltage-gated sodium channels, are known to be water-filled pores. Gramicidin conducts many cations, whereas Na^+ channels preferentially conduct Na^+ and Li^+, but both conduct protons efficiently across the water wire that they contain. The proton impermeability of water channels (aquaporins) shows that not every water-filled pore

conducts protons, although aquaporins exclude all cations by a similar mechanism. It is likely that any water-filled cation-selective channel will also conduct protons, although the H^+ flux may be quite small (see sect. IV*B*). In all of the highly H^+-selective channels, the pathway is formed at least in part by protonatable sites on amino acids or groups capable of forming hydrogen bonds. These are termed HBC, implying that at least part of the pathway is formed by the protein itself, although strictly speaking, a pure water wire is a subset of HBC. In most of the HBCs, the pathway includes both protonatable amino acid residues and water molecules. Three channels, M_2, carbonic anhydrase II, and the voltage sensor of a voltage-gated potassium channel, comprise a water-filled pore interrupted by a single His residue (one His per channel subunit, which is present in multiple copies in the tetrameric channels). One conclusion that can be drawn immediately from current information is that extremely high selectivity (e.g., $P_H > 10^6 P_{cation}$) occurs when the pathway is a HBC, not a simple water wire. The "selectivity filter" (442) of proton-selective channels is thus a protonatable amino acid residue that forms part of the conduction pathway. Selectivity is accomplished because such a group can bind protons but not other cations. Implicit in this mechanism of selectivity is the requirement that protons permeate as H^+ rather than as H_3O^+. The high selectivity of voltage-gated proton channels suggests a HBC conduction mechanism (238).

The maximum H^+ flux varies over seven orders of magnitude. Gramicidin channels conduct protons at a higher rate than any other narrow-pore ion channel conducts any ion, reflecting the efficiency of the water-wire conduction pathway. The rates of H^+ conduction through HBCs that include amino acids vary widely. The high turnover rate of carbonic anhydrase II reflects efficient proton transfer directly between buffer and a His at the mouth of the pore. Lower rates can occur for various reasons, one of which is limited proton supply to the channel, which will depend on pH. This problem is discussed in section IV*O*.

Solvent isotope effects are often substantially larger in HBCs in Table 1 than in bulk solution (65, 325, 612, 624, 844) or in water wires such as gramicidin (14, 171). An isotope effect of 7 was found for a single rate-limiting proton transfer at a Glu residue in cytochrome *c* oxidase (525); thus HBCs can have quite large isotope effects. Similarly, the temperature dependence of proton conduction through water-filled pores is not much different from that of H^+ conduction in bulk solution, whereas HBCs often exhibit strong temperature dependence. The strong deuterium isotope effect and temperature dependence of H^+ permeation through voltage-gated proton channels are consistent with the conduction pathway being a HBC and not a water-filled pore (242, 243).

The frequency with which divalent cations appear in Table 1 as inhibitors of various H^+ channels is striking. The titratable groups on amino acids, in particular the sulfhydryl group on Cys and the imidazole nitrogen on His, as well as carboxylate oxygens of Glu and Asp, are notorious metal binders (119, 1031, 1032). Competition between divalent metal ions and protons for binding sites on proteins is common. Zinc is a potent inhibitor of the mitochondrial bc_1 complex, binding with a K_i of 10^{-7} M to a protonation site at which H^+ and Zn^{2+} exhibit negative cooperativity (622). Two His residues in the glutamate transporter EAAT4 bind Zn^{2+}, which then inhibits an anion conductance (699). Zinc binds to titratable His residues in serum albumin and insulin (119). The binding of Cu^{2+} to CA (possibly to a His residue) is inhibited at low pH (1021). A Cys residue, in cooperation with a His, binds Zn^{2+} competitively with protons and mediates proton inhibition of an inward rectifier K^+ channel (187). Zinc inhibits *N*-methyl-D-aspartate receptors by interacting with His residues, apparently by "flexible coordination"; mutation of each of the 3 most critical His lowered Zn^{2+} affinity >100-fold, mutation of any of 4 other His lowered Zn^{2+} affinity 4- to 8-fold (626). It is not too surprising that metals would tend to bind at the same protonatable sites on a protein that comprise the HBC conduction pathway, although this requires the sites to be accessible to the solution. A skeptic could argue that any protein is apt to have many sites that could bind divalent metals, and certainly the effects of heavy metals on normal ion channels are qualitatively similar to their effects on voltage-gated proton channels, although H^+ channels are demonstrably more sensitive (163, 642).

Table 2 shows the proposed composition of proton pathways in a number of molecules whose function involves proton translocation across membranes. Several points emerge. The specific amino acid composition of proton pathways varies dramatically. It would require both intuition and exceedingly good luck to identify the voltage-gated proton channel by deducing possible proton pathways and searching the GenBank for candidates. The pathways comprise a variety of amino acid residues intercalated by water molecules as required to fill in gaps. Most of the amino acids are titratable and presumably are protonated transiently during proton permeation, although the specific function of each residue is controversial in many instances. Some of the amino acids in the pathways in Table 2 may act to stabilize within the channel the water molecules that actually translocate protons. Some are critical because they interact with other parts of the molecule in essential ways. Interpretation of site-directed mutagenesis studies is rarely unambiguous, demonstrating that an amino acid mutation that prevents proton conduction does not discriminate which role this residue plays. As discussed in section III*D*, the archetypal proton channel may comprise a water wire interrupted by only one or two titratable amino acids residues, as origi-

TABLE 1. *Proton-permeable and selected other channels*

	HBC or H_2O?	H^+ Selectivity	Maximum Flux, H^+/s	H_2O/D_2O Flux	Q_{10}	Inhibitors	Gated by	Reference Nos.
Gramicidin	H_2O	Low	2.2×10^8	1.2–1.37	1.23–1.34	?	Dimerization	14, 171, 172
Voltage-gated Na^+ channel*	H_2O	Low				TTX, metals	Voltage	743
K^+ channel voltage sensor†	H_2O + His	High	650		2.6	?	Voltage	960
M_2 viral H^+ channel	H_2O + His	High	7–26, $\sim 10^4$	2.1	1.9–3.9	amantadine, Cu^{2+}	Low pH	220, 340, 617, 712, 811
F_o component of H^+-ATPase	HBC	Low/high		1.7	1.89	venturicidin, DCCD, oligomycin	?	21, 306
Serotonin transporter	HBC?	High	300	?	?	desipramine	?	146
MotA/MotB	HBC	?	15,000	1.28–1.6	2.1–3	imidazole reagents	?	97, 160, 183, 682
Bacteriorhodopsin (*ex*tracellular/*cy*toplasmic)	HBC	?		4.5–6.5*ex* 1.3–2.75*cy*	1.7*ex* 2.1–3.1*cy*	dark?	Light	127, 144, 562, 601
Carbonic anhydrase II	H_2O + His	?	1.4×10^6	3.45–3.8	1.3–1.7	Cu^{2+}, Hg^{2+}	?	358, 507, 533, 879, 963, 1021
BRC	HBC	Low/high	10^5 (1,200)	3	1.8	Cd^{2+}, Ni^{2+}, Zn^{2+}	?	43, 355, 657, 787, 790, 990
Cytochrome *c* oxidase								
D channel	HBC	?	8,000	7.1	1.6–1.9	Zn^{2+}, Cd^{2+}, Cu^{2+}	?	1, 524, 526
K channel	HBC	?	2,000	2–3	1.8		?	8, 407, 862
Exit channel	HBC	?				Zn^{2+}, Cd^{2+}	Voltage?	690, 692
Uncoupling protein 1	HBC?	?	10	?	?	ADP, GDP	Fatty acids,	548, 549, 754
Water channels	H_2O	Impermeable	0	?	1.2	DCCD, Hg^{2+}, Zn^{2+}		13
Voltage activated	HBC?	High	$\approx 10^5$	1.9	2–5	Cd^{2+}, Zn^{2+}, others	Voltage, pH	168, 236, 242, 243, 1008

The conduction pathway is described as a continuous water wire (H_2O), a hydrogen-bonded chain (HBC) that might include some water molecules, or a water wire with a single occlusion formed by His residue(s) (H_2O + His). Proton selectivity is defined unambiguously by the Goldman-Hodgkin-Katz (GHK) voltage equation (368,444,456) for channels that span the entire membrane, but hard to define for access channels that conduct protons to an active site within a protein. The "low/high" H^+ selectivity designation for bacterial reaction center (BRC) and F_o reflects evidence that small weak acids (989) or *N*-ethylmaleimide and Ag^+ (306), respectively, can enter far into the proton channel, although ultimately only protons interact with the active site. Other columns refer to H^+ flux or measurable parameters that reflect H^+ flux. For BRC, the proton transfer rate constant is 10^5 s^{-1} (787), but coupling to electron transfer reduces the rate in situ to ~1,200 s^{-1}. Temperature effects are expressed as a Q_{10} value, which in some cases was converted from activation energy (E_a) arbitrarily at 20–30°C. For bacteriorhodopsin, *cy* is the cytoplasmic pathway and *ex* is the extracellular pathway (cf. Table 2). For cytochrome *c* oxidase, D, K, and exit refer to proton pathways (cf. Table 2; see sect. IV*J*). DPI, diphenylene iodonium; DCCD, dicyclohexylcarbodiimide; TTX, tetrodotoxin. * Ref. 743; divalent cations have similar effects on Na^+ channel gating as they do on voltage-gated proton channels (444). † R371H (960). The Q_{10} listed is for H^+ transport through the R365H mutant, which functions as a proton carrier rather than a channel (961).

nally proposed for the H^+-ATPase (111). Ten amino acids that are proposed to form the F_o proton channel are shown in Table 2, but these may mainly provide a matrix for the water molecules that conduct protons. The actual proton pathway may be a water wire leading to the Asp^{61}, as emphasized by recent studies (306).

Three titratable amino acids with pK_a lower than physiological pH, Glu, Asp, and His, are prominent in Table 2, presumably reflecting their suitability for H^+ conduction. Groups with higher pK_a are reluctant to release the proton and thus as HBC elements would slow conduction. However, the pK_a of an amino acid inside a protein can differ substantially from that in free solution, depending on the extent to which the group is buried in the protein and also on the hydrophobicity or hydrophilicity of the local microenvironment (677, 899). In several cases, conformational changes in the protein dramatically change the pK_a of crucial amino acids during proton transport (e.g., bacteriorhodopsin and H^+-ATPase). His seems to appear with regularity in proton pathways. This should perhaps not be too surprising, since His has a nominal pK_a of 6.0, which means that it can be protonated at physiological pH, but does not hold the proton too tightly. Three minimal HBC pathways comprise aqueous pores occluded by His at one point: the M_2 viral proton channel, CA II, and a channel constructed artificially by mutation of the voltage sensor of voltage-gated K^+ channels, resulting in aqueous pathways that are occluded at one point by a His residue. The His occlusion imparts strong proton selectivity and may allow protons to pass by means of a hypothetical ring flip (811), as was first proposed for the CA proton channel (735, 932).

Titratable amino acids can serve two important functions in proton channels. In addition to forming part of the conduction pathway, they can mediate molecular functions, in particular, pH sensitivity. It is vital to the function of most proton channels that they respond appropriately to pH. The exquisite regulation by pH of the voltage dependence of voltage-gated proton channels has been proposed to be mediated by the degree of protonation of titratable sites that are accessible to external and internal solutions (166), with the external sites comprising three

TABLE 2. *Proposed proton pathways through various molecules*

Generic ion channel	$H_2O \rightarrow (H_2O)_n \rightarrow H_2O$
K^+ channel voltage sensor	$(H_2O)_n \rightarrow His^{371} \rightarrow (H_2O)_n$
M_2	$H_2O \rightarrow (H_2O)_n \rightarrow His^{37} \rightarrow H_2O$
F_o (residues that form channel)	$H_2O \rightarrow$ **Asn — Ser — Glu — His — Asp — Asn — Asn — Gln — Arg —** Asp^{61}
F_o (possible proton pathway)	$(H_2O)_n \rightarrow Asp^{61} \rightarrow (H_2O)_n$
MotA-MotB	$(H_2O)_n \rightarrow Asp^{32} \rightarrow (H_2O)_n$
bR minimal pathway	$(H_2O)_n \rightarrow$ Asp $\rightarrow (H_2O)_n \rightarrow$ Retinal Schiff base $\rightarrow$ Asp $\rightarrow (H_2O)_n$
bR cytoplasmic pathway	Asp $\rightarrow (H_2O)_n \rightarrow$ Retinal Schiff base
bR extracellular pathway	Retinal $\rightarrow$ Asp $\rightarrow (H_2O)_2 \rightarrow$ Arg $\rightarrow H_2O \rightarrow$ Glu $\rightarrow H_2O \rightarrow$ Glu
BRC - 1	$H_2O \rightarrow$ His $\rightarrow (H_2O)_n \rightarrow$ Asp $\rightarrow H_2O \rightarrow$ Asp $\rightarrow$ Ser $\rightarrow Q_B$
BRC - 2	$H_2O \rightarrow$ His $\rightarrow (H_2O)_n \rightarrow$ Asp $\rightarrow H_2O \rightarrow$ Asp $\rightarrow (H_2O)_2 \rightarrow$ Glu $\rightarrow H_2O \rightarrow Q_B$
Cytochrome *c* oxidase (D)	$Asp^{132} \rightarrow H_2O \rightarrow (H_2O)_n \rightarrow H_2O \rightarrow$ Glu $\rightarrow (H_2O)_n \rightarrow$ binuclear center/exit path
Cytochrome *c* oxidase* (K)	$Glu^{101} \rightarrow$ Ser $\rightarrow H_2O \rightarrow$ $Lys^{362} \rightarrow$ Thr $\rightarrow H_2O \rightarrow$ Tyr $\rightarrow$ binuclear center
CA II	$BH \rightarrow His^{64} \rightarrow H_2O \rightarrow (H_2O)_n \rightarrow H_2O \rightarrow$ E-Zn-OH^-
CA III	$BH \rightarrow H_2O \rightarrow H_2O \rightarrow (H_2O)_n \rightarrow H_2O \rightarrow$ E-Zn-OH^-
UCP1	Asp $\rightarrow$ FA-$COO^- \rightarrow$ (FA-COO^-)$_n \rightarrow$ Asp $\rightarrow$ His $\rightarrow$ His $\rightarrow H_2O$

These are mainly hypothetical attempts to illustrate the pathway of the proton. Amino acid residues are in bold and the three most common are color-coded. In most cases, the number of water molecules is arbitrary. Selected crucial amino acid residues are numbered. The pathway through F_o includes residues that may contribute to the hydrogen-bonded matrix of the channel (835), but the implied linear path is arbitrary; another possibility includes only a single titratable amino acid interrupting aqueous channels, as suggested by recent work (306). Not shown are important amino acids that line the pore and stabilize the waters in the cytochrome *c* oxidase D channel (1074). Various other models have been proposed for the bR release (extracellular-facing) channel (632). BH, protonated buffer; bR, bacteriorhodopsin; BRC, bacterial photosynthetic reaction center (two parallel paths); CA, human carbonic anhydrase; UCP1, uncoupling protein of brown fat; FA-COO^-, carboxyl groups of fatty acids. References: K^+ channel voltage sensor (960), M_2 (811), F_o (835), MotB (1100), bR (417,436,631,632) BRC (9,788), cytochrome *c* oxidase D channel (458,525,843,1075), cytochrome *c* oxidase K channel (116,639,1075), CA II (176,931,963), CA V (104), UCP1 (278,548). * The postulated Glu^{89} at the entrance to the K channel is based on data from cytochrome bo_3 (639).

His residues (163). There are numerous other examples of titratable residues serving as regulatory protonation sites. Proton-pumping nicotinamide nucleotide transhydrogenases use a proton gradient to synthesize NADPH from NADH. The activity of this enzyme is regulated by the degree of protonation of a His residue (95). Gating of the ClC-1 Cl^- channel is regulated by pH_o (475, 476, 791, 864, 1063). The bulk of site-directed mutagenesis evidence points to Cys residue involvement in ClC-0 and ClC-1 channel gating as well as Zn^{2+} and Cd^{2+} binding and block by anthracene-9-carboxylic acid (7, 577, 578, 618, 863). The inhibition of ROMK1 channels by low pH_i is mediated by four His residues (151), but also by a Lys (899).

A general rule seems to be that titratable groups at the entrance to a proton channel can increase the proton flux by an order of magnitude or more. Mutational excision of the two His at the mouth of the BRC proton channel slows proton uptake by at least two orders of magnitude (787). Introducing His near the entrance to the CA III proton channel enhances activity ~10-fold (491), and Asp or Glu (K64E or K64D mutations) increases the proton transfer rate 20-fold (829). Proton currents through gramicidin channels are enhanced 12.5-fold by formic acid, which evidently supplies protons by binding transiently to the mouth of the channel (230). Apparent rate constants for protonation of membrane-associated protonophores that greatly exceed the diffusion limit can be accounted for by a direct proton transfer reaction of the Eigen variety (83).

The "chemical rescue" technique (1011, 1015) has become a fashionable way to support the idea that a particular titratable group plays a role in H^+ conduction. The amino acid in question is eliminated by mutation, resulting in loss of function, and then function is restored by addition of titratable compounds such as imidazole or pyridine derivatives (25, 10, 787, 1017, 1023), or azide, formate, or cyanate for amino acids with lower pK_a (126, 990, 1011). The titratable group must be accessible to the solution, such as His^{64} in CA II (25). A novel variant of the chemical rescue approach was the restoration of proton uptake via the D channel in D132N or D132A mutants of cytochrome *c* oxidase by exogenous long-chain unsaturated fatty acids, such as arachidonic acid (304).

O. Dependence of H^+ Current on H^+ Concentration (pH)

The expectation of the GHK equation (368, 444, 456) is that the single-channel H^+ current should be proportional to $[H^+]$, and thus should increase 10-fold/unit decrease in pH. This prediction is borne out for several channels. Figure 13 illustrates the pH dependence of single-channel proton current for every ion channel reported to conduct protons. For gramicidin and certain synthetic channels, the unitary H^+ current is nearly proportional to $[H^+]$ between pH ~0 and pH 3.75, except for a "shoulder" region between pH 1 and pH 2 (see sect. IV*A3*). This proportionality may be extended to pH 4.6 by including noise measurements of Neher, Sandblom, and Eisenman (292) (two left-most points in Fig. 13), or based on more

indirect measurements, to pH 7.5 (571) or even pH 8.5 (396). Simple extrapolation of the H^+ current measured in various channels at low pH into the physiological range, on the GHK assumption of direct proportionality, provides an estimate of <0.1 fA at pH 7. Voltage-gated proton channels and several other channels deviate from this pattern in two important respects. First, their H^+ current has a weaker dependence on pH. Second, at pH >6, the estimated single-channel H^+ current is higher than the nominal diffusion limit, indicated on the graph by a dashed red line.

Some lack of proportionality between H^+ concentration and H^+ current is evident for voltage-gated proton channels, CF_o, M_2, the 5-HT receptor, and the K^+ channel voltage sensor mutant R371H, all studied reasonably near the physiological pH range. The macroscopic $g_{H,max}$ of voltage-gated proton channels increased only approximately twofold/unit decrease in pH_i (234) (see sect. V*F*). Surprisingly, single H^+ channel currents appear to depend more strongly on pH_i (168); nevertheless, the dependence is less than directly proportional. The proportionality between gramicidin H^+ current and $[H^+]$ generally has been taken to indicate that the current is limited by the diffusional supply of protons to the mouth of the channel, rather than by permeation through the channel (230). Protons diffuse through gramicidin channels essentially unhindered, at a rate comparable to that in bulk solution (206). The anomalous behavior of voltage-gated proton channels has been interpreted to indicate that the rate-determining step in conduction occurs within the channel itself and not in the diffusional approach (166, 238, 239, 244, 245). However, it should be emphasized that strict proportionality has not been demonstrated for any proton channel in the physiological pH range.

The second complication in Figure 13 is that for several molecules (CF_o, MotA, the BRC, cytochrome *c* oxidase, and voltage-gated proton channels), the estimated elementary proton flux exceeds the diffusion limit, indicated on the graph by a dashed red line, by 1–2 orders of magnitude. The problem of proton supply is most severe for CF_o proton channels, whose estimated unitary conductance is nearly 1 pS and appears to be pH independent between 5.5 and 8.0 (21, 512). The maximum current permitted by diffusion (I_{max}; dashed line in Fig. 13), is given by (27, 71, 441, 593)

$$I_{max} = 2\pi F r_o D_H c_H \qquad (2)$$

for a hemispherical approach, where *F* is Faraday's constant, r_o is the capture radius, D_H is the H^+ diffusion constant, 8.65×10^{-5} cm^2/s at 20°C (845), and c_H is the H^+ concentration. Applying *Equation 2* to H^+ channels is complicated by uncertainty as to the appropriate value of r_o, the effects of buffer, and the actual c_H near the membrane. On a macroscopic scale, r_o is defined as the difference between the radius of the (spherical) permeating ion and the radius of the (cylindrical) pore. The probability of permeation is assumed to be unity when the entire molecule enters the pore without hitting the edges but is presumed to be zero when any part of the molecule collides with the pore mouth (303). On the molecular scale, r_o becomes an operationally defined parameter (26, 452), which may be effectively increased by various mechanisms. Due to the special mechanism of H^+ movement through water, its effective reaction distance is large and thus r_o might be larger than for ordinary ions (287). For proton currents, r_o has been estimated to be 1 Å for a synthetic proton channel (599) and 0.87 Å for gramicidin (230), much larger than 0.12–0.33 Å for "ordinary" monovalent cations in gramicidin (26, 27). Calculations by Sacks et al. (867) suggest that even larger distances (i.e., perhaps tens of Å) might apply for H^+ movement in the plane of the membrane (see sect. II*D*).

Because protonated buffer is present at 10^6 higher concentration than H^+, buffer ought to compensate to some extent for H^+ depleted by current flow. However, the calculated effects of buffer on H^+ diffusion toward a channel, based on the model of Nunogaki and Kasai (768), indicate that the effective diffusion limit is increased less than twofold by 100 mM buffer (240). Similarly weak enhancement by weak acid buffers was calculated by Decker and Levitt (230). However, they found that formic acid increased the H^+ current through gramicidin ~12-fold, apparently by transiently binding to the mouth of the channel and then dissociating (230). The formic acid effect appears to be analogous to the enhanced H^+ conductance in CA, where large buffer effects occur (see sect. IV*K*) when His or another protonatable amino acid is present at the mouth of the proton channel (507, 860, 933, 934, 1022). Evidently, the proton supply can be enhanced by buffer to a much greater extent if there is direct proton transfer between buffer and a proton acceptor on the target molecule. In fact, if protonated buffer were the permeating species, the unitary current limit according to *Equation 2* increases to 1.9 pA (238). However, the insensitivity of voltage-gated proton currents to buffer concentration between 1–100 mM rules out direct proton transfer from buffer to the channel as a rate-determining step for this channel (240).

If we assume that r_o is 0.87 Å as in gramicidin (230), then the diffusion-limited single-channel H^+ current given by *Equation 2* is 1.4 fA at pH 5.5 and only 14 aA at pH 7.5. Incorporating the effects of 100 mM buffer according to Nunogaki and Kasai (768) increases these estimates only by a factor of 1.26 or 1.42, respectively for MES or HEPES buffers (240). Up to a point, arbitrary scaling of r_o can be justified by postulating that the entire membrane acts as a "proton-collecting antenna" (see sect. II*D*) and then simply calculating how much surface area each channel could

use for this purpose (244). With the use of values derived below (see sect. VI*H6*), each H^+ channel in an eosinophil, with the highest H^+ channel expression of any native cell, has a surface area of 5–8 $\times$ 10^3 nm^2 to draw from. With the use of r_o determined for H^+ current in gramicidin, 0.87 Å (230), to estimate the effective "capture distance," i.e., the distance from the membrane surface from which a proton could leap to the membrane in a single bound, converting the resulting volume enclosed by the disk to its hemispherical equivalent, and determining its radius, for the voltage-gated H^+ channel at pH 6.5, the effective capture radius is ~60–70 Å.[4] This value is 70- to 80-fold greater than r_o assumed in Figure 13. As evident from *Equation 2*, the "diffusion limit" scales up in direct proportion to r_o. The estimated unitary H^+ currents for voltage-gated proton channels fall within this new upper limit, indicating that sufficient membrane area is available to provide an adequate supply of protons to each H^+ channel. Among several crude assumptions in this calculation is the nontrivial assumption that surface H^+ conduction is infinitely rapid.

The unitary H^+ currents for MotA-MotB, the bacterial reaction center, cytochrome *c* oxidase, as well as voltage-gated proton channels, are all reasonably close to these rough limits, although the CF_o proton channel at high pH remains well above. Several mechanisms that could increase the supply of protons to a channel and thus effectively increase r_o in the above equation (593), include *1*) a negatively charged vestibule that funnels protons toward the mouth of the channel (26, 155, 214, 508); *2*) hydrolysis (527); *3*) rapid conduction of protons at the surface of the membrane (404, 418, 706, 724, 820, 821); *4*) buffers (399, 768); *5*) electrodiffusion, which may increase r_o by one Debye length (806); *6*) increased local proton concentration due to negative surface charges on the membrane (32, 215, 378, 401, 554, 988) or on the channel itself (31, 362, 382), a single negative charge can double the conductance at low salt concentration (140, 383); *7*) titratable membrane groups acting as proton antennae (253a, 400); and *8*) buffering by phospholipid head groups (390, 536). Some of these mechanisms overlap conceptually. A fundamental problem is that although there are ample protons in H_2O and bound to buffers, any proton concentrating mechanism that involves charge (*mechanisms 1*, *3*, *5*, *6*, *7*, *8*) will only work with free H_3O^+. Furthermore, negative charges concentrate protons at the surface most effectively when the ionic strength is low (214, 988) or if H^+ is the only cation present, although the smaller size of H_3O^+ than a hydrated cation may be advantageous from this perspective (342). No mechanism that invokes the consumption of a transient store of protons is viable, because voltage-gated proton channels do not inactivate (238) and carry sustained current for minutes (85, 236). The effect of surface charges (on the membrane or channel) on local pH can be large. In positively charged ethylated diphytanoyl phosphatidylcholine membranes, the surface pH can be 2 pH units higher than in bulk solution, although this result applies to pure HCl solutions (253a). Conversely, at high pH, the pH near negatively charged biological membranes can be 2 pH units lower than in bulk solution (215, 554), with larger effects seen at low ionic strength (987, 988). If the surface pH were two units lower than bulk, the problematic supply of protons would immediately be resolved for all proton channels except CF_o.

Kasianowicz, Benz, and McLaughlin (527) considered three mechanisms by which H^+ might reach the membrane from bulk solution. H^+ can arrive as a free proton (protolysis mechanism), by hydrolysis of water, or by direct proton transfer from protonated buffer. The rate at which H^+ channels are protonated, assuming the protolysis mechanism, was 4.9 $\times$ 10^9 $M^{-1} \cdot s^{-1}$ at pH_i 5.5 and 2.0 $\times$ 10^{11} $M^{-1} \cdot s^{-1}$ at pH_i 7.5 (240). Kasianowicz et al. (527) obtained higher apparent rates than these and thus concluded that hydrolysis was the only possible source of protons. The apparent protonation rate of H^+ channels is faster than the fastest reaction occurring in free solution, the recombination of H^+ with OH^- at 1.3–1.4 $\times$ 10^{11} $M^{-1} \cdot s^{-1}$ (80, 287), but within those reported for proton transfer reactions between groups at the surface of the membrane (see sect. II*D*). Thus protolysis remains a viable mechanism, but hydrolysis is not ruled out as a possible source of protons.

Because five different molecules (the BRC, MotA-MotB, cytochrome *c* oxidase, CA III, and voltage-gated proton channels) studied in very different ways all exhibit comparably large unitary H^+ flux in the physiological pH range, it seems evident that nature does not view proton supply as a problem, whether or not we fully understand the mechanisms involved. In at least two cases, CA II and the BRC, proton flux is enhanced by the presence of one or more His residues at the channel entrance (10, 419, 491, 787). The higher proton flux through CA II is facilitated by direct proton transfer from protonated buffer to the channel (see sect. IV*K*).

V. VOLTAGE-GATED PROTON CHANNELS: GENERAL PROPERTIES

A. What Are Voltage-Gated Proton Channels?

Voltage-gated proton channels are ion channel-like entities characterized by a number of properties that distinguish them from other ion channels and other proton

[4] Purely by coincidence, this value falls within the range (23–83 Å) calculated in section VI*J* for λ, the effective space constant of proton depletion at the mouth of a proton channel in the presence of buffer. The effective r_o depends on channel density, whereas λ does not.

transporters. Their main features are described in subsequent sections. They open and conduct H^+ current upon depolarization of the membrane. Their gating is exquisitely sensitive to pH_o and pH_i. They are extremely selective for protons, with no detectable permeability to any other ion. Their single-channel currents are exceedingly small, which is not entirely surprising in light of the tiny concentration of permeant ions in physiological solutions. They are inhibited by external Zn^{2+}, Cd^{2+}, and other polyvalent metal cations, but they are resistant to blockade by organic ions. They have extraordinarily large temperature dependencies of both conductance and gating kinetics and exhibit large deuterium isotope effects. Many of these properties suggest that these channels are not water-filled pores, but rather HBCs comprising at least one amino acid side group.

B. History

Voltage-gated proton channels were first identified explicitly as a distinct entity by Thomas and Meech (1008) in their pioneering study of snail neurons (Fig. 14). Proton currents likely had been observed in earlier studies in *Helix*, *Limnea*, and *Planorbis* neurons but were misidentified as Cd^{2+}-sensitive nonspecific currents (133, 569). Earlier, Thomas (1005) had observed Na^+-independent pH_i recovery after HCl injection in snail neurons depolarized with high $[K^+]$ that probably was mediated by voltage-gated proton channels, but suggested K^+/H^+ exchange as a possible mechanism. Byerly, Meech, and Moody (134) thoroughly characterized the electrophysiological properties of voltage-gated proton currents in snail neurons under voltage clamp. Shortly thereafter, Barish and Baud (70) described similar voltage-gated proton currents in *Ambystoma* (axolotl) oocytes. For almost a decade, snail neurons and newt oocytes were the only cells known to express these channels. In 1991, voltage-gated proton channels were first described in mammalian cells, rat alveolar epithelial cells (232). H^+ currents in human cells were reported in 1993 (236, 258). To date, nearly 100 voltage-clamp studies and reviews of voltage-gated proton channels have been published.

Early reports of voltage-gated proton channels were met with normal scientific skepticism. Are H^+ currents actually conducted through other ion channels? Are H^+ currents an artifact of the unusual pH and ionic conditions used to study them? Do H^+ currents serve any useful function in cells of interest to anthropocentrists? Because these issues arise logically, they will be discussed briefly. First, the idea that H^+ current might simply reflect H^+ permeation through other ion channels, specifically voltage-gated K^+ channels, can be refuted unequivocally. First, it is possible to inhibit other ionic currents that are superimposed on H^+ currents, including Ca^{2+}, Ca^{2+}-activated K^+, voltage-gated K^+, or Cl^- currents by various channel blockers listed in Table 6 or by ion substitution, without effect on H^+ currents (70, 237, 499, 641, 710). In searching (in vain) for specific inhibitors, numerous investigators have tried batteries of blockers of other ion channels and ion transporters, without

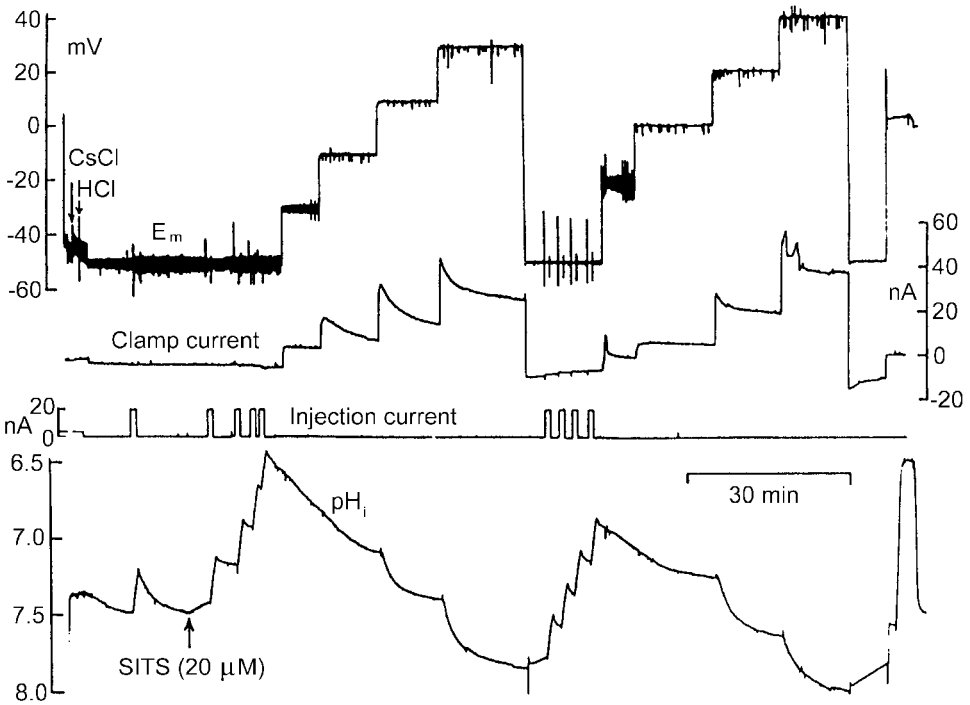

FIG. 14. The first description of voltage-gated proton channels was based on elegant simultaneous measurements (from *top* to *bottom*) of membrane potential (E_m), voltage-clamp current, HCl injection current, and pH_i in snail neurons (*Helix aspersa*) by Thomas and Meech (1008). Several HCl injections lowered pH_i to <6.5, then the membrane was depolarized stepwise. At −10 mV and at more positive voltages, a decaying outward current was observed. The recovery of pH_i (bottom trace) from the acid load clearly is faster at more positive voltages, consistent with the outward current being carried by H^+. The outward H^+ current decays because the driving force (V-E_H) decreases as pH_i increases (due to the continuous H^+ efflux). Large H^+ currents in small cells decay two orders of magnitude faster because of the much smaller cell volume than in snail neurons. The neuron was pretreated with CsCl to inhibit K^+ currents and SITS to inhibit other endogenous pH regulatory mechanisms. [From Thomas and Meech (1008), as modified by Eder and DeCoursey (280).]

identifying any that block voltage-gated proton channels (Table 6). Conversely, H^+ channels are more sensitive to inhibition by Zn^{2+} than are other ion channels in the same cells (85, 163, 474, 642). H^+ current could not be mediated by delayed rectifier K^+ channels, because these currents had different Q_{10} values and different distributions in both whole cell and excised patch configurations (136). H^+ current could not be mediated by Ca^{2+} channels, because Ca^{2+} currents "wash out" with time, but H^+ currents do not (498). Finally, it is clear that the unitary conductance of voltage-gated proton channels is very small indeed (see sect. v*G*), with the best estimates being $\sim 10^3$ smaller than that of voltage-gated K^+, Na^+, or Ca^{2+} channels in physiological solutions. The size of whole cell H^+ currents at low pH_i in several cells is as large or larger than conventional ionic currents in the same cells (134, 232, 281, 372, 574, 641). Therefore, there must be $\sim 10^3$ more voltage-gated proton channels than other ion channels. For example, if one assumed that the 130 voltage-gated K^+ channels in the average rat alveolar epithelial cell (250) could conduct protons, these K^+ channels would carry <1 pA of H^+ current at physiological pH, assuming a gramicidin-like H^+ conductance, which would be difficult to detect in the presence of macroscopic voltage-gated proton currents approaching 1 nA. Clearly, voltage-gated H^+ current is mediated by a unique channel.

Voltage-gated proton channels are usually studied by removing permeant ions (K^+, Ca^{2+}, Na^+, and Cl^-) from the solutions to preclude contamination by other types of ionic currents. As a result, the question arises whether H^+ currents might somehow be caused by unusual ionic conditions and whether they are still detectable under physiological ionic conditions. This question has been resolved unambiguously. H^+ currents can be seen at physiological pH, in quasi-physiological solutions such as Ringer solution (68, 70, 74, 232, 236, 372, 473, 498, 499, 574, 676, 1008), in large cells with intact cytoplasm (70, 74, 473, 641, 676, 1008), in cell-attached patches exposed to cytoplasm (239), in permeabilized patch studies (165, 246–248, 387), and at physiological temperatures (136, 243, 259, 311, 574) where H^+ currents are much larger than at room temperature (136, 170, 243, 574).

Finally, strong evidence exists that H^+ currents in intact cells serve a variety of important physiological functions. Voltage-gated proton currents are activated by various agonists of the respiratory burst in phagocytes that are studied using permeabilized patch technique, i.e., with intact cytoplasm and during physiological responses (165, 246, 248). H^+ efflux attributed to H^+ current is elicited in airway epithelial monolayers by histamine or ATP (311). Voltage-gated proton channels in intact cells are activated during recovery from acid loads (574, 641, 676, 762, 1006, 1008) and during various other physiological responses (see sect. vi).

C. Where Are Proton Channels Found?

The cells in which voltage-gated proton channels have been demonstrated by direct voltage-clamp measurement are listed in Table 3. Table 3 is dominated by leukocytes and related cell lines, although epithelia are also well represented. The proposal of a specific function for H^+ channels in human neutrophils (429), even before their existence was confirmed by voltage clamp (236), provided strong motivation to study neutrophils and related cells. Essentially every leukocyte that has been examined expresses voltage-gated proton channels. It is tempting to remark on the prevalence in Table 3 of cells that are subject to extreme pH in their local environment, namely, epithelia, kidney cells, oocytes, and leukocytes. The pH_o in abscesses, tumors, or synovial fluid in septic arthritis is typically lower and more variable than in normal tissue (365, 423, 942, 996, 1061) and can drop to pH 5.8 (996). On the other hand, the difficulty in finding cells that do not express H^+ channels, e.g., to serve as a heterologous expression system, suggests that other cells that have not yet been examined systematically may also express these channels. Each year H^+ currents are reported in several new cell types.

The H^+ current density in different cells varies over approximately three orders of magnitude. The highest expression is in eosinophils, whose respiratory burst (see sect. vi*H*) is more intense than in other phagocytes (246, 360). Very few cells have been identified as having no H^+ channels. The common expression systems, CHO and HEK-293 cells, both express low levels of voltage-gated proton channels. A literature search for "lymphocyte" and "ion channel" reveals 735 publications, but until recently (886), the presence of voltage-gated proton channels had not been detected. One explanation is that H^+ currents in T lymphocytes are quite small: the whole cell current at $+60$ mV is only 1.5 pA at pH_o 7.5 and pH_i 6.0 (886) and presumably is smaller at physiological pH_i. Thus far, only COS-7 cells have been reported to lack detectable H^+ currents (668, 705).

Table 3 excludes reports that deduce the possible existence of voltage-gated proton channels from pH measurements, because of the difficulty in excluding other mechanisms, such as other proton transporters. $ZnCl_2$-inhibitable H^+ efflux in chicken enterocytes induced by phorbol esters or by an acid load might reflect voltage-gated proton channels (141, 802). A Zn^{2+}-sensitive proton influx reported in leech central neurons during recovery from an intracellular alkaline load (322) appears distinct from voltage-gated proton channels, which mainly conduct outward currents. The OK cell line has a passive proton pathway that conducts inward or outward currents and is insensitive to Zn^{2+} (376). The plasma membrane of *Elodea densa* leaves is extremely selective for H^+ at high pH, and the existence of H^+ channels has been

TABLE 3. *I_H density in cells reported to have H^+ channels*

Cell Type	Species	$I_{H,max}$, pA/pF (pH_i)	Reference Nos.
Neuron	*Helix aspersa*	4.5 (~6.8)	676
	Lymnaea stagnalis	14.6 (5.9)	136
Oocyte	*Ambystoma*	8.4 (~7.2)	70
	Rana esculenta	~32	473
Epithelium			
Alveolar	Rat	27.3 (5.5)	232
Lung A549	Human	~2 (5.5)	238
Prostate PC-3	Human	~4 (5.5)	238
Kidney HEK-293	Human	~1 (6.5)	280
Renal proximal tubule	*Rana pipiens*	<75 (6.5)	391
Ovary CHO	Hamster	1.6 (5.5)	164
Airway JME/CF15	Human	1.38* (5.3)	311
Airway gland Calu-3	Human	1.95 (5.3)	H. Fischer, personal communication
Cervical HeLa	Human	1.38 (5.3)	H. Fischer, personal communication
Connective tissue			
fibroblast 3T3	Mouse	6.75 (5.3)	H. Fischer, personal communication
Skeletal muscle			
myocyte	Human	~10 (5.5)	85
Lymphocyte			
Human T lymphocyte	Human	0.9 (6.0)	886
Human B lymphocyte	Human	94.7 (6.0)	886
Jurkat E6-1	Human	36.3 (6.0)	886
Macrophage			
Peritoneal	Mouse	~30 (6.0)	519
Alveolar	Rat	~2 (7.5)	280
Osteoclast	Rabbit	6.7 (6.0)	762
Osteoclast	Chicken	?† (7.3)	1066
THP-1 monocyte	Human	22 (5.5)	241
Granulocyte			
Neutrophil	Human	17 (6.0)	236
Eosinophil	Human	~200 (6.0)	372
Basophil	Human	~100 (5.5)	170
Mast cell	Mouse	9.6 (5.5)	574
HL-60	Human	133 (5.5)	258
K-562	Human	~5 (6.0)	238
Microglia			
Microglia	Mouse	42 (6.0)	281
Microglia	Human	?† (7.3)	670
Microglia	Rat	~66† (7.2)	1047
Microglia BV-2	Mouse	~20 (5.5)	280
Microglia GM1-R1	Rat	2–20 (5.5)	709
Microglia MLS-9	Rat	0.22 (5.5)	280

This table includes only cells in which the existence of H^+ channels was established by direct voltage-clamp studies and excludes inferences from indirect measurements such as pH changes. $I_{H,max}$ is the largest H^+ current measured in a given cell (normalized to capacitance, which reflects surface area), usually at ~150 mV positive to reversal potential (V_{rev}); $g_{H,max}$ values were converted to current at V_{rev} + 150 mV. In studies where typical values or cell size were not specified, estimates were based on data in figures and are preceded by a tilde (~), as are values from surveys including a small number of cells. All values are at room temperature (20–25°C), except where noted (*) at 37°C., † Identity of the conductance not established with certainty. [Updated from Eder and DeCoursey (280).]

proposed (687). A La^{3+}-sensitive, arachidonic acid-activatable proton conductance has been described in platelets, based on pH measurements (149). Intriguingly, aldosterone activates a proton conductance in Madin-Darby canine kidney (cultured kidney) cells that is inhibited by $ZnCl_2$ and is voltage sensitive in the sense that hyperpolarization increases H^+ influx (349). However, a large H^+ influx was observed at −90 mV with a small pH gradient (pH_o 7.4, pH_i approaching 6.7), apparently incompatible with the threshold potential ($V_{threshold}$) of voltage-gated proton channels, even in phorbol 12-myristate 13-acetate (PMA)-activated phagocytes in which $V_{threshold}$ is shifted by −40 mV (cf. Fig. 19).

D. Varieties of Voltage-Gated Proton Channels

Although voltage-gated proton channels share a number of distinctive properties, it is possible to distinguish four or five varieties based on several functional properties that are summarized in Table 4. The functional categories are certainly arbitrary but will have to suffice until proton channel molecules are definitively identified. Future structure-function studies will reveal whether the apparent differences reflect structural or regulatory differences. All voltage-gated proton channels are activated by membrane depolarization, and all are sensitive to pH. The most dramatic difference between types of H^+ chan-

TABLE 4. *Varieties of voltage-gated H^+ channels*

Type	Invertebrate: ***n*** (Neuron)	Amphibian: ***o*** (Oocyte)	Mammalian Cells		
			e (Epithelial)	***p*** (Phagocyte)	***x*** (Oxidase related)
Gated by	*V*, ΔpH	*V*, ΔpH	*V*, ΔpH	*V*, ΔpH	*V*, pH_o, pH_i, AA?, NADPH oxidase activity?
τ_{act} (at +60 mV)	Fast (2.3 ms)[a]	Medium (120 ms)[b]	Slow (4–20 s)[c]	Slower (≥5 s)[d]	Slow (1.6 s)[d]
Sigmoid activation?	No	No	Pronounced	Yes	Yes
τ_{tail} (at −40 mV)	Fast (~1 ms)	Medium (50 ms)	Medium (70 ms)[e]	Slow (200 ms)	Very slow (1 s)
τ_{tail} components	1	1	2	1	1
$[Ca^{2+}]_i$ enhances I_H?	No	?	Slight	Maybe	Yes?
Cells expressing	Snail neurons	Frog and newt oocytes	Alveolar epithelium	Microglia, neutrophils, eosinophils, mast cells, macrophages, basophils, HL-60, THP-1, CHO, PLB	Eosinophils, neutrophils, PLB cells

V, voltage (depolarization); ΔpH, pH gradient ($pH_o - pH_i$); τ_{act}, activation (channel opening) time constant (room temperature, +60 mV, "physiological" pH); τ_{tail}, tail current (channel closing) time constant (room temperature, −40 mV, "physiological" pH). The τ_{act} values are arbitrary, because activation often is not single exponential (sometimes there is an additional slow component), depends strongly on pH_i (239), and data here are not all at the same pH_i. Types ***p*** and ***x*** are probably different functional modes of the same channel rather than distinct molecules. [a] Reference 134; [b] Reference 70; [c] References 239,242; [d] Reference 246; [e] Reference 166. [Adapted and extended from Eder and DeCoursey (280).]

nels is in gating kinetics. The rates of channel opening and closing (indicated by the time constants τ_{act} and τ_{tail}, respectively, which are larger when gating is slower) vary over three orders of magnitude. The sigmoidicity of the activation time course appears to differ, but this is a subtle distinction. The H^+ channel tail current decays with two clear exponential components in alveolar epithelial cells at potentials positive to V_{rev} (166). In other cells, deactivation is well described by a single exponential, except at voltages positive to $V_{threshold}$ at which in the steady-state some channels remain open. The slower component of channel closing appears to be related kinetically to the process that governs channel opening, and both are exquisitely sensitive to pH_o, in contrast to the rapid tail current component that is weakly dependent on either pH_o or voltage (166).

The type ***x*** (oxidase-related) channel complicates the picture. This was proposed to be a distinct H^+ channel that is active only when NADPH oxidase is functioning (67c). More recent work strongly suggests that type ***x*** behavior is instead a gating mode of the type ***p*** (phagocyte) channel (see sect. VI*H2*). Several types of evidence suggest that type ***p*** channels shift into the type ***x*** gating mode upon stimulation of phagocytes with agonists that activate NADPH oxidase (165, 246–248). After removal of the stimulus, type ***x*** gating behavior sometimes gradually reverts back to type ***p*** behavior (165, 246). For these reasons, the properties of type ***x*** behavior are somewhat elusive and have not been characterized thoroughly.

The sensitivity of voltage-gated proton channels to $[Ca^{2+}]_i$ is controversial and is discussed in more detail below (see sect. VI*B2*). Although modulatory effects have been reported (372, 895), it is clear that most voltage-gated proton channels are not Ca^{2+} activated (134, 739, 886). A Ca^{2+}-activated H^+ current in HEK-293 cells transfected with the gp91^{phox} homolog *Nox*5 has been reported but not characterized (67b).

E. High Proton Selectivity

Measurement of the V_{rev} of voltage-gated proton currents at various pH indicates extremely high H^+ selectivity. The relative permeability of H^+ to other cations can be demonstrated by comparing V_{rev} with the Nernst potential for H^+, E_H (751), or by comparing the slope of V_{rev} values as a function of ΔpH. In most studies there is not perfect agreement between V_{rev} and E_H and the slope of the V_{rev} versus E_H relationship is more often 40–50 mV/unit pH (85, 134, 232, 242, 258, 281, 519, 668, 710, 762, 886, 895), or even <40 mV/unit (259, 391, 574, 641), than near the ideal (at 20°C) of 58 mV/unit (70, 164, 166, 170, 241, 247, 372, 518). However, in part because $[H^+]$ is 4–7 orders of magnitude smaller than the concentration of the predominant cation, the relative permeability of H^+ to the other cations when calculated by the GHK voltage equation (368, 444, 456) is typically $>10^6$ (166, 170, 237, 238, 241, 242, 247, 258, 372, 519, 886), and is as high as 2×10^8 in deuterium solutions (242). Even though these permeability ratios are impressive, they probably underestimate the true selectivity of H^+ channels. In fact, they should not be taken to reflect finite permeability of the H^+ channel to other cations. Most telling is that the measured V_{rev} does not change when the predominant cation or anion in the solution is changed, once one corrects for liquid junction potential differences (70, 85, 236, 237, 258, 281, 372, 473, 519, 574, 641, 830). Most likely, small deviations of V_{rev} from E_H reflect experimental error in measuring V_{rev},

a contribution from leak current, or imperfect control over pH, rather than genuine permeability of H^+ channels to other cations.

In principle, it is difficult to distinguish between conductance of protons per se or proton equivalents, such as H_3O^+ permeation or flux of OH^- or HCO_3^- in the opposite direction. The Nernst potential for OH^- is always equal to that for H^+. However, several types of evidence indicate that the current carried through voltage-gated proton channels is in fact a proton current.

The maximum conductance ($g_{H,max}$) increases when pH_i is decreased, consistent with the increase in $[H^+]$ on the side of the membrane from which the current flows, whereas intracellular $[OH^-]$ decreases and extracellular $[OH^-]$ (the source of any OH^- current) is not changed. The increase is less than proportional to the change in $[H^+]$ (see sect. v*F*).

The proton conductance decreases almost 50% when deuterium replaces water (242). In terms of the classical square-root dependence of reaction rates on the mass of the reactants (366), one would predict isotope effects of 41% (for D^+ vs. H^+) and 3% (for OD^- vs. OH^-). The same argument speaks against bodily (hydrodynamic) permeation of H_3O^+, which compared with D_3O^+ has a predicted isotope effect of only 8% (242).

The extremely high selectivity can be explained readily if the conduction pathway is a HBC (see sect. III*D*) but is difficult to explain if the H^+ channel is a water-filled pore. There is strong evidence that the pathway is a HBC; this mechanism permits H^+, but not H_3O^+ permeation.

Indirect but compelling evidence thus supports the conclusion that the permeating ionic species is the proton (H^+) and not the hydronium ion (H_3O^+) or an anion like OH^- moving in the opposite direction. If the proton channel were a HBC and the transported species were OH^-, then the actual mechanism of transport would still comprise H^+ hopping in the same direction across the membrane, but from H_2O to OH^-. This would result in net OH^- translocation in the opposite direction.

F. Anomalously Weak Dependence of g_H on H^+ Concentration

The expectation of the GHK equation is that the single-channel H^+ current should be proportional to $[H^+]$ and should thus increase 10-fold/unit decrease in pH. Figure 13 shows that this prediction is borne out for several proton-conducting channels, but not for others. The $g_{H,max}$ increased only ~2-fold/unit decrease in pH_i in essentially every whole cell study of voltage-gated proton currents in which the data permit such a comparison (summarized in Fig. 1 of Ref. 234), with the exceptions of a 2.5-fold/unit increase in human basophils (170) and a 3-fold/unit increase in human lymphocytes (886). This remarkable property was confirmed directly in inside-out patches from alveolar epithelial cells. Compared in the same patch of membrane, the H^+ conductance increased only 1.7-fold/unit decrease in pH_i (239). This anomalously weak dependence of g_H on $[H^+]$ has been interpreted to indicate that the rate-determining step in conduction occurs within the H^+ channel itself (234, 238, 239).

Surprisingly, single H^+ channel currents appear to depend more strongly on $[H^+]$ than macroscopic currents (168). The unitary H^+ conductance, based on H^+ current noise (see sect. v*G*), increased approximately fourfold at pH_i 5.5 compared with pH_i 6.5 in excised patches from human eosinophils (168). Because the macroscopic $g_{H,max}$ increases only ~2-fold/unit, the number of functional channels must decrease substantially at lower pH_i. Evidently intracellular protons inhibit H^+ channel function, in a sort of self-inhibition. Although these single-channel data still indicate a less-than-proportional dependence of H^+ current on $[H^+]$, the discrepancy has been attenuated.

G. Small Unitary Conductance

Proton channels at physiological pH have a very small conductance. To some extent, the small unitary conductance may reflect the tiny concentration of the permeant ion H^+. Extrapolating the H^+ current of single gramicidin channels, which at low pH conduct larger H^+ currents than any other channel (see sect. IV*A2*), to pH 7 (Fig. 13) indicates a predicted current of 44 aA (aA = attoampere = 10^{-18} amperes). This value is far too small to be detectable directly by present technology. The estimated conductance of voltage-gated proton channels is in fact about an order of magnitude larger, and recently, apparent single-channel H^+ currents in the range 5–15 fA were observed by direct electrical recording at low pH_i (5.0 or 5.5) (168).

The single-channel conductance can also be estimated from current variance analysis. Early attempts to resolve H^+ channel gating-induced current fluctuations (85, 136, 236) met with limited success, due to poor signal-to-noise ratios (S/N). Byerly and Suen (136) established an upper bound at <50 fS at pH_i 5.9 (136). No excess fluctuations were seen (S/N = 0), but the data had to be filtered at 1 kHz because of the rapid gating kinetics in snail neurons. Bernheim et al. (85) filtered at 5 kHz, and from a 6% reduction of variance in the presence of Cd^{2+} (S/N = 0.06), estimated 90 fS at pH_i 5.5 (85). DeCoursey and Cherny improved the S/N ratio to 0.5 and estimated the unitary conductance to be ~10 fS at pH_i 6.0 in human neutrophils (236). Distinct excess fluctuations (presumably generated by H^+ channel gating) were detected at 200 Hz but not 2-kHz low-pass filtering. All of these estimates are compromised by poor S/N ratios and should be considered very rough.

More recently, we have exploited the very slow gating in human eosinophils, combined with appropriate filtering, to improve the S/N ratio to >100 routinely, and sometimes >1,000 (168). Distinct excess fluctuations ascribable to H^+ channel gating can be seen at voltages where H^+ current is activated (Fig. 15). At low pH_i the variance was maximal near the midpoint of the g_H-V relationship, precisely as expected from the simple assumption that gating events (random opening and closing of channels) are most frequent when half the channels are open, decreasing with further depolarization because most channels stay open most of the time. This behavior strongly supports the idea that the noise is generated by H^+ channel gating. These recent estimates place the unitary H^+ channel conductance at 30–40 fS at pH_i 6.5 and perhaps four times higher at pH_i 5.5 (168).

Although the conductance of H^+ channels is miniscule compared with other ion channels, in view of the low concentration of protons at physiological pH, the conductance seems implausibly large. Estimated unitary H^+ currents are an order of magnitude greater than the diffusion limit (Fig. 13). Mechanisms that might reconcile this apparent paradox are discussed elsewhere (see sect. IV*P*). Judged solely on their conductance, voltage-gated proton channels cannot be distinguished from carriers. For example, the H^+ efflux through Na^+/H^+ antiporters at pH_i 6.0 at their maximum turnover rate in human fibroblasts is equivalent to 0.5–1.7 fA (927). Nevertheless, the presence of H^+ current fluctuations provides strong evidence of gating, a defining property of ion channels, and thus support for the designation of voltage-gated proton channels as ion channels.

H. Strong Temperature Dependence

Voltage-gated proton channels are extraordinarily sensitive to temperature (136, 170, 243, 574). Both the open-channel conductance and the kinetics of gating have higher temperature sensitivity than almost any other ion channel. In a survey of voltage-gated proton channels in six cell types, the time course of H^+ current activation was fit by a single exponential after a delay to obtain τ_{act} and deactivation was fit with a single exponential to obtain the closing time constant τ_{tail}. Surprisingly, the delay, τ_{act}, and τ_{tail} all had Q_{10} values of 6–9 (243). The Q_{10} is the relative change in rate for a 10°C increase in temperature; these values correspond with activation energies of 30–38 kcal/mol. Only 1 of 24 studies of gating of other ion channels reported a higher value (825). The large Q_{10} suggests that gating involves substantial conformational changes in the channel. The similarity of temperature sensitivity of the three gating parameters was surprising, because they had been envisioned as reflecting different, if overlapping, kinetic processes. The delay presumably reflects transitions between closed states; τ_{act} is slow and must reflect the entire opening process that by analogy with other voltage-gated channels might require conformational changes in multiple channel subunits, whereas τ_{tail} ought to reflect the first closing step. Nevertheless, the similar activation energies for these three processes,

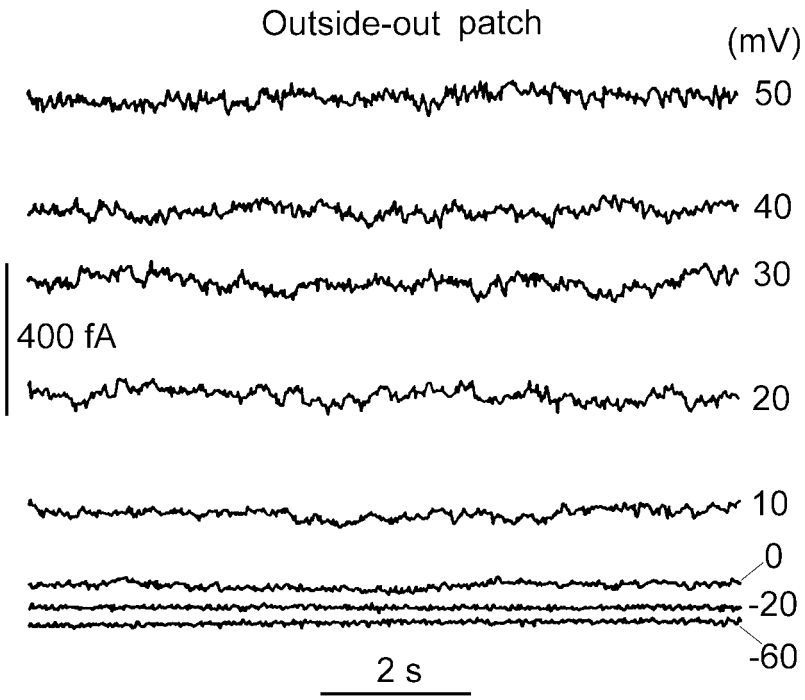

FIG. 15. Membrane current fluctuations recorded in an excised outside-out patch of membrane from a rat alveolar epithelial cell. The current fluctuation (noise) is clearly greater at voltages where the g_H is activated, at 0 mV and more positive. Currents at various voltages are shown on the same absolute scale without correction for leak; the distance between the records at −60 and −20 mV, both subthreshold, reflects a seal resistance of ~900 GΩ. Filter, 20 Hz; pipette solution, pH 6.5; bath solution, pH 6.0 (V. V. Cherny and T. E. DeCoursey, unpublished data.)

30–38 kcal/mol, suggest that the same kinetic process underlies each. This might occur if H^+ channel gating occurred generally as in the Hodgkin-Huxley model for K^+ and Na^+ channels (454). Each H^+ channel might have several subunits, each of which must undergo a kinetically similar first-order conformational change during opening, whereas closing would occur as soon as one subunit underwent the reverse transition.

It is more difficult to determine the temperature dependence of the open-channel conductance, for several reasons. One must distinguish between gating and conductance. A Q_{10} of 9.9 reported for the g_H in mast cells (574) is an overestimate that reflects a complex mixture of smaller conductance and less complete activation of H^+ channels at lower temperatures. In this study, the H^+ current was measured at the end of a voltage ramp of fixed duration applied at different temperatures; at low temperature a much smaller number of H^+ channels would open by the end of the depolarizing voltage ramp. It is difficult to achieve steady-state H^+ current at low temperature even with long pulses, because of the slow activation of H^+ current (τ_{act} can be >100 s). The pH changes due to large H^+ fluxes cause droop and distortion of the current, especially at high temperatures. Single-channel H^+ currents have not been estimated at different temperatures and would be technically difficult to resolve. It is therefore necessary to make assumptions, the most significant of which is that increasing the temperature does not change the number of channels that open during a depolarizing pulse (P_{open}, if the total number of channels is constant). The g_H-V relationship is either unchanged or may shift negatively by ~10 mV at high temperature, and all kinetic parameters scale with temperature (243), suggesting that no qualitative changes in gating occur. More convincing is evidence from noise analysis that indicates that P_{open} reaches ~0.95 during large depolarizations at pH_i 5.5 at 20°C (168), which means that any increase in P_{open} at high temperature could not exceed 5%. Correction for the temperature dependence of the pK_a of buffer slightly decreased observed Q_{10} values (243).

With all of these caveats in mind, the g_H is still strongly temperature sensitive. The Q_{10} was 2.1 in snail neurons (136) and 2.1–3.1 in whole cell studies in six mammalian cell types (243). The temperature sensitivity was greater in excised patches, perhaps because there is less propensity toward H^+ depletion during large currents. The Q_{10} in patches was 2.8 at >20°C (18.3 kcal/mol) and 5.1 at <20°C (27 kcal/mol). The temperature dependence of several processes external to the channel (buffer diffusion, H^+ diffusion) is expected to be much weaker than this, suggesting that permeation itself is rate determining (243). One possible exception is protolysis, donation of a proton from neutral water to the channel, which has a Q_{10} of ~2 (371). The Q_{10} for H^+ conductance is larger than in any of 20 studies of other ion channels (references in Ref. 243), indicating that H^+ permeation through voltage-gated proton channels is more demanding than ion permeation through most ion channels, presumably reflecting the HBC conduction mechanism. The Q_{10} values for all proton channels in Table 1 that are not water-filled pores are substantially higher than typical values for ordinary ion channels, ~1.2–1.5.

The biological implication of the extraordinary temperature sensitivity of voltage-gated proton channels is that at body temperature H^+ channels open much faster and conduct far more current than at room temperature. With the assumption of a Q_{10} value of 2.8, the $g_{H,max}$ at 37°C would be 5.8 times larger than that measured at room temperature. Although a τ_{act} of 1 s at room temperature seems very slow, if Q_{10} is 8, τ_{act} is 30 ms at 37°C.

I. Large Deuterium Isotope Effects

Most ion channels are only subtly affected by heavy water, typically exhibiting a slightly lower conductance and slightly slower gating. Voltage-gated proton currents are more sensitive to deuterium, a result that perhaps is not surprising in light of H^+ or D^+ being the permeating ion species, as well as the profound sensitivity of H^+ channel gating to pH. The currents in deuterium are qualitatively similar to those in water, indicating that the channels are permeable to D^+ and continue to exhibit voltage- and time-dependent gating. Quantitatively, the current is 1.9 times larger in H_2O than D_2O; the activation time constant τ_{act} is 3-fold slower in D_2O; the deactivation time constant τ_{tail} is hardly changed, being 1.0–1.5 times slower in D_2O; and the position of the g_H-V relationship appears similar in both solvents (242).

The isotope effect on permeation through most ion channels is similar to the isotope effect on the conductivity of the ion in bulk aqueous solution (references in Ref. 242). In contrast, the 1.9-fold larger H^+ current than D^+ current in voltage-gated proton channels is much larger than the ratio of mobilities or conductivities of H^+/D^+ in bulk solution, which are consistently 1.390–1.404 when measured electrically (65, 325, 612, 624), 1.32–1.35 in recent measurements (172), and slightly higher, 1.43–1.52 when measured polarographically (844). These values correspond with *process 3* in Figure 16. The isotope effects for dielectric relaxation and for viscosity are also substantially weaker than this (180, 412). The low D^+ conductance suggests that *1*) the rate-determining step in conduction occurs within the channel, and *2*) the conduction pathway is a HBC and not a water-filled pore (242) (see sect. v*J*).

The slower activation of H^+ current in D_2O is consistent with a rate-limiting step in channel opening being deprotonation of a site on the channel, as we proposed previously (166) (see sect. v*M*) (Fig. 20). The pK_a of most

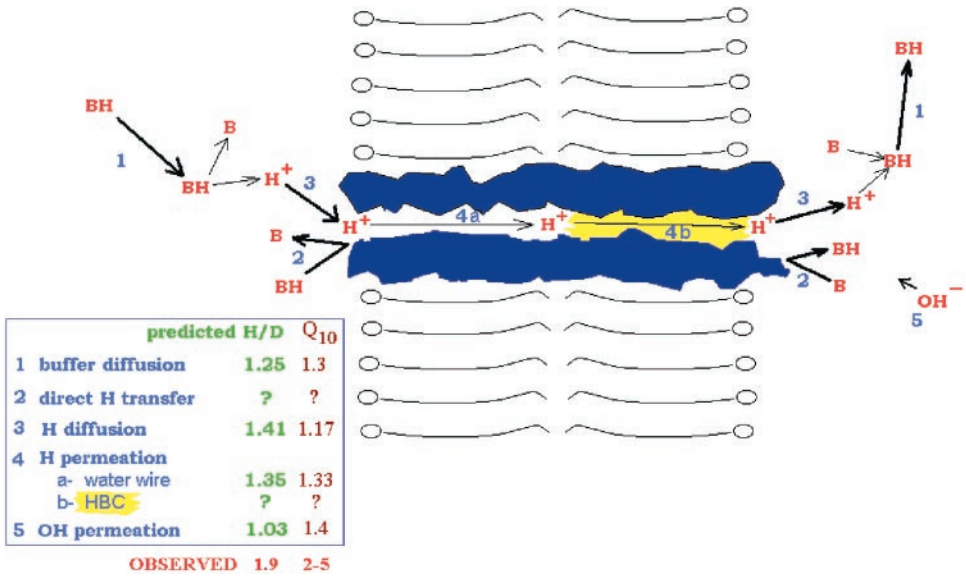

FIG. 16. Diagram illustrating the various processes that occur when H^+ current flows through a proton channel. Many biophysical measurements on voltage-gated proton channels have been directed toward determining the rate-limiting process. *Inset*: predicted values for the deuterium isotope effect (predicted ratio in H_2O to that in D_2O) and the Q_{10} for H^+ current if each step, in turn, were rate determining. The predicted value for the isotope effect on buffer diffusion (*step 1*) is based on the higher viscosity (412), and H^+ diffusion (*step 3*) is based on the relative conductivity (65, 325, 612, 624, 844). The isotope effect for *step 5* assumes a square-root dependence on the masses of OH^- vs. OD^- (366). Both the isotope effect and temperature dependence of *step 4a* are based on measurements of H^+ current through gramicidin channels (14). The Q_{10} predictions are based on the temperature dependence of the viscosity of water (300, 813) (*step 1*), the temperature dependence of H^+ mobility (606) and conductivity (786, 845) (*step 3*), and the conductivity of KOH solutions (628) (*step 5*). Observed values for voltage-gated proton channels are from Refs. 242, 243. See text for further details.

carboxylic and ammonium acids increases in D_2O by 0.5–0.6 units (894), because deuterons generally are held more tightly than protons. If the pK_a of the putative external regulatory protonation site were increased by 0.5 units, this would slow activation by threefold. The minimal slowing of deactivation in D_2O, in contrast, suggests that if deprotonation of a regulatory site occurs during channel closing, it is not rate determining. Alternatively, the chemical nature of the site might be different; sulfhydryl acids tend to exhibit smaller pK_a changes (894). In view of the different sensitivity of τ_{act} and τ_{tail} to D_2O, it was surprising that the overall g_H-V relationship did not shift. In the oversimplified case of a two-state channel, slowing the opening rate more than the closing rate ought to shift the g_H-V relationship toward more negative voltages. Not only was no such shift detected, there was remarkable similarity between the relationship between V_{rev} and $V_{threshold}$ in both H_2O and D_2O (+ and ○, respectively, in Fig. 19). This paradox awaits explanation.

J. What Is the Rate-Determining Step in Conduction?

This question provides a useful framework for evaluating such properties as deuterium isotope effects and temperature dependence, as illustrated in Figure 16. Following Andersen's lucid analysis of the determinants of ionic currents through gramicidin channels (27, 30), we can identify various steps that must occur. The fact that almost all protons are not free ions, but are bound to buffer or are constituents of H_2O, increases the complexity of the problem compared with ordinary ion channels. It is necessary to consider several additional requisite processes, any of which could conceivably affect the rate of conduction. These include diffusion of protonated buffer, BH (*step 1*), and direct proton transfer from BH to a site at the mouth of the channel (*step 2*). Complementary processes that occur at the distal end of the channel could also be involved. *Steps 4a* and *4b* indicate that conduction through the channel could occur by two qualitatively different mechanisms, diffusion through a water-filled pore like an ordinary ion channel (*step 4a*) and transmission through a HBC (*step 4b*). Figure 16, *inset*, gives estimates of the deuterium isotope effect and Q_{10} expected if each process in turn were rate determining.

The effects of buffer, deuterium, and temperature eliminate all processes occurring in the bulk solution (*steps 1–3*) from being rate determining. Direct proton transfer (cf. Fig. 1) from protonated buffer (BH) to a site at the entry of the channel (*step 2*) can be ruled out

because when either external or internal buffer concentrations were varied over a range 1–100 mM, the H^+ current amplitude changed less than twofold (240). The deuterium isotope effect on conductance, $I_H/I_D = 1.9$, is larger than for buffer diffusion (*step 1*), free H^+ diffusion (*step 3*), and for the H^+ current through the gramicidin channel (*step 4a*) (14), which we use as a prototypical ion channel of the water-filled pore variety (310, 611). An objection to this analysis is that it is widely felt that water inside ion channels is likely to be constrained and might behave more like ice (see sect. III*E*), where the isotope effect is reportedly much higher than in liquid water (289, 575). Gramicidin provides a counterexample, because its H^+-to-D^+ ratio is only 1.20–1.37 (14, 172) (see sect. IV*A5*), similar to that in bulk solution (see sect. V*I*). The profound sensitivity of H^+ currents to temperature provides more dramatic evidence that the pathway through the pore is not likely to be a water wire. The Q_{10} for macroscopic currents was >2 and in excised patches at low temperatures was as high as 5 (243), far beyond that expected for any of the steps in Figure 16. The overwhelming conclusions from this analysis are that *1*) the rate-limiting step in H^+ permeation occurs within the pore and *2*) the pathway is most likely a HBC comprising at least one titratable amino acid residue.

One additional conclusion can be drawn from this analysis. The possibility that what we consider to reflect outward H^+ current might instead be OH^- moving inward is contradicted by both the large isotope effect and the profound temperature dependence.

K. Voltage-Dependent Gating

The voltage dependence of H^+ channel gating is not absolute, but is strongly modulated by pH, as discussed in section V*L*. Figure 3 shows that the voltage dependence of gating is monotonic. H^+ channels are closed at negative voltages and open and conduct current upon depolarization and continue to do so over a range of >380 mV. This property is typical for ion channels and is strong evidence that the H^+ channel is an ion channel rather than a carrier (see sect. III*C*).

Like delayed rectifier K^+ currents, H^+ currents rectify outwardly in the steady state, and this rectification is the result of strongly voltage-dependent gating. Although open H^+ channels can carry inward or outward current, the channels open only at depolarized voltages where H^+ current is outward (excepting type ***x*** behavior). The single open-channel current-voltage relationship has not been measured directly but can be approximated by the macroscopic "instantaneous" current-voltage relationship. In the conventional "tail current" analysis (455), a depolarizing prepulse is applied to open H^+ channels, and then the membrane potential is stepped to a range of voltages. The instantaneous current at the start of the test pulse passes through the same number of open channels, but with a different driving force ($V - E_H$). At negative voltages where the channels close, the instantaneous current is often obtained by extrapolating a fitted exponential curve back to the start of the test pulse. The instantaneous current-voltage relationship of voltage-gated proton channels was either linear (70, 241, 391, 473, 641, 710) or exhibited moderate outward rectification at symmetrical pH (134, 166, 242, 258). Similarly, the instantaneous current-voltage relationship was either linear (391, 518) or exhibited moderate outward rectification (85, 237, 241, 519, 709) with an outward ΔpH ($pH_i < pH_o$). It is abundantly clear that open voltage-gated proton channels conduct inward and outward current almost equally well.

The steepness of the voltage dependence of the g_H can be estimated in one of two ways. If one makes the simplest possible assumptions that the channel has a single closed and single open state and the open-channel current-voltage relationship is linear, then the g_H-V relationship may be describable by a Boltzmann function

$$\frac{g_H}{g_{H,max}} = \frac{1}{1 + \exp\frac{V - V_{1/2}}{k}} \quad (3)$$

where $g_{H,max}$ is the maximum attainable g_H, $V_{½}$ is the midpoint potential at which half the available channels are open, and k is a slope factor that indicates the steepness of the voltage dependence. In a variety of cells, the slope factor of such fits is generally 7–14 mV, indicating a net movement of 1.8–3.6 charges across the membrane field (238). As is evident in Figure 17, this model is almost certainly an oversimplification, and as discussed in section V*M*, at least four chemically and conformationally distinct gating states must be postulated to account for pH- and voltage-dependent gating. A more reliable method for evaluating the movement of charges in the channel molecule during gating is to determine the limiting slope of the g_H-V relationship plotted semi-logarithmically (18, 930). The reliability of this estimate increases as the range of P_{open} is extended. By combining macroscopic with single-channel measurements, a range of P_{open} down to 10^{-7} has been achieved for other voltage-gated channels (450, 482). Such estimates have provided evidence that the gating charge movement is much larger than had been thought previously, up to 12–14 charges per channel for voltage-gated sodium and potassium channels (450, 482). Because single H^+ channel currents are too small to record reliably using current technology, the range of P_{open} that has been explored is limited to $<10^{-3}$. At this limit, g_H changes *e*-fold/4.65 mV, which corresponds with 5.4 gating charges and should be regarded as a lower limit (242). Thus voltage-gated proton channels are at least half as steeply voltage dependent as traditional ion channels.

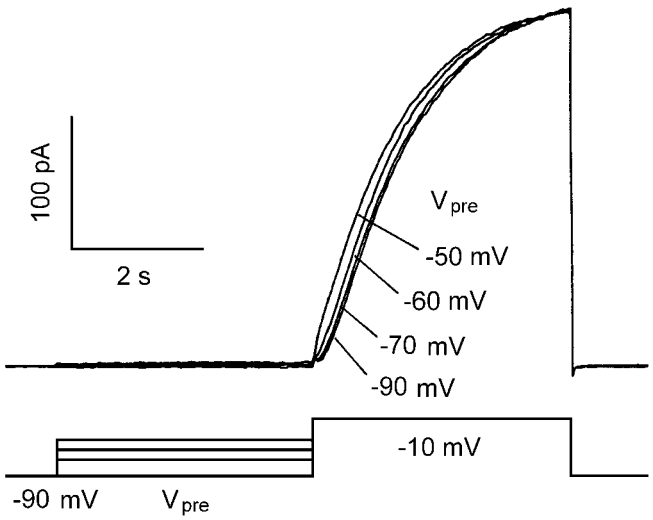

FIG. 17. Evidence that voltage-gated proton channels have multiple closed states. Prepulses to large negative voltages increase the sigmoidicity of turn-on of H^+ current during a depolarizing pulse to −10 mV. After more negative prepulses, there is a distinct delay before the H^+ current turns on. Currents were recorded in an alveolar epithelial cell at pH_o 8.0 and pH_i 6.5, with both external and internal solutions containing tetramethylammonium methanesulfonate and 100 mM buffer (tricine and Bis-Tris at pH 8.0 and 6.5, respectively). [From DeCoursey and Cherny (238), copyright 1994 Springer-Verlag.]

Voltage-gated proton channels do not inactivate. When large, prolonged H^+ currents are elicited, the currents decay or droop (68, 232, 236, 238, 258, 372, 473, 519, 676, 709, 895, 1006, 1008). However, careful examination of this phenomenon reveals that H^+ current decay is not the result of inactivation (channels entering a long-lived closed state), but is the result of increased pH_i due directly to H^+ efflux (see sect. VI*A*), which progressively shifts E_H to more positive voltages, reducing the driving force for H^+ current.

One of the features that distinguishes various types of voltage-gated proton channels is gating kinetics (Table 4). The primordial (type ***n***) H^+ channels in snail neurons open within a few milliseconds after depolarization (134). The intriguing question whether rapid gating is a property of neurons or snails awaits measurement of H^+ current in mammalian neurons. Mammalian H^+ channels open much more slowly, with activation time constants (τ_{act}) in the range of seconds to tens of seconds at room temperature (85, 163, 164, 170, 232, 236, 239, 241, 246, 311, 372, 518, 519, 574, 762, 886). The slowest H^+ channels to open are type ***p***. The rate of channel closing (essentially the inverse of τ_{tail}) is similarly variable and ranges over three orders of magnitude. Type ***n*** channels are again the fastest, but the sequence of types ***p*** and ***x*** are switched. When type ***p*** channels are stimulated and adopt type ***x*** gating behavior, τ_{act} becomes faster and τ_{tail} becomes slower (246–248).

We initially resisted fitting the time course of H^+ current activation with a simple function. No Hodgkin-Huxley-type gating parameter raised to a constant exponent fitted the data at all voltages in rat alveolar epithelial cells (166), although an exponent of 1.5–2.0 provided a reasonable fit in human neutrophils (236). In addition, we were concerned that depletion of buffer and resulting pH_i changes during pulses would distort and compromise the observed time course. Instead, we quantified the maximum rate of rise (237). However, the usefulness of having a simple, easily-defined parameter that embodies at least generally the rates of gating outweighed such concerns, and we now generally fit both activation and deactivation with exponential functions. The activation time course is sigmoid in most cells, which can be accommodated by introducing an initial delay. Sometimes an additional component of H^+ current increases very slowly (246). For all of these reasons, the values obtained for τ_{act} are somewhat arbitrary.

The voltage dependence of H^+ channel gating kinetics has been reported only sporadically. Data that exist are summarized in Table 5, expressed as the voltage required to change the time constant *e*-fold. The underlying assumption that τ_{act} and τ_{tail} are exponentially dependent on voltage is arbitrary but appears to be justified empirically (166, 170, 241, 243, 246). The values obtained in various cells are remarkably similar. It is evident that τ_{act} has a weaker voltage dependence than does τ_{tail}. In studies reporting deactivation kinetics, the tail current decay is monoexponential, with one exception. As was indicated in Table 4, H^+ currents in rat alveolar epithelial cells exhibit a distinct slower decay component between V_{rev} and $V_{threshold}$ (166). The faster component has similar voltage dependence to τ_{tail} in other cells. The slow component, in contrast, is very steeply voltage dependent and appears kinetically related to activation (see sect. V*L*); τ_{act} and τ_{tail} of the slower component are similar in absolute value at comparable voltages (166).

TABLE 5. *Voltage dependence of H^+ channel gating kinetics*

Cell	τ_{act}, mV/*e*-fold	τ_{tail}, mV/*e*-fold	Reference Nos.
Ambystoma oocyte	72	39	70
Rat alveolar epithelium		35–40 (Fast)	166
Rat alveolar epithelium		8–15 (Slow)	166
Rat alveolar epithelium	46–64		243
Human neutrophil		39–44	243
Human basophil	54	42	170
Human eosinophil	58.7	32.2	246
THP-1 macrophage	40	38	241
Jurkat lymphocyte		26	886

Values indicate the change in voltage required to produce an *e*-fold change in τ (which reflects the slope of the τ-*V* relationship), assuming exponential dependence on voltage. Inspection of data from mouse macrophages (518) suggests that τ_{act} has a weaker voltage dependence than does τ_{tail} in these cells as well.

L. pH Dependence of Gating

One of the most important properties of voltage-gated proton channels is their exquisite sensitivity to pH. Although H^+ channel gating is steeply voltage dependent, the position of the voltage-activation relationship depends strongly on both pH_o and pH_i. In all cells studied, the voltage-activation curve is shifted toward more negative voltages (thus promoting channel opening) when pH_o increases or pH_i decreases. The practical consequence of this pH sensitivity is that H^+ channels open only when the electrochemical gradient is outward, when outward current will result (1007). One exception is type ***x*** channel behavior seen in phagocytes when NADPH oxidase is active (see sects. v*D* and vi*H2*). The general implication of this pH regulation is that voltage-gated proton channels evidently function to extrude acid from cells.

A systematic study in rat alveolar epithelial cells revealed that the voltage-activation curve could be predicted from the pH gradient, $\Delta pH = pH_o - pH_i$ (166). The current-voltage relationships in Figure 18 illustrate that there is a shift of precisely 40 mV/unit change in ΔpH, whether this is accomplished by changing pH_o or pH_i. The ΔpH dependence is equivalent to saying that pH_o and pH_i have equal and opposite effects on gating. Because the g_H-V relationship is rarely a tidy Boltzmann function, its position is difficult to quantify accurately. As a practical solution, we determine the position of the voltage-activation relationship from the $V_{threshold}$ defined as the most negative voltage at which detectable H^+ current is activated. If other time-dependent conductances are absent, due to omission of permeant ions from the solutions or inclusion of blockers, then the onset of time-dependent current occurs at $V_{threshold}$. Empirically, $V_{threshold}$ in alveolar epithelial cells is given by (242)

$$V_{threshold} = 0.76\ V_{rev} + 18\ mV \quad (4)$$

The data that formed the basis for this relationship are plotted in Figure 19 as (+). An earlier formulation, $V_{threshold} = 40\Delta pH + 20$ mV (166), describes a similar relationship, but in terms of the nominal applied ΔpH. Because the actual ΔpH is more accurately defined by the observed V_{rev}, the relationship in *Equation 4* is more generally applicable.

The relationships just discussed apply to voltage-gated proton channels in rat alveolar epithelial cells over a wide pH range (pH_i 5.5–7.5 and pH_o 6–8). At pH_o >8.0, the shift of $V_{threshold}$ appears to saturate, which could indicate the approach of pH_o to the pK_a of the external regulatory protonation site (166). Quite similar apparent saturation was observed in snail neurons (134) and *Ambystoma* oocytes (70) when pH_o was increased from 7.4 to 8.4. However, a subsequent study in which the range was extended to pH_o 10 (242) revealed a peculiar phenomenon. The shift in the g_H-V relationship between pH_o 8 and 9 again was small, and there was no shift between pH_o 9 and 10. However, V_{rev} was found to deviate substantially from E_H at high pH_o. V_{rev} was close to E_H from pH_o 6 to 8, but there was only a small shift in V_{rev} at pH_o 9, and no shift between pH_o 9 and 10. Similarly, Byerly et al. (134) observed an anomalously small shift in V_{rev} when pH_o was increased to 8.4. Taken at face value, these results indicate that the apparent saturation of both V_{rev} and $V_{threshold}$ are artifacts of our inability to control pH. Strikingly, a plot of V_{rev} versus $V_{threshold}$ (Fig. 19, + and ○) was linear over the entire pH range, without the slightest hint of saturation at either ΔpH extreme. Because it seems improbable that pH_o (in an effectively infinite bath volume, with 100 mM buffer) could deviate far from its nominal value, pH_i must increase when pH_o is increased above 8 (242). One speculative explanation is the action of a Cl^-/OH^- exchanger (603, 975, 1044) that is active at very high pH_o.

Although qualitatively similar pH dependence occurs in other cells, analogous relationships have not yet been defined quantitatively. Figure 19 includes data from a large number of studies on a variety of cells. For studies done in conventional whole cell configuration, each cell type is labeled with a letter. These data exhibit some scatter, but in general they fall near the linear relationship observed for alveolar epithelial H^+ channels. The solid line in this graph shows the linear regression on all the data plotted and is defined by a relationship remarkably similar to *Equation 4*

$$V_{threshold} = 0.79\ V_{rev} + 23\ mV \quad (5)$$

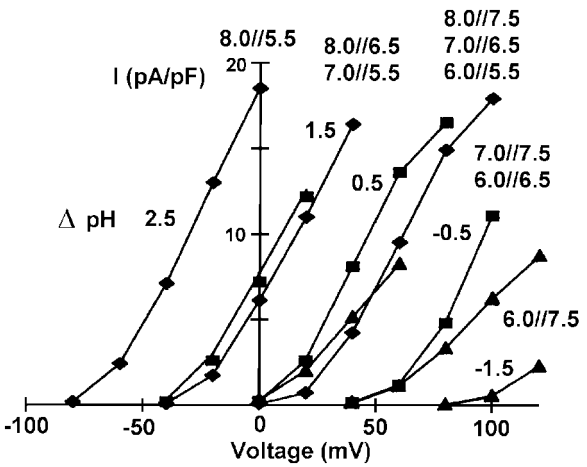

FIG. 18. Current-voltage relationships at a range of pH_o and pH_i reveal that the position of the voltage-activation curve is determined by the pH gradient, $\Delta pH = pH_o - pH_i$. Mean H^+ current measured at the end of 4-s pulses is plotted for cells studied at various pH_o and pH_i and normalized to cell size (capacitance). Symbols indicate pH_i 5.5 (◆), 6.5 (■), and 7.5 (▲), and the labels follow the convention pH_o//pH_i. [Modified from Cherny et al. (166).]

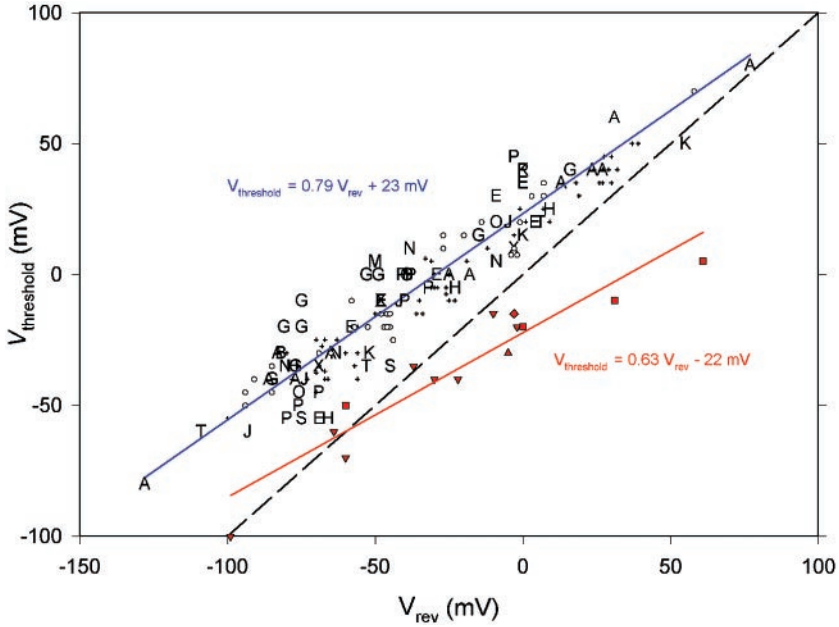

FIG. 19. Relationship between threshold potential ($V_{threshold}$) and reversal potential (V_{rev}) for all existing data on voltage-gated proton channels. The dashed line indicates equality between $V_{threshold}$ and V_{rev}. Data above the line indicate that only outward currents will be activated, whereas data below the line indicate that inward H^+ currents should be detected just negative to V_{rev}. Red symbols are from phagocytes under conditions in which NADPH oxidase was active: in permeabilized patch studies (human eosinophils, ▲, Ref. 165, and ▼, unpublished data of the same authors), (human neutrophils, ♦, Ref. 248), or in whole cell configuration with NADPH in the pipette (human eosinophils, ■, Ref. 67c). Data from conventional whole cell studies are plotted as letters, which indicate cell type as follows: A, rat alveolar epithelium (166, 232); C, CHO (164); B, peripheral blood monocytes (742); E, human eosinophil (165, 372, 895); G, rat or mouse microglia (281, 546, 710); H, HL-60 cells differentiated with DMSO (258, 830); J, Jurkat human lymphocyte (886); K, frog renal proximal tubule (391); M, mouse mast cell (574); N, snail neuron (134); O, rabbit osteoclast (762); P, mouse macrophage (518, 519, 977); S, human skeletal myotube (85); T, THP-1 cells (241); X, HEK-293 cells transfected with NOH-1 (67a). Also plotted are data in rat alveolar epithelial cells in water and in deuterium solutions (+ and ○, respectively) studied at various pH_o, pH_i, and in the presence of NH_4^+ gradients to alter pH_i (242). The solid blue line indicates the relationship obtained by linear regression for all whole cell data plotted and is described by $V_{threshold} = 0.79\ V_{rev} + 23$ mV. The relationship found previously for alveolar epithelial cells was $V_{threshold} = 0.76\ V_{rev} + 18$ mV (242). The red line shows the relationship obtained by linear regression on all permeabilized-patch data and is described by $V_{threshold} = 0.63\ V_{rev} - 22$ mV. Data plotted here were compiled from cited values or from figures illustrating mean values in some cases, but individual representative cells in others.

In most studies, the relationship roughly paralleled the line for all data, suggesting that to a first approximation, all voltage-gated proton channels have identical ΔpH-dependent gating. Data from all classes of voltage-gated proton channels are represented in this figure, with the exception of oocytes, which were excluded because pH_i was not known. Nevertheless, their pH_o dependence appears to be qualitatively similar (70, 473), and thus the four classes of voltage-gated proton channels other than type ***x*** (see below) share astonishingly similar ΔpH-dependent gating. It is noteworthy that nearly every data point falls above the dashed line that indicates $V_{threshold} = V_{rev}$. Thus, within the physiological pH range, voltage-gated proton channels open only when there is an outward electrochemical gradient, i.e., when outward H^+ current will occur. This universal property leads inescapably to the conclusion that the main function of voltage-gated proton channels is to extrude acid from cells.

Although $V_{threshold}$ shifts 40 mV/unit change in ΔpH, V_{rev} changes more steeply. As a result, at large positive voltages, $V_{threshold}$ approaches V_{rev}. Extrapolation of the relationship in Figure 19 (*Eq. 5*) predicts that with a very large inward ΔpH, $V_{threshold}$ should be negative to V_{rev}. With a large inward ΔpH of −1.5 units, $V_{threshold}$ is in fact very close to V_{rev} in alveolar epithelial cells (166), and $V_{threshold}$ was slightly negative to V_{rev} in renal proximal tubule cells (391).

The data plotted as red symbols in Figure 19 clearly deviate from the general pattern. These data are from studies of neutrophils and eosinophils under conditions in which NADPH oxidase was active (permeabilized patch studies or whole cell studies with NADPH and GTPγS in the pipette), as discussed in section VI*H2*. This deviant behavior led to the suggestion that a novel variety of voltage-gated proton channel (type ***x***, Table 4) becomes active when NADPH oxidase is functioning, in addition to the type ***p*** H^+ channels in unstimulated cells (67c). Our interpretation is that respiratory burst agonists both acti-

vate NADPH oxidase and also alter the properties of voltage-gated proton channels (165, 246–248, 705). Channels in this enhanced gating mode exhibit type ***x*** behavior. A defining property is activation in a voltage range just negative to V_{rev}. In Figure 19 it appears that $V_{threshold}$ for type ***x*** channels is ~40 mV more negative than for other voltage-gated proton channels at any given V_{rev}. The red linear regression line describing type ***x*** behavior

$$V_{threshold} = 0.63\ V_{rev} - 22\ mV \quad (6)$$

has a slope similar to that of other H^+ channels, which might indicate a similar dependence on ΔpH. At symmetrical pH (V_{rev} = 0 mV), $V_{threshold}$ is 43 mV more negative in the type ***x*** gating mode. Evidence that type ***x*** channels are simply modified type ***p*** channels is discussed in section VI, *H2* and *I*.

Surprisingly, the parameters reflecting the opening and closing of voltage-gated proton channels, τ_{act} and τ_{tail}, respectively, do not share the same pH dependence as the g_H-*V* relationship. The simplest expectation would be that all voltage-dependent parameters shift along the voltage axis to the same extent that the g_H-*V* relationship shifts (i.e., by ~40 mV/unit change in ΔpH). H^+ channel activation is profoundly slowed at higher pH_i or lower pH_o (134, 164, 166, 170, 239, 241, 519, 886). Although these changes are in the direction expected if τ_{act} simply shifted along with the g_H-*V* relationship, in many cases, there is also an overall slowing at high pH_i or low pH_o. In other words, after correcting for the shift in the g_H-*V* relationship, an additional slowing persists. In inside-out patches from alveolar epithelial cells, changes in pH_o produced nearly pure shifts along the voltage axis, whereas increases in pH_i caused profound slowing in addition to the voltage shifts (239). Comparing the τ_{act}-*V* relationship at identical ΔpH, increasing pH_i appears to slow τ_{act} uniformly at all voltages by substantial amounts: threefold for ΔpH 0.5, sevenfold for ΔpH 1.5 (170), and four- to fivefold for ΔpH 0 or 1.0 (239).

In contrast, τ_{tail} appears to be less sensitive to pH than τ_{act}, exhibiting smaller shifts with changes in pH_i or pH_o than expected from the g_H-*V* relationship (166, 242). In fact, in several cells the τ_{tail}-voltage relationship appears to be completely independent of pH_o (164, 170, 241) and possibly also of pH_i (170).

M. Model of the Mechanism of pH- and Voltage-Dependent Gating

An almost inescapable conclusion from the strong dependence of the g_H-*V* relationship on both pH_o and pH_i is that protonation sites that regulate the voltage dependence of gating must exist and must be accessible to the external and internal solutions. Titratable sites that regulate function have been proposed for many membrane transporters and channels. The Na^+/H^+ antiporter binds protons at internal and external sites; an internal site allosterically activates exchange, whereas the external site simply functions in transport (37, 38, 785, 840). Anion exchangers including the Cl^-/HCO_3^- exchanger and the Cl^-/OH^- exchanger (603, 966) also are regulated by pH via protonation sites. The activity of proton-pumping transhydrogenases is regulated by the degree of protonation of a critical His residue (95). The gating of muscle Cl^- channels is altered substantially by pH (1063). Several channels are inhibited by protons, either by block within the pore (manifested as voltage dependent block) (161, 1082), by reduction of single-channel current amplitude (187), or by downregulation of channel availability (voltage-independent "block"), such as a plant voltage-gated K^+ channel (SKOR from *Arabidopsis*) (580), the "maxi-K" Ca^{2+}-activated K^+ channel of *Chara australis* (634), skeletal muscle Cl^- channels (476, 864), and inward rectifier K^+ channels by internal protons (100, 704). Other channels are activated by protons: cation conductances in neurons (88, 381, 563), a conductance in toad skin (579), a plant inward rectifier K^+ channel (99), several Na^+ channels (1055), and aquaporin-0, the latter by protonation of a His residue (750). A cation channel formed by phallolysin, which is derived from the deadly *Amanita phalloides* mushroom, exhibits an astonishing 130-mV shift in its voltage-dependent gating for a 1 unit change in pH (1080). Low pH activates stomatal guard cell K^+ channels in *Solanum tuberosum* by protonation of two extracellular His residues (467). The transcendental KcsA channel is activated by intracellular protonation (205, 420). Protonation of a mutant alamethicin channel switches the selectivity from cation to anion (105). Protonation of Ca^{2+} channels converts them from divalent cation selective to Na^+ permeable (557). A notable feature of the regulation of proton channels by pH is that H^+ is also the permeant ion. The gating of a few other channels is also regulated by the permeant ion concentration: inward rectifier K^+ channels (17, 403, 456) and the ClC-0 Cl^- channel (158, 824, 826). Finally, a model of the influence on pH_o, pH_i, and voltage on the operation of a H^+-coupled oligopeptide transporter (769) incorporates many of the features described below (Fig. 20).

Increasing either internal or external $[H^+]$ shifts the g_H-*V* relationship in the direction expected if protons screened or neutralized negative charges at the surface of the membrane or channel protein. Most voltage-gated cation channels are affected by pH in a stereotypical manner: at low pH_o, gating occurs at more positive voltages and the maximum conductance is decreased (444). These effects can be accounted for by the binding of protons to negative charges at the surface of the membrane or the channel molecule, which has two effects. As proposed by Huxley, Frankenhaeuser, and Hodgkin (320),

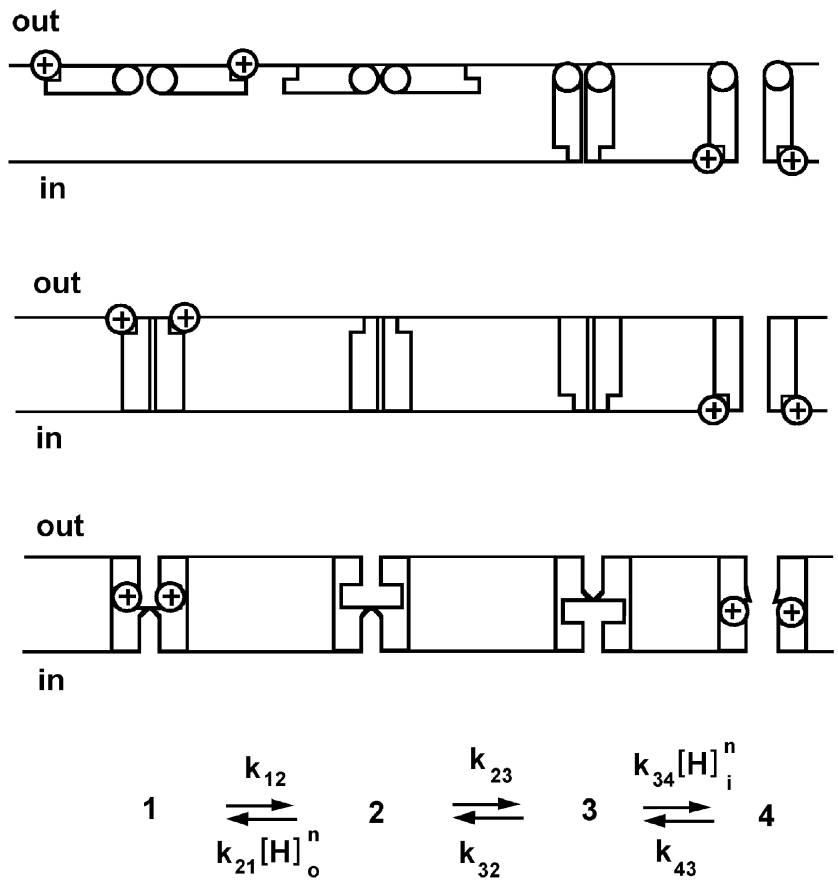

FIG. 20. The voltage and pH dependence of gating of voltage-gated proton channels can be explained by a simple model that postulates regulatory protonation sites. Five required assumptions are described in the text. Three possible physical representations of the model defined by the state diagram and rate constants are illustrated. The mechanism can be envisioned as follows: *top*, a "butterfly" in which the protonation site on each channel protomer or "wing" moves across the membrane; *middle*, distinct external and internal sites which when protonated allosterically prevent protonation at the opposite site; *bottom*, a protonation site in a proton well whose accessibility depends on a small conformational change, or other variants not illustrated. The bottom diagram would be a proton carrier (594) if the conformational change occurred in the protonated state, i.e., if there were direct transitions between states 1 and 4 and if no conducting pore were formed. In each case, the formation of a conducting H^+ channel requires a conformational change in each channel protomer which can occur only when the regulatory site is deprotonated. The closed channel conformation is stabilized by external protons, and the open conformation is stabilized by internal protonation of the same site, which is possible only after the conformational change exposes the protonation site to the internal solution. The open channel probability is therefore increased by high pH_o or low pH_i. The voltage dependence of gating could arise either from voltage-dependent binding/unbinding of protons to the regulatory protonation site, from a voltage-dependent conformational change, or from a combination of the two. To fit the data, we assigned all of the voltage dependence to proton binding so that the regulatory sites behave like "proton wells" as postulated for the proton channel of H^+-ATPases (596, 698). H^+ currents in rat alveolar epithelial cells were simulated using the following parameters, which are defined in Ref. 166: $d_{in} = d_{out} = 0.71$, $K_w = 10$, $m = 0$, $n = 1.5$, $k_{12} = 1{,}000\ s^{-1}$, $k_{32} = 10^6\ s^{-1}$, $k_{43,fast} = 3\ s^{-1}$, $k_{43,slow} = 0.05\ s^{-1}$, $pK_{in} = pK_{out} = 8.5$. [From Cherny et al. (166) by copyright permission of The Rockefeller University Press.]

the additional positive charge at the external side of the membrane biases the electrical field perceived by the voltage sensor, tricking the channel into thinking that the membrane potential is more negative than it really is. Thus more depolarization is required to produce the same gating. Another consequence of protonation (neutralization) of external negative charges is that cation concentrations near the membrane tend to be reduced, which reduces the maximum conductance (362, 440).

Several proposals have been made regarding mechanisms of pH regulation of voltage-gated proton channels. Byerly et al. (134) noted that a simple screening mechanism must be ruled out for voltage-gated proton channels because of the low concentration of protons compared with other monovalent cations, as well as the presence of millimolar levels of divalent cations, and suggested that protonation of specific acidic sites must be invoked. The voltage shifts that they observed when pH_i was changed were small enough to be ascribed to changes in the interior surface potential, but the shifts when pH_o was varied were considered too large to be accounted for by this mechanism. They concluded that external protons di-

rectly inhibit channel opening (134). Based on a marked increase in the rate of H^+ efflux from acidified neutrophils at $pH_o > 7.4$, Kapus et al. (520) proposed that "dissociation of H^+ from an externally facing H^+-binding site induces a higher conductivity state or probability of the H^+ channel being open."

After systematically evaluating H^+ channel gating over a wide range of pH, Cherny et al. (166) proposed a simple quantitative model to account for the voltage and pH dependence of gating. The fundamental observation was that the position of the voltage-activation curve depends on the pH gradient, ΔpH (see sect. v*L*). The state diagram at the bottom of Figure 20 is the model, and the three cartoons show various mechanistic ways that this model could be embodied, all of which share certain features. *1*) The channel is an oligomer formed from the association of several monomers. *2*) The degree of protonation of regulatory protonation sites communicates the pH to the channel gating machinery. *3*) Protonation of sites accessible to the external solution stabilizes a closed configuration of the channel; conversely, protonation of sites accessible to the internal solution stabilizes the open channel. *4*) The protonation sites are accessible only to one side of the membrane at a time. *5*) The accessibility is switched by a conformational change in the protein that can occur only when the sites are deprotonated. Simulations with this model using a single set of parameters reproduced the essential features of pH- and voltage-dependent gating (166). The top cartoon shows a "butterfly" version of the model, in which one end of each channel protomer flips across the membrane. A similar gating mechanism occurs in an assortment of channel-forming peptides including alamethicin (291, 406, 1010, 1084), colicin (5, 191), δ-endotoxin from *Bacillus thuringiensis* (345), melittin from honey bee venom (78, 532), the antibiotic monazomycin (437), and zervamicins (66, 659). In this form of the model, the same protonation sites are alternately accessible to the external or internal solution. The middle diagram illustrates an allosteric mechanism in which the internal and external protonation sites are different, but they are not accessible to both solutions simultaneously; a conformational change in the protein alters their accessibility. In the bottom cartoon, a conformational change alters the accessibility of a site deep inside the membrane that is accessible to bulk solution via "proton wells," as proposed by Mitchell and Moyle for H^+-ATPases (694, 698). The model is clearly very general, yet it incorporates several features that are likely to be necessary to account for the observed pH- and voltage-dependent gating. External and internal regulatory protonation sites seem essential, and alternating access was required for the model to reproduce the data.

Some details of the model (Fig. 20) need to be adjusted. That deuterium slowed activation threefold but hardly affected deactivation (242) is indirect evidence that the internal and external protonation sites are chemically distinct (see sect. v*I*). Alternatively, the rate-determining step in channel closing may not be the initial deprotonation step; a voltage-dependent closing step may precede deprotonation (242). Surprisingly, all three gating parameters (τ_{act} and the delay as well as τ_{tail}) exhibit the same profound temperature dependence (Q_{10} 6–9), suggesting that the same rate-determining process underlies each kinetic parameter (243).

N. Impervious to Blockers

No potent, high-affinity blockers of voltage-gated proton channels are known. Table 6 encapsulates the ineffectiveness of a variety of agents tested for inhibitory effects on H^+ currents. Most ion channels are blocked by small peptides found in toxins or venom from bees, scorpions, snakes, sea anemones, puffer fish, frog skin, etc.[5] Attempts to isolate voltage-gated proton channels have been frustrated by the absence of such blockers. Although it is possible that high-affinity inhibitors will be discovered, it is also possible that the proton conduction pathway may be inherently incompatible with lock-and-key type inhibition. The entrance to other channels is often a wide vestibule, which provides a large concave protein surface that is ideally suited for interaction with inhibitors and for block by simple steric occlusion. The entrance to voltage-gated proton channels may be a simple protonatable group accessible to the solution. The only other molecular requirement is that there must also be regulatory protonatable groups that are accessible to the external or internal solutions. Although the proposed mechanism for pH regulation of gating discussed in the previous section may not be correct, it is difficult to imagine how voltage-gated proton channels could respond so precisely to pH_o and pH_i without such groups. The relative simplicity of the entrance to voltage-gated proton channels may impede or preclude high-affinity binding of inhibitors.

Two general classes of inhibitors of voltage-gated proton channels have been reported: weak bases and polyvalent metal cations. Inhibition by polyvalent metal cations is discussed in section v*O*. The effects of other inhibitors share many qualifying properties. For example, no inhibitor abolishes H^+ currents. Inhibition is only partial, and in many cases is overcome by depolarization. Often the g_H-V relationship is shifted. All of these properties indicate that simple block by physical steric occlusion is not the operative mechanism. Meech and Thomas (676)

[5] The channel-blocking action of toxins and venoms probably reflects the desire of their hosts to avoid interaction with animals that use ion channels to move and think. If analogous toxins do not exist for voltage-gated proton channels, this could reflect the minimal survival advantage conferred by an ability to inflict a gradual death by blocking voltage-gated proton channels.

TABLE 6. *Drugs that do not block H^+ currents*

Compound	Concentration	I_H Reduction, %	Reference Nos.
Amantadine	0.1–1 mM	Via ↑ pH_i?	238
Amiloride	200 μM	0	710
Amiloride	100 μM	0	642
Amiloride	100 μM	weak, *V* dependent	237
Apamin	300 nM	0	642
4-AP	10 mM	67	134
4-AP	1 mM	50	762
4-AP	10 mM	Via ↑ pH_i?	676
4-AP	1 mM	50	281
4-AP	5 mM	Strong	473
A9C	1 mM	0	238
Bafilomycin A	200 nM	0	709,710
Ba^{2+}	1 mM	0	574
Bromophenacyl bromide	≤1 mM*	0	V. Cherny and T. DeCoursey, unpublished data
CCmP	20 μM	0	676
Charybdotoxin	100 nM	0	238
Cinnamate	?	0	85
D600	100 μg/ml	*V* dependent	676
DCCD	100 μM	0	676
DCCD	200 μM	0	238
Diethylpyrocarbonate	1 mM	0	642
DIDS	100 μM	0	710
DPI	1 μM	0	248
DPI	3 μM	0	246
Dimethylamiloride	10 μM	0	237
Mefenamic acid	100 μM	0	238
N-ethylmaleimide	2 mM	0	642
Nicardipine	10 μM	Small	1007
Nifedipine	1 μM	0	85
Noxiustoxin	100 nM	0	238
Oligomycin	10 μg/ml	0	676
Phencyclidine	200 μM	0	238
Rimantadine	0.1–1 mM	Via ↑ pH_i?	238
SITS	20 μM	0	676
Strophanthidin	2 mM	0	238
TEA^+	10 mM	35	85
TEA^+	52 mM	34	134
TEA^+	Isotonic	0	473
TEA^+	5 mM	5	762
TEA^+	1 mM	29	281
TEA^+	50 mM	*V* dependent	676
Tetrapentylammonium	1 mM	0	136
Tetrapentylammonium	10 mM	0	499
Venturicidin	10 μM	0	238

A9C, anthracene-9-carboxylic acid; CCmP, carbonyl cyanide-*m*-chlorophenylhydrazone; D600, methoxyverapamil; DCCD, *N*,*N*′-dicyclohexylcarbodiimide; mefenamic acid, 2-[(2,3-dimethylphenyl)amino]benzoic acid; *V* dependent, I_H inhibition can be overcome by additional depolarization.

* Bromophenacyl bromide was a saturated solution, nominally 1 mM.

found that 4-aminopyridine increased pH_i and considered that this effect might account for its reduction of I_H. Although there are several reports of moderate reduction of H^+ current by tetraethylammonium$^+$ (TEA^+), it is possible to record large H^+ currents in unilateral (70) or symmetrical isotonic TEA^+ solutions (236, 372). The nature of any effect of TEA^+ is therefore obscure, and in any case, it does not act as a simple channel blocker.

The weak base mechanism of block may account for the effects of most of the agents in Table 6 that appear to reduce H^+ currents. As was illustrated in Figure 2, a weak base added to the bathing solution will partially dissociate, and the neutral form will permeate the membrane and enter the cell. Depending on its pK_a and pH_i, the base will become protonated. This process has the effect of lowering pH_o as protons are "left behind" and raising pH_i as the base binds protons. As long as influx continues, there will be dynamic local pH gradients, and both the lower pH_o and higher pH_i will tend to shift the g_H-V relationship in a positive direction and reduce I_H during a test pulse. In a patch-clamped cell, the pipette acts as an infinite sink for anything diffusing into the cell, and thus pseudo-steady-state inhibition will be observed even if the agent has no direct effect on voltage-gated proton channels. Whether this mechanism can account for the effects of the agents listed in Table 6 remains to be tested rigorously.

O. Inhibition by Polyvalent Metal Cations

All voltage-gated proton channels studied to date are sensitive to inhibition by polyvalent cations. In fact, sensitivity to $CdCl_2$ and $ZnCl_2$ has classically been considered a requisite characteristic to identify these channels. A majority of polyvalent cations have similar effects. A compilation of existing literature (234) provided the following "consensus" potency sequence among divalent metal inhibitors:

$$Cu^{2+} \approx Zn^{2+} > Ni^{2+} > Cd^{2+} > Co^{2+} > Mn^{2+} > Ba^{2+}, Ca^{2+}, Mg^{2+} \approx 0.$$

The trivalent cations La^{3+}, Gd^{3+}, and Al^{3+} also inhibit H^+ current (238, 281, 676, 895, 1008), as do Be^{2+}, Pb^{2+}, and Hg^{2+} (136, 238) (Cherny and DeCoursey, unpublished observations). There is some question whether Ba^{2+}, Ca^{2+}, and Mg^{2+} are weak inhibitors or completely ineffective. In human myotubes, Ba^{2+}, Ca^{2+}, and Mg^{2+} inhibited weakly (85); in murine microglia, Ba^{2+} inhibited but Ca^{2+} did not (281); in alveolar epithelium, neither Mg^{2+} nor Ca^{2+} inhibited detectably (234); and in snail neurons, Ba^{2+}, Ca^{2+}, and Mg^{2+} were completely ineffective (134, 136). Although metal sensitivity may depend on the channel isoform, these three metals have such weak effects that they are difficult to measure. The inhibition by Zn^{2+} is quite potent, with marked effects at ≤ 1 μM (67c, 163, 372, 1007). Voltage-gated proton channels are inhibited at lower concentrations of Zn^{2+} than are K^+ channels in the same cells (163, 642).

Consistent with the observation that nothing blocks H^+ channels (see sect. v*N*), the effects of metals cannot be described as block in any normal sense of the word. Similar to their effects on virtually all voltage-gated ion channels, polyvalent metal cations shift the voltage dependence of gating toward more positive voltages, slow channel opening, and may reduce the maximal conductance. The reduction of $g_{H,max}$ is the only effect that could be considered to qualify as "block," but it appears to be a relatively minor component of the effects of these metals and occurs only at high concentrations (163). The slowing of activation and depolarizing shift of the g_H-V relationship can be explained largely in terms of alteration of the membrane potential sensed by the channel. As first proposed for calcium by Huxley, Frankenhaeuser, and Hodgkin (320), but also applicable to protons (440, 446), the binding of a divalent metal cation or proton to negatively charged groups at the outer side of the membrane (or the channel itself) will alter the apparent transmembrane potential perceived by the voltage sensor of the channel. As a result, a greater depolarization must be imposed for the channel to respond (see sect. v*M*). Careful examination of the effects of metals reveals some discrepancies with the simplest form of this model. Byerly et al. (134) noted that activation was slowed more than could be accounted for by the shift in the g_H-V relationship and proposed that Cd^{2+} has the additional specific effect of interfering with channel opening. Similar observations have been made in other cells (70, 519). In alveolar epithelial cells, the effects of Cd^{2+} were consistent with a simple and equal shift of the τ_{act}-V and g_H-V relationships, but Zn^{2+} had a distinct additional slowing effect (163).

The effects of metals on voltage-gated proton channels are extraordinarily sensitive to pH_o (163). Lowering pH_o reduces the apparent potency of metals, as illustrated in Figure 21. At pH_o 7.0, 1 μM $ZnCl_2$ has distinct effects (Fig. 21, top row). To achieve the same effects at pH_o 6.0 requires 10 μM $ZnCl_2$ (Fig. 21, second row). Lowering the pH_o by one unit from 6.0 to 5.0 reduces the apparent potency by ~100-fold (Fig. 21, third row). Evidently, protons and Zn^{2+} compete for a binding site on the external surface of H^+ channels. The large (100-fold) decrease in apparent potency between pH_o 6.0 and 5.0 rules out 1:1 competition between H^+ and Zn^{2+} for a single site, because simple competition would reduce the apparent potency of Zn^{2+} by at most 10-fold/unit. Also ruled out is the idea that the active species is $ZnOH^+$ rather than Zn^{2+} (163), because the concentration of $ZnOH^+$ increases only 10-fold/unit decrease in pH (64). The concentration-response relationships for Zn^{2+} effects on both channel opening (τ_{act}) and the g_H-V relationship at pH_o from 5.0 to 8.0 were well described by assuming that H^+ channels cannot open when Zn^{2+} is bound to an externally accessible receptor. To account for the strong competition at pH 5 required that the Zn^{2+} receptor consist of at least two or three titratable groups with pK_a 6.2–7.0, most likely His residues. Protonation of one group lowers the affinity of the receptor for Zn^{2+} by 30- to 100-fold (163). Based on the qualitative similarity between the effects of external protons and Zn^{2+}, we proposed (163) that external protons and Zn^{2+} bind at the same regulatory protonation sites that mediate the pH_o sensitivity of gating (166) (cf. Fig. 20). Thus the external regulatory site on voltage-gated proton channels may comprise several His residues. This hypothetical identification of the critical amino acid as His based only on its pK_a should be tempered by the examples of the ClC-1 Cl^- channel which displays strongly pH-dependent block by Cd^{2+} and Zn^{2+} (474), with pK_a 6.8 (863), although the metal receptor comprises three Cys residues (577), and the $K_{ir}1.1$ channel with a critical Lys residue whose pK_a is shifted from 10.5 in solution to 6.8 in situ by proximity to two Arg residues (899).

In contrast to the potent inhibition of H^+ currents by

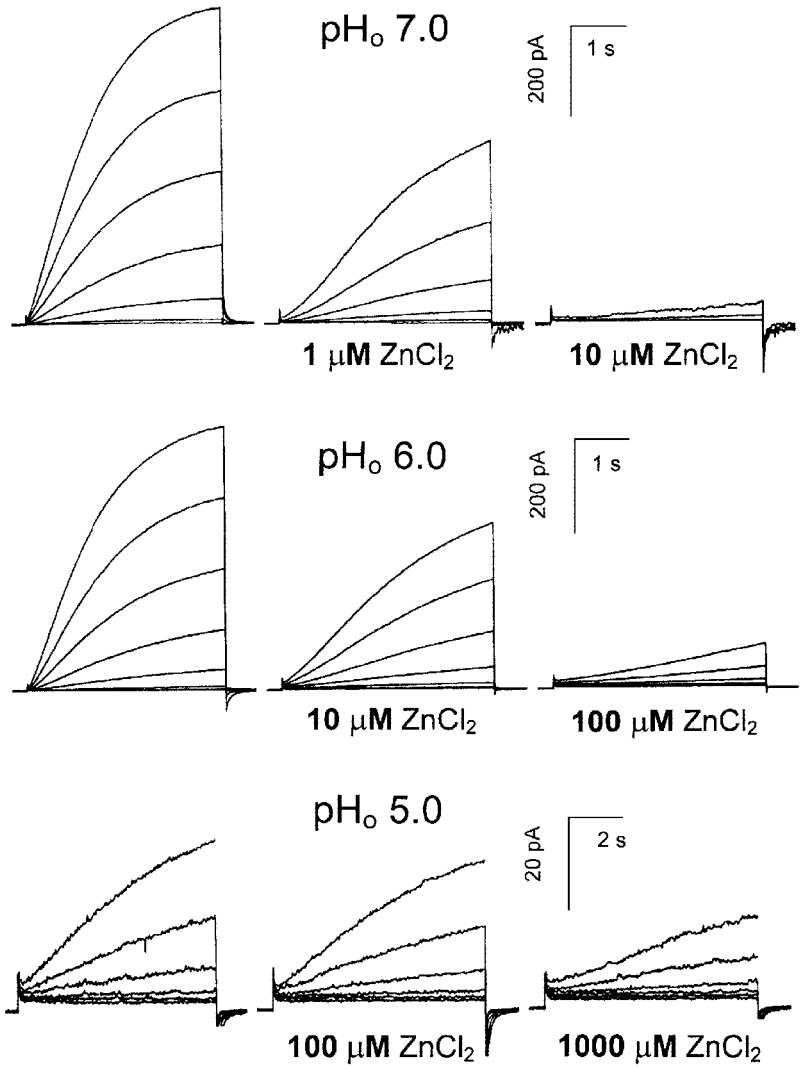

FIG. 21. The effects of Zn^{2+} on voltage-gated proton channels depend strongly on pH_o. Families of voltage-clamp currents are shown in rat alveolar epithelial cells at pH_o 7.0, 6.0, and 5.0, all at pH_i 5.5, recorded in the absence (left-most family in each row) and presence of the indicated concentration of $ZnCl_2$. Data in each row were recorded from the same cell during identical families of voltage pulses, applied in 10-mV increments. The cell at pH_o 7.0 was held at −60 mV, and currents are shown from −40 to +20 mV. The cell at pH_o 6.0 was held at −20 mV, and pulses are from +10 to +70 mV. The cell at pH_o 5.0 was held at −20 mV, and pulses are from +50 to +100 mV. [From Cherny and DeCoursey (163) by copyright permission of The Rockefeller University Press.]

external metals, internal application results in only weak inhibition in alveolar epithelial cells, with increased τ_{tail} (slower deactivation) at high $ZnCl_2$ concentrations (163). Competition between Zn^{2+} and H^+ for an internal site has not been demonstrated.

A peripheral issue is the contamination of chemicals or water with heavy metal cations that may inhibit H^+ currents. Because voltage-gated proton channels are highly sensitive to metal cations, trace levels of these ions may produce distinct effects. The H^+ channel voltage-activation curve was shifted 15–20 mV toward more negative voltages when the external bath solution containing nominally 2 mM Ca^{2+} was replaced by 3 mM Ca^{2+} and 1 mM EGTA, which has the same free Ca^{2+} (166). Similar metal contamination was detected for the NMDG receptor channel, which has a very high affinity for Zn^{2+} (22, 792). Some students of H^+ currents routinely add EGTA to bath solutions to minimize metal contamination.

VI. VOLTAGE-GATED PROTON CHANNELS: FUNCTIONS AND PROPERTIES IN SPECIFIC CELLS

By virtue of their efficient conduction of H^+, voltage-gated proton channels are intricately involved in the vast area of cellular pH regulation (850). Except in highly specific circumstances (see sect. VI*H2*), H^+ channels open only when there is an outward electrochemical gradient for protons. Therefore, the result of their activation is acid extrusion from cells, which is generally accepted as their primary function. During times of high metabolic activity, H^+ channels act as relief valves to permit rapid and efficient H^+ efflux. The appearance of the type ***x*** gating mode in activated phagocytes (see sect. VI*H2*), in which H^+ channels can conduct inward current, might conceivably reflect a different type of function (67c). Alternatively, this may simply be an inadvertent consequence of

the cell's attempt to prepare for massive H^+ efflux with any depolarization above E_H. Specific situations in which H^+ channels become activated in various cells are discussed here.

Determining specific functions of ion channels is often far more difficult than determining their biophysical or biochemical properties. Standard pharmacological lesion experiments can be done with $ZnCl_2$ or $CdCl_2$, but must be tempered by caution regarding possible nonspecific effects as well as inadvertent chelation. In some cells, the knowledge that we have relating to possible functions of proton channels is based on modulation of channel activity or properties by various stimuli. These responses are discussed in the context of the cells in which the behavior has been reported. Although some responses may occur in all cells with proton channels, others occur only in certain cells or groups of cells. For example, H^+ channels in human neutrophils and eosinophils studied in the permeabilized-patch configuration respond vigorously to stimulation by PMA (a phorbol ester), whereas H^+ channels in rat alveolar epithelial cells studied under identical conditions do not respond (68, 246, 248). In contrast, the response of H^+ channels studied in whole cell configuration to arachidonic acid is similar in phagocytes (236, 372, 518, 895, 977) and alveolar epithelial cells (Cherny and DeCoursey, unpublished data).

A. Proton Currents Increase pH_i Rapidly and Efficiently

It is obvious that outward proton current must increase pH_i. The rate and extent of cytoplasmic alkalinization depends on the H^+ channel density (the number of channels per unit area of membrane), the buffering power of cytoplasm, and cell geometry. In their original description of voltage-gated proton channels (see Fig. 14), Thomas and Meech (1008) injected HCl under voltage-clamp conditions. Massive H^+ efflux at depolarizing voltages raised pH_i to bring E_H toward the command potential. It required ~10–30 min to establish each new pH_i because the snail neurons used in these experiments were large cells with a diameter of ~100–200 μm (R. C. Thomas, personal communication) and with substantial cytoplasmic buffering power.

Proton currents increase pH_i much more rapidly in small cells such as phagocytes or alveolar epithelial cells with diameters ranging from 8 to 20 μm. During large depolarizing pulses lasting several seconds, H^+ currents increase to a peak and then decay with a time constant of seconds (232). When large, prolonged H^+ currents are elicited, the currents decay or droop in large cells (676, 1006, 1008) as well as small cells (68, 232, 236, 238, 258, 372, 473, 519, 709, 895). Careful examination of this phenomenon reveals that current decay is not the result of inactivation (channels entering a long-lived closed state), but is a direct manifestation of the increased pH_i caused by H^+ efflux. V_{rev} shifts toward more positive voltages, reflecting increased pH_i, roughly in proportion to the integral of the outward H^+ current during prepulses of different length or to different voltages (70, 232, 238, 372, 473, 519, 709, 895). Increased pH_i during large H^+ currents has been measured directly by intracellular pH electrodes (676, 1008) and by fluorescent pH-sensitive dyes (258, 518, 519, 762, 895). Large H^+ currents can increase pH_i by 1 unit in only ~7 s (519). Droop is exacerbated at lower intracellular buffer concentration (232, 238–240, 519). Voltage-gated proton currents droop much less in excised, inside-out membrane patches than in whole cell measurements, although some droop persisted in large patches, probably due to a sizable volume of solution enclosed at the tip of the pipette (239). Finally, during identical depolarizing pulses, droop appears at high temperatures as the H^+ current amplitude increases dramatically (243).

The ability of voltage-gated proton channels to extrude acid has been demonstrated in several cells after acid loading. In fact, voltage-gated proton channels were discovered when Thomas and Meech (1008) identified H^+ channels as the pathway responsible for mediating recovery of pH_i after HCl injection. Figure 22 illustrates that H^+ channel inhibition with 100 μM Zn^{2+} profoundly slows pH_i recovery in rabbit osteoclasts, whereas the H^+-ATPase inhibitor bafilomycin A does not (762). A similar role of H^+ channels in pH_i recovery was demonstrated in murine mast cells (574), rat microglia (710), spreading

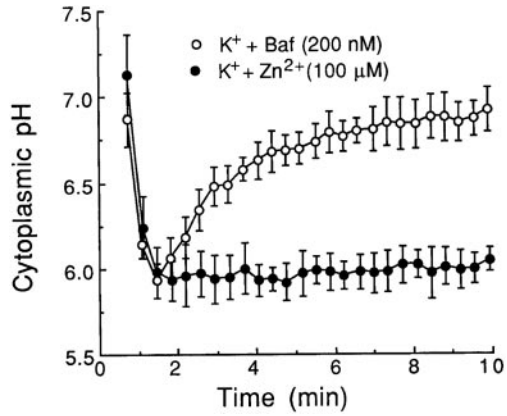

FIG. 22. Evidence that voltage-gated H^+ channels in rabbit osteoclasts contribute to pH_i recovery after an acid load. Osteoclasts were loaded with BCECF-AM and incubated with 40 mM NH_4Cl for 20 min at 37°C. Some cells were superfused with K^+ medium containing 100 μM Zn^{2+} (●). Other cells were pretreated with 200 nM bafilomycin A during the final 5 min of the acid-loading step and then exposed to K^+ medium containing bafilomycin (○). The H^+-ATPase inhibitor bafilomycin A did not prevent recovery, but the H^+ channel inhibitor Zn^{2+} greatly slowed acid extrusion. [From Nordström et al. (762), copyright 1995 American Society for Biochemistry and Molecular Biology.]

neutrophils (257), and osteoclasts exposed to chronic extracellular acidosis (763).

B. Modulation by Physiological Mediators

1. Arachidonic acid

The first physiological mediator shown to alter H^+ channel function was arachidonic acid (AA) (236). AA is a 20-carbon fatty acid with 4 unsaturated bonds that is produced by phagocytes during the respiratory burst. It acts in an autocrine manner, stimulating phagocytes to produce O_2^- (see sect. VI*H5*). In fact, it has been proposed that AA is the final link in the signaling cascade that activates NADPH oxidase (123, 434). AA also activates the electrogenic H^+ efflux that occurs during the respiratory burst (428). AA may also mediate the enhancement of H^+ efflux produced by purinergic receptor stimulation by ATP (976). Under whole cell voltage-clamp conditions, AA produces similar changes in H^+ currents in human neutrophils (236), murine macrophages (518, 977), human eosinophils (372, 895), and rat alveolar epithelial cells (Cherny and DeCoursey, unpublished data). The g_H-V relationship is shifted toward negative voltages by 15–20 mV, $g_{H,max}$ is increased roughly twofold, and both activation and deactivation are accelerated. The acceleration of tail current decay seems remarkable for two reasons. First, the other three effects would tend to increase g_H at any given membrane potential in an intact cell, whereas faster deactivation (smaller τ_{tail}) would reduce it. Second, this effect is opposite to that expected for a simple hyperpolarizing shift of all voltage-dependent gating parameters, which appears to rule out a weak acid mechanism. Perhaps AA lowers the energy barrier to activation, thus increasing both forward and backward gating rate constants. Studied with the permeabilized-patch technique in human eosinophils, AA had similar but larger effects, except that, in contrast to whole cell studies, AA had little effect on τ_{tail} (165). AA may have two opposing effects on H^+ channel deactivation, one direct and the other indirect. The direct effect seen in whole cell studies is to speed τ_{tail}. In addition, AA can slow τ_{tail} indirectly, by activating NADPH oxidase (165). NADPH oxidase activity is associated with a slowing of τ_{tail} of H^+ currents (67c, 165, 246–248) (see sect. VI, *H2*, *H5*, and *J*).

2. Intracellular free calcium

In their seminal study of voltage-gated proton channels, Byerly et al. (134) found that varying intracellular free calcium concentrations ($[Ca^{2+}]_i$) between 0.1 and 10 μM had no discernable effect on H^+ currents in snail neurons. Similarly, little effect of large changes in $[Ca^{2+}]_i$ was observed on H^+ currents in HEK-293 cells (67b). In phagocytes, however, several groups have reported that increasing $[Ca^{2+}]_i$ increased H^+ currents. These studies provide a lesson in the utility of using buffered solutions. Holevinsky et al. (459) used essentially unbuffered pipette solutions and concluded that the entire proton conductance in macrophages was Ca^{2+} activated. However, the putative proton currents were small, the reversal potential was not convincingly shown to change when pH was changed, and the currents were inhibited by DIDS, in contradiction to studies of clearly identified voltage-gated proton channels in other cells (710) (Table 6). Therefore, it seems more likely that these were Ca^{2+}-activated Cl^- currents, which have a generally similar appearance (39, 69, 663). Schrenzel et al. (895) reported that I_H in eosinophils increased about twofold and $V_{threshold}$ shifted ~30 mV more negative at 1 μM $[Ca^{2+}]_i$ compared with an undefined low $[Ca^{2+}]_i$. Gordienko et al. (372) also compared H^+ currents in eosinophils studied with weakly or strongly buffered (to pCa ~8.1) pipette solutions. The H^+ current was several times larger, and $V_{threshold}$ shifted toward substantially more negative voltages when the unbuffered solution was used, similar to the results of Schrenzel et al. (895). However, when well-buffered solutions were used, increasing $[Ca^{2+}]_i$ from 10 to 100 nM had no effect, and when $[Ca^{2+}]_i$ was increased to 1 μM, I_H increased about twofold at pH_i 7.0 and by just 40% at pH_i 6.0. In neither case was there a shift in $V_{threshold}$ (372). In summary, increasing $[Ca^{2+}]_i$ may enhance voltage-gated proton currents in phagocytes by twofold or less, depending on pH_i, but H^+ currents clearly are not Ca^{2+} activated. On the other hand, increased $[Ca^{2+}]_i$ is neither sufficient nor required to activate the H^+ conductance in neutrophils (739).

All of these were whole cell studies. Direct comparison in excised, inside-out patches from Jurkat (lymphocyte-related) cells revealed no detectable effect on H^+ currents of $[Ca^{2+}]_i$ up to 1 μM (886). Perhaps under some conditions, high $[Ca^{2+}]_i$ may enhance H^+ current indirectly by effects on other molecules or by changing pH_i. At least some of the measurements in eosinophils (895) were done only 2 min after establishing whole cell configuration. Perhaps elevated $[Ca^{2+}]_i$ promotes type ***p*** to type ***x*** conversion, which might transiently enhance H^+ currents before the cytoplasm is fully dialyzed by the pipette solution.

3. Phosphorylation

There is indirect evidence that H^+ channel activation is enhanced by phosphorylation. The protein kinase C activator PMA increases g_H in intact cells whether assessed indirectly via pH changes (429–431, 520, 521, 627, 737, 738) or assessed directly by voltage clamp (246–248). In voltage-clamp studies, the PMA response occurred only in permeabilized-patch and not in conventional whole cell configuration, indicating that diffusible intracellular sec-

ond messengers mediate the PMA effect on H^+ channels (as well as on NADPH oxidase). The phosphotyrosine phosphatase inhibitor vanadyl hydroperoxide activated the g_H in HL-60 cells, suggesting a role for tyrosine phosphorylation (90). Tyrosine kinase inhibition with erbstatin also prevents activation by formyl-methionyl-leucyl-phenylalanine (fMLP) of either conductive H^+ efflux or the H^+-ATPase in neutrophils (739). Days after THP-1 cells are induced by PMA to differentiate from monocyte-like to macrophage-like, H^+ channel expression and gating kinetics change (241) (see sect. VI*B6*). Identical changes in H^+ currents occur 1 day after treatment of human B lymphocytes with PMA (886). Given the time scales involved, however, any link with PMA-initiated phosphorylation events may be remote.

Voltage-gated proton channels do not require ATP to function. Similar H^+ currents were seen in macrophages with or without ATP in the pipette solution (519). The H^+ current in whole cell studies with ATP-free pipette solutions is stable (166, 886) or may increase slightly during 1- to 2-h experiments (166). Profound rundown of H^+ currents was reported in one study of human eosinophils, but rundown occurred independently of whether ATP was included in the pipette solution (895). When membrane patches from *Lymnaea* neurons are excised into ATP-free solutions, the H^+ current remains stable, while the Ca^{2+} current runs down (498). ATP has subtle effects on H^+ currents (574, 710) that are unrelated to phosphorylation (710) (Cherny and DeCoursey, unpublished data).

Schumann et al. (903) claimed that a 10-s exposure to fMLP or tumor necrosis factor-α (TNF-α) activated H^+ current "waves" in human neutrophils studied in whole cell configuration. The currents shown only vaguely resemble voltage-gated proton currents in human neutrophils (236) or other leukocytes (170, 258, 281, 372, 519, 574, 762, 886, 895, 977), but closely resemble currents reported previously by the same group that were described variously as voltage-dependent Cl^- currents (904), calcium-activated Cl^- currents (902), or nonselective cation currents (905). In each of their four incarnations, the currents were supposedly activated by a subset of neutrophil agonists including fMLP, PMA, TNF-α, or Ca^{2+} ionophores. However, in no case was the selectivity of the conductance demonstrated convincingly. Thus the attribution of these responses to H^+ channels is dubious at best. Furthermore, neither NADPH oxidase nor H^+ current is stimulated by PMA in human phagocytes studied in whole cell configuration (246, 248). Similarly, Bánfi et al. (67c) saw type ***x*** H^+ channel behavior only under conditions that permitted NADPH oxidase activity, which does not occur in whole cell configuration without NADPH in the pipette solution (896). Thus, although the reports by Schumann et al. appear to contradict existing literature, their data are simply uninterpretable.

4. Cytoskeletal interactions: volume regulation in microglia

Microglia are macrophages of the brain. In their resting state they are highly ramified, but upon activation they become amoeboid, more macrophage-like, and capable of phagocytosis (279). Microglia express high levels of voltage-gated proton channels (281). Subtle changes in proton currents were seen in cultured microglia treated with lipopolysaccharide to simulate the "activated" amoeboid state, or treated with astrocyte-conditioned media to induce the ramified, resting state (546). Surprisingly, both treatments reduced the H^+ current density ~50% and slowed activation kinetics (1.5- to 2.1-fold), giving no indication of a correlation between functional state and H^+ channel properties. Nearly identical changes in H^+ channel gating and expression occur in THP-1 cells induced by PMA to differentiate from monocyte-like to macrophage-like (241) and in human B lymphocytes treated with PMA (886). Because transformation of microglial functional state is associated with cytoskeletal changes, Klee et al. (545) tested the hypothesis that cytoskeletal interactions with proton channels underlie the modulation of proton current properties. After 24-h treatment with the disruptive agents cytochalasin D or colchicine, H^+ current density was reduced by 49 or 27%, respectively, and τ_{act} was increased by <1.5-fold. Treatment with the cytoskeletal stabilizers phalloidin and taxol had no discernable effects (545). These results suggest that cytoskeletal interactions may modulate the gating properties of voltage-gated proton channels, although the functional implications of these changes remain to be elucidated.

Morihata et al. (710) reported that swelling greatly enhanced voltage-gated proton currents; increasing cell diameter by 80% increased the H^+ current density 10-fold. In most cases, swelling was induced by dialyzing cells with low pH pipette solutions. Because cytoplasmic acidification in itself enhances H^+ currents, part of this response simply reflects the lower pH_i. Furthermore, the measurements were done using voltage ramps too brief to allow full activation of the g_H. In swollen cells, activation was faster (τ_{act} decreased) and $V_{½}$ was shifted more negative by 13 mV, both of which would exaggerate the difference between ramp currents in control and swollen cells. However, swelling induced by hypotonic bath solutions also increased H^+ currents, suggesting that part of the response was attributable to cell swelling per se. The increase in H^+ current and the swelling in response to low pH_i were prevented by replacing Na^+ in the bath with $NMDG^+$, suggesting that Na^+/H^+ antiport mediates or initiates the swelling. Swelling and the increase in H^+ current were also prevented by phalloidin (cytoskeletal stabilizer), cytochalasin D (cytoskeletal disrupter), or removal of ATP from the pipette solution (although hydro-

lysis of ATP was not required). Intriguingly, swelling of guinea pig neutrophils enhances O_2^- production in response to 1-oleoyl-2-acetylglycerol (OAG) (451), fMLP, PMA, and other stimuli (700). The interpretation of these results remains obscure, but they reinforce the idea that there are interactions between H^+ channels and the cytoskeleton.

5. Chronic acidosis in osteoclasts

Voltage-gated proton currents are altered, either irreversibly or slowly reversibly, in osteoclasts maintained at pH_o 6.5 for several hours. The current density was reduced 41%, and $V_{threshold}$ was shifted ~30 mV to more positive voltages, teleologically explainable as an attempt by the cell to preclude the possibility of H^+ influx (763).

6. Changes during differentiation in phagocytes

The promyelocytic cell line HL-60 can be induced to differentiate toward a granulocytic phenotype by DMSO treatment. Within 1 wk, the cells expressed the NADPH oxidase components required for O_2^- production (see sect. VI*H*) and H^+ currents increased sevenfold (830).

The monocytic cell line THP-1 differentiates toward a macrophage phenotype upon incubation with phorbol ester. The expression of several ion channels changed dramatically during this differentiation process (251, 539). Changes in the expression and properties of voltage-gated proton channels were relatively subtle in comparison: $g_{H,max}$ was reduced by 50% and τ_{act} was doubled (i.e., the H^+ current was smaller and turned on more slowly) (241).

C. Excitable Cells: Snail Neurons and Skeletal Myotubes

Voltage-gated proton channels in excitable cells probably open during the action potential. The resulting H^+ efflux may be a way for the cell to extrude acid that is produced by metabolic activity (85, 676). Because activation in snail neurons is quite rapid (Table 4), significant numbers of H^+ channels would open during each action potential. H^+ currents in human skeletal myotubes appear to activate slowly, but a fast component of activation was described (85) that would facilitate significant H^+ channel opening during one or a train of action potentials.

The scenario envisioned by Thomas and colleagues (676, 907) for the opening of H^+ channels in snail neurons is illustrated in Figure 23. Depolarization during the action potential opens voltage-gated calcium channels resulting in Ca^{2+} influx, which increases the local proton concentration by two mechanisms. First, Ca^{2+} tends to bind to similar sites in the cell as protons, thus displacing some previously bound protons. Second, Ca^{2+}/H^+ exchange is activated, extruding Ca^{2+} at the expense of H^+ influx. The local decrease in pH_i in conjunction with the depolarization during the action potential will tend to activate H^+ channels resulting in H^+ efflux. Recent confocal microscopy (908) supports this hypothesis. A 1-s depolarization to +40 mV alkalinized the lamellipodia region of the neuron by 0.4 units, and this alkalinization was prevented by 50 μM Zn^{2+}.

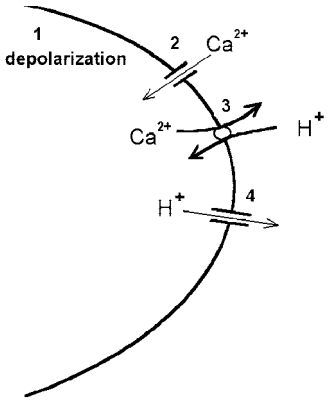

FIG. 23. Cartoon illustrating the proposed operation of voltage-gated proton channels during action potentials in snail neurons. See text for details. The Ca^{2+}/H^+ exchanger may be ATP driven (907).

D. Amphibian Oocytes: *Ambystoma* and *Rana esculenta*

The voltage-gated proton current is the most prominent conductance in immature *Ambystoma* oocytes (70). During maturation induced by progesterone, pH_i increases, the membrane potential depolarizes, the g_H disappears, and a Na^+ conductance appears (74). The physiological significance of these changes remains tantalizingly obscure.

Mature *Rana esculenta* oocytes express large H^+ currents (473). Membrane current oscillations related to Ca^{2+} release from inositol trisphosphate ($InsP_3$)-sensitive stores were inhibited by the H^+ channel inhibitor Ni^{2+} and were proposed to be regulated by H^+ channels via the pH dependence of the $InsP_3$ receptor (472).

E. Alveolar and Airway Epithelium

Rat alveolar epithelial cells were the first mammalian cells shown to express voltage-gated proton channels (232), but a specific function of H^+ channels in alveolar epithelium has not been demonstrated. As in other cells, H^+ channels likely serve as a relief valve to dissipate acid under conditions of acute metabolic activity. The exquisite regulation of the gating of H^+ channels by pH (see sect. V*L*) effectively prevents acid influx, even upon challenge by apical pH 6.4 (510). This property is essential in light of the normally low pH of the alveolar subphase

(282, 757). Low pH_o at the basolateral membrane of alveolar epithelial monolayers elicits H^+ influx via Na^+/H^+ antiport (510).

The high density of H^+ channels in alveolar epithelium (Table 2) suggests a specialized purpose. One hypothesis is that H^+ channels might participate in the main function of the lungs, namely, elimination of CO_2 from the body (235). This proposal is illustrated in Figure 24. The diffusion of CO_2 across the thin barrier that separates blood in the alveolar capillaries from air in the alveolar spaces is facilitated by the presence of CA located within the alveolar-capillary tissue barrier (284, 296, 297, 346, 388, 389, 398, 478, 551, 624a, 984, 986, 1062). Facilitated diffusion works because dissociation of CO_2 into HCO_3^- and H^+ increases the concentration of diffusible species ~10- to 20-fold at physiological pH. This principle is also the basis for CO_2 transport in the blood, where, on each passage through the systemic circulation, CO_2 is taken up, converted to HCO_3^- and H^+, and brought to the lungs, where CO_2 is reconstituted and eliminated. Inhibition of CA II, which is present in alveolar epithelial cells, appears to reduce CO_2 transport (424, 614, 972). Hereditary absence of CA II is associated with impaired CO_2 elimination (993) and restrictive lung disease (770), although the CO_2 retention in these patients might be a consequence of the restrictive lung disease resulting from osteopetrosis, rather than the CA II deficiency per se (E. R. Swenson, personal communication). Although it is usually assumed that CO_2 simply diffuses across the apical membrane, certain epithelial cells have low CO_2 permeability (1054); exit of H^+ and HCO_3^- would be an alternative pathway. There are at least two potential flaws in the mechanism proposed in Figure 24. First, extrusion of H^+ through proton channels must be accompanied by HCO_3^- extrusion, but the mechanism of the latter process can only be speculated for the present. Second, and perhaps more severe, the rate of spontaneous recombination of H^+ and HCO_3^- in the alveolar subphase (liquid lining the alveolus) is probably too slow to account for more than a tiny fraction of the total CO_2 elimination (985), because this fluid lacks CA (283, 284). It is possible that this mechanism operates only under extreme conditions, e.g., at high rates of CO_2 excretion during exercise or with lung dysfunction, such as adult respiratory distress syndrome (ARDS), in which CA may be released into the alveolar fluid with cell injury and lysis. No effect on CO_2 exchange was observed when 0.5 mM $ZnCl_2$ was added to perfusate in rabbit lungs (983), but it is not clear that sufficient Zn^{2+} reached the apical membranes of alveolar epithelial cells to inhibit H^+ channels. A specific test of this hypothesis would be welcome but requires a specific blocker, or perhaps a tissue-specific genetic knock-out, neither of which is feasible at this time.

A voltage-gated proton conductance was recently reported in the cystic fibrosis JME/CF15 airway cell line, along with evidence that a similar conductance is present in human airway epithelial cultures (311). Like the alveolar subphase fluid (282, 757), the liquid lining the apical surface of the airways is acidic. Acid secretion across the epithelium was stimulated by histamine or ATP and was inhibited by $ZnCl_2$, but not by amiloride, ouabain, bafilomycin A1, or Sch-28080 (a gastric K^+-H^+-ATPase inhibitor). Thus Fischer et al. (311) proposed that voltage-gated proton channels secrete acid into this fluid and that this histamine response might acidify the airway surface liquid, exacerbating asthma attacks.

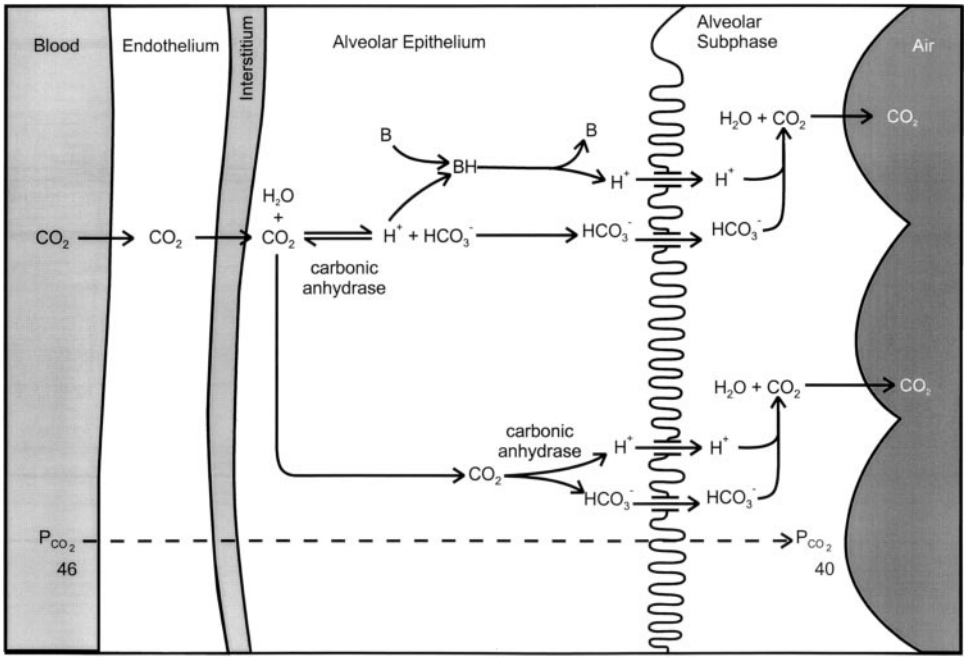

FIG. 24. Diagram illustrating the essential features of a proposed mechanism in which H^+ channels contribute to CO_2 elimination by the lung. Briefly, CO_2 leaves the blood and crosses the endothelial cell layer to reach the alveolar epithelium. There is evidence that carbonic anhydrase-catalyzed facilitated diffusion may contribute to CO_2 movement across endothelial cells (284, 624a). Carbonic anhydrase II, present in the cytoplasm of alveolar epithelial cells, catalyzes the conversion of CO_2 and H_2O to HCO_3^- and H^+ (via H_2CO_3, not shown). These ions diffuse across the cell, the H^+ bound to mobile buffer (B). H^+ leaves by permeating voltage-gated H^+ channels in the apical membrane, and HCO_3^- leaves by Cl^-/HCO_3^- exchange or through anion channels. The extruded HCO_3^- and H^+ recombine to form CO_2 and H_2O in the aqueous subphase, a thin layer of liquid lining the epithelial surface. CO_2 then enters the gas phase, and H_2O is reabsorbed. See text for further details of the proposed mechanism. [From DeCoursey (235).]

F. Pulmonary Smooth Muscle: Hypoxic Pulmonary Vasoconstriction

A major difference between pulmonary and systemic arteries is that pulmonary vessels constrict under hypoxic conditions, whereas systemic arteries relax. Hypoxic pulmonary vasoconstriction shunts blood flow away from poorly ventilated regions of the lung. It was proposed that NADPH oxidase or a homolog may act as an oxygen sensor in pulmonary vessels, initiating hypoxic pulmonary vasoconstriction (504, 506, 660). Exposure of cultures of pulmonary smooth muscle to hypoxia results in O_2^- release (660). Additional support for this hypothesis is based on the demonstration that diphenylene iodonium (DPI) (660, 1003), iodinium diphenyl, Cd^{2+}, and Zn^{2+} (505, 506), all of which directly or indirectly inhibit NADPH oxidase (195, 200, 252), inhibit hypoxic pulmonary vasoconstriction. Because Cd^{2+} and Zn^{2+} do not directly inhibit NADPH oxidase (252, 896), but act by inhibiting proton channels (163, 195, 252, 1008) (see sect. VI*H7*), this result implicates H^+ channels in this response. That hypoxic pulmonary vasoconstriction occurs in cultures of pure pulmonary artery smooth muscle (721) suggests the presence of voltage-gated proton channels in these cells, which remains to be tested. Hypoxic pulmonary vasoconstriction is also attenuated by CA inhibition, perhaps via pH_i changes (253). The hypoxic vasoconstriction response is preserved in gp91^{phox} knock-out mice (35), which suggests that NADPH oxidase does not mediate this response. However, the O_2 response of pulmonary neuroepithelial bodies, the presumed airway chemoreceptors, was abolished in gp91^{phox} knock-out mice, suggesting that NADPH oxidase does act as an O_2 sensor in these cells (326).

G. Lymphocytes

Human T and B lymphocytes, as well as the intensely studied Jurkat cell line, all express voltage-gated proton channels (886). H^+ currents in T lymphocytes are tiny, ~1.5 pA/cell, but are 100 times larger in both Jurkat cells and B lymphocytes. H^+ channel expression correlates with the capacity to produce superoxide anion. T lymphocytes do not produce significant O_2^- (516a, 1035), whereas both human B lymphocytes (600, 646, 647, 1048) and Jurkat cells (81) generate O_2^- in response to several agonists. Presumably, H^+ channels perform the same function in lymphocytes that they do in phagocytes (see sect. VI*H*), of charge compensation during NADPH oxidase activity. One day after stimulation with PMA, H^+ currents in T lymphocytes increased 13-fold, perhaps a reflection of the cell gearing up for greater metabolic activity (886).

H. Phagocytes: Macrophages, Eosinophils, Neutrophils, Microglia

Voltage-gated proton channels have been studied extensively in phagocytes, in part because a specific physiological function had been proposed even before the existence of these channels was demonstrated directly by voltage clamp. Henderson et al. (429) first postulated the existence of proton channels in human neutrophils, on the basis of measurements of pH, membrane potential, and superoxide anion production stimulated by the potent respiratory burst agonist PMA. They recognized that the electrogenic action of NADPH oxidase would rapidly depolarize the membrane unless the hypothetical proton channel opened, and that agonists that activate the oxidase must also somehow activate proton efflux (431).

1. The respiratory burst and NADPH oxidase

The function and perhaps even the structure of voltage-gated proton channels in phagocytes is intertwined intimately with that of NADPH oxidase (Fig. 25). In unstimulated cells, this enzyme complex is inactive; it is actually physically unassembled, with components segregated in the membrane and in the cytosol (55). Upon challenge with a variety of agents, it assembles and becomes active, converting oxygen, O_2, to superoxide anion, O_2^-, which exerts limited bactericidal activity itself (57), but more importantly, is a precursor to even more reactive species (56) such as H_2O_2 and HOCl. This process is called the "respiratory burst" because one manifestation is increased oxygen consumption by phagocytes (67, 881, 912).

The NADPH oxidase complex is formed from a single copy of each (1027) of six protein components: two membrane-bound components, gp91^{phox} and p22^{phox}, that combine to form cytochrome b_{558}, and three cytosolic components, p67^{phox}, p47^{phox}, and the small molecular weight protein Rac, either Rac1 or Rac2, depending on cell type.[6] A fourth cytosolic protein, p40^{phox}, coisolates with the cytosolic oxidase components. Phosphorylation of p47^{phox} results in its conformational reorganization, such that domains cryptic in the nonphosphorylated protein become exposed and competent to interact with docking sites on the membrane-bound cytochrome b_{558} and thereby mediate its translocation to the membrane and assembly of a functional oxidase (255, 747, 915). Stoichiometric evidence suggests that p67^{phox} may act catalytically, that is, it helps activate the complex, but may not remain attached during O_2^- generation (198). The p40^{phox} component may modulate NADPH oxidase activity, but is not essential (3, 178, 196, 880, 1071). In fact, none of the cytosolic components is absolutely re-

[6] Key to NADPH oxidase subunit nomenclature: p, protein; gp, glycoprotein; molecular mass in kDa; *phox*, *ph*agocyte *ox*idase.

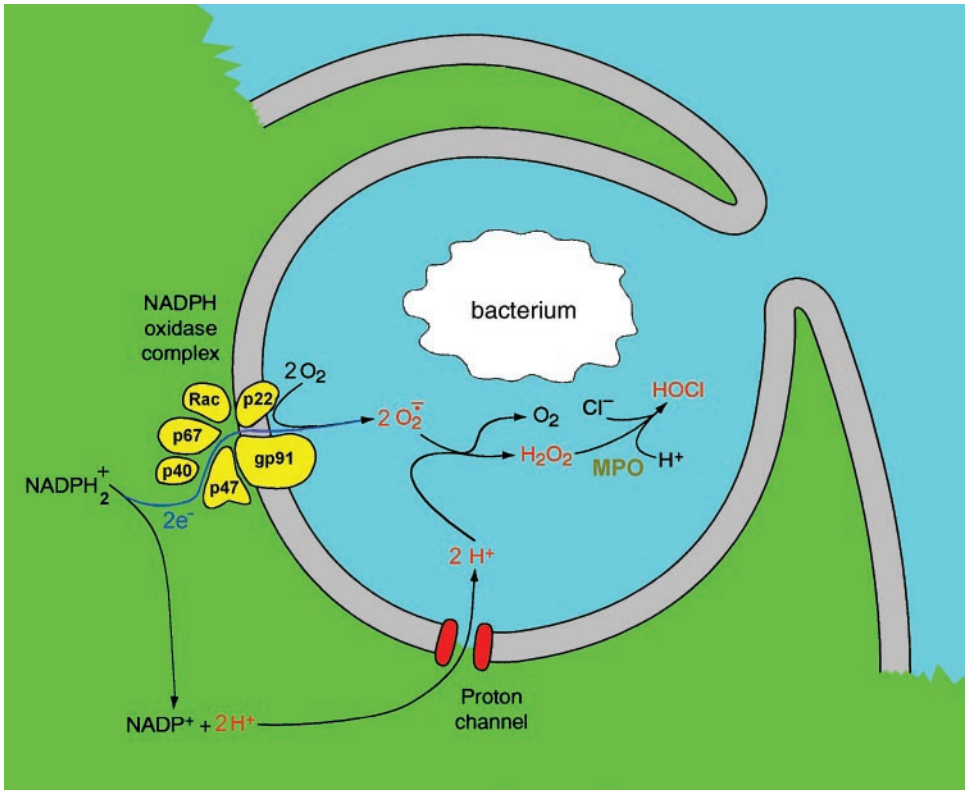

FIG. 25. Cartoon illustrating the relationship between electron and proton currents during the respiratory burst in phagocytes. The depicted stoichiometry is generally accepted (53, 58, 201, 330, 644, 853). Although superoxide dismutase is present in neutrophils and can catalyze the conversion (dismutation) of O_2^- to H_2O_2, its release into the phagosome has not been demonstrated (201, 543), and disproportionation of O_2^- (oxidation and reduction in the same reaction) probably occurs spontaneously. The half time of disappearance of O_2^- ($t_{1/2}$) due to spontaneous disproportionation to form O_2 and H_2O_2 can be calculated from (derived by Ricardo Murphy from Ref. 93)

$$t_{1/2} = \frac{K\left(1 + \frac{K}{[H^+]}\right)}{(k_1[H^+] + k_2K)[O_2^-]_{t=0}}$$

where $k_1 = 7.61 \times 10^5\ M^{-1} \cdot s^{-1}$, $k_2 = 8.86 \times 10^7 M^{-1} \cdot s^{-1}$, and $K = 10^{-4.75}$ M. At pH <7.5 for $[O_2^-] > 10\ \mu M$, the $t_{1/2}$ is <1 s. The conversion of H_2O_2 to HOCl is catalyzed by myeloperoxidase (MPO), which is released into the phagosome from primary or azurophilic granules in neutrophils (542, 543) and is present in lysosomes in macrophages but is absent from eosinophils (54). The high concentration of MPO in neutrophils causes pus to be green (542). Loss of MPO function, hereditary or acquired in humans or in MPO knock-out mice, has far less severe consequences than CGD but is associated with susceptibility to *Candida albicans* (33, 354, 409, 591, 746). [Modified from DeCoursey and Grinstein (249).]

quired in a cell-free system (565, 567, 568, 608). Nevertheless, optimal in vivo operation of NADPH oxidase likely requires all components (256). Another required ingredient is an amphiphile or detergent such as AA or SDS.

The importance of a functional NADPH oxidase in promoting phagocytic killing of bacteria, parasites, and other invaders is demonstrated by the clinical morbidity and mortality associated with its deficiency in chronic granulomatous disease (CGD). An inherited disease afflicting four to five individuals per million (202), CGD occurs when a mutation renders any one of four of the major components of NADPH oxidase absent or defective (851). This observation, by the way, emphasizes the importance in vivo of these four components. The phagocytes can still ingest microbes normally, but cannot kill many specific organisms, particularly those that are catalase positive (463). CGD is extremely heterogeneous genetically, with reported cases resulting from at least 353 different mutations of $gp91^{phox}$, 25 of $p22^{phox}$, 10 of $p47^{phox}$, and 18 of $p67^{phox}$ (202, 439, 796, 851) (A. R. Cross, personal communication). No variants due to a deficiency of $p40^{phox}$ are known, perhaps because this component is not essential, and only a single patient with defective Rac2 and phenotypic features of CGD has been reported (23). If untreated, CGD is usually lethal; the patients typically die in childhood of chronic recurrent bacterial or fungal infections (461). Standard clinical management includes prophylactic antibiotics and maintenance γ-interferon. Two hallmark clinical features are recurrent life-threatening infections and excessive inflammation that

leads to granuloma formation, sometimes resulting in obstruction of hollow organs (462).

The active enzyme complex removes two electrons from NADPH inside the cell and transports them sequentially across the membrane via an electron transport pathway, probably comprising (201, 256, 568, 853)

$$NADPH_2^+ \rightarrow FAD \rightarrow heme\ 1 \rightarrow heme\ 2 \rightarrow O_2^-$$

The electrons reduce extracellular or intraphagosomal O_2 to the superoxide anion, O_2^- (57, 204, 644, 916). Either catalyzed by superoxide dismutase or, more likely, spontaneously, O_2^- is rapidly converted into H_2O_2, which is then converted by myeloperoxidase (MPO) into HOCl (hypochlorous acid or household bleach, e.g., Chlorox). A variety of other reactive species can also be formed (543). Although many different species can be generated in vitro and all of these reactive oxygen species are capable of killing bacteria, their relative contribution to intraphagosomal killing is unsettled (409). HOCl is a particularly powerful oxidant (543) and is probably the major product of NADPH oxidase (409, 494). Neutrophils contain several types of granules that fuse with the phagosomal membrane and release their contents, which participate in the inflammatory response and help to digest phagocytosed material (107). It has been suggested that effective microbicidal activity requires both lytic enzymes and reactive oxygen species (837, 1012). Neutrophils possess other, oxygen-independent microbicidal systems, because certain organisms are killed under anaerobic conditions, when NADPH oxidase cannot function (648). Presumably, the physiological microbicidal response within the phagosome reflects the complementary and precisely integrated activities of a variety of systems whose coordinated release and activation mediate effective containment, killing, and degradation of the invading microbe. Of special interest to protonophiles, for each electron transported across the cell membrane by NADPH oxidase, one proton is left behind in the cell. The immediate source of these protons is $NADPH_2^+$, which is generated by the ongoing activity of the hexose monophosphate shunt (108). The main purpose of voltage-gated proton channels in phagocytes is thought to be to compensate for the charge separation that results from NADPH oxidase activity (236, 429–431, 520, 521, 738). Approximately 6% of the charge compensation has been ascribed to K^+ entry into the phagosome, which may render the phagosome hypertonic and help activate granule enzymes (837).

The topology in the cartoon in Figure 25 is intentionally ambiguous. Although originating as plasma membrane, the phagosomal membrane eventually will pinch off and become intracellular (121) as the nascent phagosome matures along the endocytic pathway en route to fusion with the lysosome. Furthermore, in human neutrophils, assembly of the NADPH oxidase may begin in secretory granules that are entirely intracellular, and which may eventually fuse with the plasma membrane and release their contents (55, 122, 179, 211, 497, 522, 553, 635, 1030). A practical consequence of this geometry is that neither NADPH oxidase-related electron currents, nor proton currents, nor superoxide anion generation can be detected in standard assays unless the relevant molecules are located in the plasma membrane. The exuberant respiratory burst detected in response to the soluble agonist PMA likely reflects the more extensive assembly of the NADPH oxidase complex in the surface membrane than would occur in a living neutrophil that is phagocytosing bacteria (772, 773) (W. M. Nauseef, personal communication). Eosinophils (286), whose job description includes attacking parasites like helminths that are too large to engulf (550, 994), normally assemble NADPH oxidase in the surface membrane and secrete O_2^- and other secretory products extracellularly (321, 581, 852).

NADPH oxidase is activated by a variety of pathophysiological or artificial stimuli. Physiological or pathophysiological agonists of the respiratory burst include TNF (544), platelet activating factor (853), leukotriene B_4 (853), eosinophil granule major basic protein (713), chemotactic peptides such as fMLP, AA, and numerous other unsaturated long-chain fatty acids (61, 62, 123, 432, 516), C5a (complement) (675), and opsonized zymosan or latex particles that interact with Fc receptors (57, 544, 853, 916). Artificial stimuli include phorbol esters such as PMA (673, 916), retinoids (63), calcium ionophores (e.g., A23187), phosphotyrosine phosphatase inhibitors (82), and lectins like concanavalin A (853). It seems likely that NADPH oxidase can be activated through multiple signaling pathways (522, 838, 853).

2. Activation of H^+ current during the respiratory burst by H^+ channel modulation

During the respiratory burst in human neutrophils, protons appear extracellularly in 1:1 stoichiometry with the consumption of O_2 and production of O_2^- (108, 330, 991, 1037). Protons are not released directly from the enzyme into the extracellular space, but rather intracellularly, from whence they are transported across the membrane (201). If proton channels are inhibited with Zn^{2+} or Cd^{2+} (thus preventing H^+ efflux), the pH_i drops drastically during NADPH oxidase activity (430). One $NADPH_2^+$ provides two electrons that pass through the electron transport chain across the membrane and two protons that appear in the cytoplasm, but are then extruded across the membrane, presumably through H^+ channels (Fig. 25). Simultaneously with the discovery that NADPH oxidase is electrogenic, Henderson et al. (429) reported that PMA stimulates electrogenic H^+ efflux, as well as NADPH oxidase. This conductive H^+ efflux is

observed both with PMA (429, 738) and AA as stimuli (428, 516a, 516b, 521). Two questions arise. What is the molecular mechanism responsible for mediating this H^+ efflux, and what turns it on?

The molecular mechanism of H^+ efflux can be narrowed down to four candidates: Na^+/H^+ antiport, CO_2 efflux, H^+-ATPase, and voltage-gated proton channels. Although Na^+/H^+ antiport is likely activated during the respiratory burst under physiological conditions (385, 386, 430, 919, 935, 936, 981), it cannot contribute to conductive H^+ efflux, because the one-for-one exchange of Na^+ for H^+ is electroneutral (541, 935, 936, 938). Furthermore, the bulk of proton secretion is not inhibited by amiloride, ruling out Na^+/H^+ antiport as the mechanism (719, 991). Equivalent proton extrusion by diffusion of CO_2 across the membrane and subsequent dissociation into H^+ and HCO_3^- similarly is electroneutral and does not occur at a quantitatively sufficient rate (1037). V-type H^+-ATPase activity can be demonstrated in stimulated neutrophils (739, 741) and macrophages (719, 982). Bianchini et al. (90) concluded that all three transporters were activated concomitantly during the respiratory burst in HL-60 granulocytes. However, H^+-ATPase inhibition by bafilomycin had no effect on pH_i responses in activated neutrophils (257). Furthermore, direct inhibition of V-ATPase by concanamycin did not affect NADPH oxidase activity (489). Numerous studies have demonstrated conductive H^+ efflux in phagocytes during the respiratory burst that is inhibited by Cd^{2+} or Zn^{2+} but is insensitive to bafilomycin A (90, 428, 429, 520, 521, 627, 737–739, 741, 977). Thus there is strong evidence that voltage-gated proton channels are activated during the respiratory burst and contribute to electrogenic H^+ extrusion.

Given that electrogenic H^+ efflux is activated during the respiratory burst and is mediated largely by voltage-gated proton channels, what causes the channels to open? Two distinct possibilities exist. First, local effects of NADPH oxidase activity might directly open H^+ channels, even without their properties changing. H^+ channels open upon membrane depolarization, decreased pH_i, or increased pH_o, all of which result directly from NADPH oxidase activity. The second possibility is that the properties of H^+ channels are modified in a manner that promotes channel opening. The exciting discovery that PMA-stimulated (and Zn^{2+}-sensitive) H^+ efflux was greatly diminished in CGD neutrophils (740) was therefore ambiguous. H^+ channels might be abnormal in CGD, either in their expression or properties. Alternatively, the fact that NADPH oxidase was not active in CGD cells means that the stimulation of H^+ current by NADPH oxidase activity simply would not occur. The first evidence suggesting that the properties of H^+ channels were modulated during the respiratory burst was the discovery that AA alters H^+ channel properties, promoting their activation (236, 518). In addition, nearly normal levels of H^+ efflux are activated by PMA in certain forms of CGD despite the lack of NADPH oxidase activity, strongly suggesting that H^+ channels are activated during the respiratory burst independently of NADPH oxidase activity (737), and therefore by some mechanism that does not simply reflect the metabolic changes produced by the oxidase.

The current view is that H^+ channels are activated in vivo mainly by modulation of their properties, but also by depolarization and possibly pH changes. Thus the original possibilities suggested by Henderson et al. (429) have proven exceedingly accurate: "The mechanism for initiating the opening of this channel is unknown at present, but could be a voltage decrease (depolarization), an increase in the internal concentration of protons or a phosphorylation/conformational change." An important discovery was that under conditions that permit NADPH oxidase activity, voltage-gated proton channels exhibit properties radically different from those under resting conditions (67c). The properties were so different that Bánfi et al. (67c) concluded that a new type of H^+ channel was activated (type ***x*** in Table 4). Compared with "normal" H^+ channels (type ***p***) that are observed in conventional whole cell recordings and which account for the g_H in unstimulated phagocytes, the "novel" H^+ channels activated more rapidly, had slower tail current decay, were activated at much more negative voltages, and reportedly were more sensitive to inhibition by Zn^{2+} (67c). The more negative voltage range of activation was especially noteworthy because at some pH it resulted in activation of the g_H negative to E_H and thus inward H^+ current could be elicited in a small voltage range near threshold. Activation of inward H^+ currents previously had been reported only under extreme pH conditions (391), and thus this behavior near physiological pH was surprising. Attenuation by Zn^{2+} of the dissipation of phagosomal acidification (H^+ "leak" from phagosome to cytosol) in DPI-treated neutrophils during phagocytosis is direct evidence that channel-mediated H^+ influx can occur in vivo (489).

Bánfi et al. (67c) observed type ***x*** H^+ channel behavior in whole cell configuration when they included NADPH and other ingredients to enable NADPH oxidase to function. We found that it was possible to detect NADPH oxidase activity directly as electron current in phagocytes studied with the permeabilized-patch configuration (165, 246, 248), which preserves diffusible intracellular second messenger pathways, and thus permits responses to various agonists. Using permeabilized-patch recording (with an applied NH_4^+ gradient to control pH_i), we confirmed that in neutrophils or eosinophils activated by PMA, the properties of voltage-gated proton channels were indeed altered radically, with faster activation, slower deactivation, larger $g_{H,max}$, and a 40-mV negative shift in the g_H-V relationship (246, 248). Our interpretation that the properties of type ***p*** H^+ channels are modified

rather than a new type of channel being activated is discussed in section VI*I*. Each of these four changes promotes H^+ current. It is thus clear that the activation of H^+ current during the respiratory burst occurs to a large extent as a result of the altered properties of the channels themselves. It is conceivable that H^+ channel activation might occur even without requiring any change in pH or membrane potential. It is therefore of interest to examine possible mechanisms of activation.

3. *What is the resting membrane potential of phagocytes, and how much do they depolarize during the respiratory burst?*

The resting membrane potential of neutrophils has been estimated using potential sensitive dyes and by electrical recording using conventional microelectrode puncture or current-clamp mode in patch-clamped cells. All three measurements are subject to errors. Potential-sensitive dyes can report potentials of organelle membranes (315, 488), can alter cell function (918), can be quenched by the reactive oxygen species released by phagocytes during the respiratory burst (918), and are difficult to calibrate accurately (348). Simple microelectrode puncture in small cells may cause a leak that is greater than the entire membrane conductance, which undoubtedly accounts for the remarkable estimates of −2.4 mV for the resting potential of human monocytes (758) and −7.4 mV in human lymphocytes (645). With the use of tight-seal or "patch-clamp" recording, a zero current potential can be measured, but it will be attenuated by any leak present and will also depend on the ionic composition imposed by the pipette solution, and is thus artificial. Finally, it is likely that there is no fixed resting potential in small cells. Due to the high membrane resistance and the often small number of ion channels present, the resting potential may normally fluctuate over a range of tens of millivolts (139, 1039). Early microelectrode puncture measurements of resting potentials in human macrophages produced what probably were artificially depolarized values, −2.4 mV (758), −13 to −15 mV (336, 339), or −30 to −40 mV (481), although some cells (presumably the ones less damaged by the electrode) had more reasonable values of −60 to −90 mV (337). Gallin (334) showed how the relative amplitudes of leak and inwardly rectifying K^+ conductances determine the measured resting potential and can even produce two stable resting potentials in some cells. The membrane (i.e., zero current) potential in patch-clamped human macrophages was −51 mV (338) and in human eosinophils was −63 mV (372). The resting potential of neutrophils estimated in patch-clamp studies was −50 to −60 mV (570), and estimated from ion fluxes was −59 mV (941). Resting potentials estimated in neutrophils using fluorescent dyes, in chronological order, are −26.7 mV (561), −100 mV (501), −66 to −86 mV (1000), −58.3 mV (576), −59 mV (941), −73 mV (662), −75 mV (73, 643), −74 mV (597), and −58 mV (488).

A variety of membrane potential responses of phagocytes to various stimuli have been reported, the first being in macrophages stimulated with chemotactic agents (336). Of most interest here are responses to PMA, a highly effective activator of NADPH oxidase, although chemotactic peptides elicit a weak respiratory burst under some conditions. Activation of NADPH oxidase is associated with depolarization of the plasma membrane (267a, 428, 429, 488, 502, 561, 598, 738, 911, 945, 1069). A key observation was that the large membrane depolarization seen with several stimuli was absent in CGD neutrophils (917, 1069), and thus most likely arises as a result of the respiratory burst. Seligmann and Gallin (917) further pointed out that because chemotaxis and secretion were unaffected in CGD neutrophils, the membrane potential changes were most closely associated with the respiratory burst. Subsequent studies have confirmed the absence of a depolarizing response in CGD phagocytes (13a, 67c, 1069), when NADPH oxidase was inhibited by DPI or by chlorpromazine (429, 488, 738, 1069), and in myeloid precursor cells that lack the ability to undergo a respiratory burst (974). Bánfi et al. (67c) found that patch-clamped eosinophils studied using solutions lacking most permeant ions, but containing ingredients necessary to support NADPH oxidase activity, depolarized to near E_H over a wide range of ΔpH, but depolarized to +80 mV in the presence of Zn^{2+}. This result indicates that NADPH oxidase activity tends to drive the membrane potential toward +80 mV in these conditions, but that activation of the voltage-gated proton conductance clamps the potential near E_H. Using more physiological solutions in intact human neutrophils, Jankowski and Grinstein (488) found that after careful correction for the many possible errors in this kind of measurement, the best estimate of the membrane potential attained during the respiratory burst was +58 mV. This represents a depolarization of >100 mV from the resting potential of −58 mV and would easily suffice to activate the voltage-gated proton conductance.

In early studies, enthusiastic investigators speculated that electrical signals might be critical in triggering the respiratory burst, because membrane potential changes appeared to precede the onset of O_2^- release (502, 561, 945, 1069). Ion channels certainly are capable of triggering a variety of cellular responses and can do so very rapidly. Most recent evidence indicates that depolarization is a direct consequence (rather than the cause) of the activation of the electrogenic NADPH oxidase enzyme. Furthermore, simple depolarization of the membrane does not seem to trigger the respiratory burst, but rather has little effect (460, 576, 722, 998) or even partially inhibits O_2^- production stimulated by PMA or other agonists (315, 662). Nevertheless, the finding that depolarization precedes measurable O_2^- generation remains puzzling if the

depolarization is the result of electrogenic NADPH oxidase activity. One explanation is that depolarization requires translocation of only a very small number of electrons, whereas the cytochrome *c* reduction assay for O_2^- may have a substantially higher threshold of detection. The lag before the onset of O_2^- release may simply reflect the time required for enough cytochrome *c* to be reduced to be detected spectrophotometrically. An alternative explanation is that part of the depolarization reflects activation of another conductance that is superimposed on the electrical effects of NADPH oxidase function. It has been proposed that activation of Ca^{2+}-activated Cl^- efflux is responsible for the depolarization (722). Depolarization was seen in neutrophils stimulated with concentrations of PMA too low to produce measurable O_2^- production (911), suggesting that at least part of this response may be mediated by an electrogenic process other than NADPH oxidase. A novel, speculative explanation of these results involves the activation of H^+ channels. PMA or AA shift the voltage dependence of H^+ channels negatively by 40 mV, resulting in a voltage range where inward H^+ current can occur (165, 246, 248). The gating of H^+ channels was altered temporally before NADPH oxidase-mediated electron current, I_e, turned on (246, 248) and also by lower concentrations of AA than those that elicited measurable I_e (165). Activation of H^+ influx would depolarize the membrane toward E_H. After NADPH oxidase is activated, the much larger ensuing depolarization would activate H^+ efflux in accordance with the traditional view (Fig. 25). Whether or not all the temporal details can be explained, it is clear that NADPH oxidase is electrogenic and its activity tends to depolarize cells.

4. *Do pH changes contribute to H^+ channel activation during the respiratory burst?*

Although the functioning NADPH oxidase produces intracellular protons and consumes extracellular protons when O_2^- dismutates into H_2O_2 (Fig. 25), under physiological conditions the resulting pH changes are substantially attenuated by the Na^+/H^+ antiporter (701). Chemotactic peptides specifically activate the Na^+/H^+ antiporter, increasing its sensitivity to pH_i, and thus tend to produce cytoplasmic alkalinization (385, 919, 935, 936). The antiporter will also tend to reduce changes in pH_o that might occur. Even without H^+ equivalent transporters, intracellular buffers blunt pH_i changes. With the assumption that the intracellular buffering capacity is 50 mM (see sect. II*F*), the respiratory burst in a human eosinophil would require ~20 s to lower pH_i by 0.1 unit. In comparison, the same I_e would depolarize the membrane, in the absence of other charge compensation mechanisms, from a resting potential of −60 mV to the nominal "equilibrium potential" of the NADPH oxidase electron pathway, +160 mV (see sect. VI*H6*), within 20 ms. Roughly speaking, I_e during the respiratory burst changes the membrane potential 1,000 times faster than it lowers pH_i.

Despite the damped changes in pH_i, it is possible that local proton accumulation near the membrane promotes H^+ channel activation and H^+ efflux. Two scales of local pH changes may be considered. Local proton accumulation near a source of protons, such as a single NADPH oxidase complex, will dissipate by >95% within 25 nm (see sect. VI*J*). However, in view of the massive H^+ generation at the membrane during the respiratory burst, macroscopic pH changes may also occur. There is clear evidence that large pH gradients (e.g., 1 pH unit in a cardiac myocyte) can exist inside cells subjected to a localized acid load (651, 957). This pH gradient is attenuated by CA in the presence of CO_2 (965). The gating of H^+ channels most likely responds to local pH near the channel, whereas the net H^+ current will flow according to V_{rev}.

5. *Does AA turn on proton channels during the respiratory burst?*

The signaling pathways that result in activation of NADPH oxidase and voltage-gated proton channels during the respiratory burst in phagocytes are complex. Two pathways, which are not mutually exclusive, have been proposed: phosphorylation (see sect. VI*B3*) and AA (see sect. VI*B1*).

AA is unique because it is the only physiological agonist known to directly alter the properties of voltage-gated proton channels in whole cell studies (236, 372, 830, 977). AA also plays an important role in the activation of NADPH oxidase. It has been suggested that AA is an essential second messenger that activates NADPH oxidase during the respiratory burst (123, 434, 672). Recent evidence indicates that AA induces conformational changes in $p47^{phox}$ that facilitate its assembly with the other NADPH oxidase components (924, 980).

In comparing effective concentrations of AA, its extreme lability must be taken into account. Although care was taken in early studies to avoid oxidation, optimal stimulation of O_2^- release was reported to occur at ~40–200 μM AA (61, 62, 190, 672), whereas in recent studies the optimal concentration is ~10 μM (165, 434, 619). Similarly, despite the precautions taken, we observed an order-of-magnitude lower potency of AA in enhancing H^+ currents in an early study (236) compared with a recent one (165). Recent estimates of the optimal concentration of AA for enhancing H^+ currents are 5 μM (165) or 10 μM (518), similar to optimal concentrations for activating NADPH oxidase. Oxidation of AA reduces its apparent potency (672). The reliability of commercially available AA may have improved over the years.

AA is released from phagocytes upon stimulation by a number of agonists including calcium ionophores, zy-

mosan, PMA, TNF-α, fMLP, OAG, platelet activating factor, bacterial lipoteichoic acid, concanavalin A, and wheat germ agglutinin (40, 102, 123, 332, 736, 756, 910, 997, 999, 1019, 1057). Exogenous AA stimulates O_2^- generation in various phagocytes: neutrophils (6, 61, 165, 210, 213, 516, 861, 962), macrophages (123, 263, 872), eosinophils (165, 619), related cell lines (212), including nonphagocytic cells transfected with NADPH oxidase components (822), and NADPH oxidase in a cell-free system (197, 209, 674).

It is AA itself that is important, and not one of its many interesting metabolites, because inhibiting either the lipoxygenase or cyclooxygenase pathways has no effect on O_2^- generation (216, 607, 655, 951, 952). The requirement for AA appears to be somewhat nonspecific, in that other anionic amphiphilic detergents, such as SDS, deoxycholate, digitonin, or saponin, have similar effects (190, 516, 952). In addition, other unsaturated long-chain (14–20 carbons) fatty acids, such as linolenic acid, linoleic acid, and oleic acid, have activity similar to that of AA, whereas saturated fatty acids are ineffective (6, 61, 62, 123, 438, 516). Although phosphorylation alone may stimulate a small level of NADPH oxidase activity in a cell-free system without added amphiphiles (625), the respiratory burst in a cell-free system is greatly enhanced by anionic amphiphiles like AA (197, 209, 438, 793, 962).

Many studies have shown that superoxide generation is inhibited by a variety of inhibitors of phospholipase A_2 (PLA_2), including bromophenacyl bromide (BPB), quinacrine (Mepacrine), Ro-31–4639, and scalaradial (213, 216, 434, 655, 952). PLA_2 is the enzyme responsible for releasing AA from membrane phospholipids (1057). However, Suszták et al. (977) found that an analog of AA inhibited PLA_2 without reducing O_2^- production in macrophages. Also, the effects of some inhibitors have been ascribed to suppression of glucose uptake rather than PLA_2 inhibition (1019). Quinacrine can inhibit NADPH oxidase in a cell-free system (203). Nevertheless, the concentration-response relationship for inhibition of AA release by quinacrine (655) or by cAMP (756) closely paralleled that for inhibition of O_2^- generation. Furthermore, after inhibition of O_2^- release by PLA_2 inhibitors, the full PMA response was restored by exogenous AA (213). The latter is the more remarkable because AA alone in this study stimulated only ~20% of the O_2^- generation observed with PMA, yet AA restored the full response. Additional strong evidence supporting a requirement for AA is that a PLB-985 cell line transfected to express antisense mRNA for PLA_2 did not produce O_2^- in response to PMA, fMLP, or opsonized zymosan, but did respond to AA (212). Similarly, electrogenic H^+ efflux was stimulated by PMA in control PLB-985 cells but not in PLA_2 knock-out cells and was restored by addition of exogenous AA (627).

The ability of AA to upregulate H^+ channel function parallels that for NADPH oxidase activation. The requirement for unsaturated long-chain fatty acids closely resembles that for NADPH oxidase activation (518, 516b). Inhibition of AA metabolic pathways similarly has no effect (372, 518). PLA_2 inhibition prevents the activation of H^+ efflux by PMA (518). Pretreatment of eosinophils with BPB did not prevent subsequent enhancement of whole cell H^+ currents by AA (895). In eosinophils, direct comparison of the effects of AA on H^+ channels and NADPH oxidase indicated that the two molecules were regulated separately but in parallel (165). Thus H^+ current was enhanced at lower concentrations of AA than required to elicit detectable electron current. Furthermore, AA speeds H^+ current activation before it turns on electron current (165), in which respect it resembles PMA (246). In summary, AA exerts most of its effects on voltage-gated proton channels directly, and this mechanism probably contributes to the enhancement of H^+ flux during the respiratory burst.

6. *Kinetic competence: how many H^+ channels and NADPH oxidase molecules are there in phagocytes?*

It is clear that *1*) electrogenic H^+ efflux is activated during the respiratory burst, *2*) this efflux is inhibited by the H^+ channel inhibitors Zn^{2+} and Cd^{2+}, *3*) the local effects of NADPH oxidase activity promote H^+ channel activation, and *4*) respiratory burst agonists strongly modulate and enhance voltage-gated proton channels as well as activating NADPH oxidase. Nevertheless, the evidence that voltage-gated proton channels mediate the H^+ efflux arguably is indirect. Here we consider whether the H^+ current likely to be activated in intact cells during the respiratory burst is sufficient to compensate the charge translocated by NADPH oxidase.

All cells known to produce O_2^- via NADPH oxidase also express voltage-gated proton channels. As shown in Figure 26, the expression levels of voltage-gated proton channels in phagocytes are roughly proportional to the maximum rate of O_2^- production in each cell type. Furthermore, in every case, the $g_{H,max}$ is adequate by a >10-fold safety margin to compensate fully for the entire acid load during maximal NADPH oxidase activity (280).

The NADPH oxidase complex reconstituted in vitro translocates 300 (204) to 330 (566) electrons/s. In intact cells, the rate may be higher (179). The flux of electrons through each NADPH oxidase complex generates an electron current of ~50 aA. In comparison, the H^+ current through a single channel has been estimated to be on the order of a few femtoamperes for a moderate driving force (e.g., ~40 mV) (168, 236). Thus one voltage-gated proton channel can easily compensate for ~100 maximally activated NADPH oxidase complexes.

An eosinophil with 1.5 nS $g_{H,max}$ at pH_i 6.5 (372) has 5×10^4 channels if the unitary conductance is 30 fS (168). This calculation depends on the assumption that most H^+ channels open with a large depolarization, which is sup-

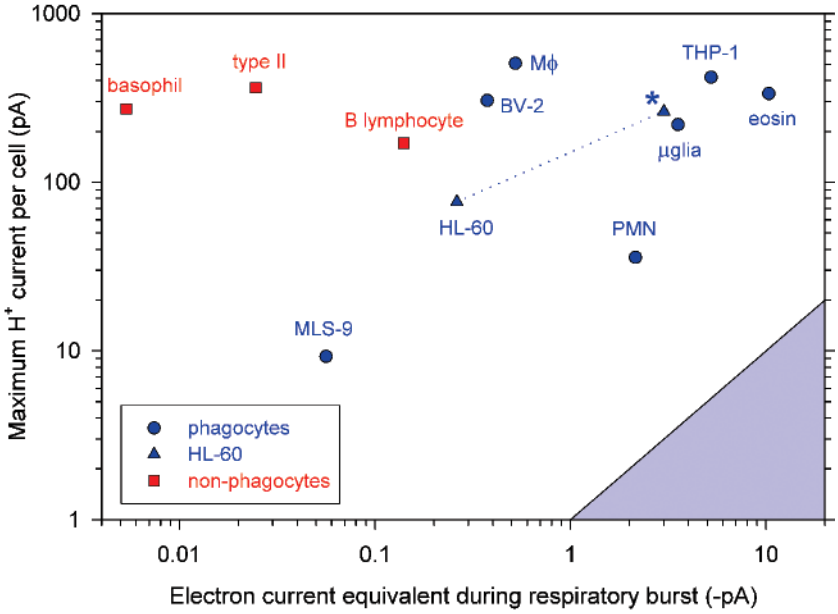

FIG. 26. Comparison of the maximum whole cell voltage gated proton current in various phagocytes or nonphagocytic cells and the rate of superoxide anion production in response to PMA (or lipopolysaccharide for THP-1 cells). In some of the cell lines that are categorized as phagocytes in this figure, phagocytic activity has not been studied and the designation is based arbitrarily on cellular origin. Superoxide anion production is expressed as the equivalent electron current that would be generated (and which must be compensated electrically). The line indicates the H^+ current required to fully compensate NADPH oxidase activity during the respiratory burst; the shaded area shows H^+ current amplitudes that would be inadequate to serve this purpose. These data were collected by many different groups, in a wide variety of conditions, and although the results are "standardized," they are not all directly comparable. The intent is to give a general impression of the relative magnitudes of these two cellular processes. The "standard" conditions are the peak rate of O_2^- release at 37°C after PMA stimulation, and the maximum I_H measured in the whole cell configuration at pH_i 5.5 and pH_o 7.0, usually at room temperature. However, O_2^- release was measured in different ways, and the attempt to standardize the results ignores nonlinearity in the temporal response. Similarly, some measurements of I_H were at different pH_i: in cases where multiple values were given, data at the lowest pH_i studied were used. Two values connected by a dotted line are for HL-60 cells (▲) before and after (*) being induced to differentiate by DMSO (830) (S. Grinstein, personal communication). Other sources of data for this figure: I_H, Refs. 170, 232, 236, 281, 372, 519, 886, 895 and unpublished data of V. V. Cherny and T. E. DeCoursey; I_e derived from O_2^-, Refs. 154, 280, 604, 807, 982, 999, 1034. Cell types as indicated in the figure are as follows: basophil, human basophil; type II, rat type II alveolar epithelial cell; MLS-9, rat microglial cell line; BV-2, mouse microglial cell line; Mϕ, mouse macrophage; PMN, human neutrophil; THP-1, human monocytic cell line; μglia, mouse microglia; eosin, human eosinophil. There is uncertainty about the rate of O_2^- release by nonphagocytes because the rates are very low and may be contaminated by release from other types of cells (especially problematic is contamination by phagocytes). Several cells that express voltage-gated proton channels but may not produce superoxide anion (snail neurons, amphibian oocytes, kidney epithelial cells, mast cells, T lymphocytes) are not included on the graph. The total current in the whole cell membrane is plotted, which reflects cell size as well as current density. For example, eosinophils are small cells with 10 times denser H^+ channel expression than THP-1 cells, but because THP-1 cells have 10 times larger membrane surface area, their whole cell H^+ current is similar. [Modified from Eder and DeCoursey (280).]

ported by noise measurements, at least at low pH_i (168, 720). Assuming a smooth membrane, an 8-μm-diameter (360) eosinophil has a surface area of 201 μm^2. Many cell membranes are not smooth, and the average capacitance of eosinophils is 2.5–4.0 pF (372, 895), which, assuming a specific capacitance of 1 $\mu F/cm^2$ (444), corresponds to a membrane area of 250–400 μm^2. There are most likely 125–200 (at most 250, if the membrane is smooth) H^+ channels/μm^2. The electron current in a human eosinophil is −6 pA at 21°C (246) and roughly −40 pA at 37°C (167). Given a turnover rate of ~300 s^{-1} (199, 566), this corresponds to 8.3×10^5 NADPH oxidase complexes/eosinophil. This number is in good agreement with an estimate that 5×10^5 molecules of each of the cytosolic NADPH oxidase components translocate to the plasma membrane of a neutrophil within 20 min of PMA stimulation (832), especially considering that eosinophils have an approximately threefold larger respiratory burst than neutrophils (229, 246, 581, 807, 926, 956, 1086, 1087, 1090). Given the above assumptions, there are 2,100–3,300 active NADPH oxidase complexes/μm^2 membrane. Thus there are roughly 20 active NADPH oxidase complexes for each voltage-gated proton channel, which, incidentally, is evidence that the channel is not part of the NADPH oxidase complex (see sect. VI*I*).

The I_e generated by NADPH oxidase in PMA-stimulated human neutrophils is −2.3 pA at 20°C (248). This I_e would depolarize the neutrophil, with an average capaci-

tance of 2.1 pF (236), by 1.1 V/s, or by 100 mV in 91 ms. An eosinophil at 37°C would depolarize by ~1.1 kV/min. For continuous function of the NADPH oxidase, it is clearly necessary to balance this charge movement by an efficient mechanism that is capable of responding rapidly to depolarization. Voltage-gated proton channels are ideally suited to this task.

One might ask teleologically why the electron and proton fluxes are carried through separate molecules, in contrast to a number of molecules important in bioenergetics, in which electron and proton movement is strictly coupled (51, 130, 194, 394, 447, 526, 584, 694, 696, 775, 862, 1014, 1072–1074). Part of the answer is that voltage-gated proton channels differ fundamentally in opening to form a continuous passive pathway through which protons can cross the entire membrane without interruption. In contrast, the proton channels in molecules that serve bioenergetic processes must function in a vectorial manner, and this unidirectionality is accomplished by interrupting the proton's journey partway across the membrane. At the active site, the proton participates in accomplishing the goal of the molecule, and then it moves on through a different hemi-channel. It is possible to uncouple proton and electron movements in cytochrome oxidase by mutation, but then the proton pumping function is abolished because vectoriality is lost (351). The division of labor between NADPH oxidase and H^+ channel molecules may be advantageous because it permits the H^+ flux to occur independently of and without strict stoichiometric coupling to electron flux. H^+ channels can thus respond to the immediate needs of the cell or vesicle. Because NADPH oxidase may assemble in the plasma membrane or in vesicle or phagosome membranes, the relevant membrane potential may be across any of these membranes. Voltage-gated proton channels respond to the voltage across the membrane in which they are located, with modulation by the pH on both sides of the membrane. In essence, they are activated automatically when the need arises. Furthermore, if another conductance contributed to or interfered with the charge compensation process, then an independently regulated H^+ channel could adjust accordingly. On the other hand, if H^+ flux through voltage-gated proton channels were strictly coupled to I_e through NADPH oxidase, the elegantly designed voltage and pH sensitivity of H^+ channels would be wasted.

7. *The respiratory burst is inhibited by H^+ channel inhibitors because depolarization inhibits NADPH oxidase*

Given that H^+ channels open during the respiratory burst, how crucial is their function? Seven studies have reported that H^+ channel inhibitors inhibit O_2^- production. However, the concentrations of metals that inhibit PMA-stimulated O_2^- production appear to be much higher than those that inhibit voltage-gated proton channels. Partial inhibition by Cd^{2+} was seen at 250 μM (430) or 80–640 μM (521). Partial inhibition by Zn^{2+} in PLB-985 cells occurred at 50 μM (627), but at 1 mM in human neutrophil cytoplasts (431), or granulocytes (87), although the latter study was compromised by the presence of phosphate in the buffer. Simchowitz et al. (939) showed that La^{3+}, Zn^{2+}, Cd^{2+}, and several other divalent cations completely inhibited O_2^- production in human neutrophils stimulated with fMLP but not with PMA. The agonist dependence suggests that the fMLP response is mediated by a metal-sensitive signaling pathway, attributed by the authors to Na^+/Ca^{2+} exchange. However, Ca^{2+} influx via calcium release-activated Ca^{2+} (CRAC) channels, which has been postulated to trigger the respiratory burst (379), is inhibited by several of these metals, although the ion potency sequence for inhibiting superoxide production (939)

$$Zn^{2+} > Sr^{2+} > Cd^{2+} > Ba^{2+} > Co^{2+} \approx Ni^{2+} \approx Mg^{2+}$$

does not completely agree with that for inhibiting Ca flux through CRAC channels (466)

$$Zn^{2+} > Cd^{2+} > Be^{2+} \approx Co^{2+} \approx Mn^{2+} > Ni^{2+} > Sr^{2+} \approx Ba^{2+}$$

or with that for inhibiting voltage-gated proton currents (234)

$$Cu^{2+} \approx Zn^{2+} > Ni^{2+} > Cd^{2+} > Co^{2+} > Mn^{2+} > Ba^{2+}, Ca^{2+}, Mg^{2+} \approx 0.$$

Because of the dearth of information on this vital question, we recently measured the concentration dependence of Zn^{2+} inhibition of PMA-stimulated O_2^- production in human neutrophils (252). Inhibition was distinct at 300 μM Zn^{2+} and nearly complete at 3 mM. In contrast, similar measurements in COS-7 cells transfected with the four main NADPH oxidase components revealed no inhibition by 3 mM Zn^{2+}. Because these transfected COS-7 cells lack voltage-gated proton channels (705), this result supports the idea that the inhibition by Zn^{2+} in phagocytes was mediated by H^+ channels. Reassuring as this result was, there remained a disquieting apparent discrepancy between the Zn^{2+} sensitivity of O_2^- production and of H^+ channels, which in phagocytes are distinctly affected by 1 μM Zn^{2+} (67c, 246).

Even if Zn^{2+} blocked H^+ channels by steric occlusion, which it does not (see sect. v*O*), there would be no reason to expect a direct proportionality between the $[Zn^{2+}]$ required for inhibition of H^+ currents and O_2^- production. The effect on O_2^- generation is not mediated by direct binding of Zn^{2+} to the oxidase, but rather to

proton channels. Failure of up to 5 mM Zn^{2+} to inhibit I_e in a voltage-clamped cell demonstrates directly the insensitivity of NADPH oxidase itself to Zn^{2+} (252). Because of the complex actions of Zn^{2+} on H^+ channel gating, it is difficult to predict how large the Zn^{2+} effects need to be to prevent enough H^+ channels from opening to impair compensation for electron flux through NADPH oxidase. If activation of 5% of all H^+ channels normally sufficed for compensation (cf. Fig. 26), then in the presence of Zn^{2+}, a larger depolarization would be required to activate the same H^+ efflux.

The specific mechanism by which metals inhibit NADPH oxidase function is presumably by inhibiting H^+ channels and thus permitting excessive membrane depolarization. An alternative possibility is that H^+ currents serve to prevent cytoplasmic acidification and phagosomal alkalinization. It is true that NADPH oxidase in a cell-free system has a pH optimum of 7.0–7.5 (177, 179, 190, 329, 438, 674) and that in intact cells NADPH oxidase is profoundly inhibited by low pH_i (613, 745, 854, 937, 982). However, electron flux changes the membrane potential far more quickly than it changes pH_i (see sect. vi*H4*), and thus depolarization is more likely to represent a limiting process. It has been shown that when NADPH oxidase is active, the membrane potential of eosinophils closely approaches E_H, but depolarizes to +80 mV in the presence of 10 μM Zn^{2+} (67c), indicating that the NADPH oxidase is indeed capable of producing extreme depolarization if H^+ channels are prevented from compensating charge.

The role of H^+ channels in phagocytes is universally believed to be charge compensation, with the presumption that NADPH oxidase would be inhibited by depolarization. However, until recently, this assumption had never been tested. Because NADPH oxidase transports electrons across the cell membrane it must be voltage sensitive (596). The standard redox potentials at the ends of the electron transport pathway are −320 mV for $NADPH_2^+$ in the cytoplasm and −160 mV for O_2^- at the extracellular/intraphagosomal end (131, 201, 430, 846, 1081). Thus the nominal driving force for electron movement across the chain is +160 mV, although this pseudo-equilibrium potential is defined by the standard conditions of redox potential measurements, and in practice will depend on actual concentrations (596). The rapid reactions that O_2^- undergoes after its generation likely make this reaction irreversible; thus there is no true reversal potential. Depolarization of the phagocyte membrane to the equilibrium potential of the electron transport pathway should prevent electron transport by NADPH oxidase. We recently measured the voltage dependence of I_e in human eosinophils and found that depolarization of the membrane to +190 mV abolished I_e (252). This result confirms that depolarization itself can prevent NADPH oxidase from translocating electrons across the membrane. A surprising aspect of the I_e-voltage relationship was that I_e was nearly constant between −100 mV and ~+50 mV but was steeply inhibited by further depolarization. This unexpected feature explains the concentration dependence of Zn^{2+} and upon reflection reveals the brilliant design of the enzyme.

Divalent metal cations inhibit H^+ currents mainly by shifting the voltage dependence of gating to more positive voltages (70, 134, 232, 236, 246, 258, 372, 519, 762, 886) (see sect. v*O*). Distinct inhibition of O_2^- production in neutrophils first occurred at 300 μM Zn^{2+} (252), which at pH 7.4 would shift the threshold for activating the g_H by ~90 mV (163), i.e., from −20 mV in PMA-activated cells (246, 248) to +70 mV. Consequently, activation of sufficient H^+ efflux to compensate I_e can occur only at voltages positive to +70 mV that are within the range where I_e is inhibited directly by voltage. Because the I_e-*V* relationship is voltage independent from the normal resting potential up to roughly +50 mV, lower [Zn^{2+}] that shift the g_H-*V* relationship within this voltage range do not inhibit NADPH oxidase. Analogously, depolarization to ~0 mV with high K^+ concentration had little (315, 460, 662) or no effect on O_2^- production by eosinophils, macrophages, or neutrophils (576, 722, 998). In summary, Zn^{2+} inhibits O_2^- production by shifting H^+ channel activation into or beyond the voltage-dependent region of the I_e-*V* relationship.

Careful measurements during the respiratory burst in neutrophils indicate that the membrane depolarizes to +58 mV (488). This is close to the point at which depolarization begins to inhibit I_e. Importantly, despite this depolarization of >100 mV from the resting potential, there is minimal "self-inhibition" because the I_e-*V* relationship is practically voltage independent in this range (252). The surprisingly large range over which NADPH oxidase is independent of membrane potential provides a safety factor that ensures continued optimal function of this enzyme unless it is confronted by drastic membrane depolarization. The depolarization that occurs during the respiratory burst is sufficient to activate substantial H^+ efflux through H^+ channels without significantly inhibiting the NADPH oxidase.

8. Could other ion channels serve the same function?

Phagocytes express a variety of ion channels in addition to H^+ channels (249, 335). It has been proposed based on pharmacological lesion studies that various ion channels (Ca^{2+}, K^+, and Cl^-) play important roles in the respiratory burst (182, 534, 871, 889, 909), although blocking the inward rectifier (Kir2.1) channel had no effect on O_2^- production (998). In eosinophils, PMA enhances Cl^- currents but has no effect on K^+ currents, and Cl^- channel inhibitors reduce O_2^- production by about one-third (909). Roles proposed for K^+ channels include the one

already proposed for H^+ channels, namely, balancing NADPH oxidase-generated electron flux (837, 889), or facilitating the activity of proteolytic enzymes (837). Proposed roles for Cl^- channels include signaling during assembly of the oxidase (683), blunting calcium influx (1068), and charge compensation (909). Swelling-activated Cl^- currents in neutrophils may also contribute to regulatory volume decrease (968). Although a partial reduction of O_2^- production by the Cl^- transport inhibitor DIDS was reported in eosinophils (909), in neutrophils this inhibitor either had no effect (560) or enhanced O_2^- production (656). Activation of Cl^- influx attenuated O_2^- production (1068); conversely, Cl^- efflux has been proposed to be an essential step in activating NADPH oxidase (683). It was suggested recently that the severity of CGD results not only from the lack of reactive oxygen species, but also from altered phagosomal and cytoplasmic ion composition due to disruption of ion fluxes across phagosomal membranes as a consequence of the lack of the electrogenic NADPH oxidase function (348).

With respect to balancing the electron flux mediated by NADPH oxidase, H^+ channels have a distinct advantage over other channels. The operation of other channels would result in osmotic changes in the phagosome, leading to swelling (K^+ influx) or shrinking (Cl^- efflux). In contrast, the extruded H^+ may be consumed stoichiometrically with O_2^- in the dismutation reaction (Fig. 25). H^+ current can balance electron flux perfectly and can do so with no net osmotic effect. In contrast, K^+ influx or Cl^- efflux would cease by self-inhibition when the phagosome was filled with K^+ or depleted of Cl^-, and thus the ability of these lesser conductances to compensate for continuous NADPH oxidase activity is limited. Because the H^+ transported by channels is consumed metabolically, H^+ efflux can continue indefinitely. This is crucial in light of the continuous activity of NADPH oxidase over tens of minutes. Reeves et al. (837) proposed recently that although electron flux is balanced mostly by H^+, up to 6% is compensated by K^+ efflux, which consequently results in controlled alkalinization of the phagosome (837), as was observed previously (914). In this view, the imperfect control of phagosomal pH and osmolarity due to the small K^+ efflux component is crucial to somehow facilitating activation of bactericidal proteases (837).

9. *Other functions: do voltage-gated proton channels acidify organelles or phagosomes?*

Although voltage-gated proton channels are studied almost exclusively in the plasma membrane of cells, which is accessible by voltage-clamp techniques, an intriguing possibility is that they may play a specific function in organelle membranes. Endosomes become progressively more acidic as they evolve into lysosomes. The orientation of voltage-gated proton channels in the plasma membrane is such that upon endocytosis they will "point inward," tending to conduct H^+ current into the interior of an endosome. Voltage-gated proton channels appear to be well suited to this task, functioning as ideal rectifiers, allowing only H^+ influx. Two factors make it unlikely that typical endosomal acidification is attributable to H^+ channels. First, endosomes and many other organelles already have V-type H^+-ATPases in their membranes that acidify the interior (596). Second, even if H^+ channels were available to function in this capacity, they function passively; thus for every H^+ conducted into the vesicle, one positive charge-equivalent would have to be extruded actively. Teleologically, the cell appears to gain nothing by this mechanism.

These arguments are not persuasive for phagocytes during the respiratory burst. At least in the case of neutrophils, and possibly for other phagocytes, the major site of physiological NADPH oxidase activity is precisely in the phagosomal membrane, and perhaps also in presecretory vesicles or granules (55, 179, 553, 581). The driving force for channel-mediated H^+ influx is provided by NADPH oxidase itself. This enzyme produces O_2^- by pumping electrons into the phagosome, which rapidly depolarizes the membrane (interior relative to cytoplasm) and activates H^+ channels. No additional energy source is needed. The larger cytoplasmic vesicles in neutrophils are ~300 nm in diameter, with ~3 fF capacitance (767). A single NADPH oxidase molecule with a turnover rate of 300/s (199, 566) would depolarize the membrane of the vesicle by 16 mV/s. Given that roughly 250,000 NADPH oxidase molecules assemble in a single neutrophil within 6 min of PMA stimulation (832) and that the neutrophil membrane capacity increases upon stimulation by ~5.4 pF (767), the average vesicle, assuming uniform distribution in all membranes, would have 139 functional NADPH oxidase complexes. The vesicle membrane potential would depolarize by 2.2 V/s, or by 100 mV in 45 ms. Viewed differently, neutrophils consume 0.2 fmol O_2 for each opsonized particle phagocytosed (912). Without any charge compensation, the same 3 fF phagosome would depolarize by 6,400 V. Long before such extreme depolarization could occur, the huge opposing membrane potential would shut down the oxidase (see sect. VI*H7*). Depolarization would rapidly activate H^+ channels in the phagosomal or plasma membrane, which would conduct H^+ into the vesicle to keep up with the electron flux. Although there is no direct evidence, it is highly probable that H^+ channels serve the same function in phagosomal or vesicular membranes in phagocytes that they serve in the plasma membrane.

An additional benefit of the balancing of electron and proton fluxes is that the phagosomal pH is thereby maintained (or any change is minimized). The superoxide anions produced by NADPH oxidase rapidly dismutate into H_2O_2 (Fig. 25). The dismutation reaction consumes pro-

tons and would increase the phagosomal pH, thus inhibiting the oxidase because its pH optimum is 7.0–7.5 (179). That the phagosomal pH does increase detectably (914) indicates that proton excretion lags slightly behind electron extrusion, confirming that these processes are not strictly coupled. Alternatively, the alkalinization may reflect a small component of charge compensation by K^+ flux (837).

I. Molecular Identity of Voltage-Gated Proton Channels: Is Part of the NADPH Oxidase Complex a Voltage-Gated Proton Channel?

The molecular identity of voltage-gated proton channels is not known at this time. For some time it has been speculated that a component of NADPH oxidase might act as a proton channel. When Henderson et al. (429) presented the first evidence of electrogenic H^+ efflux in human neutrophils, they proposed that the molecule responsible might resemble the Zn^{2+}- and Cd^{2+}-sensitive voltage-gated proton channel reported 5 years earlier in snail neurons by Thomas and Meech (1008). They later considered the idea that a component of the NADPH oxidase complex might carry out the electrogenic H^+ efflux required to compensate for electrogenic electron translocation (430, 431). A variety of evidence can be interpreted to support the idea that part of the oxidase complex, presumably one of the membrane-bound components, $gp91^{phox}$ or $p22^{phox}$, can function as a proton channel (67c, 426–428, 433, 649, 668, 740, 830). The opinion of this reviewer is that these arguments are either circumstantial or unproven. A number of studies indicate that $gp91^{phox}$ is not a proton channel (246–248, 705, 737, 742). Because this issue has become controversial,[7] the evidence for and against $gp91^{phox}$ being a proton channel will now be summarized, using the conversational format employed by Galileo in his *Dialogue Concerning the Two Chief World Systems* in 1632 (333). Simplicio advocates $gp91^{phox}$ being a proton channel, Salviati believes it is not, and Sagredo is nonpartisan.[8]

Simplicio: Many bioenergetic molecules have strictly coupled electron and proton transport.

The original (429–431) and still-accepted explanation of the function of voltage-gated proton channels in phagocytes is to compensate for the electrogenic electron transport performed by the working NADPH oxidase complex (249, 252, 280, 348). In light of the precedent of many bioenergetic molecules that transport both electrons and protons in a stoichiometrically coupled fashion (51, 130, 194, 394, 447, 526, 584, 694, 696, 775, 862, 1014, 1072–1074), Henderson et al. (430, 431) considered the idea that the NADPH oxidase itself might carry out the electrogenic H^+ efflux required to compensate for its electrogenic nature.

Salviati: Protons and electrons move independently of each other in many situations.

Unlike bioenergetic molecules in which electron translocation and proton translocation are strictly and stoichiometrically coupled, the translocation of electrons through NADPH oxidase is unequivocally separable from compensatory H^+ efflux through H^+ channels. Several lines of evidence demonstrate functional independence of NADPH oxidase and H^+ channels. It is possible to measure continuous DPI-sensitive I_e in a cell that is voltage-clamped at a potential that does not allow H^+ channels to open (67c, 165, 246–248, 896), or when H^+ current is inhibited by Zn^{2+} (252, 896). In this situation, the normal requirement for H^+ current to balance the electron flux is satisfied by the feedback amplifier of the patch-clamp circuit, which supplies the required compensatory current. Conversely, inhibition of NADPH oxidase activity by DPI does not prevent activation of H^+ efflux by vanadate peroxides in HL-60 cells (90), nor does it prevent or reverse the dramatic enhancement of the g_H in stimulated phagocytes (165, 246, 248). Stimulation with AA in the presence of DPI increases H^+ currents and speeds τ_{act} without activating electron current through NADPH oxidase (165). H^+ flux is inhibited by lower concentrations of Zn^{2+} or Cd^{2+} than are required to reduce O_2^- release in neutrophils (521) (see sect. VI*H7*).

Simplicio: The $gp91^{phox}$ molecule has several His residues that might conduct protons.

It has been considered likely that the conduction pathway through voltage-gated proton channels is a HBC (see sect. III*D*) rather than a water-filled pore (166, 238–240, 242, 244, 245, 426, 433, 649, 668). With a pK_a near neutral and precedents in M_2 (811), CA II (176, 931), and the K^+ channel voltage sensor (960), His has been considered a likely candidate to form part of a HBC conduction pathway, although inspection of Table 2 indicates that other amino acids can serve this function. Henderson and Meech (426, 433) reported loss of AA-activatable H^+ efflux in CHO cells transfected with variants of $gp91^{phox}$ in which His^{111}, His^{115}, and His^{119} all were mutated to Leu, or in the single H115L mutation; H115D preserved some function. The H115L result was duplicated by Maturana et al. (668). Henderson (426) proposed that His^{115} shuttles protons across the membrane.

Salviati: The His residues are too busy coordinating heme groups to conduct protons.

It is clear that $gp91^{phox}$ is the key heme-binding component of NADPH oxidase (1094) and that His^{115} binds one of the two hemes in the electron transport chain (91).

[7] Note added in proof: many of the arguments presented here are discussed in the Perspectives section of the December 2002 issue of the *Journal of General Physiology*.

[8] The names of the discussants are those used by Galileo. The Latin term *simplicitas* means straightforwardness, honesty, and candor.

Maturana et al. (668) proposed that His^{115} might function both in heme ligation and proton conduction, "thereby coupling electron and proton transport." However, if $gp91^{phox}$ and the H^+ channel are separate molecules, such convoluted mechanisms need not be considered.

Simplicio: The histidine modifying reagent diethylpyrocarbonate (DEPC) reportedly inhibits AA-induced superoxide release and H^+ flux in human neutrophil cytoplasts (649), as well as type ***x*** H^+ current in eosinophils (67c).

Salviati: DEPC could affect any protein containing His. $gp91^{phox}$ is not the only molecule with solvent-accessible His residues. Inhibition of H^+ flux by His modification could reflect effects on any protein with an accessible His residue, including the H^+ channel (whatever its identity) or an accessory protein. Competition between Zn^{2+} and H^+ suggests that the external Zn^{2+} receptor of voltage-gated proton channels comprises several His residues (163).

Sagredo: The H-X-X-X-H-X-X-X-H motif proposed by Henderson and Meech (426, 433) to comprise part of the proton pathway was used by Bánfi et al. (67a) to identify $gp91^{phox}$ homologs that have putative H^+ channel function.

Salviati: Neither $gp91^{phox}$ nor any of its homologs has been demonstrated to function as a proton channel. Furthermore, this motif is present only in *Nox*1 (but not in rat) and *Nox*2 ($gp91^{phox}$) but is absent in other *Nox* isoforms, including *Nox*3, *Nox*4, *Nox*5, *Duox*1, and *Duox*2.

Simplicio: Expression of voltage-gated proton channels is correlated with NADPH oxidase activity.

Cells with the highest levels of NADPH oxidase activity (e.g., eosinophils) have large proton currents. Furthermore, as shown in Figure 26, H^+ channel expression among phagocytes is roughly proportional to the maximum rate of O_2^- production in each cell type. The promyelocytic HL-60 cell line, induced to differentiate in the granulocyte pathway, acquires the ability to produce O_2^- in parallel with increased H^+ channel expression (830).

Salviati: Direct comparison of the amplitude of I_e and I_H in individual human neutrophils activated by PMA revealed no correlation (248).

Sagredo: Direct correspondence between numbers of various NADPH oxidase components is not required. Apparently, $gp91^{phox}$ is present at about fourfold excess over the cytosolic NADPH oxidase components in human neutrophils (832). One neutrophil contains 2,260,000 $gp91^{phox}$ molecules, although most are not in the plasma membrane, but only 600,000 $p67^{phox}$ molecules (A. R. Cross, personal communication).

Salviati: The correlation between H^+ channel expression and NADPH oxidase activity is weak or absent in some cells. In any case, the H^+ channel in unstimulated cells is not $gp91^{phox}$.

Several cells that express voltage-gated proton channels have no detectable NADPH oxidase activity. Voltage-gated proton channels were discovered in snail neurons, which may lack NADPH oxidase. Human basophils have large H^+ currents (170), but do not produce detectable O_2^- (222). Rat alveolar epithelial cells express high levels of H^+ channels (166, 232) but are capable of at most a low level of O_2^- release (1034). The properties of type ***e*** channels are sufficiently distinct from type ***p*** to be reasonably considered a different isoform, but basophil H^+ channels exhibit type ***p*** properties, and basophils share a granulocyte lineage with eosinophils and neutrophils. Endothelial cells apparently produce O_2^- by an NADPH oxidase mechanism (954), yet no detectable H^+ current has been reported. Human T lymphocytes express H^+ channels (886) but have no detectable cytochrome b_{558} (516a).

The correlation shown in Figure 26 is for H^+ currents in unstimulated cells. Even some proponents of the theory that $gp91^{phox}$ is a proton channel agree that the H^+ channel in resting cells is not $gp91^{phox}$ (67a, 67c, 668); thus any correlation is irrelevant. On the other hand, if activation converts H^+ channels from the type ***p*** to the type ***x*** gating mode, as seems likely (165, 246–248), the apparent correlation between g_H and NADPH oxidase activity in phagocytes is meaningful and indicates that cells regulate expression of H^+ channels in accordance with their need for them.

Finally, estimates of the number of H^+ channels and NADPH oxidase complexes in human eosinophils (see sect. VI*H6*) indicate that there are ~20 times more active NADPH oxidase complexes per cell (8.3×10^5) than H^+ channels (5×10^4). In contrast, most H^+ channels are open at large positive voltages where their density is estimated (720). The discrepancy increases if one considers the total number of cytochrome b_{558} molecules (including inactive ones) which is $0.8–1.0 \times 10^6$/cell for neutrophils (832). Larger numbers occur in eosinophils, which have two to three times as much cytochrome b_{558} (913) and correspondingly an approximately threefold larger respiratory burst (229, 581, 807, 926, 956, 1086, 1087). All things considered, eosinophils most likely have ~100 times more $gp91^{phox}$ molecules than proton channels.

Simplicio: The same things turn on NADPH oxidase and voltage-gated proton channels.

There is a temporal and phenomenological coincidence of O_2^- release and electrogenic H^+ efflux in phagocytes stimulated with PMA and other agonists (108, 165, 246–248, 428–431, 521, 738).

Salviati: This is a good thing, because they both need to work at the same time!

In light of the function of H^+ channels during the respiratory burst, it is teleologically beneficial that the g_H is enhanced by the same agonists that activate the respiratory burst (431). However, these agonists also activate many distinct processes in cells, such as chemotaxis,

granule secretion, cytokine release, Na^+/H^+ antiport, etc. Signaling pathways frequently affect several distinct processes.

Simplicio: The H^+ channels active during the respiratory burst have properties markedly different from those in resting cells (two types of channels).

Bánfi et al. (67c) made the important observation that under conditions that enable NADPH oxidase activity, the properties of voltage-gated proton channels were radically different from in cells studied under conventional whole cell conditions, in which NADPH oxidase cannot function. They concluded that NADPH oxidase activity was associated with the appearance of a distinct variety of H^+ channel, not observed in unstimulated cells, and that this channel was formed by $gp91^{phox}$. The simultaneous presence of two types of channels was supported by altered gating properties and enhanced sensitivity to DEPC and Zn^{2+} (67c).

Salviati: H^+ channel properties change during activation of NADPH oxidase (one channel with two gating modes).

The permeabilized-patch configuration allows direct comparison of the properties of H^+ currents in a single phagocyte before, during, and after activation of NADPH oxidase with PMA, AA, or other agonists (165, 246–248). These studies confirm the observation of Bánfi et al. (67c) that the properties of H^+ channels are profoundly different when NADPH oxidase is activated, but also provide strong evidence that agonists alter the properties of preexisting H^+ channels, rather than inducing the appearance of a novel variety of channel. The PMA-enhanced g_H in individual neutrophils was strongly correlated with that before stimulation, even though there was an order of magnitude range of resting g_H (248). There was a progressive shift of tail current kinetics and the g_H-V relationship with no indication of two components (248). When NADPH oxidase is inhibited by DPI, the H^+ currents remain large (165, 246, 248). Inhibition by DPI immediately reverses only one of the four H^+ channel gating properties that is altered by PMA, τ_{tail}, thus demonstrating that the novel properties of the NADPH oxidase-associated H^+ channel are separable from one another, rather than being invariant properties of a distinct channel type. Furthermore, AA activates I_e in permeabilized patch studies and produces changes in H^+ currents that mostly are quantitatively identical to those produced by PMA (165). However, AA does not slow τ_{tail}, again demonstrating that the properties of putative type ***x*** channels are not invariant. Finally, the reported difference in Zn^{2+} sensitivity between type ***p*** and ***x*** channels was a predictable outcome of their experimental design and is not observed when equivalent measurements are evaluated (see appendix of Ref. 246).

Sagredo: Are H^+ current properties consistent with the known cellular localization of cytochrome b_{558}?

In resting neutrophils ~75% of the cytochrome b_{558} is located in intracellular granules and ~25% is in the plasma membrane (179). If $gp91^{phox}$ were the type ***x*** proton channel, then it should be detectable in unstimulated cells, and its density in the surface membrane should increase upon stimulation. Is this observed?

Salviati: No. The NADPH oxidase-related (type ***x***) H^+ channel is not detected in the plasma membrane of unstimulated phagocytes (236, 246, 248, 258, 372, 518, 519, 895). Upon activation, all of the channels in the cell uniformly exhibit type ***x*** behavior, and no detectable type ***p*** channel behavior remains (246–248).

Sagredo: Maybe $gp91^{phox}$ is inactive in resting cells. Type ***p*** channels may disappear when phagocytes are activated, or perhaps upon stimulation type ***p*** channels, like chameleons, adopt properties indistinguishable with type ***x***, simultaneous with the appearance of new type ***x*** channels. It could happen.

Simplicio: Maybe $gp91^{phox}$ functions as a proton channel only when NADPH oxidase is active.

Nanda et al. (737) concluded that although NADPH oxidase does not conduct H^+ current, optimal activation of H^+ efflux requires normal assembly of oxidase components.

Salviati: This idea is apparently disproved by studies reporting putative H^+ channel behavior of $gp91^{phox}$ expressed in CHO (426, 427, 433, 649) or COS-7 cells (668). Neither of these cells has the biochemical machinery to assemble NADPH oxidase or to produce O_2^-.

Simplicio: H^+ efflux is subnormal in some CGD cells with dysfunctional NADPH oxidase.

Nanda and Grinstein (740) reported that the PMA-stimulated, Zn^{2+}-sensitive cytoplasmic alkalinization (interpreted as H^+ channel activity) was reduced in CGD patients who lack $gp91^{phox}$. Bánfi et al. (67c) reported that CGD patients lacking either $gp91^{phox}$ or $p47^{phox}$ lacked the type ***x*** H^+ channel, although both had normal H^+ currents at pH_i 6.1. The absence of putative $gp91^{phox}$-mediated currents in the patient lacking $p47^{phox}$ is paradoxical, but might be explained by the suggestion that proper assembly of the NADPH oxidase complex is required for activation of its associated H^+ channel (737).

Salviati: Altered H^+ currents are consistent with channel modulation. H^+ currents are normal in phagocytes from CGD patients.

An obvious alternative interpretation of the report of Nanda and Grinstein (740) was that CGD neutrophils might have normal H^+ channels that are not activated by PMA stimulation because the defective NADPH oxidase in these cells does not acidify the cytoplasm and depolarize the membrane as in normal cells. At that time it was conceivable that voltage-gated proton channels were activated in a purely indirect manner, by the depolarization and lower pH_i that result from the action of NADPH oxidase. In fact, the same lab immediately disproved their

initial hypothesis in a voltage-clamp study of peripheral blood monocytes that demonstrated that patients lacking gp91^{phox} had H^+ currents with properties and amplitude identical to those in normal subjects (742). This result has been confirmed by others (67c, 247). They also showed that in several rare forms of CGD, activation of H^+ efflux was normal in mutations that permitted assembly of a dysfunctional NADPH oxidase complex, and that in patients with reduced gp91^{phox} expression, activation of the g_H was not reduced proportionately (737). This disparity between cytochrome b_{558} levels and voltage-gated proton current density speaks against the idea that NADPH oxidase might contain the H^+ channel.

Simplicio: The H^+ currents are normal in CGD because whole cell studies detect only the resting type ***p*** channel. They would not reveal the absence of type ***x*** NADPH oxidase-related channels.

Salviati: H^+ currents are normal in gp91^{phox} knock-out cells and phagocytes from CGD patients. Furthermore, PMA increases H^+ currents to the same extent whether gp91^{phox} is present or absent.

The strongest evidence against gp91^{phox} being a proton channel comes from genetic knock-out studies. PLB-985 cells are of the myelocytic lineage and after induction by dimethylformamide are capable of producing O_2^- via a fully functional NADPH oxidase system (1099). Identical large voltage-gated proton currents with completely normal properties were observed in wild-type PLB cells, gp91^{phox} knock-outs, and in knock-outs rescued by retransfection with gp91^{phox} (247). Studied in permeabilized-patch configuration, the H^+ currents in gp91^{phox} knock-outs also responded to PMA stimulation with increased $g_{H,max}$ and faster τ_{act}, similar to controls. The slowing of τ_{tail} was not observed, consistent with this parameter being closely linked to NADPH oxidase activity, which obviously was absent in the gp91^{phox} knock-out cells. As shown in Figure 27, similar results were obtained with CGD granulocytes from patients lacking gp91^{phox}. Unstimulated neutrophils from CGD patients had normal H^+ currents, and PMA stimulation increased the H^+ current to the same extent. This study demonstrated that when NADPH oxidase is activated, $g_{H,max}$ increases in the complete absence of gp91^{phox} and this increase cannot be ascribed to gp91^{phox} being a proton channel.

Simplicio: Heterologous expression of gp91^{phox} and homologs results in voltage-gated proton currents.

Henderson et al. (427) reported that heterologous expression of gp91^{phox} in CHO cells resulted in pH changes suggestive of conductive H^+ flux, a result supported by subsequent studies (426, 433, 435, 649, 668). Recently, several gp91^{phox} homologs were reported to function as H^+ channels, increasing background H^+ currents by four- to fivefold in heterologous expression systems (67a, 67b, 668).

Salviati: Heterologous expression either upregulates

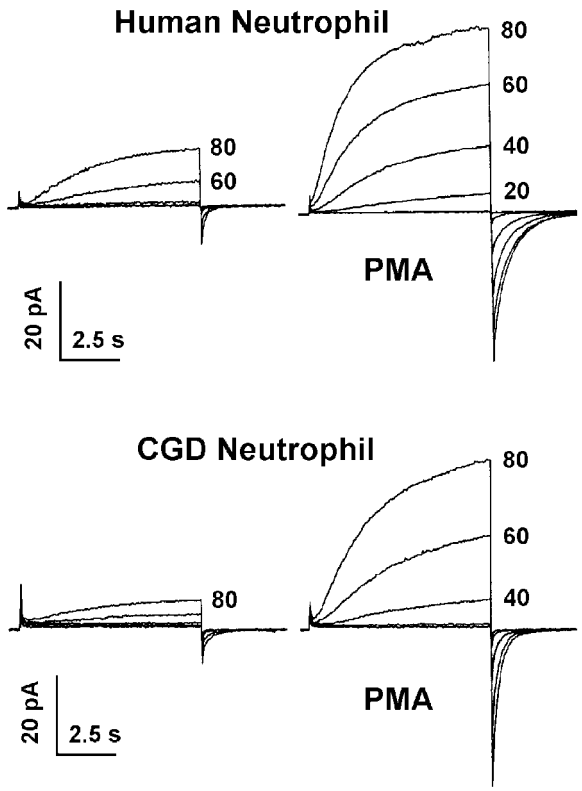

FIG. 27. Families of H^+ currents recorded in neutrophils from a normal individual (*top*) and from a patient with chronic granulomatous disease (CGD) who lacked gp91^{phox} expression (*bottom*). Voltage pulses were applied in 20-mV increments as labeled. Cells were studied in permeabilized patch configuration, with a symmetrical NH_4^+ gradient applied to clamp pH_i to pH_o, which was 7.0. The currents on the *left* were recorded before stimulation, those on the *right* after stimulation with PMA. The average H^+ current amplitudes are the same in CGD and normal cells (247). The small inward current at the holding potential in the normal cell is due to electron current through the activated NADPH oxidase complex, which is absent in the CGD cell. The proton conductance in both resting and activated cells is the same in the absence of gp91^{phox}, which is inconsistent with the proposal that gp91^{phox} is a proton channel (V. V. Cherny, A. G. DeCoursey, and T. E. DeCoursey, unpublished data.)

background voltage-gated proton channels or produces a conductance that differs from genuine voltage-gated proton channels.

The heterologous expression data are unconvincing. Of the three cell lines used for expression, two (CHO and HEK-293 cells) already express voltage-gated proton channels (67a, 164, 280, 668). Expression of either *Nox*1 or gp91^{phox} in HEK-293 cells resulted in H^+ currents that were only approximately fourfold larger than in the background (67a, 668), which could reflect upregulation of intrinsic H^+ channels. Upregulation of endogenous ion channels by transfection with irrelevant proteins is a well-known phenomenon (922). We observed H^+ current densities in HEK-293 cells transfected with the biologically inert green fluorescent protein (280) (V. V. Cherny, B. L. Davidson, R. Haskell, and T. E. DeCoursey, unpublished data) that were similar to those in HEK-293 cells trans-

fected with *Nox*1 (67a) or gp91^{phox} (668). In both *Nox*1 or gp91^{phox} transfected HEK-293 cells, H^+ current densities were small, <4 pA/pF (at +60 mV at pH_o 7.5, pH_i 5.7). Under the same conditions (+60 mV at pH_o 7.5, pH_i 5.7) this group reported voltage-gated H^+ currents >300 pA/pF in human eosinophils (895). Putative H^+ currents in gp91^{phox}-transfected CHO cells were >10,000 pA (433).

The putative voltage-gated proton channels in gp91^{phox}-expressing CHO cells (433) differ markedly from H^+ currents in phagocytes. They activate very rapidly; the currents are extremely large, >10 nA in some cells, but surprisingly do not exhibit the droop characteristically observed during large H^+ currents (68, 232, 238, 258, 372, 473, 519, 709, 895). Increasing pH_i by ~0.6 units abolished the putative H^+ currents. In stark contrast, increasing pH_i by 1 unit reduces $g_{H,max}$ only by one-half (234) and shifts the g_H-V relationship by ~40 mV in every extant study of voltage-gated proton channels in native cells (Fig. 19). To account for the mysterious disappearance of the putative H^+ currents in CHO cells would require a shift of at least 140 mV; larger depolarizations were not described. Finally, 200 μM Zn^{2+} only partially inhibited the current and did not appear to slow activation (433). In phagocytes and other cells, 1 μM Zn^{2+} slows H^+ current activation by ~3- to 10-fold at pH ≥7 (163, 246, 886). Thus, although the conductance in gp91^{phox}-expressing CHO cells superficially resembles voltage-gated proton current, it is fundamentally different.

Sagredo: COS-7 cells appear to lack endogenous H^+ currents and therefore present a cleaner expression system (668). What happens in COS-7 cells transfected with gp91^{phox}?

Salviati: The putative H^+ currents in gp91^{phox} expressing COS-7 cells have not been characterized thoroughly, and the data that exist indicate a nonselective conductance. The currents in Figure 1*A* of Maturana et al. (668) were recorded at pH_o 7.5 and pH_i 5.7; thus E_H was −105 mV. However, the large inward tail current upon repolarization to −60 mV, as well as the activation of inward current during the pulse to 0 mV, both indicate that V_{rev} >0 mV. The conductance in gp91^{phox}-transfected COS-7 cells therefore is not H^+ selective, because V_{rev} deviates from E_H by >100 mV. In contrast, the currents in gp91^{phox}-transfected HEK-293 cells in the same figure and recorded under identical conditions, exhibit outward tail currents at −60 mV, consistent with their being H^+ selective. Thus H^+-selective currents were observed only in cells with endogenous voltage-gated proton channels.

In another study, gp91^{phox} was expressed in COS-7 cells together with the other three main NADPH oxidase components (705). The expression of gp91^{phox} was confirmed by antibody staining and by demonstration that the cells generated O_2^- upon stimulation (705, 822). No proton currents were detected in whole cell or permeabilized patch studies, or after stimulation under conditions that enhanced H^+ currents in neutrophils, eosinophils, or PLB cells (705). Thus H^+-selective currents were not detected in either study in the COS-7 expression system.

Simplicio: Maybe homologs of gp91^{phox} are proton channels (67a, 67b). An alternatively spliced variant of *Nox*1 mRNA was detected in leukocytes and HL-60 cells (67a).

Salviati: Most of the gp91^{phox} homologs are not expressed detectably in peripheral blood leukocytes (538, 582), including *Nox*1 (973), *Nox*3, *Nox*4 (162), and *Nox*5 (67b). However, *Nox*4 has been detected in osteoclasts (1088), which do have proton currents (762). Recent data suggest that the short form of *Nox*1, called NOH-1S and reported to be a proton channel by Bánfi et al. (67a), is not a natural product (T. L. Leto and M. Geiszt, personal communication).

Sagredo: Anyway, the question is whether gp91^{phox} is a proton channel. Why don't you put gp91^{phox} into phospholipid bilayers and see if it acts as a channel?

Salviati: We tried that (J. Tang, A. R. Cross, D. Morgan, V. V. Cherny, and T. E. DeCoursey, unpublished data). We added cytochrome b_{558} plus FAD, and then at intervals of several minutes, added neutrophil cytosol to restore the cytosolic components, then guanosine 5′-*O*-(3-thiotriphosphate), NADPH, PMA, and finally AA. At no stage (for up to >2 h) did we observe currents above the tiny leak conductance through the bilayer alone (<1 pA over +/−100 mV, bilayer resistance ~200 GΩ). Addition of OmpF porin channels to the same bilayer produced single-channel currents within seconds.

Summary: Although early studies were tantalizing, the preponderance of the evidence indicates that the voltage-gated proton channel is a separate entity from the NADPH oxidase complex. Ignoring the circumstantial evidence on both sides leaves the more definitive heterologous expression studies. The studies claiming proton channel function for gp91^{phox} are unconvincing. In some cases, the putative H^+ currents in gp91^{phox} transfected cells simply do not have the properties of voltage-gated proton currents in native cells. Those studies showing genuine H^+ currents in gp91^{phox}-transfected cells were done in an expression system that constitutively exhibits H^+ currents of amplitude similar to those in the transfected cells. When gp91^{phox} is expressed in COS-7 cells that have no endogenous H^+ channels, no H^+ current could be detected (668, 705), although expression was confirmed both by antibody staining and functional studies (705). Genetic knock-out of gp91^{phox} in PLB-985 cells or in CGD patients does not affect H^+ currents in unstimulated cells nor prevents the PMA-stimulated increase in H^+ currents (247). It is time to abandon the idea that gp91^{phox} is a proton channel and reinstate a search for this elusive molecule.

J. Functional Link Between NADPH Oxidase Activity and H^+ Channel Gating

A remarkably similar constellation of effects on voltage-gated proton channels is observed when NADPH oxidase is activated by PMA (246–248), by AA (165), or spontaneously (246). This coincidence suggests that a common signaling pathway may be involved. On the other hand, it is possible to dissect some of these changes temporally or pharmacologically. The most rapid effect of PMA is an increase in the rate of channel opening (246, 248). The increase in I_H also occurs more rapidly than the appearance of I_e. Thus H^+ channel opening is enhanced before significant activation of NADPH oxidase has occurred, strongly suggesting that modifications of channel gating occur as a primary effect and not as a consequence of NADPH oxidase activation.

In contrast, the slowing of τ_{tail} (indicating the rate of H^+ channel closing upon repolarization) appears to be tightly coupled to NADPH oxidase activity. When neutrophils, eosinophils, or PLB-985 cells are stimulated with PMA or when they become activated spontaneously, I_e turns on with a time course that generally parallels the slowing of τ_{tail} (246–248). Furthermore, when I_e turns off spontaneously or when NADPH oxidase is inhibited by DPI (200), τ_{tail} becomes faster again (246–248). The speeding of τ_{tail} by DPI occurs only when τ_{tail} has first been slowed by activation of the cell. DPI has no effect on τ_{tail} in unstimulated cells (248), or after the I_e turns off spontaneously, as occasionally happens in eosinophils (246). Thus DPI does not have a direct pharmacological effect on H^+ channels, but acts indirectly on H^+ channels by inhibiting NADPH oxidase. The apparent sensitivity of τ_{tail} to NADPH oxidase activity is surprising. Evidently, there is a strong functional connection between the rate of H^+ channel closing and the activity of NADPH oxidase. Intriguingly, a β-subunit of K^+ channels that is structurally similar to oxidoreductase enzymes has been speculated to function as a link between cellular redox chemistry and electrical excitability, or alternatively to act as a voltage-dependent enzyme (393).

How this link occurs is a mystery. The hypothesis that the H^+ channel is part of the NADPH oxidase complex is untenable, as discussed in section VI, *H* and *I*. There could be direct molecular interaction if the H^+ channel were in close physical proximity to the NADPH oxidase complex, perhaps as an as-yet-unidentified auxiliary protein or in a lipid micro-raft. A higher-order regulatory molecule might simultaneously govern the activity of NADPH oxidase and H^+ channels. Finally, the H^+ channel might sense the effects of NADPH oxidase activity. The latter idea seems the most likely in view of there being one to two orders of magnitude more NADPH oxidase complexes than H^+ channels in phagocytes (see sect. VI*H6*). Possible effects of NADPH oxidase activity include depolarization, global or local decreases in pH_i and increases in pH_o, and appearance of reactive oxygen species. Preliminary studies indicate little effect of H_2O_2 applied to the bath solution (Cherny and DeCoursey, unpublished data), but these studies were not extensive, nor did they examine possible effects of O_2^- or a myriad other reactive oxygen species that can be formed (543). We proposed that H^+ channels sense the local accumulation of protons during the respiratory burst (248).

K. How Far Apart Are Proton Channels and NADPH Oxidase Complexes?

For the H^+ channel to sense local accumulation of protons (248), it must be physically near the source of protons. The analogous problem of how far Ca^{2+} can diffuse from the point source of a Ca^{2+} channel into bulk cytoplasm has been addressed (964). The length constant λ (roughly the average distance the free ion diffuses before it is consumed by buffer) is given approximately by

$$\lambda \approx \sqrt{\frac{D_H}{B_{free} k}} \qquad (7)$$

where D_H is the diffusion constant for H^+ and is 1.08×10^{-4} cm^2/s at 37°C (845), B_{free} is the free buffer concentration, which corresponds roughly with the buffering capacity of phagocyte cytoplasm, which has been estimated to be 15.6–50 mM at physiological pH_i (324, 940). Stern (964) and others (950) have discussed the limitations of this calculation. The bimolecular rate constant of protonation of buffer (k) is assumed to be diffusion limited at $1–4 \times 10^{10}$ $M^{-1} \cdot s^{-1}$ (80, 287, 290, 768). Given these rough assumptions, λ is 2.3–8.3 nm. Neglecting buffer diffusion and background proton concentration, the concentration of protons (c_H) at distance r from a source such as NADPH oxidase is given approximately by (E. Ríos, personal communication)

$$c_H \approx \frac{H^+ \text{generation rate}}{4\pi D_H r} e^{-r/\lambda} \qquad (8)$$

The exponential term incorporates the attenuation by buffer of the c_H that would have resulted from diffusion from the source alone.

Distances can be estimated from the previous estimates of 125–200 H^+ channels/μm^2 and 2,100–3,300 active NADPH oxidase complexes/μm^2 of eosinophil membrane (see sect. VI*H6*). The following geometric analysis is by Ricardo Murphy. With the assumption of a uniform distribution in a square grid pattern, each H^+ channel would be 70–90 nm from its nearest neighbor, and each active NADPH oxidase complex would be 17–22 nm from

its neighbors. If the membrane area associated with each H^+ channel ($A = 5–8 \times 10^3$ nm^2) is approximated as a circle of radius $R = \sqrt{(A/\pi)} = 40–50$ nm, then on average, no NADPH oxidase molecule could be farther than this distance from a H^+ channel. If H^+ channels and NADPH oxidase complexes were distributed uniformly, the average distance of an NADPH oxidase molecule from the nearest H^+ channel, r_{mean}, would be

$$r_{mean} = \int_0^R r\left(\frac{2r}{R^2}\right)dr = \frac{2}{R^2}\int_0^R r^2 dr = \frac{2}{3}R \qquad (9)$$

or 27–33 nm. The minimum estimated distance is thus 3λ, which from *Equation 8* means that a H^+ channel would sense <5% of the increased [H^+] near the NADPH oxidase complex (assuming the effective radius of the NADPH oxidase complex is ≤λ). In other phagocytes with a lower density of both H^+ channels and NADPH oxidase components, the distances would be greater. Thus, in the absence of some structural link, such as colocalization of H^+ channels and NADPH oxidase molecules in "lipid rafts" (480), it is unlikely that H^+ channels would uniformly sense highly localized changes in pH due to the activity of a single NADPH oxidase complex. These calculations ignore any enhancement that would result by processes that facilitate the movement of protons in the plane of the membrane surface (see sect. II*D*).

On the other hand, there is a large decrease in global pH_i during the respiratory burst when Na^+/H^+ antiport and H^+ channels are inhibited (430, 431, 738, 977), which demonstrates that protons are generated at a rate sufficient to overload the entire cytoplasmic buffering capacity. It is likely that during the respiratory burst, protons are concentrated near the membrane and that there is a proton gradient that dissipates toward the center of the cell. Direct evidence that this can occur is seen in permeabilized-patch studies. Although the applied NH_4^+ gradient provides excellent control of pH_i in the absence of a load (248, 387), when the NADPH oxidase is activated under these conditions the observed V_{rev} of H^+ currents shifts −3.7 mV in neutrophils (248) and −5.8 mV or −5.3 mV in eosinophils stimulated with PMA (246) or AA (165), respectively. Eosinophils are the same size as neutrophils but have a more active NADPH oxidase. NADPH oxidase activity thus lowers pH_i by ~0.1 unit in spite of the NH_4^+ gradient (and in spite of application of occasional depolarizing pulses to observe currents).

In summary, voltage-gated proton channels are likely too far from NADPH oxidase complexes to sense acute local pH changes, but they may respond to more global pH_i changes that accumulate during sustained NADPH oxidase activity.

VII. SUMMARY AND CONCLUSIONS

Protons are unique among cations in their tiny size, low free but enormous total concentration, reactivity with other molecules, and Grotthuss conduction mechanism. Proton channels have a unique conduction mechanism, the HBC, which in nonselective channels is a simple water wire, but in highly proton-selective channels includes at least one titratable amino acid residue. These protonation sites at once preclude the conduction of other cations, thus acting as "selectivity filters," and provide a mechanism that mediates the interaction between pH and the molecular conformation and function of the channel. The key to proton selectivity is that the proton is conducted through a HBC as H^+ rather than H_3O^+. Many different molecules have proton channels that are of central importance to their function. Most of these channels are HBCs comprising water wires interrupted at crucial points by titratable amino acid residues. In several cases, proton conduction is enhanced by the presence of titratable groups at the entrance to the channel. Proton entry into (or exit from) a channel that occurs by direct Eigen-type proton transfer between buffer and a titratable group on the channel can increase the rate of proton transport far beyond that obtained with simple diffusion. Heavy metal cations often bind competitively with protons to titratable sites on proton channels, where they produce a variety of effects on molecular function.

Unique properties of voltage-gated proton channels, compared with other ion channels that are water-filled pores, include extraordinarily high selectivity, tiny unitary conductance, strong temperature and deuterium isotope effects on both conductance and gating kinetics, and insensitivity to block by steric occlusion. Many of these properties are manifestations of the HBC conduction mechanism. The gating of voltage-gated proton channels is regulated tightly by pH and voltage, with the result that under normal conditions, the channels open only when the electrochemical gradient is outward. The general function of these channels is therefore acid extrusion from cells. Their responsiveness to the voltage across the membrane in which they are located, with modulation by the local pH on both sides of the membrane, means that they are activated automatically when the need arises. Voltage-gated proton channels are expressed in many cells and appear to comprise at least four isoforms. The evidence for specific function is strongest in phagocytes, in which H^+ channels extrude protons during the respiratory burst to compensate for electron extrusion by NADPH oxidase. Activation of H^+ current during the respiratory burst is due to a combination of depolarization, pH changes, and profound modulation of the properties of the H^+ channels. The functions of voltage-gated proton channels and NADPH oxidase are intimately interconnected, but the bulk of evidence indicates that the

channel is a molecular entity distinct from any known NADPH oxidase component. Although much progress has been made, the most exciting discoveries lie in the future.

I thank Vladimir V. Cherny for nearly a decade of invaluable collaboration and Tatiana Iastrebova for prodigious work organizing the references. For generously providing comments, suggestions, answers, preprints, and permission to use figures and unpublished data, I am indebted to Noam Agmon, Jennifer Bankers-Fulbright, Michael E. Barish, Howard C. Berg, Allan Bretag, Peter Brzezinski, Vladimir V. Cherny, Anatoly Chernyshev, David W. Christianson, Andrew R. Cross, Sam Cukierman, Beverly L. Davidson, Audrey G. DeCoursey, Wesley F. DeCoursey, J. Paul Devlin, Mary C. Dinauer, Claudia Eder, Shelagh Ferguson-Miller, Horst Fischer, Robert H. Fillingame, Miklós Geiszt, Mark E. Girvin, Sergio Grinstein, Menachem (Hemi) Gutman, Sharon Hammes-Schiffer, Ronald Haskell, Robert A. Lamb, Janos K. Lanyi, Eric V. Leaver, Tom L. Leto, Paul A. Loach, Vladislav S. Markin, Robert Meech, Denise A. Mills, Deri Morgan, Ricardo Murphy, John F. Nagle, William M. Nauseef, Mel Y. Okamura, Mark L. Paddock, Pamela A. Pappone, Lawrence H. Pinto, Eduardo Ríos, Dirk Roos, Tom Schilling, Mark F. Schumaker, David N. Silverman, Clifford L. Slayman, Erik R. Swenson, John Tang, Justin Teissie, Roger C. Thomas, Mårten Wikström, Dixon J. Woodbury, and Colin A. Wraight. This review was truly a collective effort; many of these individuals patiently critiqued or in some cases essentially rewrote sections of this review.

This work was supported by National Heart, Lung, and Blood Institute Grants HL-52671 and HL-61437.

Address for reprint requests and other correspondence: T. DeCoursey, Dept. of Molecular Biophysics and Physiology, Rush Presbyterian St. Luke's Medical Center, 1750 West Harrison, Chicago, IL 60612 (E-mail: tdecours@rush.edu).

REFERENCES

1. Aagaard A and Brzezinski P. Zinc ions inhibit oxidation of cytochrome *c* oxidase by oxygen. *FEBS Lett* 494: 157–160, 2001.
2. Aagaard A, Namslauer A, and Brzezinski P. Inhibition of proton transfer in cytochrome *c* oxidase by zinc ions: delayed proton uptake during oxygen reduction. *Biochim Biophys Acta* 1555: 133–139, 2002.
3. Abo A, Boyhan A, West I, Thrasher AJ, and Segal AW. Reconstitution of neutrophil NADPH oxidase activity in the cell-free system by four components: p67-*phox*, p47-*phox*, p21*rac*1, and cytochrome b_{245}. *J Biol Chem* 267: 16767–16770, 1992.
4. Abrahams JP, Leslie AG, Lutter R, and Walker JE. Structure at 2.8 Å resolution of F_1-ATPase from bovine heart mitochondria. *Nature* 370: 621–628, 1994.
5. Abrams CK, Jakes KS, Finkelstein A, and Slatin SL. Identification of a translocated gating charge in a voltage-dependent channel Colicin E1 channels in planar phospholipid bilayer membranes. *J Gen Physiol* 98: 77–93, 1991.
6. Abramson SB, Leszczynska-Piziak J, and Weissmann G. Arachidonic acid as a second messenger. Interactions with a GTP-binding protein of human neutrophils. *J Immunol* 147: 231–236, 1991.
7. Accardi A, Ferrera L, and Pusch M. Drastic reduction of the slow gate of human muscle chloride channel (ClC-1) by mutation C277S. *J Physiol* 534: 745–752, 2001.
8. Ädelroth P, Brzezinski P, and Malmström BG. Internal electron transfer in cytochrome *c* oxidase from *Rhodobacter sphaeroides*. *Biochemistry* 34: 2844–2849, 1995.
9. Ädelroth P, Paddock ML, Sagle LB, Feher G, and Okamura MY. Identification of the proton pathway in bacterial reaction centers: both protons associated with reduction of Q_B to Q_BH_2 share a common entry point. *Proc Natl Acad Sci USA* 97: 13086–13091, 2000.
10. Ädelroth P, Paddock ML, Tehrani A, Beatty JT, Feher G, and Okamura MY. Identification of the proton pathway in bacterial reaction centers: decrease of proton transfer rate by mutation of surface histidines at H126 and H128 and chemical rescue by imidazole identifies the initial proton donors. *Biochemistry* 40: 14538–14546, 2001.
10a. Agmon N. The Grotthuss mechanism. *Chem Phys Lett* 244: 456–462, 1995.
11. Agmon N. Hydrogen bonds, water rotation and proton mobility. *J Chim Phys* 93: 1714–1736, 1996.
11a. Agmon N. Proton solvation and proton mobility. *Isr J Chem* 39: 493–502, 1999.
11b. Agmon N. Mechanism of hydroxide mobility. *Chem Phys Lett* 319: 247–252, 2000.
12. Agre P, King LS, Yasui M, Guggino WB, Ottersen OP, Fujiyoshi Y, Engel A, and Nielsen S. Aquaporin water channels: from atomic structure to clinical medicine. *J Physiol* 542: 3–16, 2002.
13. Agre P, Preston GM, Smith BL, Jung JS, Raina S, Moon C, Guggino WB, and Nielsen S. Aquaporin CHIP: the archetypal molecular water channel. *Am J Physiol Renal Fluid Electrolyte Physiol* 265: F463–F476, 1993.
13a. Åhlin A, Gyllenhammar H, Ringertz B, and Palmblad J. Neutrophil membrane potential changes and homotypic aggregation kinetics are pH-dependent: studies of chronic granulomatous disease. *J Lab Clin Med* 125: 392–401, 1995.
13b. Åkerfeldt KS, Kim RM, Camac D, Groves JT, Lear JD, and Degrado WF. Tetraphilin: a four-helix proton channel built on a tetraphenylporphyrin framework. *J Am Chem Soc* 26: 191–197, 1992.
13c. Åkerfeldt KS, Lear JD, Wasserman ZR, Chung LA, and Degrado WF. Synthetic peptides as models for ion channel proteins. *Acc Chem Res* 26: 191–197, 1993.
14. Akeson M and Deamer DW. Proton conductance by the gramicidin water wire model for proton conductance in the F_1F_o ATPases? *Biophys J* 60: 101–109, 1991.
15. Al-Baldawi NF and Abercrombie RF. Cytoplasmic hydrogen ion diffusion coefficient. *Biophys J* 61: 1470–1479, 1992.
16. Alix SN, Woodbury DJ, and Brusilow WS. An unexpectedly large cation conductance following reconstitution of the bacterial F_o proton channel into bilayers (Abstract). *FASEB J* 9: A67, 1995.
17. Almers W. *The Potassium Permeability of Frog Muscle Membrane* (PhD thesis). Rochester, NY: Univ. of Rochester, 1971.
18. Almers W. Gating currents and charge movements in excitable membranes. *Rev Physiol Biochem Pharmacol* 82: 96–190, 1978.
19. Almers W and Armstrong CM. Survival of K^+ permeability and gating currents in squid axons perfused with K^+-free media. *J Gen Physiol* 75: 61–78, 1980.
20. Altendorf K, Stalz W-D, Greie J-C, and Deckers-Hebestreit G. Structure and function of the F_o complex of the ATP synthase from *Escherichia coli*. *J Exp Biol* 203: 19–28, 2000.
21. Althoff G, Lill H, and Junge W. Proton channel of the chloroplast ATP synthase, CF_o: its time-averaged single-channel conductance as a function of pH, temperature, isotopic and ionic medium composition. *J Membr Biol* 108: 263–271, 1989.
22. Amar M, Perin-Dureau F, and Neyton J. High-affinity Zn block in recombinant *N*-methyl-D-aspartate receptors with cysteine substitutions at the Q/R/N site. *Biophys J* 81: 107–116, 2001.
23. Ambruso DR, Knall C, Abell AN, Panepinto J, Kurkchubasche A, Thurman G, Gonzalez-Aller C, Hiester A, deBoer M, Harbeck RJ, Oyer R, Johnson GL, and Roos D. Human neutrophil immunodeficiency syndrome is associated with an inhibitory Rac2 mutation. *Proc Natl Acad Sci USA* 97: 4654–4659, 2000.
24. Amorena CE, Wilding TJ, Manchester JK, and Roos A. Changes in intracellular pH caused by high K in normal and acidified frog muscle. Relation to metabolic changes. *J Gen Physiol* 96: 959–972, 1990.
25. An H, Tu C, Duda D, Montanez-Clemente I, Math K, Laipis PJ, McKenna R, and Silverman DN. Chemical rescue in catalysis by

human carbonic anhydrases II and III. *Biochemistry* 41: 3235–3242, 2002.
26. ANDERSEN OS. Ion movement through gramicidin A channels. Interfacial polarization effects on single-channel current measurements. *Biophys J* 41: 135–146, 1983.
27. ANDERSEN OS. Ion movement through gramicidin A channels. Single-channel measurements at very high potentials. *Biophys J* 41: 119–133, 1983.
28. ANDERSEN OS. Ion movement through gramicidin A channels. Studies on the diffusion-controlled association step. *Biophys J* 41: 147–165, 1983.
29. ANDERSEN OS, FINKELSTEIN A, KATZ I, AND CASS A. Effect of phloretin on the permeability of thin lipid membranes. *J Gen Physiol* 67: 749–771, 1976.
30. ANDERSEN OS AND PROCOPIO J. Ion movement through gramicidin A channels. On the importance of the aqueous diffusion resistance and ion-water interactions. *Acta Physiol Scand Suppl* 481: 27–35, 1980.
31. APELL HJ, BAMBERG E, ALPES H, AND LÄUGER P. Formation of ion channels by a negatively charged analog of gramicidin A. *J Membr Biol* 31: 171–188, 1977.
32. APELL HJ, BAMBERG E, AND LÄUGER P. Effects of surface charge on the conductance of the gramicidin channel. *Biochim Biophys Acta* 552: 369–378, 1979.
33. ARATANI Y, KOYAMA H, NYUI S, SUZUKI K, KURA F, AND MAEDA N. Severe impairment in early host defense against *Candida albicans* in mice deficient in myeloperoxidase. *Infect Immun* 67: 1828–1836, 1999.
34. ARCHER RJ AND LA MER VK. The rate of evaporation of water through fatty acid monolayers. *J Phys Chem* 59: 200–208, 1955.
35. ARCHER SL, REEVE HL, MICHELAKIS E, PUTTAGUNTA L, WAITE R, NELSON DP, DINAUER MC, AND WEIR EK. O_2 sensing is preserved in mice lacking the gp91 *phox* subunit of NADPH oxidase. *Proc Natl Acad Sci USA* 96: 7944–7949, 1999.
36. ARMSTRONG KM, QUIGLEY EP, QUIGLEY P, CRUMRINE DS, AND CUKIERMAN S. Covalently linked gramicidin channels: effects of linker hydrophobicity and alkaline metals on different stereoisomers. *Biophys J* 80: 1810–1818, 2001.
37. ARONSON PS, NEE J, AND SUHM MA. Modifier role of internal H^+ in activating the Na^+-H^+ exchanger in renal microvillus membrane vesicles. *Nature* 299: 161–163, 1982.
38. ARONSON PS, SUHM MA, AND NEE J. Interaction of external H^+ with the Na^+-H^+ exchanger in renal microvillus membrane vesicles. *J Biol Chem* 258: 6767–6771, 1983.
39. ARREOLA J, MELVIN JE, AND BEGENISICH T. Inhibition of Ca^{2+}-dependent Cl^- channels from secretory epithelial cells by low internal pH. *J Membr Biol* 147: 95–104, 1995.
40. ATKINSON YH, MURRAY AW, KRILIS S, VADAS MA, AND LOPEZ AF. Human tumour necrosis factor-alpha (TNF-α) directly stimulates arachidonic acid release in human neutrophils. *Immunology* 70: 82–87, 1990.
41. AUSTIN C AND WRAY S. An investigation of intrinsic buffering power in rat vascular smooth muscle cells. *Pflügers Arch* 429: 325–331, 1995.
42. AUTY RP AND COLE RH. Dielectric properties of ice and solid D_2O. *J Chem Phys* 20: 1309–1314, 1952.
43. AXELROD HL, ABRESCH EC, PADDOCK ML, OKAMURA MY, AND FEHER G. Determination of the binding sites of the proton transfer inhibitors Cd^{2+} and Zn^{2+} in bacterial reaction centers. *Proc Natl Acad Sci USA* 97: 1542–1547, 2000.
44. AYRTON WE AND PERRY J. Ice as an electrolyte. *Proc Phys Soc* 2: 171–182, 1877.
51. BABCOCK GT. How oxygen is activated and reduced in respiration. *Proc Natl Acad Sci USA* 96: 12971–12973, 1999.
52. BABCOCK GT AND WIKSTRÖM M. Oxygen activation and the conservation of energy in cell respiration. *Nature* 356: 301–309, 1992.
53. BABIOR BM. Oxygen-dependent microbial killing by phagocytes (first of two parts). *N Engl J Med* 298: 659–668, 1978.
54. BABIOR BM. Oxidants from phagocytes: agents of defense and destruction. *Blood* 64: 959–966, 1984.
55. BABIOR BM. NADPH oxidase: an update. *Blood* 93: 1464–1476, 1999.
56. BABIOR BM, CURNUTTE JT, AND KIPNES RS. Biological defense mechanisms. Evidence for the participation of superoxide in bacterial killing by xanthine oxidase. *J Lab Clin Med* 85: 235–244, 1975.
57. BABIOR BM, KIPNES RS, AND CURNUTTE JT. Biological defense mechanisms The production by leukocytes of superoxide, a potential bactericidal agent. *J Clin Invest* 52: 741–744, 1973.
58. BABIOR BM AND PETERS WWA. The O_2^--producing enzyme of human neutrophils. Further properties. *J Biol Chem* 256: 2321–2323, 1981.
59. BACKGREN C, HUMMER G, WIKSTRÖM M, AND PUUSTINEN A. Proton translocation by cytochrome *c* oxidase can take place without the conserved glutamic acid in subunit I. *Biochemistry* 39: 7863–7867, 2000.
60. BACKX PH AND YUE DT. Proton permeation through cardiac sodium channels (Abstract). *Biophys J* 59: 26a, 1991.
61. BADWEY JA, CURNUTTE JT, AND KARNOVSKY ML. *cis*-Polyunsaturated fatty acids induce high levels of superoxide production by human neutrophils. *J Biol Chem* 256: 12640–12643, 1981.
62. BADWEY JA, CURNUTTE JT, ROBINSON JM, BERDE CB, KARNOVSKY MJ, AND KARNOVSKY ML. Effects of free fatty acids on release of superoxide and on change of shape by human neutrophils. Reversibility by albumin. *J Biol Chem* 259: 7870–7877, 1984.
63. BADWEY JA, ROBINSON JM, CURNUTTE JT, KARNOVSKY MJ, AND KARNOVSKY ML. Retinoids stimulate the release of superoxide by neutrophils and change their morphology. *J Cell Physiol* 127: 223–228, 1986.
64. BAES CF AND MESMER RE. *The Hydrolysis of Cations*. New York: Wiley, 1976.
65. BAKER WN AND LA MER K. The conductance of potassium chloride and hydrochloride-deuterochloric acid in H_2O-D_2O mixtures. The viscosity of H_2O-D_2O. *J Chem Phys* 3: 406–410, 1935.
66. BALARAM P, KRISHNA K, SUKUMAR M, MELLOR IR, AND SANSOM MSP. The properties of ion channels formed by zervamicins. *Eur Biophys J* 21: 117–128, 1992.
67. BALDRIDGE CW AND GERARD RW. The extra respiration of phagocytosis. *Am J Physiol* 103: 235–236, 1933.
67a. BÁNFI B, MATURANA A, JACONI S, ARNAUDEAU S, LAFORGE T, SINHA B, LIGETI E, DEMAUREX N, AND KRAUSE KH. A mammalian H^+ channel generated through alternative splicing of the NADPH oxidase homolog NOH-1. *Science* 287: 138–142, 2000.
67b. BÁNFI B, MOLNÁR G, MATURANA A, STEGER K, HEGEDÛS B, DEMAUREX N, AND KRAUSE KH. A Ca^{2+}-activated NADPH oxidase in testis, spleen, and lymph nodes. *J Biol Chem* 276: 37594–37601, 2001.
67c. BÁNFI B, SCHRENZEL J, NÜSSE O, LEW DP, LIGETI E, KRAUSE KH, AND DEMAUREX N. A novel H^+ conductance in eosinophils: unique characteristics and absence in chronic granulomatous disease. *J Exp Med* 190: 183–194, 1999.
68. BANKERS-FULBRIGHT JL, KITA H, GLEICH GJ, AND O'GRADY SM. Regulation of human eosinophil NADPH oxidase activity: a central role for PKCδ. *J Cell Physiol* 189: 306–315, 2001.
69. BARISH ME. A transient calcium-dependent chloride current in the immature *Xenopus* oocyte. *J Physiol* 342: 309–325, 1983.
70. BARISH ME AND BAUD C. A voltage-gated hydrogen ion current in the oocyte membrane of the axolotl, *Ambystoma*. *J Physiol* 352: 243–263, 1984.
71. BARRY PH AND DIAMOND JM. Effects of unstirred layers on membrane phenomena. *Physiol Rev* 64: 763–872, 1984.
72. BARTL F, BRZEZINSKI B, RÓZALSKI B, AND ZUNDEL G. FT-IR study of the nature of the proton and Li^+ motions in gramicidin A and C. *J Phys Chem B* 102: 5234–5238, 1998.
73. BASHFORD CL AND PASTERNAK CA. Plasma membrane potential of neutrophils generated by the Na^+ pump. *Biochim Biophys Acta* 817: 174–180, 1985.
74. BAUD C AND BARISH ME. Changes in membrane hydrogen and sodium conductances during progesterone-induced maturation of *Ambystoma* oocytes. *Dev Biol* 105: 423–434, 1984.
78. BECHINGER B. Structure and functions of channel-forming peptides: magainins, cecropins, melittin and alamethicin. *J Membr Biol* 156: 197–211, 1997.
79. BEGENISICH T AND DANKO M. Hydrogen ion block of the sodium pore in squid giant axons. *J Gen Physiol* 82: 599–618, 1983.
80. BELL RP. *The Proton in Chemistry*. Ithaca, NY: Cornell University Press, 1973.
81. BENICHOU G, KANELLOPOULOS JM, MITENNE F, GALANAUD P, AND LECA

G. T-cell chemiluminescence. A novel aspect of T-cell membrane activation studied with a Jurkat tumour cell line. *Scand J Immunol* 30: 265–269, 1989.
82. Bennett PA, Finan PM, Dixon RJ, and Kellie S. Tyrosine phosphatase antagonist-induced activation of the neutrophil NADPH oxidase: a possible role for protein kinase C. *Immunology* 85: 304–310, 1995.
83. Benz R and McLaughlin S. The molecular mechanism of action of the proton ionophore FCCP (carbonylcyanide *p*-trifluoromethoxyphenylhydrazone). *Biophys J* 41: 381–398, 1983.
84. Bernal JD and Fowler RH. A theory of water and ionic solution, with particular reference to hydrogen and hydroxyl ions. *J Chem Phys* 1: 515–548, 1933.
85. Bernheim L, Krause RM, Baroffio A, Hamann M, Kaelin A, and Bader C-R. A voltage-dependent proton current in cultured human skeletal muscle myotubes. *J Physiol* 470: 313–333, 1993.
86. Berry RM and Berg HC. Torque generated by the flagellar motor of *Escherichia coli* while driven backward. *Biophys J* 76: 580–587, 1999.
87. Beswick PH, Brannen PC, and Hurles SS. The effects of smoking and zinc on the oxidative reactions of human neutrophils. *J Clin Lab Immunol* 21: 71–75, 1986.
88. Bevan S and Yeats J. Protons activate a cation conductance in a sub-population of rat dorsal root ganglion neurones. *J Physiol* 433: 145–161, 1991.
89. Bezanilla F and Armstrong CM. Negative conductance caused by entry of sodium and cesium ions into the potassium channels of squid axons. *J Gen Physiol* 60: 588–608, 1972.
90. Bianchini L, Nanda A, Wasan S, and Grinstein S. Activation of multiple pH-regulatory pathways in granulocytes by a phosphotyrosine phosphatase antagonist. *Biochem J* 301: 539–544, 1994.
91. Biberstine-Kinkade KJ, DeLeo FR, Epstein RI, LeRoy BA, Nauseef WM, and Dinauer MC. Heme-ligating histidines in flavocytochrome b_{558}: identification of specific histidines in gp91^{phox}. *J Biol Chem* 276: 31105–31112, 2001.
92. Bidani A, Brown SE, and Heming TA. pH_i regulation in alveolar macrophages: relative roles of Na^+-H^+ antiport and H^+-ATPase. *Am J Physiol Lung Cell Mol Physiol* 266: L681–L688, 1994.
93. Bielski A and Allen AO. Mechanism of the disproportionation of superoxide radicals. *J Phys Chem* 81: 1048–1050, 1977.
94. Bienengraeber M, Echtay KS, and Klingenberg M. H^+ transport by uncoupling protein (UCP-1) is dependent on a histidine pair, absent in UCP-2 and UCP-3. *Biochemistry* 37: 3–8, 1998.
95. Bizouarn T, Meuller J, Axelsson M, and Rydström J. The transmembrane domain and the proton channel in proton-pumping transhydrogenases. *Biochim Biophys Acta* 1459: 284–290, 2000.
96. Bjerrum N. Structure and properties of ice. *Science* 115: 385–390, 1952.
97. Blair DF and Berg HC. The MotA protein of *E. coli* is a proton-conducting component of the flagellar motor. *Cell* 60: 439–449, 1990.
98. Blair DF and Berg HC. Mutations in the MotA protein of *Escherichia coli* reveal domains critical for proton conduction. *J Mol Biol* 221: 1433–1442, 1991.
99. Blatt MR. K^+ channels of stomatal guard cells. Characteristics of the inward rectifier and its control by pH. *J Gen Physiol* 99: 615–644, 1992.
100. Blatz AL. Asymmetric proton block of inward rectifier K channels in skeletal muscle. *Pflügers Arch* 401: 402–407, 1984.
101. Bogomolni RA, Baker RA, Lozier RH, and Stoeckenius W. Light-driven proton translocations in *Halobacterium halobium*. *Biochim Biophys Acta* 440: 68–88, 1976.
102. Bonney RJ, Wightman PD, Davies P, Sadowski SJ, Kuehl FA Jr, and Humes JL. Regulation of prostaglandin synthesis and of the selective release of lysosomal hydrolases by mouse peritoneal macrophages. *Biochem J* 176: 433–442, 1978.
103. Boorer KJ, Frommer WB, Bush DR, Kreman M, Loo DD, and Wright EM. Kinetics and specificity of a H^+/amino acid transporter from *Arabidopsis thaliana*. *J Biol Chem* 271: 2213–2220, 1996.
104. Boriack-Sjodin PA, Heck RW, Laipis PJ, Silverman DN, and Christianson DW. Structure determination of murine mitochondrial carbonic anhydrase V at 2.45-Å resolution: implications for catalytic proton transfer and inhibitor design. *Proc Natl Acad Sci USA* 92: 10949–10953, 1995.
105. Borisenko V, Sansom MSP, and Woolley GA. Protonation of lysine residues inverts cation/anion selectivity in a model channel. *Biophys J* 78: 1335–1348, 2000.
106. Boron WF. Transport of H^+ and of ionic weak acids and bases. *J Membr Biol* 72: 1–16, 1983.
107. Borregaard N and Cowland JB. Granules of the human neutrophilic polymorphonuclear leukocyte. *Blood* 89: 3503–3521, 1997.
108. Borregaard N, Schwartz JH, and Tauber AI. Proton secretion by stimulated neutrophils. Significance of hexose monophosphate shunt activity as source of electrons and protons for the respiratory burst. *J Clin Invest* 74: 455–459, 1984.
109. Boss O, Samec S, Paoloni-Giacobino A, Rossier C, Dulloo A, Seydoux J, Muzzin P, and Giacobino JP. Uncoupling protein-3: a new member of the mitochondrial carrier family with tissue-specific expression. *FEBS Lett* 408: 39–42, 1997.
110. Bowman EJ, Siebers A, and Altendorf K. Bafilomycins: a class of inhibitors of membrane ATPases from microorganisms, animal cells, and plant cells. *Proc Natl Acad Sci USA* 85: 7972–7976, 1988.
111. Boyer PD. A model for conformational coupling of membrane potential and proton translocation to ATP synthesis and to active transport. *FEBS Lett* 58: 1–6, 1975.
112. Boyer PD. Bioenergetic coupling to protonmotive force: should we be considering hydronium ion coordination and not group protonation? *Trends Biochem Sci* 13: 5–7, 1988.
113. Boyer PD. The binding change mechanism for ATP synthase—some probabilities and possibilities. *Biochim Biophys Acta* 1140: 215–250, 1993.
114. Bramhall J. Conductance routes for protons across membrane barriers. *Biochemistry* 26: 2848–2855, 1987.
115. Brändén M, Sigurdson H, Namslauer A, Gennis RB, Ädelroth P, and Brzezinski P. On the role of the K-proton transfer pathway in cytochrome *c* oxidase. *Proc Natl Acad Sci USA* 98: 5013–5018, 2001.
116. Brändén M, Tomson F, Gennis RB, and Brzezinski P. The entry point of the K-proton-transfer pathway in cytochrome *c* oxidase. *Biochemistry* 41: 10794–10798, 2002.
117. Brandsburg-Zabary S, Fried O, Marantz Y, Nachliel E, and Gutman M. Biophysical aspects of intra-protein proton transfer. *Biochim Biophys Acta* 1458: 120–134, 2000.
118. Breed J, Sankararamakrishnan R, Kerr ID, and Sansom MSP. Molecular dynamics simulations of water within models of ion channels. *Biophys J* 70: 1643–1661, 1996.
119. Breslow E. Metal-protein complexes. In: *Inorganic Biochemistry*, edited by Eichhorn GL. Amsterdam: Elsevier Scientific, 1973, p. 227–249.
120. Brewer ML, Schmitt UW, and Voth GA. The formation and dynamics of proton wires in channel environments. *Biophys J* 80: 1691–1702, 2001.
121. Briggs RT, Drath DB, Karnovsky ML, and Karnovsky MJ. Localization of NADH oxidase on the surface of human polymorphonuclear leukocytes by a new cytochemical method. *J Cell Biol* 67: 566–586, 1975.
122. Briggs RT, Robinson JM, Karnovsky ML, and Karnovsky MJ. Superoxide production by polymorphonuclear leukocytes. A cytochemical approach. *Histochemistry* 84: 371–378, 1986.
123. Bromberg Y and Pick E. Unsaturated fatty acids as second messengers of superoxide generation by macrophages. *Cell Immunol* 79: 240–252, 1983.
123a. Brönsted JN and Pedersen K. Die katalytische Zersetzung des Nitramids und ihre physikalisch-chemische Bedeutung. *Z Phys Chem* 108: 185–235, 1923.
124. Brookes PS, Hulbert AJ, and Brand MD. The proton permeability of liposomes made from mitochondrial inner membrane phospholipids: no effect of fatty acid composition. *Biochim Biophys Acta* 1330: 157–164, 1997.
125. Brown GC. The leaks and slips of bioenergetic membranes. *FASEB J* 6: 2961–2965, 1992.
126. Brown LS and Lanyi JK. Determination of the transiently lowered pK_a of the retinal Schiff base during the photocycle of bacteriorhodopsin. *Proc Natl Acad Sci USA* 93: 1731–1734, 1996.
127. Brown LS, Needleman R, and Lanyi JK. Origins of deuterium

kinetic isotope effects on the proton transfers of the bacteriorhodopsin photocycle. *Biochemistry* 39: 938–945, 2000.
129. Brusilow WS and Monticello RA. Synthesis and assembly of the F_o proton channel from F_o genes cloned into bacteriophage λ and integrated into the *Escherichia coli* chromosome. *J Biol Chem* 269: 7285–7289, 1994.
130. Brzezinski P. Proton-transfer reactions in bioenergetics. *Biochim Biophys Acta* 1458: 1–5, 2000.
131. Burton K and Wilson TH. The free-energy changes for the reduction of diphosphopyridine nucleotide and the dehydrogenation of L-malate and L-glycerol 1-phosphate. *Biochem J* 54: 86–94, 1953.
132. Busath DD, Thulin CD, Hendershot RW, Phillips LR, Maughan P, Cole CD, Bingham NC, Morrison S, Baird LC, Hendershot RJ, Cotten M, and Cross TA. Noncontact dipole effects on channel permeation. I. Experiments with (5F-indole)Trp_{13} gramicidin A channels. *Biophys J* 75: 2830–2844, 1998.
133. Byerly L and Hagiwara S. Calcium currents in internally perfused nerve cell bodies of *Limnea stagnalis*. *J Physiol* 322: 503–528, 1982.
134. Byerly L, Meech R, and Moody W Jr. Rapidly activating hydrogen ion currents in perfused neurones of the snail, *Lymnaea stagnalis*. *J Physiol* 351: 199–216, 1984.
135. Byerly L and Moody WJ Jr. Membrane currents of internally perfused neurones of the snail, *Lymnaea stagnalis*, at low intracellular pH. *J Physiol* 376: 477–491, 1986.
136. Byerly L and Suen Y. Characterization of proton currents in neurones of the snail, *Lymnaea stagnalis*. *J Physiol* 413: 75–89, 1989.
137. Cadenas S and Brand MD. Effects of magnesium and nucleotides on the proton conductance of rat skeletal-muscle mitochondria. *Biochem J* 348: 209–213, 2000.
138. Cadenas S, Echtay KS, Harper JA, Jekabsons MB, Buckingham JA, Grau E, Abuin A, Chapman H, Clapham JC, and Brand MD. The basal proton conductance of skeletal muscle mitochondria from transgenic mice overexpressing or lacking uncoupling protein-3. *J Biol Chem* 277: 2773–2778, 2002.
139. Cahalan MD, Chandy KG, DeCoursey TE, and Gupta S. A voltage-gated potassium channel in human T lymphocytes. *J Physiol* 358: 197–237, 1985.
140. Cai M and Jordan PC. How does vestibule surface charge affect ion conduction and toxin binding in a sodium channel? *Biophys J* 57: 883–891, 1990.
141. Calonge ML and Ilundáin AA. PKC activators stimulate H^+ conductance in chicken enterocytes. *Pflügers Arch* 431: 594–598, 1996.
142. Camplin GC, Glen JW, and Paren JG. Theoretical models for interpreting the dielectric behavior of HF-doped ice. *J Glaciology* 85: 123–141, 1978.
143. Cao NJ, Brusilow WSA, Tomashek JJ, and Woodbury DJ. Characterization of reconstituted F_o from wild-type *Escherichia coli* and identification of two other fluxes copurifying with F_o. *Cell Biochem Biophys* 34: 305–320, 2001.
144. Cao Y, Brown LS, Sasaki J, Maeda A, Needleman R, and Lanyi JK. Relationship of proton release at the extracellular surface to deprotonation of the Schiff base in the bacteriorhodopsin photocycle. *Biophys J* 68: 1518–1530, 1995.
145. Cao Y, Li M, Mager S, and Lester HA. Amino acid residues that control pH modulation of transport-associated current in mammalian serotonin transporters. *J Neurosci* 18: 7739–7749, 1998.
146. Cao Y, Mager S, and Lester HA. H^+ permeation and pH regulation at a mammalian serotonin transporter. *J Neurosci* 17: 2257–2266, 1997.
147. Cass A and Finkelstein A. Water permeability of thin lipid membranes. *J Gen Physiol* 50: 1765–1784, 1967.
148. Cattell KJ, Lindop CR, Knight IG, and Beechey RB. The identification of the site of action of *NN′*-dicyclohexylcarbodi-imide as a proteolipid in mitochondrial membranes. *Biochem J* 125: 169–177, 1971.
149. Cavallini L, Coassin M, Borean A, and Alexandre A. Arachidonic acid activates a proton conductance pathway and the Na^+/H^+ exchanger in platelets. *Biochem J* 319: 567–574, 1996.
150. Célis H. 1-Butanol extracted proteolipid. Proton conducting properties. *Biochem Biophys Res Commun* 92: 26–31, 1980.
151. Chanchevalap S, Yang Z, Cui N, Qu Z, Zhu G, Liu C, Giwa Lr, Abdulkadir L, and Jiang C. Involvement of histidine residues in proton sensing of ROMK1 channel. *J Biol Chem* 275: 7811–7817, 2000.
152. Chander A, Johnson RG, Reicherter J, and Fisher AB. Lung lamellar bodies maintain an acidic internal pH. *J Biol Chem* 261: 6126–6131, 1986.
153. Chandy G, Grabe M, Moore HP, and Machen TE. Proton leak and CFTR in regulation of Golgi pH in respiratory epithelial cells. *Am J Physiol Cell Physiol* 281: C908–C921, 2001.
154. Chao CC, Hu S, and Peterson PK. Modulation of human microglial cell superoxide production by cytokines. *J Leukoc Biol* 58: 65–70, 1995.
155. Checover S, Nachliel E, Dencher NA, and Gutman M. Mechanism of proton entry into the cytoplasmic section of the proton-conducting channel of bacteriorhodopsin. *Biochemistry* 36: 13919–13928, 1997.
156. Chen K, Hirst J, Camba R, Bonagura CA, Stout CD, Burgess BK, and Armstrong FA. Atomically defined mechanism for proton transfer to a buried redox centre in a protein. *Nature* 405: 814–817, 2000.
157. Chen M-S, Onsager L, Bonner J, and Nagle J. Hopping of ions in ice. *J Chem Phys* 60: 405–419, 1974.
158. Chen TY and Miller C. Nonequilibrium gating and voltage dependence of the ClC-0 Cl^- channel. *J Gen Physiol* 108: 237–250, 1996.
159. Chen X and Berg HC. Solvent-isotope and pH effects on flagellar rotation in *Escherichia coli*. *Biophys J* 78: 2280–2284, 2000.
160. Chen X and Berg HC. Torque-speed relationship of the flagellar rotary motor of *Escherichia coli*. *Biophys J* 78: 1036–1041, 2000.
161. Chen Xh, Bezprozvanny I, and Tsien RW. Molecular basis of proton block of L-type Ca^{2+} channels. *J Gen Physiol* 108: 363–374, 1996.
162. Cheng G, Cao Z, Xu X, Meir EG, and Lambeth JD. Homologs of gp91*phox:* cloning and tissue expression of Nox3, Nox4, and Nox5. *Gene* 269: 131–140, 2001.
163. Cherny VV and DeCoursey TE. pH-dependent inhibition of voltage-gated H^+ currents in rat alveolar epithelial cells by Zn^{2+} and other divalent cations. *J Gen Physiol* 114: 819–838, 1999.
164. Cherny VV, Henderson LM, and DeCoursey TE. Proton and chloride currents in Chinese hamster ovary cells. *Membr Cell Biol* 11: 337–347, 1997.
165. Cherny VV, Henderson LM, Xu W, Thomas LL, and DeCoursey TE. Activation of NADPH oxidase-related proton and electron currents in human eosinophils by arachidonic acid. *J Physiol* 535: 783–794, 2001.
166. Cherny VV, Markin VS, and DeCoursey TE. The voltage-activated hydrogen ion conductance in rat alveolar epithelial cells is determined by the pH gradient. *J Gen Physiol* 105: 861–896, 1995.
167. Cherny VV, Morgan D, Thomas LL, Xu W, and DeCoursey TE. Complex temperature dependence of electron current generated by the phagocyte NADPH oxidase (Abstract). *Biophys J* 84: 456a, 2003.
168. Cherny VV, Murphy R, and DeCoursey TE. Single proton channel currents are really small (Abstract). *Biophys J* 82: 639a, 2002.
169. Cherny VV, Simonova MV, Sokolov VS, and Markin VS. Transport of the neutral form of amphiphilic drugs through a planar bilayer lipid membrane: the role of the pH gradient. *Bioelectrochem Bioenerget* 23: 17–25, 1990.
170. Cherny VV, Thomas LL, and DeCoursey TE. Voltage-gated proton currents in human basophils. *Biologicheskie Membrany* 18: 458–465, 2001.
171. Chernyshev A and Cukierman S. Thermodynamic view of activation energies of proton transfer in various gramicidin A channels. *Biophys J* 82: 182–192, 2002.
172. Chernyshev A, Pomès R, and Cukierman S. Kinetic isotope effects of proton transfer in gramicidin channels in aqueous and methanol containing solutions. *Biophys Chem* 103: 179–190, 2003.
173. Chiu SW, Subramaniam S, and Jakobsson E. Simulation study of a gramicidin/lipid bilayer system in excess water and lipid. II. Rates and mechanisms of water transport. *Biophys J* 76: 1939–1950, 1999.
174. Chiu SW, Subramaniam S, Jakobsson E, and McCammon JA. Water and polypeptide conformations in the gramicidin channel. A molecular dynamics study. *Biophys J* 56: 253–261, 1989.

175. Chizhmakov IV, Geraghty FM, Ogden DC, Hayhurst A, Antoniou M, and Hay AJ. Selective proton permeability and pH regulation of the influenza virus M2 channel expressed in mouse erythroleukaemia cells. *J Physiol* 494: 329–336, 1996.
176. Christianson DW and Fierke CA. Carbonic anhydrase: evolution of the zinc binding site by nature and by design. *Acc Chem Res* 29: 331–339, 1996.
177. Clark RA. The human neutrophil respiratory burst oxidase. *J Infect Dis* 161: 1140–1147, 1990.
178. Clark RA. Activation of the neutrophil respiratory burst oxidase. *J Infect Dis* 179 *Suppl* 2: S309–S317, 1999.
179. Clark RA, Leidal KG, Pearson DW, and Nauseef WM. NADPH oxidase of human neutrophils. Subcellular localization and characterization of an arachidonate-activatable superoxide-generating system. *J Biol Chem* 262: 4065–4074, 1987.
180. Collie CH, Hasted JB, and Ritson DM. The dielectric properties of water and heavy water. *Proc R Soc Lond* 60: 145–160, 1948.
181. Collier WB, Ritzhaupt G, and Devlin JP. Spectroscopically evaluated rates and energies for proton transfer and Bjerrum defect migration in cubic ice. *J Phys Chem* 88: 363–368, 1984.
182. Colton CA, Jia M, Li MX, and Gilbert DL. K^+ modulation of microglial superoxide production: involvement of voltage-gated Ca^{2+} channels. *Am J Physiol Cell Physiol* 266: C1650–C1655, 1994.
183. Conley MP and Berg HC. Chemical modification of *Streptococcus* flagellar motors. *J Bacteriol* 158: 832–843, 1984.
184. Conway BE, Bockris JOM, and Linton H. Proton conductance and the existence of the H_3O ion. *J Chem Phys* 24: 834–850, 1956.
185. Cooper GJ, Zhou Y, Bouyer P, Grichtchenko II, and Boron WF. Transport of volatile solutes through AQP1. *J Physiol* 542: 17–29, 2002.
186. Coronado R, Rosenberg RL, and Miller C. Ionic selectivity, saturation, and block in a K^+-selective channel from sarcoplasmic reticulum. *J Gen Physiol* 76: 425–446, 1980.
187. Coulter KL, Perier F, Radeke CM, and Vandenberg CA. Identification and molecular localization of a pH-sensing domain for the inward rectifier potassium channel HIR. *Neuron* 15: 1157–1168, 1995.
188. Cowin JP, Tsekouras AA, Iedema MJ, Wu K, and Ellison GB. Immobility of protons in ice from 30 to 190 K. *Nature* 398: 405–407, 1999.
189. Cox GB, Fimmel AL, Gibson F, and Hatch L. The mechanism of ATP synthase: a reassessment of the functions of the *b* and *a* subunits. *Biochim Biophys Acta* 849: 62–69, 1986.
190. Cox JA, Jeng AY, Blumberg PM, and Tauber AI. Comparison of subcellular activation of the human neutrophil NADPH-oxidase by arachidonic acid, sodium dodecyl sulfate (SDS), and phorbol myristate acetate (PMA). *J Immunol* 138: 1884–1888, 1987.
191. Cramer WA, Heymann JB, Schendel SL, Deriy BN, Cohen FS, Elkins PA, and Stauffacher CV. Structure-function of the channel-forming colicins. *Annu Rev Biophys Biomol Struct* 24: 611–641, 1995.
192. Criddle RS, Packer L, and Shieh P. Oligomycin-dependent ionophoric protein subunit of mitochondrial adenosinetriphosphatase. *Proc Natl Acad Sci USA* 74: 4306–4310, 1977.
193. Crider BP, Xie XS, and Stone DK. Bafilomycin inhibits proton flow through the H^+ channel of vacuolar proton pumps. *J Biol Chem* 269: 17379–17381, 1994.
194. Crofts AR and Wraight CA. The electrochemical domain of photosynthesis. *Biochim Biophys Acta* 726: 149–185, 1983.
195. Cross AR. Inhibitors of the leukocyte superoxide generating oxidase: mechanisms of action and methods for their elucidation. *Free Radic Biol Med* 8: 71–93, 1990.
196. Cross AR. $p40^{phox}$ participates in the activation of NADPH oxidase by increasing the affinity of $p47^{phox}$ for flavocytochrome b_{558}. *Biochem J* 349: 113–117, 2000.
197. Cross AR, Erickson RW, and Curnutte JT. Simultaneous presence of $p47^{phox}$ and flavocytochrome b_{-245} are required for the activation of NADPH oxidase by anionic amphiphiles. Evidence for an intermediate state of oxidase activation. *J Biol Chem* 274: 15519–15525, 1999.
198. Cross AR, Erickson RW, and Curnutte JT. The mechanism of activation of NADPH oxidase in the cell-free system: the activation process is primarily catalytic and not through the formation of a stoichiometric complex. *Biochem J* 341: 251–255, 1999.
199. Cross AR, Erickson RW, Ellis BA, and Curnutte JT. Spontaneous activation of NADPH oxidase in a cell-free system: unexpected multiple effects of magnesium ion concentrations. *Biochem J* 338: 229–233, 1999.
200. Cross AR and Jones OT. The effect of the inhibitor diphenylene iodonium on the superoxide-generating system of neutrophils. Specific labelling of a component polypeptide of the oxidase. *Biochem J* 237: 111–116, 1986.
201. Cross AR and Jones OT. Enzymic mechanisms of superoxide production. *Biochim Biophys Acta* 1057: 281–298, 1991.
202. Cross AR, Noack D, Rae J, Curnutte JT, and Heyworth PG. Hematologically important mutations: the autosomal recessive forms of chronic granulomatous disease (first update). *Blood Cells Mol Dis* 26: 561–565, 2000.
203. Cross AR, Parkinson JF, and Jones OT. The superoxide-generating oxidase of leucocytes. NADPH-dependent reduction of flavin and cytochrome *b* in solubilized preparations. *Biochem J* 223: 337–344, 1984.
204. Cross AR, Parkinson JF, and Jones OT. Mechanism of the superoxide-producing oxidase of neutrophils. O_2 is necessary for the fast reduction of cytochrome *b*-245 by NADPH. *Biochem J* 226: 881–884, 1985.
205. Cuello LG, Romero JG, Cortes DM, and Perozo E. pH-dependent gating in the *Streptomyces lividans* K^+ channel. *Biochemistry* 37: 3229–3236, 1998.
206. Cukierman S. Flying protons in linked gramicidin A channels. *Isr J Chem* 39: 419–426, 1999.
207. Cukierman S. Proton mobilities in water and in different stereoisomers of covalently linked gramicidin A channels. *Biophys J* 78: 1825–1834, 2000.
208. Cukierman S, Quigley EP, and Crumrine DS. Proton conduction in gramicidin A and in its dioxolane-linked dimer in different lipid bilayers. *Biophys J* 73: 2489–2502, 1997.
209. Curnutte JT. Activation of human neutrophil nicotinamide adenine dinucleotide phosphate, reduced (triphosphopyridine nucleotide, reduced) oxidase by arachidonic acid in a cell-free system. *J Clin Invest* 75: 1740–1743, 1985.
210. Curnutte JT, Badwey JA, Robinson JM, Karnovsky MJ, and Karnovsky ML. Studies on the mechanism of superoxide release from human neutrophils stimulated with arachidonate. *J Biol Chem* 259: 11851–11857, 1984.
211. Dahlgren C, Johansson A, Lundqvist H, Bjerrum OW, and Borregaard N. Activation of the oxygen-radical-generating system in granules of intact human neutrophils by a calcium ionophore (ionomycin). *Biochim Biophys Acta* 1137: 182–188, 1992.
212. Dana R, Leto TL, Malech HL, and Levy R. Essential requirement of cytosolic phospholipase A_2 for activation of the phagocyte NADPH oxidase. *J Biol Chem* 273: 441–445, 1998.
213. Dana R, Malech HL, and Levy R. The requirement for phospholipase A_2 for activation of the assembled NADPH oxidase in human neutrophils. *Biochem J* 297: 217–223, 1994.
214. Dani JA. Ion-channel entrances influence permeation. Net charge, size, shape, and binding consideration. *Biophys J* 49: 607–618, 1986.
215. Danielli JF. The relations between surface *p*H, ion concentrations and interfacial tension. *Proc R Soc Lond B Biol Sci* 122: 155–174, 1937.
216. Daniels I, Lindsay MA, Keany CI, Burden RP, Fletcher J, and Haynes AP. Role of arachidonic acid and its metabolites in the priming of NADPH oxidase in human polymorphonuclear leukocytes by peritoneal dialysis effluent. *Clin Diagn Lab Immunol* 5: 683–689, 1998.
217. Danneel H. Notiz über Ionengeschwindigkeiten. *Zeitschrift für Elektrochemie und angewandte physikalische Chemie* 11: 249–252, 1905.
218. Darken LS and Meier HF. Conductances of aqueous solutions of the hydroxides of lithium, sodium and potassium at 25°. *J Am Chem Soc* 64: 621–623, 1942.
219. Daumas P and andersen OS. Proton block of rat brain sodium channels. Evidence for two proton binding sites and multiple occupancy. *J Gen Physiol* 101: 27–43, 1993.

220. DAVIES WL, GRUNERT RR, HAFF RF, MCGAHEN JW, NEUMAYER EM, PAULSHOCK M, WATTS JC, WOOD TR, HERMANN EC, AND HOFFMANN CE. Antiviral activity of 1-adamantanamine (amantadine). *Science* 144: 862–863, 1964.
221. DAY TJF, SCHMITT UW, AND VOTH GA. The mechanism of hydrated proton transport in water. *J Am Chem Soc* 122: 12027–12028, 2000.
222. DE BOER M AND ROOS D. Metabolic comparison between basophils and other leukocytes from human blood. *J Immunol* 136: 3447–3454, 1986.
225. DEAMER DW. Proton permeability in biological and model membranes. In: *Intracellular pH: Its Measurement, Regulation, and Utilization in Cellular Functions*. New York: Liss, 1982, p. 173–187.
226. DEAMER DW. Proton permeation of lipid bilayers. *J Bioenerg Biomembr* 19: 457–479, 1987.
227. DEAMER DW AND NICHOLS JW. Proton-hydroxide permeability of liposomes. *Proc Natl Acad Sci USA* 80: 165–168, 1983.
228. DEAMER DW AND NICHOLS JW. Proton flux mechanisms in model and biological membranes. *J Membr Biol* 107: 91–103, 1989.
229. DECHATELET LR, SHIRLEY PS, MCPHAIL LC, HUNTLEY CC, MUSS HB, AND BASS DA. Oxidative metabolism of the human eosinophil. *Blood* 50: 525–535, 1977.
230. DECKER ER AND LEVITT DG. Use of weak acids to determine the bulk diffusion limitation of H^+ ion conductance through the gramicidin channel. *Biophys J* 53: 25–32, 1988.
231. DECORNEZ H, DRUKKER K, AND HAMMES-SCHIFFER S. Solvation and hydrogen-bonding effects on proton wires. *J Phys Chem* 103: 2891–2898, 1999.
232. DECOURSEY TE. Hydrogen ion currents in rat alveolar epithelial cells. *Biophys J* 60: 1243–1253, 1991.
233. DECOURSEY TE. Mechanism of K^+ channel block by verapamil and related compounds in rat alveolar epithelial cells. *J Gen Physiol* 106: 745–779, 1995.
234. DECOURSEY TE. Four varieties of voltage-gated proton channels. *Front Biosci* 3: d477–d482, 1998.
235. DECOURSEY TE. Hypothesis: do voltage-gated H^+ channels in alveolar epithelial cells contribute to CO_2 elimination by the lung? *Am J Physiol Cell Physiol* 278: C1–C10, 2000.
236. DECOURSEY TE AND CHERNY VV. Potential, pH, and arachidonate gate hydrogen ion currents in human neutrophils. *Biophys J* 65: 1590–1598, 1993.
237. DECOURSEY TE AND CHERNY VV. Na^+-H^+ antiport detected through hydrogen ion currents in rat alveolar epithelial cells and human neutrophils. *J Gen Physiol* 103: 755–785, 1994.
238. DECOURSEY TE AND CHERNY VV. Voltage-activated hydrogen ion currents. *J Membr Biol* 141: 203–223, 1994.
239. DECOURSEY TE AND CHERNY VV. Voltage-activated proton currents in membrane patches of rat alveolar epithelial cells. *J Physiol* 489: 299–307, 1995.
240. DECOURSEY TE AND CHERNY VV. Effects of buffer concentration on voltage-gated H^+ currents: does diffusion limit the conductance? *Biophys J* 71: 182–193, 1996.
241. DECOURSEY TE AND CHERNY VV. II. Voltage-activated proton currents in human THP-1 monocytes. *J Membr Biol* 152: 131–140, 1996.
242. DECOURSEY TE AND CHERNY VV. Deuterium isotope effects on permeation and gating of proton channels in rat alveolar epithelium. *J Gen Physiol* 109: 415–434, 1997.
243. DECOURSEY TE AND CHERNY VV. Temperature dependence of voltage-gated H^+ currents in human neutrophils, rat alveolar epithelial cells, and mammalian phagocytes. *J Gen Physiol* 112: 503–522, 1998.
244. DECOURSEY TE AND CHERNY VV. An electrophysiological comparison of voltage-gated proton channels, other ion channels, and other proton channels. *Isr J Chem* 39: 409–418, 1999.
245. DECOURSEY TE AND CHERNY VV. Common themes and problems of bioenergetics and voltage-gated proton channels. *Biochim Biophys Acta* 1458: 104–119, 2000.
246. DECOURSEY TE, CHERNY VV, DECOURSEY AG, XU W, AND THOMAS LL. Interactions between NADPH oxidase-related proton and electron currents in human eosinophils. *J Physiol* 535: 767–781, 2001.
247. DECOURSEY TE, CHERNY VV, MORGAN D, KATZ BZ, AND DINAUER MC. The $gp91^{phox}$ component of NADPH oxidase is not the voltage-gated proton channel in phagocytes, but it helps. *J Biol Chem* 276: 36063–36066, 2001.
248. DECOURSEY TE, CHERNY VV, ZHOU W, AND THOMAS LL. Simultaneous activation of NADPH oxidase-related proton and electron currents in human neutrophils. *Proc Natl Acad Sci USA* 97: 6885–6889, 2000.
249. DECOURSEY TE AND GRINSTEIN S. Ion channels and carriers in leukocytes. In: *Inflammation: Basic Principles and Clinical Correlates*, edited by Gallin JI and Snyderman R. Philadelphia, PA: Lippincott Williams & Wilkins, 1999, p. 639–659.
250. DECOURSEY TE, JACOBS ER, AND SILVER MR. Potassium currents in rat type II alveolar epithelial cells. *J Physiol* 395: 487–505, 1988.
251. DECOURSEY TE, KIM SY, SILVER MR, AND QUANDT FN. III. Ion channel expression in PMA-differentiated human THP-1 macrophages. *J Membr Biol* 152: 141–157, 1996.
252. DECOURSEY TE, MORGAN D, AND CHERNY VV. The voltage dependence of NADPH oxidase reveals why phagocytes need proton channels. *Nature*. In press.
253. DEEM S, HEDGES RG, KERR ME, AND SWENSON ER. Acetazolamide reduces hypoxic pulmonary vasoconstriction in isolated perfused rabbit lungs. *Respir Physiol* 123: 109–119, 2000.
253a. DE GODOY CM AND CUKIERMAN S. Modulation of proton transfer in the water wire of dioxolane-linked gramicidin channels by lipid membranes. *Biophys J* 81: 1430–1438, 2001.
254. DEGRADO WF AND LEAR JD. Conformationally constrained α-helical peptide models for protein ion channels. *Biopolymers* 29: 205–213, 1990.
254a. DE GROTTHUSS CJT. Sur la décomposition de l'eau et des corps qu'elle tient en dissolution à l'aide de l'électricité galvanique. *Ann Chim* LVIII: 54–74, 1806.
255. DELEO FR, ALLEN LA, APICELLA M, AND NAUSEEF WM. NADPH oxidase activation and assembly during phagocytosis. *J Immunol* 163: 6732–6740, 1999.
256. DELEO FR AND QUINN MT. Assembly of the phagocyte NADPH oxidase: molecular interaction of oxidase proteins. *J Leukoc Biol* 60: 677–691, 1996.
257. DEMAUREX N, DOWNEY GP, WADDELL TK, AND GRINSTEIN S. Intracellular pH regulation during spreading of human neutrophils. *J Cell Biol* 133: 1391–1402, 1996.
258. DEMAUREX N, GRINSTEIN S, JACONI M, SCHLEGEL W, LEW DP, AND KRAUSE KH. Proton currents in human granulocytes: regulation by membrane potential and intracellular pH. *J Physiol* 466: 329–344, 1993.
259. DEMAUREX N, ORLOWSKI J, BRISSEAU G, WOODSIDE M, AND GRINSTEIN S. The mammalian Na^+/H^+ antiporters NHE-1, NHE-2, and NHE-3 are electroneutral and voltage independent, but can couple to an H^+ conductance. *J Gen Physiol* 106: 85–111, 1995.
260. DEVLIN JP, URAS N, SADLEJ J, AND BUCH V. Discrete stages in the solvation and ionization of hydrogen chloride adsorbed on ice particles. *Nature* 417: 269–271, 2002.
261. DEWAR J AND FLEMING JA. Note on the dielectric constant of ice and alcohol at very low temperatures. *Proc R Soc Lond* 61: 2–18, 1897.
263. DIETER P. Relationship between intracellular pH changes, activation of protein kinase C and NADPH oxidase in macrophages. *FEBS Lett* 298: 17–20, 1992.
264. DIMROTH P. Operation of the F_o motor of the ATP synthase. *Biochim Biophys Acta* 1458: 374–386, 2000.
265. DIMROTH P, WANG H, GRABE M, AND OSTER G. Energy transduction in the sodium F-ATPase of *Propionigenium modestum*. *Proc Natl Acad Sci USA* 96: 4924–4929, 1999.
266. DINER BA, FORCE DA, RANDALL DW, AND BRITT RD. Hydrogen bonding, solvent exchange, and coupled proton and electron transfer in the oxidation and reduction of redox-active tyrosine Y_z in Mn-depleted core complexes of photosystem II. *Biochemistry* 37: 17931–17943, 1998.
267. DIPPEL T AND KREUER KD. Proton transport mechanism in concentrated aqueous solutions and solid hydrates of acids. *Solid State Ionics* 46: 3–9, 1991.
267a. DI VIRGILIO F, LEW PD, ANDERSSON T, AND POZZAN T. Plasma membrane potential modulates chemotactic peptide-stimulated cytosolic free Ca^{2+} changes in human neutrophils. *J Biol Chem* 262: 4574–4579, 1987.
268. DOYLE DA, MORAIS CABRAL J, PFUETZNER RA, KUO A, GULBIS JM,

COHEN SL, CHAIT BT, AND MACKINNON R. The structure of the potassium channel: molecular basis of K^+ conduction and selectivity. *Science* 280: 69–77, 1998.
269. DRÖSE S, BINDSEIL KU, BOWMAN EJ, SIEBERS A, ZEECK A, AND ALTENDORF K. Inhibitory effect of modified bafilomycins and concanamycins on P- and V-type adenosinetriphosphatases. *Biochemistry* 32: 3902–3906, 1993.
270. DRUKKER K, DE LEEUW SW, AND HAMMES-SCHIFFER S. Proton transport along water chains in an electric field. *J Chem Phys* 108: 6799–6808, 1998.
271. DUCA KA AND JORDAN PC. Ion-water and water-water interactions in a gramicidinlike channel: effects due to group polarizability and backbone flexibility. *Biophys Chem* 65: 123–141, 1997.
272. DUCA KA AND JORDAN PC. Comparison of selectively polarizable force fields for ion-water-peptide interactions: ion translocation in a gramicidinlike channel. *J Phys Chem B* 102: 9127–9138, 1998.
273. DUFF KC AND ASHLEY RH. The transmembrane domain of influenza A M2 protein forms amantadine-sensitive proton channels in planar lipid bilayers. *Virology* 190: 485–489, 1992.
274. DUFF KC, GILCHRIST PJ, SAXENA AM, AND BRADSHAW JP. Neutron diffraction reveals the site of amantadine blockade in the influenza A M2 ion channel. *Virology* 202: 287–293, 1994.
275. DUNCAN TM, BULYGIN VV, ZHOU Y, HUTCHEON ML, AND CROSS RL. Rotation of subunits during catalysis by *Escherichia coli* F_1-ATPase. *Proc Natl Acad Sci USA* 92: 10964–10968, 1995.
276. DUNKER AK AND MARVIN DA. A model for membrane transport through α-helical protein pores. *J Theor Biol* 72: 9–16, 1978.
277. ECHTAY KS, ROUSSEL D, ST PIERRE J, JEKABSONS MB, CADENAS S, STUART JA, HARPER JA, ROEBUCK SJ, MORRISON A, PICKERING S, CLAPHAM JC, AND BRAND MD. Superoxide activates mitochondrial uncoupling proteins. *Nature* 415: 96–99, 2002.
278. ECHTAY KS, WINKLER E, BIENENGRAEBER M, AND KLINGENBERG M. Site-directed mutagenesis identifies residues in uncoupling protein (UCP1) involved in three different functions. *Biochemistry* 39: 3311–3317, 2000.
279. EDER C. Ion channels in microglia (brain macrophages). *Am J Physiol Cell Physiol* 275: C327–C342, 1998.
280. EDER C AND DECOURSEY TE. Voltage-gated proton channels in microglia. *Prog Neurobiol* 64: 277–305, 2001.
281. EDER C, FISCHER HG, HADDING U, AND HEINEMANN U. Properties of voltage-gated currents of microglia developed using macrophage colony-stimulating factor. *Pflügers Arch* 430: 526–533, 1995.
282. EFFROS RM AND CHINARD FP. The in vivo pH of the extravascular space of the lung. *J Clin Invest* 48: 1983–1996, 1969.
283. EFFROS RM, MASON G, AND SILVERMAN P. Asymmetric distribution of carbonic anhydrase in the alveolar-capillary barrier. *J Appl Physiol* 51: 190–193, 1981.
284. EFFROS RM, MASON G, AND SILVERMAN P. Role of perfusion and diffusion in $^{14}CO_2$ exchange in the rabbit lung. *J Appl Physiol* 51: 1136–1144, 1981.
285. EHLENBECK S, GRADMANN D, BRAUN FJ, AND HEGEMANN P. Evidence for a light-induced H^+ conductance in the eye of the green alga *Chlamydomonas reinhardtii*. *Biophys J* 82: 740–751, 2002.
286. EHRLICH P. Ueber die specifischen Granulationen des Blutes. In: *Archiv für Physiologie*, edited by Du Bois-Reymond E. Leipzig: Verlag von Veit, 1879, p. 571–579.
287. EIGEN M. Proton transfer, acid-base catalysis, and enzymatic hydrolysis. Part I: elementary processes. *Angewandte Chemie, International Edition* 3: 1–19, 1964.
288. EIGEN M AND DE MAEYER L. Self-dissociation and protonic charge transport in water and ice. *Proc R Soc Lond A* 247: 505–533, 1958.
289. EIGEN M, DEMAEYER L, AND SPATZ H-C. Über das kinetische Verhalten von Protonen und Deuteronen in Eiskristallen. *Berichte der Bunsen-Gesellschaft für Physikalische Chemie* 68: 19–29, 1964.
290. EIGEN M AND HAMMES GG. Elementary steps in enzyme reactions (as studied by relaxation spectrometry). *Adv Enzymol* 25: 1–38, 1963.
291. EISENBERG M, HALL JE, AND MEAD CA. The nature of the voltage-dependent conductance induced by alamethicin in black lipid membranes. *J Membr Biol* 14: 143–176, 1973.
292. EISENMAN G, ENOS B, HÄGGLUND J, AND SANDBLOM J. Gramicidin as an example of a single-filing ionic channel. *Ann NY Acad Sci* 339: 8–20, 1980.
293. ELSTON T, WANG H, AND OSTER G. Energy transduction in ATP synthase. *Nature* 391: 510–513, 1998.
294. ENGELHARDT H. Protonic conduction in ice. In: *Physics and Chemistry of Ice*, edited by Whalley E, Jones SJ, and Gold L. Ottawa: Univ. of Toronto Press, 1973, p. 226–235.
295. ENGELS M, BASHFORD D, AND GHADIRI MR. Structure and dynamics of self-assembling peptide nanotubes and the channel-mediated water organization and self-diffusion. A molecular dynamics study. *J Am Chem Soc* 117: 9151–9158, 1995.
296. ENNS T. Facilitation by carbonic anhydrase of carbon dioxide transport. *Science* 155: 44–47, 1967.
297. ENNS T AND HILL EP. CO_2 diffusing capacity in isolated dog lung lobes and the role of carbonic anhydrase. *J Appl Physiol* 54: 483–490, 1983.
298. ERIKSSON AE, JONES TA, AND LILJAS A. Refined structure of human carbonic anhydrase II at 2.0 Å resolution. *Proteins* 4: 274–282, 1988.
299. ESCH FS, BÖHLEN P, OTSUKA AS, YOSHIDA M, AND ALLISON WS. Inactivation of the bovine mitochondrial F_1-ATPase with dicyclohexyl[^{14}C]carbodiimide leads to the modification of a specific glutamic acid residue in the β subunit. *J Biol Chem* 256: 9084–9089, 1981.
300. EWELL RH AND EYRING H. Theory of the viscosity of liquids as a function of temperature and pressure. *J Chem Phys* 5: 726–736, 1937.
301. FAIRMAN WA, SONDERS MS, MURDOCH GH, AND AMARA SG. Arachidonic acid elicits a substrate-gated proton current associated with the glutamate transporter EAAT4. *Nat Neurosci* 1: 105–113, 1998.
302. FEI YJ, ROMERO MF, KRAUSE M, LIU JC, HUANG W, GANAPATHY V, AND LEIBACH FH. A novel H^+-coupled oligopeptide transporter (OPT3) from *Caenorhabditis elegans* with a predominant function as a H^+ channel and an exclusive expression in neurons. *J Biol Chem* 275: 9563–9571, 2000.
303. FERRY JD. Statistical evaluation of sieve constants in ultra-filtration. *J Gen Physiol* 20: 95–104, 1936.
304. FETTER J, SHARPE M, QIAN J, MILLS D, FERGUSON-MILLER S, AND NICHOLLS P. Fatty acids stimulate activity and restore respiratory control in a proton channel mutant of cytochrome *c* oxidase. *FEBS Lett* 393: 155–160, 1996.
305. FETTER JR, QIAN J, SHAPLEIGH J, THOMAS JW, GARCIA-HORSMAN A, SCHMIDT E, HOSLER J, BABCOCK GT, GENNIS RB, AND FERGUSON-MILLER S. Possible proton relay pathways in cytochrome *c* oxidase. *Proc Natl Acad Sci USA* 92: 1604–1608, 1995.
306. FILLINGAME RH, ANGEVINE CM, AND DMITRIEV OY. Coupling proton movements to *c*-ring rotation in F_1F_o ATP synthase: aqueous access channels and helix rotations at the *a-c* interface. *Biochim Biophys Acta* 1555: 29–36, 2002.
307. FILLINGAME RH, GIRVIN ME, FRAGA D, AND ZHANG Y. Correlations of structure and function in H^+ translocating subunit *c* of F_1F_o ATP synthase. *Ann NY Acad Sci* 671: 323–333, 1992.
308. FILLINGAME RH, JIANG W, DMITRIEV OY, AND JONES PC. Structural interpretations of F_o rotary function in the *Escherichia coli* F_1F_o ATP synthase. *Biochim Biophys Acta* 1458: 387–403, 2000.
309. FINKELSTEIN A. Water and nonelectrolyte permeability of lipid bilayer membranes. *J Gen Physiol* 68: 127–135, 1976.
310. FINKELSTEIN A AND ANDERSEN OS. The gramicidin A channel: a review of its permeability characteristics with special reference to the single-file aspect of transport. *J Membr Biol* 59: 155–171, 1981.
311. FISCHER H, WIDDICOMBE JH, AND ILLEK B. Acid secretion and proton conductance in human airway epithelium. *Am J Physiol Cell Physiol* 282: C736–C743, 2002.
312. FISCHER WB AND SANSOM MS. Viral ion channels: structure and function. *Biochim Biophys Acta* 1561: 27–45, 2002.
313. FLEMING JA AND DEWAR J. On the dielectric constants of pure ice, glycerine, nitrobenzol, and ethylene dibromide at and above the temperature of liquid air. *Proc R Soc Lond* 61: 316–330, 1897.
314. FLEURY C, NEVEROVA M, COLLINS S, RAIMBAULT S, CHAMPIGNY O, LEVI-MEYRUEIS C, BOUILLAUD F, SELDIN MF, SURWIT RS, RICQUIER D, AND WARDEN CH. Uncoupling protein-2: a novel gene linked to obesity and hyperinsulinemia. *Nat Genet* 15: 269–272, 1997.
315. FORMAN HJ AND KIM E. Inhibition by linoleic acid hydroperoxide of alveolar macrophage superoxide production: effects upon mito-

chondrial and plasma membrane potentials. *Arch Biochem Biophys* 274: 443–452, 1989.
316. Fornili SL, Vercauteren DP, and Clementi E. Water structure in the gramicidin A transmembrane channel. *Biochim Biophys Acta* 771: 151–164, 1984.
317. Forrest LR, Kukol A, Arkin IT, Tieleman DP, and Sansom MSP. Exploring models of the influenza A M2 channel: MD simulations in a phospholipid bilayer. *Biophys J* 78: 55–69, 2000.
318. Forte M, Blachly-Dyson E, and Colombini M. Structure and function of the yeast outer mitochondrial membrane channel, VDAC. *Soc Gen Physiol Ser* 51: 145–154, 1996.
319. Franck EU, Hartmann D, and Hensel F. Proton mobility in water at high temperatures and pressures. *Disc Faraday Soc* 39: 200–206, 1965.
320. Frankenhaeuser B and Hodgkin AL. The action of calcium on the electrical properties of squid axons. *J Physiol* 137: 218–244, 1957.
321. Freiburghaus J, Jörg A, and Müller T. Luminol-dependent chemiluminescence in bovine eosinophils and neutrophils: differential increase of intracellular and extracellular chemiluminescence induced by soluble stimulants. *J Biolumin Chemilumin* 6: 115–121, 1991.
322. Frey G and Schlue WR. pH recovery from intracellular alkalinization in Retzius neurones of the leech central nervous system. *J Physiol* 462: 627–643, 1993.
323. Friedl P, Hoppe J, Gunsalus RP, Michelsen O, von Meyenburg K, and Schairer HU. Membrane integration and function of the three F_o subunits of the ATP synthase of *Escherichia coli* K12. *EMBO J* 2: 99–103, 1983.
324. Frighi V, Ng LL, Lewis A, and Dhar H. Na^+/H^+ antiport and buffering capacity in human polymorphonuclear and mononuclear leucocytes. *Clin Sci* 80: 95–99, 1991.
325. Frivold OE, Hassel O, and Hetland E. The electric conductivity of solutions of HCl in ordinary water and of DCl in heavy water. *Avhandlinger Det Norske Vid-Akad i Oslo 1 Mat-Naturv Klasse* 9: 1–11, 1943.
326. Fu XW, Wang D, Nurse CA, Dinauer MC, and Cutz E. NADPH oxidase is an O_2 sensor in airway chemoreceptors: evidence from K^+ current modulation in wild-type and oxidase-deficient mice. *Proc Natl Acad Sci USA* 97: 4374–4379, 2000.
327. Fuks B and Homblé F. Mechanism of proton permeation through chloroplast lipid membranes. *Plant Physiol* 112: 759–766, 1996.
328. Fung DC and Berg HC. Powering the flagellar motor of *Escherichia coli* with an external voltage source. *Nature* 375: 809–812, 1995.
329. Gabig TG, Bearman SI, and Babior BM. Effects of oxygen tension and pH on the respiratory burst of human neutrophils. *Blood* 53: 1133–1139, 1979.
330. Gabig TG, Lefker BA, Ossanna PJ, and Weiss SJ. Proton stoichiometry associated with human neutrophil respiratory-burst reactions. *J Biol Chem* 259: 13166–13171, 1984.
331. Gabriel B and Teissié J. Proton long-range migration along protein monolayers and its consequences on membrane coupling. *Proc Natl Acad Sci USA* 93: 14521–14525, 1996.
332. Galbraith GMP. Chemotactic peptide-induced arachidonic acid mobilization in human polymorphonuclear leukocytes. *Am J Pathol* 133: 347–354, 1988.
333. Galileo G. *Dialogue Concerning the Two Chief World System: Ptolemaic & Copernican*. Berkeley: Univ. of California Press, 1632.
334. Gallin EK. Voltage clamp studies in macrophages from mouse spleen cultures. *Science* 214: 458–460, 1981.
335. Gallin EK. Ion channels in leukocytes. *Physiol Rev* 71: 775–811, 1991.
336. Gallin EK and Gallin JI. Interaction of chemotactic factors with human macrophages. Induction of transmembrane potential changes. *J Cell Biol* 75: 277–289, 1977.
337. Gallin EK and Livengood DR. Nonlinear current-voltage relationships in cultured macrophages. *J Cell Biol* 85: 160–165, 1980.
338. Gallin EK and McKinney LC. Patch-clamp studies in human macrophages: single-channel and whole-cell characterization of two K^+ conductances. *J Membr Biol* 103: 55–66, 1988.
339. Gallin EK, Wiederhold ML, Lipsky PE, and Rosenthal AS. Spontaneous and induced membrane hyperpolarizations in macrophages. *J Cell Physiol* 86: 653–661, 1975.
340. Gandhi CS, Shuck K, Lear JD, Dieckmann GR, DeGrado WF, Lamb RA, and Pinto LH. Cu(II) inhibition of the proton translocation machinery of the influenza A virus M_2 protein. *J Biol Chem* 274: 5474–5482, 1999.
341. Garcia-Horsman JA, Puustinen A, Gennis RB, and Wikström M. Proton transfer in cytochrome *bo*3 ubiquinol oxidase of *Escherichia coli*: second-site mutations in subunit I that restore proton pumping in the mutant Asp135 → Asn. *Biochemistry* 34: 4428–4433, 1995.
342. Garlid KD, Beavis AD, and Ratkje SK. On the nature of ion leaks in energy-transducing membranes. *Biochim Biophys Acta* 976: 109–120, 1989.
343. Garlid KD, Orosz DE, Modriansk‡ M, Vassanelli S, and Jezek P. On the mechanism of fatty acid-induced proton transport by mitochondrial uncoupling protein. *J Biol Chem* 271: 2615–2620, 1996.
344. Garza AG, Harris-Haller LW, Stoebner RA, and Manson MD. Motility protein interactions in the bacterial flagellar motor. *Proc Natl Acad Sci USA* 92: 1970–1974, 1995.
345. Gazit E, La Rocca P, Sansom MSP, and Shai Y. The structure and organization within the membrane of the helices composing the pore-forming domain of *Bacillus thuringiensis* δ-endotoxin are consistent with an "umbrella-like" structure of the pore. *Proc Natl Acad Sci USA* 95: 12289–12294, 1998.
346. Geers C and Gros G. Carbon dioxide transport and carbonic anhydrase in blood and muscle. *Physiol Rev* 80: 681–715, 2000.
347. Geibel S, Friedrich T, Ormos P, Wood PG, Nagel G, and Bamberg E. The voltage-dependent proton pumping in bacteriorhodopsin is characterized by optoelectric behavior. *Biophys J* 81: 2059–2068, 2001.
348. Geiszt M, Kapus A, and Ligeti E. Chronic granulomatous disease: more than the lack of superoxide? *J Leukoc Biol* 69: 191–196, 2001.
349. Gekle M, Silbernagl S, and Oberleithner H. The mineralocorticoid aldosterone activates a proton conductance in cultured kidney cells. *Am J Physiol Cell Physiol* 273: C1673–C1678, 1997.
350. Gennis R and Ferguson-Miller S. Structure of cytochrome *c* oxidase, energy generator of aerobic life. *Science* 269: 1063–1064, 1995.
351. Gennis R, Pawate AS, Mills DA, Morgan JE, and Ferguson-Miller S. A mutation in subunit I of cytochrome oxidase from *Rhodobacter sphaeroides* results in an increase in steady state activity but completely eliminates proton pumping (Abstract). *Biophys J* 82: 287a, 2002.
352. Gennis RB. Multiple proton-conducting pathways in cytochrome oxidase and a proposed role for the active-site tyrosine. *Biochim Biophys Acta* 1365: 241–248, 1998.
353. Georgievskii Y, Medvedev ES, and Stuchebrukhov AA. Proton transport via coupled surface and bulk diffusion. *J Chem Phys* 116: 1692–1699, 2002.
354. Gerber CE, Kuçi S, Zipfel M, Niethammer D, and Bruchelt G. Phagocytic activity and oxidative burst of granulocytes in persons with myeloperoxidase deficiency. *Eur J Clin Chem Clin Biochem* 34: 901–908, 1996.
355. Gerencsér L and Maróti P. Retardation of proton transfer caused by binding of the transition metal ion to the bacterial reaction center is due to pK_a shifts of key protonatable residues. *Biochemistry* 40: 1850–1860, 2001.
356. Gertner BJ and Hynes JT. Molecular dynamics simulation of hydrochloric acid ionization at the surface of stratospheric ice. *Science* 271: 1563–1566, 1996.
357. Gertner BJ, Peslherbe GH, and Hynes JT. Acid ionization of HBr in a small water cluster. *Isr J Chem* 39: 273–281, 1999.
358. Ghannam AF, Tsen W, and Rowlett RS. Activation parameters for the carbonic anhydrase II-catalyzed hydration of CO_2. *J Biol Chem* 261: 1164–1169, 1986.
359. Gibbons C, Montgomery MG, Leslie AG, and Walker JE. The structure of the central stalk in bovine F_1-ATPase at 2.4 Å resolution. *Nat Struct Biol* 7: 1055–1061, 2000.
360. Giembycz MA and Lindsay MA. Pharmacology of the eosinophil. *Pharmacol Rev* 51: 213–340, 1999.

361. GIERER A AND WIRTZ K. Anomale H^+ und OH^- Ionenbeweglichkeit in Wasser. *Ann Physic* 6: 257–304, 1949.
362. GILBERT DL AND EHRENSTEIN G. Use of a fixed charge model to determine the pK of the negative sites on the external membrane surface. *J Gen Physiol* 55: 822–825, 1970.
363. GILBERTSON TA, AVENET P, KINNAMON SC, AND ROPER SD. Proton currents through amiloride-sensitive Na channels in hamster taste cells. Role in acid transduction. *J Gen Physiol* 100: 803–824, 1992.
364. GILBERTSON TA, ROPER SD, AND KINNAMON SC. Proton currents through amiloride-sensitive Na^+ channels in isolated hamster taste cells: enhancement by vasopressin and cAMP. *Neuron* 10: 931–942, 1993.
365. GILLIES RJ, LIU Z, AND BHUJWALLA Z. ^{31}P-MRS measurements of extracellular pH of tumors using 3-aminopropylphosphonate. *Am J Physiol Cell Physiol* 267: C195–C203, 1994.
366. GLASSTONE S, LAIDLER KJ, AND EYRING H. *The Theory of Rate Processes: The Kinetics of Chemical Reactions, Viscosity, Diffusion and Electrochemical Phenomena*. New York: McGraw-Hill, 1941.
367. GLUCK S AND AL-AWQATI Q. Vasopressin increases water permeability in inducing pores. *Nature* 284: 631–632, 1980.
368. GOLDMAN DE. Potential, impedance, and rectification in membranes. *J Gen Physiol* 27: 37–60, 1943.
369. GONG DW, MONEMDJOU S, GAVRILOVA O, LEON LR, MARCUS-SAMUELS B, CHOU CJ, EVERETT C, KOZAK LP, LI C, DENG C, HARPER ME, AND REITMAN ML. Lack of obesity and normal response to fasting and thyroid hormone in mice lacking uncoupling protein-3. *J Biol Chem* 275: 16251–16257, 2000.
370. GOOD NE, WINGET GD, WINTER W, CONNOLLY TN, IZAWA S, AND SINGH RM. Hydrogen ion buffers for biological research. *Biochemistry* 5: 467–477, 1966.
371. GOPTA OA, CHEREPANOV DA, JUNGE W, AND MULKIDJANIAN AY. Proton transfer from the bulk to the bound ubiquinone Q_B of the reaction center in chromatophores of *Rhodobacter sphaeroides*: retarded conveyance by neutral water. *Proc Natl Acad Sci USA* 96: 13159–13164, 1999.
372. GORDIENKO DV, TARE M, PARVEEN S, FENECH CJ, ROBINSON C, AND BOLTON TB. Voltage-activated proton current in eosinophils from human blood. *J Physiol* 496: 299–316, 1996.
373. GOUBERN M, YAZBECK J, CHAPEY MF, DIOLEZ P, AND MOREAU F. Variations in energization parameters and proton conductance induced by cold adaptation and essential fatty acid deficiency in mitochondria of brown adipose tissue in the rat. *Biochim Biophys Acta* 1015: 334–340, 1990.
374. GOWEN JA, MARKHAM JC, MORRISON SE, CROSS TA, BUSATH DD, MAPES EJ, AND SCHUMAKER MF. The role of Trp side chains in tuning single proton conduction through gramicidin channels. *Biophys J* 83: 880–898, 2002.
375. GRABE M, WANG H, AND OSTER G. The mechanochemistry of V-ATPase proton pumps. *Biophys J* 78: 2798–2813, 2000.
376. GRABER M, DIPAOLA J, HSIANG FL, BARRY C, AND PASTORIZA E. Intracellular pH in the OK cell. I. Identification of H^+ conductance and observations on buffering capacity. *Am J Physiol Cell Physiol* 261: C1143–C1153, 1991.
377. GRADMANN D, HANSEN UP, LONG WS, SLAYMAN CL, AND WARNCKE J. Current-voltage relationships for the plasma membrane and its principal electrogenic pump in *Neurospora crassa*. I. Steady-state conditions. *J Membr Biol* 39: 333–367, 1978.
378. GRAHAME DC. The electrical double layer and the theory of electrocapillarity. *Chem Rev* 41: 441–501, 1947.
379. GRANFELDT D, SAMUELSSON M, AND KARLSSON A. Capacitative Ca^{2+} influx and activation of the neutrophil respiratory burst. Different regulation of plasma membrane- and granule-localized NADPH-oxidase. *J Leukoc Biol* 71: 611–617, 2002.
380. GRÄNICHER H, JACCARD C, SCHERRER P, AND STEINEMANN A. Dielectric relaxation and the electrical conductivity of ice crystals. *Disc Faraday Soc* 23: 50–62, 1957.
381. GRANTYN R AND LUX HD. Similarity and mutual exclusion of NMDA- and proton-activated transient Na^+-current in rat tectal neurons. *Neurosci Lett* 89: 198–203, 1988.
382. GREEN WN AND ANDERSEN OS. Surface charges and ion channel function. *Annu Rev Physiol* 53: 341–359, 1991.
383. GREEN WN, WEISS LB, AND ANDERSEN OS. Batrachotoxin-modified sodium channels in planar lipid bilayers. Ion permeation and block. *J Gen Physiol* 89: 841–872, 1987.
384. GRESSER MJ, MYERS JA, AND BOYER PD. Catalytic site cooperativity of beef heart mitochondrial F_1 adenosine triphosphatase. Correlations of initial velocity, bound intermediate, and oxygen exchange measurements with an alternating three-site model. *J Biol Chem* 257: 12030–12038, 1982.
385. GRINSTEIN S AND FURUYA W. Amiloride-sensitive Na^+/H^+ exchange in human neutrophils: mechanism of activation by chemotactic factors. *Biochem Biophys Res Commun* 122: 755–762, 1984.
386. GRINSTEIN S AND FURUYA W. Cytoplasmic pH regulation in phorbol ester-activated human neutrophils. *Am J Physiol Cell Physiol* 251: C55–C65, 1986.
387. GRINSTEIN S, ROMANEK R, AND ROTSTEIN OD. Method for manipulation of cytosolic pH in cells clamped in the whole cell or perforated-patch configurations. *Am J Physiol Cell Physiol* 267: C1152–C1159, 1994.
388. GROS G AND MOLL W. Facilitated diffusion of CO_2 across albumin solutions. *J Gen Physiol* 64: 356–371, 1974.
389. GROS G, MOLL W, HOPPE H, AND GROS H. Proton transport by phosphate diffusion—a mechanism of facilitated CO_2 transfer. *J Gen Physiol* 67: 773–790, 1976.
390. GRZESIEK S AND DENCHER NA. Dependency of ΔpH-relaxation across vesicular membranes on the buffering power of bulk solutions and lipids. *Biophys J* 50: 265–276, 1986.
391. GU X AND SACKIN H. Effect of pH on potassium and proton conductance in renal proximal tubule. *Am J Physiol Renal Fluid Electrolyte Physiol* 269: F289–F308, 1995.
392. GUERRIERI F AND PAPA S. Effect of chemical modifiers of amino acid residues on proton conduction by the H^+-ATPase of mitochondria. *J Bioenerg Biomembr* 13: 393–409, 1981.
393. GULBIS JM, MANN S, AND MACKINNON R. Structure of a voltage-dependent K^+ channel β subunit. *Cell* 97: 943–952, 1999.
394. GUNNER MR AND ALEXOV E. A pragmatic approach to structure based calculation of coupled proton and electron transfer in proteins. *Biochim Biophys Acta* 1458: 63–87, 2000.
395. GUTKNECHT J. Proton/hydroxide conductance through lipid bilayer membranes. *J Membr Biol* 82: 105–112, 1984.
396. GUTKNECHT J. Proton conductance through phospholipid bilayers: water wires or weak acids? *J Bioenerg Biomembr* 19: 427–442, 1987.
397. GUTKNECHT J. Proton conductance caused by long-chain fatty acids in phospholipid bilayer membranes. *J Membr Biol* 106: 83–93, 1988.
398. GUTKNECHT J, BISSON MA, AND TOSTESON FC. Diffusion of carbon dioxide through lipid bilayer membranes: effects of carbonic anhydrase, bicarbonate, and unstirred layers. *J Gen Physiol* 69: 779–794, 1977.
399. GUTKNECHT J AND TOSTESON DC. Diffusion of weak acids across lipid bilayer membranes: effects of chemical reactions in the unstirred layers. *Science* 182: 1258–1261, 1973.
400. GUTMAN M AND NACHLIEL E. Time-resolved dynamics of proton transfer in proteinous systems. *Annu Rev Phys Chem* 48: 329–356, 1997.
401. GUTMAN M, NACHLIEL E, AND TSFADIA Y. Propagation of protons at the water membrane interface. Microscopic evaluation of a macroscopic process. In: *Permeability and Stability of Lipid Bilayers*, edited by Disalvo EA and Simon SA. Ann Arbor, MI: CRC, 1995, p. 259–276.
402. GUTMAN M, TSFADIA Y, MASAD A, AND NACHLIEL E. Quantitation of physical-chemical properties of the aqueous phase inside the phoE ionic channel. *Biochim Biophys Acta* 1109: 141–148, 1992.
403. HAGIWARA S AND TAKAHASHI K. The anomalous rectification and cation selectivity of the membrane of a starfish egg cell. *J Membr Biol* 18: 61–80, 1974.
404. HAINES TH. Anionic lipid headgroups as a proton-conducting pathway along the surface of membranes: a hypothesis. *Proc Natl Acad Sci USA* 80: 160–164, 1983.
405. HAINES TH. Do sterols reduce proton and sodium leaks through lipid bilayers? *Prog Lipid Res* 40: 299–324, 2001.
406. HALL JE, VODYANOY I, BALASUBRAMANIAN TM, AND MARSHALL GR. Alamethicin A rich model for channel behavior. *Biophys J* 45: 233–247, 1984.

407. HALLÉN S, BRZEZINSKI P, AND MALMSTRÖM BG. Internal electron transfer in cytochrome *c* oxidase is coupled to the protonation of a group close to the bimetallic site. *Biochemistry* 33: 1467–1472, 1994.
408. HAMMES-SCHIFFER S. Mixed quantum/classical dynamics of hydrogen transfer reaction. *J Phys Chem* 102: 10443–10454, 1998.
409. HAMPTON MB, KETTLE AJ, AND WINTERBOURN CC. Inside the neutrophil phagosome: oxidants, myeloperoxidase, and bacterial killing. *Blood* 92: 3007–3017, 1998.
410. HANSEN UP, GRADMANN D, SANDERS D, AND SLAYMAN CL. Interpretation of current-voltage relationships for "active" ion transport systems: I Steady-state reaction-kinetic analysis of class-I mechanisms. *J Membr Biol* 63: 165–190, 1981.
411. HANSEN UP, TITTOR J, AND GRADMANN D. Interpretation of current-voltage relationships for "active" ion transport systems. II. Nonsteady-state reaction-kinetic analysis of class-I mechanisms with one slow time-constant. *J Membr Biol* 75: 141–169, 1983.
412. HARDY RC AND COTTINGTON RL. Viscosity of deuterium oxide and water in the range of 5° to 125°C. *J Res Natl Bureau Standards* 42: 573–578, 1949.
413. HARRIS HW, KIKERI D, JANOSHAZI A, SOLOMON AK, AND ZEIDEL ML. High proton flux through membranes containing antidiuretic hormone water channels. *Am J Physiol Renal Fluid Electrolyte Physiol* 259: F366–F371, 1990.
414. HARTNIG C, WITSCHEL W, AND SPOHR E. Molecular dynamics study of the structure and dynamics of water in cylindrical pores. *J Phys Chem B* 102: 1241–1249, 1998.
415. HASSELBALCH KA. Die Berechnung des Wasserstoffzahl des Blutes aus der freien und gebunden Kohlensäure desselben, und die Sauerstoffbindung des Blutes als Funktion der Wasserstoffzahl. *Biochem Z* 78: 112–144, 1917.
416. HAY AJ, WOLSTENHOLME AJ, SKEHEL JJ, AND SMITH MH. The molecular basis of the specific anti-influenza action of amantadine. *EMBO J* 4: 3021–3024, 1985.
417. HEBERLE J. Proton transfer reactions across bacteriorhodopsin and along the membrane. *Biochim Biophys Acta* 1458: 135–147, 2000.
418. HEBERLE J, RIESLE J, THIEDEMANN G, OESTERHELT D, AND DENCHER NA. Proton migration along the membrane surface and retarded surface to bulk transfer. *Nature* 370: 379–382, 1994.
419. HECK RW, BORIACK-SJODIN PA, QIAN M, TU C, CHRISTIANSON DW, LAIPIS PJ, AND SILVERMAN DN. Structure-based design of an intramolecular proton transfer site in murine carbonic anhydrase V. *Biochemistry* 35: 11605–11611, 1996.
420. HEGINBOTHAM L, LEMASURIER M, KOLMAKOVA-PARTENSKY L, AND MILLER C. Single *Streptomyces lividans* K^+ channels: functional asymmetries and sidedness of proton activation. *J Gen Physiol* 114: 551–560, 1999.
421. HEINEMANN SH AND SIGWORTH FJ. Estimation of Na^+ dwell time in the gramicidin A channel. Na^+ ions as blockers of H^+ currents. *Biochim Biophys Acta* 987: 8–14, 1989.
422. HELENIUS A. Unpacking the incoming influenza virus. *Cell* 69: 577–578, 1992.
423. HELMLINGER G, YUAN F, DELLIAN M, AND JAIN RK. Interstitial pH and pO_2 gradients in solid tumors *in vivo:* high-resolution measurements reveal a lack of correlation. *Nat Med* 3: 177–182, 1997.
424. HEMING TA, GEERS C, GROS G, BIDANI A, AND CRANDALL ED. Effects of dextran-bound inhibitors on carbonic anhydrase activity in isolated rat lungs. *J Appl Physiol* 61: 1849–1856, 1986.
425. HENDERSON LJ. Concerning the relationship between the strength of acids and their capacity to preserve neutrality. *Am J Physiol* 21: 173–179, 1908.
426. HENDERSON LM. Role of histidines identified by mutagenesis in the NADPH oxidase-associated H^+ channel. *J Biol Chem* 273: 33216–33223, 1998.
427. HENDERSON LM, BANTING G, AND CHAPPELL JB. The arachidonate-activatable, NADPH oxidase-associated H^+ channel. Evidence that gp91-*phox* functions as an essential part of the channel. *J Biol Chem* 270: 5909–5916, 1995.
428. HENDERSON LM AND CHAPPELL JB. The NADPH-oxidase-associated H^+ channel is opened by arachidonate. *Biochem J* 283: 171–175, 1992.
429. HENDERSON LM, CHAPPELL JB, AND JONES OT. The superoxide-generating NADPH oxidase of human neutrophils is electrogenic and associated with an H^+ channel. *Biochem J* 246: 325–329, 1987.
430. HENDERSON LM, CHAPPELL JB, AND JONES OT. Internal pH changes associated with the activity of NADPH oxidase of human neutrophils. Further evidence for the presence of an H^+ conducting channel. *Biochem J* 251: 563–567, 1988.
431. HENDERSON LM, CHAPPELL JB, AND JONES OT. Superoxide generation by the electrogenic NADPH oxidase of human neutrophils is limited by the movement of a compensating charge. *Biochem J* 255: 285–290, 1988.
432. HENDERSON LM, CHAPPELL JB, AND JONES OT. Superoxide generation is inhibited by phospholipase A_2 inhibitors. Role for phospholipase A_2 in the activation of the NADPH oxidase. *Biochem J* 264: 249–255, 1989.
433. HENDERSON LM AND MEECH RW. Evidence that the product of the human X-linked CGD gene, gp91-*phox*, is a voltage-gated H^+ pathway. *J Gen Physiol* 114: 771–786, 1999.
434. HENDERSON LM, MOULE SK, AND CHAPPELL JB. The immediate activator of the NADPH oxidase is arachidonate not phosphorylation. *Eur J Biochem* 211: 157–162, 1993.
435. HENDERSON LM, THOMAS S, BANTING G, AND CHAPPELL JB. The arachidonate-activatable, NADPH oxidase-associated H^+ channel is contained within the multi-membrane-spanning N-terminal region of gp91-*phox*. *Biochem J* 325: 701–705, 1997.
436. HENDERSON R, BALDWIN JM, CESKA TA, ZEMLIN F, BECKMANN E, AND DOWNING KH. Model for the structure of bacteriorhodopsin based on high-resolution electron cryo-microscopy. *J Mol Biol* 213: 899–929, 1990.
437. HEYER RJ, MULLER RU, AND FINKELSTEIN A. Inactivation of monazomycin-induced voltage-dependent conductance in thin lipid membranes. II. Inactivation produced by monazomycin transport through the membrane. *J Gen Physiol* 67: 731–748, 1976.
438. HEYNEMAN RA AND VERCAUTEREN RE. Activation of a NADPH oxidase from horse polymorphonuclear leukocytes in a cell-free system. *J Leukoc Biol* 36: 751–759, 1984.
439. HEYWORTH PG, CURNUTTE JT, RAE J, NOACK D, ROOS D, VAN KOPPEN E, AND CROSS AR. Hematologically important mutations: X-linked chronic granulomatous disease (second update). *Blood Cells Mol Dis* 27: 16–26, 2001.
440. HILLE B. Charges and potentials at the nerve surface. Divalent ions and pH. *J Gen Physiol* 51: 221–236, 1968.
441. HILLE B. Ionic channels in nerve membranes. *Prog Biophys Mol Biol* 21: 1–32, 1970.
442. HILLE B. Ionic selectivity of Na and K channels of nerve membranes. In: *Membranes: A Series of Advances*. New York: Dekker, 1975, p. 255–323.
443. HILLE B. The pH-dependent rate of action of local anesthetics on the node of Ranvier. *J Gen Physiol* 69: 475–496, 1977.
444. HILLE B. *Ion Channels of Excitable Membranes*. Sunderland, MA: Sinauer, 2001.
445. HILLE B AND SCHWARZ W. Potassium channels as multi-ion single-file pores. *J Gen Physiol* 72: 409–442, 1978.
446. HILLE B, WOODHULL AM, AND SHAPIRO BI. Negative surface charge near sodium channels of nerve: divalent ions, monovalent ions, and pH. *Philos Trans R Soc Lond B Biol Sci* 270: 301–318, 1975.
447. HILLE R. Electron transfer within xanthine oxidase: a solvent kinetic isotope effect study. *Biochemistry* 30: 8522–8529, 1991.
448. HILLS GJ, OVENDEN PJ, AND WHITEHOUSE DR. Proton migration in aqueous solution. *Disc Faraday Soc* 39: 207–215, 1965.
449. HINKLE PC AND HORSTMAN LL. Respiration-driven proton transport in submitochondrial particles. *J Biol Chem* 246: 6024–6028, 1971.
450. HIRSCHBERG B, ROVNER A, LIEBERMAN M, AND PATLAK J. Transfer of twelve charges is needed to open skeletal muscle Na^+ channels. *J Gen Physiol* 106: 1053–1068, 1995.
451. HIURA M, OZAWA M, OHTSUKA T, TAKESUE H, YAMAGUCHI M, OKAMURA N, AND ISHIBASHI S. Stimulation of superoxide anion production in guinea pig polymorphonuclear leukocytes by hypotonic conditions in combination with protein kinase C activators. *Arch Biochem Biophys* 291: 31–37, 1991.
452. HLADKY SB. Ion currents through pores. The roles of diffusion and external access steps in determining the currents through narrow pores. *Biophys J* 46: 293–297, 1984.
453. HLADKY SB AND HAYDON DA. Ion transfer across lipid membranes in

the presence of gramicidin A. I. Studies of the unit conductance channel. *Biochim Biophys Acta* 274: 294–312, 1972.
454. HODGKIN AL AND HUXLEY AF. A quantitative description of membrane current and its application to conduction and excitation in nerve. *J Physiol* 117: 500–544, 1952.
455. HODGKIN AL AND HUXLEY AF. The components of membrane conductance in the giant axon of *Loligo*. *J Physiol* 116: 473–496, 1952.
456. HODGKIN AL AND KATZ B. The effects of sodium ions on the electrical activity of the giant axon of the squid. *J Physiol* 108: 37–77, 1949.
457. HODGKIN AL AND KEYNES RD. The potassium permeability of a giant nerve fibre. *J Physiol* 128: 61–88, 1955.
458. HOFACKER I AND SCHULTEN K. Oxygen and proton pathways in cytochrome *c* oxidase. *Proteins* 30: 100–107, 1998.
459. HOLEVINSKY KO, JOW F, AND NELSON DJ. Elevation in intracellular calcium activates both chloride and proton currents in human macrophages. *J Membr Biol* 140: 13–30, 1994.
460. HOLIAN A AND DANIELE RP. Formyl peptide stimulation of superoxide anion release from lung macrophages: sodium and potassium involvement. *J Cell Physiol* 113: 413–419, 1982.
461. HOLLAND SM AND GALLIN JI. Evaluation of the patient with recurrent bacterial infections. *Annu Rev Med* 49: 185–199, 1998.
462. HOLLAND SM AND GALLIN JI. Disorders of phagocytic cells. In: *Inflammation: Basic Principles and Clinical Correlates*, edited by Gallin JI and Snyderman R. Philadelphia, PA: Lippincott Williams & Wilkins, 1999, p. 895–914.
463. HOLMES B, QUIE PG, WINDHORST DB, AND GOOD RA. Fatal granulomatous disease of childhood. An inborn abnormality of phagocytic function. *Lancet* 1: 1225–1228, 1966.
464. HOPPE J AND SEBALD W. The proton conducting F_o-part of bacterial ATP synthases. *Biochim Biophys Acta* 768: 1–27, 1984.
465. HORSEWILL AJ, JONES NH, AND CACIUFFO R. Evidence for coherent proton tunneling in a hydrogen bond network. *Science* 291: 100–103, 2001.
466. HOTH M AND PENNER R. Calcium release-activated calcium current in rat mast cells. *J Physiol* 465: 359–386, 1993.
467. HOTH S, DREYER I, DIETRICH P, BECKER D, MÜLLER-RÖBER B, AND HEDRICH R. Molecular basis of plant-specific acid activation of K^+ uptake channels. *Proc Natl Acad Sci USA* 94: 4806–4810, 1997.
467a. HÜCKEL E. Theorie der Beweglichkeiten des Wasserstoff- und Hydroxylions in wässriger Lösung. *Zeitschrift für Elektrochemie und angewandte physikalische Chemie* 34: 546–562, 1928.
468. HUGGINS ML. Electronic structures of atoms. *J Phys Chem* 26: 601–625, 1922.
469. HUGGINS ML. The role of hydrogen bonds in conduction by hydrogen and hydroxyl ions. *J Am Chem Soc* 53: 3190–3191, 1931.
470. HUGGINS ML. Hydrogen bridges in ice and liquid water. *J Phys Chem* 40: 723–731, 1936.
471. HUI CS. Possible origin of gating current in nerve membrane. *Biosystems* 8: 207–212, 1977.
472. HUMEZ S, COLLIN T, MATIFAT F, GUILBAULT P, AND FOURNIER F. $InsP_3$-dependent Ca^{2+} oscillations linked to activation of voltage-dependent H^+ conductance in *Rana esculenta* oocytes. *Cell Signal* 8: 375–379, 1996.
473. HUMEZ S, FOURNIER F, AND GUILBAULT P. A voltage-dependent and pH-sensitive proton current in *Rana esculenta* oocytes. *J Membr Biol* 147: 207–215, 1995.
474. HUTTER OF AND WARNER AE. Action of some foreign cations and anions on the chloride permeability of frog muscle. *J Physiol* 189: 445–460, 1967.
475. HUTTER OF AND WARNER AE. The pH sensitivity of the chloride conductance of frog skeletal muscle. *J Physiol* 189: 403–425, 1967.
476. HUTTER OF AND WARNER AE. The voltage dependence of the chloride conductance of frog muscle. *J Physiol* 227: 275–290, 1972.
478. HYDE RW, PUY RJ, RAUB WF, AND FORSTER RE. Rate of disappearance of labeled carbon dioxide from the lungs of humans during breath holding: a method for studying the dynamics of pulmonary CO_2 exchange. *J Clin Invest* 47: 1535–1552, 1968.
479. HYNES JT. The protean proton in water. *Nature* 397: 565–567, 1999.
480. IKONEN E. Roles of lipid rafts in membrane transport. *Curr Opin Cell Biol* 13: 470–477, 2001.
481. INCE C, THIO B, VAN DUIJN B, VAN DISSEL JT, YPEY DL, AND LEIJH PC. Intracellular K^+, Na^+ and Cl^- concentrations and membrane potential in human monocytes. *Biochim Biophys Acta* 905: 195–204, 1987.
482. ISLAS LD AND SIGWORTH FJ. Voltage sensitivity and gating charge in *Shaker* and *Shab* family potassium channels. *J Gen Physiol* 114: 723–742, 1999.
483. IWATA S, OSTERMEIER C, LUDWIG B, AND MICHEL H. Structure at 2.8 Å resolution of cytochrome *c* oxidase from *Paracoccus denitrificans*. *Nature* 376: 660–669, 1995.
484. JABŮREK M, VAŘECHA M, GIMENO RE, DEMBSKI M, JEŽEK P, ZHANG M, BURN P, TARTAGLIA LA, AND GARLID KD. Transport function and regulation of mitochondrial uncoupling proteins 2 and 3. *J Biol Chem* 274: 26003–26007, 1999.
485. JACKMAN JE, MERZ KM, AND FIERKE CA. Disruption of the active site solvent network in carbonic anhydrase II decreases the efficiency of proton transfer. *Biochemistry* 35: 16421–16428, 1996.
486. JACOBS MH. The production of intracellular acidity by neutral and alkaline solutions containing carbon dioxide. *Am J Physiol* 53: 457–463, 1920.
487. JAKOBSSON E AND CHIU SW. Stochastic theory of ion movement in channels with single-ion occupancy. Application to sodium permeation of gramicidin channels. *Biophys J* 52: 33–45, 1987.
488. JANKOWSKI A AND GRINSTEIN S. A noninvasive fluorometric procedure for measurement of membrane potential. Quantification of the NADPH oxidase-induced depolarization in activated neutrophils. *J Biol Chem* 274: 26098–26104, 1999.
489. JANKOWSKI A, SCOTT CC, AND GRINSTEIN S. Determinants of the phagosomal pH in neutrophils. *J Biol Chem* 277: 6059–6066, 2002.
490. JEFFREY GA. *An Introduction to Hydrogen Bonding*. New York: Oxford Univ. Press, 1997.
491. JEWELL DA, TU CK, PARANAWITHANA SR, TANHAUSER SM, LOGRASSO PV, LAIPIS PJ, AND SILVERMAN DN. Enhancement of the catalytic properties of human carbonic anhydrase III by site-directed mutagenesis. *Biochemistry* 30: 1484–1490, 1991.
492. JEZEK P AND GARLID KD. New substrates and competitive inhibitors of the Cl^- translocating pathway of the uncoupling protein of brown adipose tissue mitochondria. *J Biol Chem* 265: 19303–19311, 1990.
493. JEŽEK P, HANUŠ J, SEMRAD C, AND GARLID KD. Photoactivated azido fatty acid irreversibly inhibits anion and proton transport through the mitochondrial uncoupling protein. *J Biol Chem* 271: 6199–6205, 1996.
494. JIANG Q, GRIFFIN DA, BAROFSKY DF, AND HURST JK. Intraphagosomal chlorination dynamics and yields determined using unique fluorescent bacterial mimics. *Chem Res Toxicol* 10: 1080–1089, 1997.
495. JIANG W, HERMOLIN J, AND FILLINGAME RH. The preferred stoichiometry of *c* subunits in the rotary motor sector of *Escherichia coli* ATP synthase is 10. *Proc Natl Acad Sci USA* 98: 4966–4971, 2001.
496. JIANG Y AND MACKINNON R. The barium site in a potassium channel by X-ray crystallography. *J Gen Physiol* 115: 269–272, 2000.
497. JOHANSSON A, JESAITIS AJ, LUNDQVIST H, MAGNUSSON KE, SJÖLIN C, KARLSSON A, AND DAHLGREN C. Different subcellular localization of cytochrome *b* and the dormant NADPH-oxidase in neutrophils and macrophages: effect on the production of reactive oxygen species during phagocytosis. *Cell Immunol* 161: 61–71, 1995.
498. JOHNSON BD AND BYERLY L. A cytoskeletal mechanism for Ca^{2+} channel metabolic dependence and inactivation by intracellular Ca^{2+}. *Neuron* 10: 797–804, 1993.
499. JOHNSON BD AND BYERLY L. Photo-released intracellular Ca^{2+} rapidly blocks Ba^{2+} current in *Lymnaea* neurons. *J Physiol* 462: 321–347, 1993.
500. JOHNSTONE JHL. The electrical resistance and temperature coefficient of ice. *Proc Trans Nova Scotian Inst Sci* 13: 126–144, 1912.
501. JONES GS, VAN DYKE K, AND CASTRANOVA V. Purification of human granulocytes by centrifugal elutriation and measurement of transmembrane potential. *J Cell Physiol* 104: 425–431, 1980.
502. JONES GS, VAN DYKE K, AND CASTRANOVA V. Transmembrane potential changes associated with superoxide release from human granulocytes. *J Cell Physiol* 106: 75–83, 1981.
503. JONES PC, HERMOLIN J, JIANG W, AND FILLINGAME RH. Insights into the rotary catalytic mechanism of F_oF_1 ATP synthase from the cross-linking of subunits *b* and *c* in the *Escherichia coli* enzyme. *J Biol Chem* 275: 31340–31346, 2000.

504. JONES RD, HANCOCK JT, AND MORICE AH. NADPH oxidase: a universal oxygen sensor? *Free Radic Biol Med* 29: 416–424, 2000.
505. JONES RD AND MORICE AH. Hypoxic pulmonary vasoconstriction of isolated rat pulmonary arteries is inhibited by cadmium and zinc sulphate: antagonists of the NADPH oxidase-associated proton channel (Abstract). *Thorax* 53 *Suppl*: 46a, 1998.
506. JONES RD, THOMPSON JS, AND MORICE AH. The NADPH oxidase inhibitors iodonium diphenyl and cadmium sulphate inhibit hypoxic pulmonary vasoconstriction in isolated rat pulmonary arteries. *Physiol Res Acad Sci Bohem* 49: 587–596, 2000.
507. JONSSON BH, STEINER H, AND LINDSKOG S. Participation of buffer in the catalytic mechanism of carbonic anhydrase. *FEBS Lett* 64: 310–314, 1976.
508. JORDAN PC. How pore mouth charge distributions alter the permeability of transmembrane ionic channels. *Biophys J* 51: 297–311, 1987.
509. JORDAN PC. Ion-water and ion-polypeptide correlations in a gramicidin-like channel. A molecular dynamics study. *Biophys J* 58: 1133–1156, 1990.
510. JOSEPH D, TIRMIZI O, ZHANG XL, CRANDALL ED, AND LUBMAN RL. Polarity of alveolar epithelial cell acid-base permeability. *Am J Physiol Lung Cell Mol Physiol* 282: L675–L683, 2002.
511. JÜNEMANN S, MEUNIER B, GENNIS RB, AND RICH PR. Effects of mutation of the conserved lysine-362 in cytochrome *c* oxidase from *Rhodobacter sphaeroides*. *Biochemistry* 36: 14456–14464, 1997.
512. JUNGE W. Protons, the thylakoid membrane, and the chloroplast ATP synthase. *Ann NY Acad Sci* 574: 268–286, 1989.
513. JUNGE W. ATP synthase and other motor proteins. *Proc Natl Acad Sci USA* 96: 4735–4737, 1999.
514. JUNGE W AND MCLAUGHLIN S. The role of fixed and mobile buffers in the kinetics of proton movement. *Biochim Biophys Acta* 890: 1–5, 1987.
515. KAIM G AND DIMROTH P. Voltage-generated torque drives the motor of the ATP synthase. *EMBO J* 17: 5887–5895, 1998.
516. KAKINUMA K. Effects of fatty acids on the oxidative metabolism of leukocytes. *Biochim Biophys Acta* 348: 76–85, 1974.
516a. KÁLDI K, SZÁSZI K, KONCZ G, SUSZTÁK K, AND LIGETI E. Arachidonic acid activatable electrogenic H^+ transport in the absence of cytochrome b_{558} in human T lymphocytes. *FEBS Lett* 381: 156–160, 1996.
516b. KÁLDI K, SZÁSZI K, SUSZTÁK K, KAPUS A, AND LIGETI E. Lymphocytes possess an electrogenic H^+-transporting pathway in their plasma membrane. *Biochem J* 301: 329–334, 1994.
517. KANNT A, LANCASTER CRD, AND MICHEL H. The coupling of electron transfer and proton translocation: electrostatic calculations on *Paracoccus denitrificans* cytochrome *c* oxidase. *Biophys J* 74: 708–721, 1998.
518. KAPUS A, ROMANEK R, AND GRINSTEIN S. Arachidonic acid stimulates the plasma membrane H^+ conductance of macrophages. *J Biol Chem* 269: 4736–4745, 1994.
519. KAPUS A, ROMANEK R, QU AY, ROTSTEIN OD, AND GRINSTEIN S. A pH-sensitive and voltage-dependent proton conductance in the plasma membrane of macrophages. *J Gen Physiol* 102: 729–760, 1993.
520. KAPUS A, SUSZTÁK K, AND LIGETI E. Regulation of the electrogenic H^+ channel in the plasma membrane of neutrophils: possible role of phospholipase A_2, internal and external protons. *Biochem J* 292: 445–450, 1993.
521. KAPUS A, SZÁSZI K, AND LIGETI E. Phorbol 12-myristate 13-acetate activates an electrogenic H^+-conducting pathway in the membrane of neutrophils. *Biochem J* 281: 697–701, 1992.
522. KARLSSON A, NIXON JB, AND MCPHAIL LC. Phorbol myristate acetate induces neutrophil NADPH-oxidase activity by two separate signal transduction pathways: dependent or independent of phosphatidylinositol 3-kinase. *J Leukoc Biol* 67: 396–404, 2000.
523. KARPEFORS M, ÄDELROTH P, AAGAARD A, SIGURDSON H, SVENSSON EM, AND BRZEZINSKI P. Electron-proton interactions in terminal oxidases. *Biochim Biophys Acta* 1365: 159–169, 1998.
524. KARPEFORS M, ÄDELROTH P, AND BRZEZINSKI P. Localized control of proton transfer through the D-pathway in cytochrome *c* oxidase: application of the proton-inventory technique. *Biochemistry* 39: 6850–6856, 2000.
525. KARPEFORS M, ÄDELROTH P, AND BRZEZINSKI P. The onset of the deuterium isotope effect in cytochrome *c* oxidase. *Biochemistry* 39: 5045–5050, 2000.
526. KARPEFORS M, ÄDELROTH P, ZHEN Y, FERGUSON-MILLER S, AND BRZEZINSKI P. Proton uptake controls electron transfer in cytochrome *c* oxidase. *Proc Natl Acad Sci USA* 95: 13606–13611, 1998.
527. KASIANOWICZ J, BENZ R, AND MCLAUGHLIN S. How do protons cross the membrane-solution interface? Kinetic studies on bilayer membranes exposed to the protonophore S-13 (5-chloro-3-tert-butyl-2′-chloro-4′nitrosalicylanilide). *J Membr Biol* 95: 73–89, 1987.
530. KELL DB. On the functional proton current pathway of electron transport phosphorylation. An electrodic view. *Biochim Biophys Acta* 549: 55–99, 1979.
531. KELL MJ AND DEFELICE LJ. Surface charge near the cardiac inward-rectifier channel measured from single-channel conductance. *J Membr Biol* 102: 1–10, 1988.
532. KEMPF C, KLAUSNER RD, WEINSTEIN JN, VAN RENSWOUDE J, PINCUS M, AND BLUMENTHAL R. Voltage-dependent *trans*-bilayer orientation of melittin. *J Biol Chem* 257: 2469–2476, 1982.
533. KHALIFAH RG. The carbon dioxide hydration activity of carbonic anhydrase. I. Stop-flow kinetic studies on the native human isoenzymes B and C. *J Biol Chem* 246: 2561–2573, 1971.
534. KHANNA R, ROY L, ZHU X, AND SCHLICHTER LC. K^+ channels and the microglial respiratory burst. *Am J Physiol Cell Physiol* 280: C796–C806, 2001.
535. KHOSHTARIYA DE AND BERDZENISHVILI NO. A new dynamic elementary act model for thermal and photoinduced proton self-exchange through the lyate ion hydrogen bridges in solutions. *Chem Phys Lett* 196: 607–613, 1992.
536. KIEFER H AND JÄHNIG F. Neutral phospholipids do not buffer at neutral pH. *Biophys J* 66: 1733, 1994.
537. KIENKER P, SLATIN SL, AND FINKELSTEIN A. Colicin channels have a shockingly high proton permeability (Abstract). *Biophys J* 82: 555a, 2002.
538. KIKUCHI H, HIKAGE M, MIYASHITA H, AND FUKUMOTO M. NADPH oxidase subunit, gp91^{phox} homologue, preferentially expressed in human colon epithelial cells. *Gene* 254: 237–243, 2000.
539. KIM SY, SILVER MR, AND DECOURSEY TE. Ion channels in human THP-1 monocytes. *J Membr Biol* 152: 117–130, 1996.
540. KIMURA J, MIYAMAE S, AND NOMA A. Identification of sodium-calcium exchange current in single ventricular cells of guinea-pig. *J Physiol* 384: 199–222, 1987.
541. KINSELLA JL AND ARONSON PS. Properties of the Na^+-H^+ exchanger in renal microvillus membrane vesicles. *Am J Physiol Renal Fluid Electrolyte Physiol* 238: F461–F469, 1980.
542. KLEBANOFF SJ. Antimicrobial mechanisms in neutrophilic polymorphonuclear leukocytes. *Semin Hematol* 12: 117–142, 1975.
543. KLEBANOFF SJ. Oxygen metabolites from phagocytes. In: *Inflammation: Basic Principles and Clinical Correlates*, edited by Gallin JI and Snyderman R. Philadelphia, PA: Lippincott Williams & Wilkins, 1999, p. 721–768.
544. KLEBANOFF SJ, VADAS MA, HARLAN JM, SPARKS LH, GAMBLE JR, AGOSTI JM, AND WALTERSDORPH AM. Stimulation of neutrophils by tumor necrosis factor. *J Immunol* 136: 4220–4225, 1986.
545. KLEE R, HEINEMANN U, AND EDER C. Changes in proton currents in murine microglia induced by cytoskeletal disruptive agents. *Neurosci Lett* 247: 191–194, 1998.
546. KLEE R, HEINEMANN U, AND EDER C. Voltage-gated proton currents in microglia of distinct morphology and functional state. *Neuroscience* 91: 1415–1424, 1999.
547. KLEINFELD AM. Lipid phase fatty acid flip-flop, is it fast enough for cellular transport? *J Membr Biol* 175: 79–86, 2000.
548. KLINGENBERG M AND ECHTAY KS. Uncoupling proteins: the issues from a biochemist point of view. *Biochim Biophys Acta* 1504: 128–143, 2001.
549. KLINGENBERG M AND WINKLER E. The reconstituted isolated uncoupling protein is a membrane potential driven H^+ translocator. *EMBO J* 4: 3087–3092, 1985.
550. KLION AD, ARMANT MA, AND NUTMAN TB. Role of immunoglobulin E and eosinophils in mediating protection and pathology in parasitic helminth infections. In: *Inflammation: Basic Principles and Clinical Correlates*, edited by Gallin JI and Snyderman R. Philadelphia, PA: Lippincott Williams & Wilkins, 1999, p. 929–936.

551. KLOCKE RA. Equilibrium of CO_2 reactions in the pulmonary capillary. *J Appl Physiol* 48: 972–976, 1980.
552. KOBAYASHI C, SAITO S, AND OHMINE I. Mechanism of fast proton transfer in ice: potential energy and reaction coordinate analysis. *J Chem Phys* 113: 9090–9100, 2000.
553. KOBAYASHI T, ROBINSON JM, AND SEGUCHI H. Identification of intracellular sites of superoxide production in stimulated neutrophils. *J Cell Sci* 111: 81–91, 1998.
554. KOCH AL. The pH in the neighborhood of membranes generating a protonmotive force. *J Theor Biol* 120: 73–84, 1986.
555. KOLESNIKOV SS AND MARGOLSKEE RF. Extracellular K^+ activates a K^+- and H^+-permeable conductance in frog taste receptor cells. *J Physiol* 507: 415–432, 1998.
556. KONISHI T AND PACKER L. A proton channel in bacteriorhodopsin. *FEBS Lett* 89: 333–336, 1978.
557. KONNERTH A, LUX HD, AND MORAD M. Proton-induced transformation of calcium channel in chick dorsal root ganglion cells. *J Physiol* 386: 603–633, 1987.
558. KONSTANTINOV AA, SILETSKY S, MITCHELL D, KAULEN A, AND GENNIS RB. The roles of the two proton input channels in cytochrome *c* oxidase from *Rhodobacter sphaeroides* probed by the effects of site-directed mutations on time-resolved electrogenic intraprotein proton transfer. *Proc Natl Acad Sci USA* 94: 9085–9090, 1997.
559. KOPPEL M AND SPIRO K. Über die Wirkung von Moderatoren (Puffern) bei der Verschiebung des Säure-Basengleichgewichtes in biologischen Flüssigkeiten. *Biochemische Zeitung* 65: 409–439, 1914.
560. KORCHAK HM, EISENSTAT BA, HOFFSTEIN ST, DUNHAM PB, AND WEISSMANN G. Anion channel blockers inhibit lysosomal enzyme secretion from human neutrophils without affecting generation of superoxide anion. *Proc Natl Acad Sci USA* 77: 2721–2725, 1980.
561. KORCHAK HM AND WEISSMANN G. Changes in membrane potential of human granulocytes antecede the metabolic responses to surface stimulation. *Proc Natl Acad Sci USA* 75: 3818–3822, 1978.
562. KORENSTEIN R, SHERMAN WV, AND CAPLAN SR. Kinetic isotope effects in the photochemical cycle of bacteriorhodopsin. *Biophys Struct Mech* 2: 267–276, 1976.
563. KORKUSHKO AO AND KRYSHTAL OA. Blocking of proton-activated sodium permeability of the membranes of trigeminal ganglion neurons in the rat by organic cations. *Neirofiziologiia* 16: 557–561, 1984.
564. KORNBLATT JA. The water channel of cytochrome *c* oxidase: inferences from inhibitor studies. *Biophys J* 75: 3127–3134, 1998.
565. KOSHKIN V, LOTAN O, AND PICK E. The cytosolic component $p47^{phox}$ is not a *sine qua non* participant in the activation of NADPH oxidase but is required for optimal superoxide production. *J Biol Chem* 271: 30326–30329, 1996.
566. KOSHKIN V, LOTAN O, AND PICK E. Electron transfer in the superoxide-generating NADPH oxidase complex reconstituted in vitro. *Biochim Biophys Acta* 1319: 139–146, 1997.
567. KOSHKIN V AND PICK E. Generation of superoxide by purified and relipidated cytochrome b_{559} in the absence of cytosolic activators. *FEBS Lett* 327: 57–62, 1993.
568. KOSHKIN V AND PICK E. Superoxide production by cytochrome b_{559}. Mechanism of cytosol-independent activation. *FEBS Lett* 338: 285–289, 1994.
569. KOSTYUK PG AND KRISHTAL OA. Separation of sodium and calcium currents in the somatic membrane of mollusc neurones. *J Physiol* 270: 545–568, 1977.
570. KRAUSE KH AND WELSH MJ. Voltage-dependent and Ca^{2+}-activated ion channels in human neutrophils. *J Clin Invest* 85: 491–498, 1990.
571. KRISHNAMOORTHY G. Temperature jump as a new technique to study the kinetics of fast transport of protons across membranes. *Biochemistry* 25: 6666–6671, 1986.
572. KRISHNAMOORTHY G AND HINKLE PC. Non-ohmic proton conductance of mitochondria and liposomes. *Biochemistry* 23: 1640–1645, 1984.
573. KUKOL A, ADAMS PD, RICE LM, BRUNGER AT, AND ARKIN TI. Experimentally based orientational refinement of membrane protein models: a structure for the *Influenza* A M2 H^+ channel. *J Mol Biol* 286: 951–962, 1999.
574. KUNO M, KAWAWAKI J, AND NAKAMURA F. A highly temperature-sensitive proton current in mouse bone marrow-derived mast cells. *J Gen Physiol* 109: 731–740, 1997.
575. KUNST M AND WARMAN JM. Proton mobility in ice. *Nature* 288: 465–467, 1980.
576. KUROKI M, KAMO N, KOBATAKE Y, OKIMASU E, AND UTSUMI K. Measurement of membrane potential in polymorphonuclear leukocytes and its changes during surface stimulation. *Biochim Biophys Acta* 693: 326–334, 1982.
577. KÜRZ LL, KLINK H, JAKOB I, KUCHENBECKER M, BENZ S, LEHMANN-HORN F, AND RÜDEL R. Identification of three cysteines as targets for the Zn^{2+} blockade of the human skeletal muscle chloride channel. *J Biol Chem* 274: 11687–11692, 1999.
578. KÜRZ LL, WAGNER S, GEORGE AL, AND RÜDEL R. Probing the major skeletal muscle chloride channel with Zn^{2+} and other sulfhydryl-reactive compounds. *Pflügers Arch* 433: 357–363, 1997.
579. LACAZ-VIEIRA F. pH- and voltage-dependent conductances in toad skin. *J Membr Biol* 148: 1–11, 1995.
580. LACOMBE B, PILOT G, GAYMARD F, SENTENAC H, AND THIBAUD JB. pH control of the plant outwardly-rectifying potassium channel SKOR. *FEBS Lett* 466: 351–354, 2000.
581. LACY P, ABDEL LATIF D, STEWARD M, MUSAT-MARCU S, ROWE B, MAN SFP, AND MOQBEL R. Divergence of mechanisms regulating respiratory burst in blood and sputum eosinophils and neutrophils from atopic subjects. *J Immunol.* In press.
582. LAMBETH JD, CHENG G, ARNOLD RS, AND EDENS WA. Novel homologs of gp91*phox*. *Trends Biochem Sci* 25: 459–461, 2000.
583. LANCASTER CR, GROB R, HAAS A, RITTER M, MÄNTELE W, SIMON J, AND KRÖGER A. Essential role of Glu-C66 for menaquinol oxidation indicates transmembrane electrochemical potential generation by *Wolinella succinogenes* fumarate reductase. *Proc Natl Acad Sci USA* 97: 13051–13056, 2000.
584. LANCASTER CR, MICHEL H, HONIG B, AND GUNNER MR. Calculated coupling of electron and proton transfer in the photosynthetic reaction center of *Rhodopseudomonas viridis*. *Biophys J* 70: 2469–2492, 1996.
585. LANDE MB, DONOVAN JM, AND ZEIDEL ML. The relationship between membrane fluidity and permeabilities to water, solutes, ammonia, and protons. *J Gen Physiol* 106: 67–84, 1995.
586. LANYI JK. Proton translocation mechanism and energetics in the light-driven pump bacteriorhodopsin. *Biochim Biophys Acta* 1183: 241–261, 1993.
587. LANYI JK. Bacteriorhodopsin as a model for proton pumps. *Nature* 375: 461–463, 1995.
588. LANYI JK. Mechanism of ion transport across membranes. Bacteriorhodopsin as a prototype for proton pumps. *J Biol Chem* 272: 31209–31212, 1997.
589. LANYI JK. Crystallographic studies of the conformational changes that drive directional transmembrane ion movement in bacteriorhodopsin. *Biochim Biophys Acta* 1459: 339–345, 2000.
590. LANYI JK AND SCHOBERT B. Crystallographic structure of the retinal and the protein after deprotonation of the Schiff base: the switch in the bacteriorhodopsin photocycle. *J Mol Biol* 321: 727–737, 2002.
591. LANZA F. Clinical manifestation of myeloperoxidase deficiency. *J Mol Med* 76: 676–681, 1998.
592. LATIMER WM AND RODEBUSH W. Polarity and ionization from the standpoint of the Lewis theory of valence. *J Am Chem Soc* 42: 1419–1433, 1920.
593. LÄUGER P. Diffusion-limited ion flow through pores. *Biochim Biophys Acta* 455: 493–509, 1976.
594. LÄUGER P. Barrier models for the description of proton transport across membranes. *Methods Enzymol* 127: 465–471, 1986.
595. LÄUGER P. Dynamics of ion transport systems in membranes. *Physiol Rev* 67: 1296–1331, 1987.
596. LÄUGER P. *Electrogenic Ion Pumps*. Sunderland, MA: Sinauer, 1991.
597. LAZZARI KG, PROTO P, AND SIMONS ER. Neutrophil hyperpolarization in response to a chemotactic peptide. *J Biol Chem* 265: 10959–10967, 1990.
598. LAZZARI KG, PROTO PJ, AND SIMONS ER. Simultaneous measurement of stimulus-induced changes in cytoplasmic Ca^{2+} and in membrane potential of human neutrophils. *J Biol Chem* 261: 9710–9713, 1986.

599. Lear JD, Wasserman ZR, and Degrado WF. Synthetic amphiphilic peptide models for protein ion channels. *Science* 240: 1177–1181, 1988.
600. Leca G, Benichou G, Bensussan A, Mitenne F, Galanaud P, and Vazquez A. Respiratory burst in human B lymphocytes. Triggering of surface Ig receptors induces modulation of chemiluminescence signal. *J Immunol* 146: 3542–3549, 1991.
601. le Coutre J and Gerwert K. Kinetic isotope effects reveal an ice-like and a liquid-phase-type intramolecular proton transfer in bacteriorhodopsin. *FEBS Lett* 398: 333–336, 1996.
602. Lee HM, Das TK, Rousseau DL, Mills D, Ferguson-Miller S, and Gennis RB. Mutations in the putative H-channel in the cytochrome *c* oxidase from *Rhodobacter sphaeroides* show that this channel is not important for proton conduction but reveal modulation of the properties of heme *a*. *Biochemistry* 39: 2989–2996, 2000.
603. Leem CH, Lagadic-Gossmann D, and Vaughan-Jones RD. Characterization of intracellular pH regulation in the guinea-pig ventricular myocyte. *J Physiol* 517: 159–180, 1999.
604. Leibbrandt ME and Koropatnick J. Activation of human monocytes with lipopolysaccharide induces metallothionein expression and is diminished by z. *Toxicol Appl Pharmacol* 124: 72–81, 1994.
605. Lengyel S and Conway BE. Proton solvation and proton transfer in chemical and electrochemical processes. In: *Comprehensive Treatise of Electrochemistry. Thermodynamic and Transport Properties of Aqueous and Molten Electrolytes*, edited by Conway BE, Bockris JOM, and Yeager E. New York: Plenum, 1983, vol 5, p. 339–398.
606. Lengyel S, Giber J, and Tamás J. Determination of ionic mobilities in aqueous hydrochloric acid solutions of different concentration at various temperatures. *Acta Chim Acad Sci Hung* 32: 429–436, 1962.
607. Lennartz MR and Brown EJ. Arachidonic acid is essential for IgG Fc receptor-mediated phagocytosis by human monocytes. *J Immunol* 147: 621–626, 1991.
608. Leusen JHW, Verhoeven AJ, and Roos D. Interactions between the components of the human NADPH oxidase: a review about the intrigues in the *phox* family. *Front Biosci* 1: d72–d90, 1996.
609. Levitt DG. Electrostatic calculations for an ion channel. 1. Energy and potential profiles and interactions between ions. *Biophys J* 22: 209–219, 1978.
610. Levitt DG and Decker ER. Electrostatic radius of the gramicidin channel determined from voltage dependence of H^+ ion conductance. *Biophys J* 53: 33–38, 1988.
611. Levitt DG, Elias SR, and Hautman JM. Number of water molecules coupled to the transport of sodium, potassium and hydrogen ions via gramicidin, nonactin or valinomycin. *Biochim Biophys Acta* 512: 436–451, 1978.
612. Lewis GN and Doody TC. The mobility of ions in H^2H^2O. *J Am Chem Soc* 55: 3504–3506, 1933.
613. Liberek T, Topley N, Jörres A, Petersen MM, Coles GA, Gahl GM, and Williams JD. Peritoneal dialysis fluid inhibition of polymorphonuclear leukocyte respiratory burst activation is related to the lowering of intracellular pH. *Nephron* 65: 260–265, 1993.
614. Lien YH and Lai LW. Respiratory acidosis in carbonic anhydrase II-deficient mice. *Am J Physiol Lung Cell Mol Physiol* 274: L301–L304, 1998.
615. Lill H, Althoff G, and Junge W. Analysis of ionic channels by a flash spectrophotometric technique applicable to thylakoid membranes: CF_o, the proton channel of the chloroplast ATP synthase, and for comparison, gramicidin. *J Membr Biol* 98: 69–78, 1987.
616. Lill H, Engelbrecht S, Schönknecht G, and Junge W. The proton channel, CF_o, in thylakoid membranes. Only a low proportion of CF_1-lacking CF_o is active with a high unit conductance (169 fS). *Eur J Biochem* 160: 627–634, 1986.
617. Lin TI and Schroeder C. Definitive assignment of proton selectivity and attoampere unitary current to the M2 ion channel protein of influenza A virus. *J Virol* 75: 3647–3656, 2001.
618. Lin YW, Lin CW, and Chen TY. Elimination of the slow gating of ClC-0 chloride channel by a point mutation. *J Gen Physiol* 114: 1–12, 1999.
619. Lindsay MA, Perkins RS, Barnes PJ, and Giembycz MA. Leukotriene B_4 activates the NADPH oxidase in eosinophils by a pertussis toxin-sensitive mechanism that is largely independent of arachidonic acid mobilization. *J Immunol* 160: 4526–4534, 1998.
620. Lindskog S. Structure and mechanism of carbonic anhydrase. *Pharmacol Ther* 74: 1–20, 1997.
621. Lindskog S and Silverman DN. The catalytic mechanism of mammalian carbonic anhydrases. In: *The Carbonic Anhydrases: New Horizons*, edited by Chegwidden WR, Carter ND, and Edwards YH. Basel: Birkhäuser Verlag, 2000, p. 175–195.
622. Link TA and von Jagow G. Zinc ions inhibit the Q_p center of bovine heart mitochondrial bc_1 complex by blocking a protonatable group. *J Biol Chem* 270: 25001–25006, 1995.
623. Loewenstein A and Szöke A. The activation energies of proton transfer reactions in water. *J Am Chem Soc* 84: 1151–1154, 1962.
624. Longsworth LG and Macinnes DA. Transference numbers and ion mobilities of some electrolytes in deuterium oxide and its mixtures with water. *J Am Chem Soc* 59: 1666–1670, 1937.
624a. Lönnerholm G. Pulmonary carbonic anhydrase in the human, monkey, and rat. *J Appl Physiol* 52: 352–356, 1982.
625. Lopes LR, Hoyal CR, Knaus UG, and Babior BM. Activation of the leukocyte NADPH oxidase by protein kinase C in a partially recombinant cell-free system. *J Biol Chem* 274: 15533–15537, 1999.
626. Low CM, Zheng F, Lyuboslavsky P, and Traynelis SF. Molecular determinants of coordinated proton and zinc inhibition of *N*-methyl-D-aspartate NR1/NR2A receptors. *Proc Natl Acad Sci USA* 97: 11062–11067, 2000.
627. Lowenthal A and Levy R. Essential requirement of cytosolic phospholipase A_2 for activation of the H^+ channel in phagocyte-like cells. *J Biol Chem* 274: 21603–21608, 1999.
628. Lown DA and Thirsk HR. Proton transfer conductance in aqueous solution. Part 1. Conductance of concentrated aqueous alkali metal hydroxide solutions at elevated temperatures and pressures. *Trans Faraday Soc* 67: 132–148, 1971.
630. Lubman RL and Crandall ED. Polarized distribution of Na^+-H^+ antiport activity in rat alveolar epithelial cells. *Am J Physiol Lung Cell Mol Physiol* 266: L138–L147, 1994.
631. Luecke H, Richter HT, and Lanyi JK. Proton transfer pathways in bacteriorhodopsin at 2.3 angstrom resolution. *Science* 280: 1934–1937, 1998.
632. Luecke H, Schobert B, Richter HT, Cartailler JP, and Lanyi JK. Structural changes in bacteriorhodopsin during ion transport at 2 angstrom resolution. *Science* 286: 255–261, 1999.
633. Luecke H, Schobert B, Richter HT, Cartailler JP, and Lanyi JK. Structure of bacteriorhodopsin at 1.55 Å resolution. *J Mol Biol* 291: 899–911, 1999.
634. Lühring H. pH-sensitive gating kinetics of the maxi-K channel in the tonoplast of *Chara australis*. *J Membr Biol* 168: 47–61, 1999.
635. Lundqvist H, Follin P, Khalfan L, and Dahlgren C. Phorbol myristate acetate-induced NADPH oxidase activity in human neutrophils: only half the story has been told. *J Leukoc Biol* 59: 270–279, 1996.
636. Luz Z and Meiboom S. The activation energies of proton transfer reactions in water. *J Am Chem Soc* 86: 4768–4769, 1964.
637. Lyall V, Belcher TS, and Biber TU. Effect of changes in extracellular potassium on intracellular pH in principal cells of frog skin. *Am J Physiol Renal Fluid Electrolyte Physiol* 263: F722–F730, 1992.
638. Lyall V, Belcher TS, and Biber TU. Na^+ channel blockers inhibit voltage-dependent intracellular pH changes in principal cells of frog (*Rana pipiens*) skin. *Comp Biochem Physiol B Physiol* 105: 503–511, 1993.
639. Ma J, Tsatsos PH, Zaslavsky D, Barquera B, Thomas JW, Katsonouri A, Puustinen A, Wikström M, Brzezinski P, Alben JO, and Gennis RB. Glutamate-89 in subunit II of cytochrome bo_3 from *Escherichia coli* is required for the function of the heme-copper oxidase. *Biochemistry* 38: 15150–15156, 1999.
640. Mackay DH, Berens PH, Wilson KR, and Hagler AT. Structure and dynamics of ion transport through gramicidin A. *Biophys J* 46: 229–248, 1984.
641. Mahaut-Smith M. Separation of hydrogen ion currents in intact molluscan neurones. *J Exp Biol* 145: 439–454, 1989.
642. Mahaut-Smith M. The effect of zinc on calcium and hydrogen ion currents in intact snail neurones. *J Exp Biol* 145: 455–469, 1989.

643. MAJANDER A AND WIKSTRÖM M. The plasma membrane potential of human neutrophils. Role of ion channels and the sodium/potassium pump. *Biochim Biophys Acta* 980: 139–145, 1989.
644. MAKINO R, TANAKA T, IIZUKA T, ISHIMURA Y, AND KANEGASAKI S. Stoichiometric conversion of oxygen to superoxide anion during the respiratory burst in neutrophils. Direct evidence by a new method for measurement of superoxide anion with diacetyldeuteroheme-substituted horseradish peroxidase. *J Biol Chem* 261: 11444–11447, 1986.
645. MALOFIEJEW M, KOSTRZEWSKA A, AND KOWAL E. Intracellular potential in normal and leukemic lymphocytes. *Acta Haematol Pol* 53: 138–144, 1975.
646. MALY FE, CROSS AR, JONES OT, WOLF-VORBECK G, WALKER C, DAHINDEN CA, AND DE WECK AL. The superoxide generating system of B cell lines. Structural homology with the phagocytic oxidase and triggering via surface Ig. *J Immunol* 140: 2334–2339, 1988.
647. MALY FE, NAKAMURA M, GAUCHAT JF, URWYLER A, WALKER C, DAHINDEN CA, CROSS AR, JONES OT, AND DE WECK AL. Superoxide-dependent nitroblue tetrazolium reduction and expression of cytochrome b_{-245} components by human tonsillar B lymphocytes and B cell lines. *J Immunol* 142: 1260–1267, 1989.
648. MANDELL GL. Bactericidal activity of aerobic and anaerobic polymorphonuclear neutrophils. *Infect Immun* 9: 337–341, 1974.
649. MANKELOW TJ AND HENDERSON LM. Inhibition of the neutrophil NADPH oxidase and associated H^+ channel by diethyl pyrocarbonate (DEPC), a histidine-modifying agent: evidence for at least two target sites. *Biochem J* 358: 315–324, 2001.
650. MANOR D, HASSELBACHER CA, AND SPUDICH JL. Membrane potential modulates photocycling rates of bacterial rhodopsins. *Biochemistry* 27: 5843–5848, 1988.
651. MAOUYO D, CHU S, AND MONTROSE MH. pH heterogeneity at intracellular and extracellular plasma membrane sites in HT29–C1 cell monolayers. *Am J Physiol Cell Physiol* 278: C973–C981, 2000.
652. MARANTZ Y AND NACHLIEL E. Gauging of cytochrome *c* structural fluctuation by time-resolved proton pulse. *Isr J Chem* 39: 439–445, 1999.
653. MARANTZ Y, NACHLIEL E, AAGAARD A, BRZEZINSKI P, AND GUTMAN M. The proton collecting function of the inner surface of cytochrome *c* oxidase from *Rhodobacter sphaeroides*. *Proc Natl Acad Sci USA* 95: 8590–8595, 1998.
654. MARCUS RA. Theoretical relations among rate constants, barriers, and Brönsted slope of chemical reactions. *J Phys Chem* 72: 891–899, 1968.
655. MARIDONNEAU-PARINI I AND TAUBER AI. Activation of NADPH-oxidase by arachidonic acid involves phospholipase A_2 in intact human neutrophils but not in the cell-free system. *Biochem Biophys Res Commun* 138: 1099–1105, 1986.
656. MARKERT M, VAGLIO M, AND FREI J. Activation of the human neutrophil respiratory burst by an anion channel blocker. *J Lab Clin Med* 111: 577–583, 1988.
657. MARÓTI P AND WRAIGHT CA. Kinetics of H^+ ion binding by the P^+Q_A-state of bacterial photosynthetic reaction centers: rate limitation within the protein. *Biophys J* 73: 367–381, 1997.
658. MARRINK SJ, JAHNIG F, AND BERENDSEN HJ. Proton transport across transient single-file water pores in a lipid membrane studied by molecular dynamics simulations. *Biophys J* 71: 632–647, 1996.
659. MARSH D. Peptide models for membrane channels. *Biochem J* 315: 345–361, 1996.
660. MARSHALL C, MAMARY AJ, VERHOEVEN AJ, AND MARSHALL BE. Pulmonary artery NADPH-oxidase is activated in hypoxic pulmonary vasoconstriction. *Am J Respir Cell Mol Biol* 15: 633–644, 1996.
661. MARTIN K AND HELENIUS A. Nuclear transport of influenza virus ribonucleoproteins: the viral matrix protein (M1) promotes export and inhibits import. *Cell* 67: 117–130, 1991.
662. MARTIN MA, NAUSEEF WM, AND CLARK RA. Depolarization blunts the oxidative burst of human neutrophils. Parallel effects of monoclonal antibodies, depolarizing buffers, and glycolytic inhibitors. *J Immunol* 140: 3928–3935, 1988.
663. MARTY A, TAN YP, AND TRAUTMANN A. Three types of calcium-dependent channel in rat lacrimal glands. *J Physiol* 357: 293–325, 1984.
664. MARX D, TUCKERMAN ME, HUTTER J, AND PARRINELLO M. The nature of the hydrated excess proton in water. *Nature* 397: 601–604, 1999.
665. MATTHIAS A, JACOBSSON A, CANNON B, AND NEDERGAARD J. The bioenergetics of brown fat mitochondria from UCP1-ablated mice. UCP1 is not involved in fatty acid-induced de-energization ("uncoupling"). *J Biol Chem* 274: 28150–28160, 1999.
666. MATTHIAS A, OHLSON KB, FREDRIKSSON JM, JACOBSSON A, NEDERGAARD J, AND CANNON B. Thermogenic responses in brown fat cells are fully UCP1-dependent. UCP2 or UCP3 do not substitute for UCP1 in adrenergically or fatty acid-induced thermogenesis. *J Biol Chem* 275: 25073–25081, 2000.
667. MATTSSON JP AND KEELING DJ. [^{3}H]bafilomycin as a probe for the transmembrane proton channel of the osteoclast vacuolar H^+-ATPase. *Biochim Biophys Acta* 1280: 98–106, 1996.
668. MATURANA A, ARNAUDEAU S, RYSER S, BÁNFI B, HOSSLE JP, SCHLEGEL W, KRAUSE KH, AND DEMAUREX N. Heme histidine ligands within $gp91^{phox}$ modulate proton conduction by the phagocyte NADPH oxidase. *J Biol Chem* 276: 30277–30284, 2001.
669. MCGEOCH JEM, MCGEOCH MW, MAO R, AND GUIDOTTI G. Opposing actions of cGMP and calcium on the conductance of the F_o subunit c pore. *Biochem Biophys Res Commun* 274: 835–840, 2000.
670. MCLARNON JG, XU R, LEE YB, AND KIM SU. Ion channels of human microglia in culture. *Neuroscience* 78: 1217–1228, 1997.
671. MCLAUGHLIN SG AND DILGER JP. Transport of protons across membranes by weak acids. *Physiol Rev* 60: 825–863, 1980.
672. MCPHAIL LC, CLAYTON CC, AND SNYDERMAN R. A potential second messenger role for unsaturated fatty acids: activation of Ca^{2+}-dependent protein kinase. *Science* 224: 622–625, 1984.
673. MCPHAIL LC, DECHATELET LR, AND SHIRLEY PS. Further characterization of NADPH oxidase activity of human polymorphonuclear leukocytes. *J Clin Invest* 58: 775–780, 1976.
674. MCPHAIL LC, SHIRLEY PS, CLAYTON CC, AND SNYDERMAN R. Activation of the respiratory burst enzyme from human neutrophils in a cell-free system. Evidence for a soluble cofactor. *J Clin Invest* 75: 1735–1739, 1985.
675. MCPHAIL LC AND SNYDERMAN R. Activation of the respiratory burst enzyme in human polymorphonuclear leukocytes by chemoattractants and other soluble stimuli. Evidence that the same oxidase is activated by different transductional mechanisms. *J Clin Invest* 72: 192–200, 1983.
676. MEECH RW AND THOMAS RC. Voltage-dependent intracellular pH in *Helix aspersa* neurones. *J Physiol* 390: 433–452, 1987.
677. MEHLER EL AND GUARNIERI F. A self-consistent, microenvironment modulated screened coulomb potential approximation to calculate pH-dependent electrostatic effects in proteins. *Biophys J* 77: 3–22, 1999.
678. MEIBOOM S. Nuclear magnetic resonance study of the proton transfer in water. *J Chem Phys* 34: 375–388, 1961.
679. MEISSNER G AND MCKINLEY D. Permeability of canine cardiac sarcoplasmic reticulum vesicles to K^+, Na^+, H^+, and Cl^-. *J Biol Chem* 257: 7704–7711, 1982.
680. MEISSNER G AND YOUNG RC. Proton permeability of sarcoplasmic reticulum vesicles. *J Biol Chem* 255: 6814–6819, 1980.
681. MEISTER M, CAPLAN SR, AND BERG HC. Dynamics of a tightly coupled mechanism for flagellar rotation Bacterial motility, chemiosmotic coupling, protonmotive force. *Biophys J* 55: 905–914, 1989.
682. MEISTER M, LOWE G, AND BERG HC. The proton flux through the bacterial flagellar motor. *Cell* 49: 643–650, 1987.
683. MENEGAZZI R, BUSETTO S, DRI P, CRAMER R, AND PATRIARCA P. Chloride ion efflux regulates adherence, spreading, and respiratory burst of neutrophils stimulated by tumor necrosis factor-α (TNF) on biologic surfaces. *J Cell Biol* 135: 511–522, 1996.
684. MICHAELIS L AND MENTEN ML. Die Kinetic der Invertinwirkung. *Biochem Z* 49: 333–369, 1913.
685. MICHEL H. The mechanism of proton pumping by cytochrome *c* oxidase. *Proc Natl Acad Sci USA* 95: 12819–12824, 1998.
686. MICHEL H. Cytochrome *c* oxidase: catalytic cycle and mechanisms of proton pumping—a discussion. *Biochemistry* 38: 15129–15140, 1999.
687. MIEDEMA H, FELLE H, AND PRINS HB. Effect of high pH on the plasma membrane potential and conductance in *Elodea densa*. *J Membr Biol* 128: 63–69, 1992.

688. Miedema H, Staal M, and Prins HB. pH-induced proton permeability changes of plasma membrane vesicles. *J Membr Biol* 152: 159–167, 1996.
689. Mills DA and Ferguson-Miller S. Proton uptake and release in cytochrome *c* oxidase: separate pathways in time and space? *Biochim Biophys Acta* 1365: 46–52, 1998.
690. Mills DA and Ferguson-Miller S. Influence of structure, pH and membrane potential on proton movement in cytochrome oxidase. *Biochim Biophys Acta* 1555: 96–100, 2002.
691. Mills DA, Florens L, Hiser C, Qian J, and Ferguson-Miller S. Where is "outside" in cytochrome *c* oxidase and how and when do protons get there? *Biochim Biophys Acta* 1458: 180–187, 2000.
692. Mills DA, Schmidt B, Hiser C, Westley E, and Ferguson-Miller S. Membrane potential-controlled inhibition of cytochrome *c* oxidase by zinc. *J Biol Chem* 277: 14894–14901, 2002.
693. Mitchell DM, Fetter JR, Mills DA, Ädelroth P, Pressler MA, Kim Y, Aasa R, Brzezinski P, Malmström BG, Alben JO, Babcock GT, Ferguson-Miller S, and Gennis RB. Site-directed mutagenesis of residues lining a putative proton transfer pathway in cytochrome *c* oxidase from *Rhodobacter sphaeroides*. *Biochemistry* 35: 13089–13093, 1996.
694. Mitchell P. Coupling of phosphorylation to electron and hydrogen transfer by a chemi-osmotic type of mechanism. *Nature* 191: 144–148, 1961.
695. Mitchell P. A chemiosmotic molecular mechanism for proton-translocating adenosine triphosphatases. *FEBS Lett* 43: 189–194, 1974.
696. Mitchell P. Vectorial chemistry and the molecular mechanics of chemiosmotic coupling: power transmission by proticity. *Biochem Soc Trans* 4: 399–430, 1976.
697. Mitchell P. Molecular mechanics of protonmotive F_oF_1 ATPases: rolling well and turnstile hypothesis. *FEBS Lett* 182: 1–7, 1985.
698. Mitchell P and Moyle J. The mechanism of proton translocation in reversible proton-translocating adenosine triphosphatases. *Biochem Soc Special Publ* 4: 91–111, 1974.
699. Mitrovic Ad, Plesko F, and Vandenberg RJ. Zn^{2+} inhibits the anion conductance of the glutamate transporter EEAT4. *J Biol Chem* 276: 26071–26076, 2001.
700. Miyahara M, Watanabe Y, Edashige K, and Yagyu K. Swelling-induced O_2^- generation in guinea-pig neutrophils. *Biochim Biophys Acta* 1177: 61–70, 1993.
701. Molski TF, Naccache PH, Volpi M, Wolpert LM, and Sha'afi RI. Specific modulation of the intracellular pH of rabbit neutrophils by chemotactic factors. *Biochem Biophys Res Commun* 94: 508–514, 1980.
702. Monticello RA, Angov E, and Brusilow WS. Effects of inducing expression of cloned genes for the F_o proton channel of the *Escherichia coli* F_1F_o ATPase. *J Bacteriol* 174: 3370–3376, 1992.
703. Montrose MH and Kimmich GA. Quantitative use of weak bases for estimation of cellular pH gradients. *Am J Physiol Cell Physiol* 250: C418–C422, 1986.
704. Moody WJ and Hagiwara S. Block of inward rectification by intracellular H^+ in immature oocytes of the starfish *Mediaster aequalis*. *J Gen Physiol* 79: 115–130, 1982.
705. Morgan D, Cherny VV, Price MO, Dinauer MC, and DeCoursey TE. Absence of proton channels in COS-7 cells expressing functional NADPH oxidase components. *J Gen Physiol* 119: 571–580, 2002.
706. Morgan H, Taylor DM, and Oliveira ON. Proton transport at the monolayer-water interface. *Biochim Biophys Acta* 1062: 149–156, 1991.
707. Morgan J and Warren BE. X-ray analysis of the structure of water. *J Chem Phys* 6: 666–673, 1938.
708. Morgan JE, Verkhovsky MI, and Wikström M. The histidine cycle: a new model for proton translocation in the respiratory heme-copper oxidases. *J Bioenerg Biomembr* 26: 599–608, 1994.
709. Morihata H, Kawawaki J, Sakai H, Sawada M, Tsutada T, and Kuno M. Temporal fluctuations of voltage-gated proton currents in rat spinal microglia via pH-dependent and -independent mechanisms. *Neurosci Res* 38: 265–271, 2000.
710. Morihata H, Nakamura F, Tsutada T, and Kuno M. Potentiation of a voltage-gated proton current in acidosis-induced swelling of rat microglia. *J Neurosci* 20: 7220–7227, 2000.
711. Mould JA, Drury JE, Frings SM, Kaupp UB, Pekosz A, Lamb RA, and Pinto LH. Permeation and activation of the M_2 ion channel of influenza A virus. *J Biol Chem* 275: 31038–31050, 2000.
712. Mould JA, Li HC, Dudlak CS, Lear JD, Pekosz A, Lamb RA, and Pinto LH. Mechanism for proton conduction of the M_2 ion channel of influenza A virus. *J Biol Chem* 275: 8592–8599, 2000.
713. Moy JN, Gleich GJ, and Thomas LL. Noncytotoxic activation of neutrophils by eosinophil granule major basic protein. Effect on superoxide anion generation and lysosomal enzyme release. *J Immunol* 145: 2626–2632, 1990.
714. Mozhayeva GN and Naumov AP. The permeability of sodium channels to hydrogen ions in nerve fibres. *Pflügers Arch* 396: 163–173, 1983.
715. Mozhayeva GN, Naumov AP, and Negulyaev YA. Interaction of H^+ ions with acid groups in normal sodium channels. *Gen Physiol Biophys* 1: 5–19, 1982.
716. Muller RU and Finkelstein A. The electrostatic basis of Mg^{++} inhibition of transmitter release. *Proc Natl Acad Sci USA* 71: 923–926, 1974.
717. Muneyuki E, Ikematsu M, and Yoshida M. $\Delta\mu H^+$ dependency of proton translocation by bacteriorhodopsin and a stochastic energization-relaxation channel model. *J Phys Chem* 100: 19687–19691, 1996.
718. Murata K, Mitsuoka K, Hirai T, Walz T, Agre P, Heymann JB, Engel A, and Fujiyoshi Y. Structural determinants of water permeation through aquaporin-1. *Nature* 407: 599–605, 2000.
719. Murphy JK and Forman HJ. Effects of sodium and proton pump activity on respiratory burst and pH regulation of rat alveolar macrophages. *Am J Physiol Lung Cell Mol Physiol* 264: L523–L532, 1993.
720. Murphy R, Cherny VV, Sokolov VS, and DeCoursey TE. Power spectral analysis of voltage-gated proton current noise in human eosinophils (Abstract). *Biophys J* 84: 556a, 2003.
721. Murray TR, Chen L, Marshall BE, and Macarak EJ. Hypoxic contraction of cultured pulmonary vascular smooth muscle cells. *Am J Respir Cell Mol Biol* 3: 457–465, 1990.
722. Myers JB, Cantiello HF, Schwartz JH, and Tauber AI. Phorbol ester-stimulated human neutrophil membrane depolarization is dependent on Ca^{2+}-regulated Cl^- efflux. *Am J Physiol Cell Physiol* 259: C531–C540, 1990.
723. Myers VB and Haydon DA. Ion transfer across lipid membranes in the presence of gramicidin A. II. The ion selectivity. *Biochim Biophys Acta* 274: 313–322, 1972.
724. Nachliel E and Gutman M. Kinetic analysis of proton transfer between reactants adsorbed to the same micelle. The effect of proximity on the rate constants. *Eur J Biochem* 143: 83–88, 1984.
725. Nachliel E, Gutman M, and Zohar LE. Time resolved measurements of a single proton diffusing in the Gramicidin A channel. *Solid State Ionics* 77: 79–83, 1995.
726. Nachliel E, Pollak N, Huppert D, and Gutman M. Time-resolved study of the inner space of lactose permease. *Biophys J* 80: 1498–1506, 2001.
727. Nagel G, Kelety B, Möckel B, Büldt G, and Bamberg E. Voltage dependence of proton pumping by bacteriorhodopsin is regulated by the voltage-sensitive ratio of M_1 to M_2. *Biophys J* 74: 403–412, 1998.
728. Nagel G, Möckel B, Büldt G, and Bamberg E. Functional expression of bacteriorhodopsin in oocytes allows direct measurement of voltage dependence of light induced H^+ pumping. *FEBS Lett* 377: 263–266, 1995.
729. Nagel G, Ollig D, Fuhrmann M, Kateriya S, Musti AM, Bamberg E, and Hegemann P. Channelrhodopsin-1: a light-gated proton channel in green algae. *Science* 296: 2395–2398, 2002.
730. Nagle JF. Theory of passive proton conductance in lipid bilayers. *J Bioenerg Biomembr* 19: 413–426, 1987.
731. Nagle JF and Dilley RA. Models of localized energy coupling. *J Bioenerg Biomembr* 18: 55–64, 1986.
732. Nagle JF, Mille M, and Morowitz HJ. Theory of hydrogen bonded chains in bioenergetics. *J Chem Phys* 72: 3959–3971, 1980.
733. Nagle JF and Morowitz HJ. Molecular mechanisms for proton transport in membranes. *Proc Natl Acad Sci USA* 75: 298–302, 1978.
734. Nagle JF and Tristram-Nagle S. Hydrogen bonded chain mecha-

nisms for proton conduction and proton pumping. *J Membr Biol* 74: 1–14, 1983.
735. NAIR SK AND CHRISTIANSON DW. Unexpected pH-dependent conformation of His-64, the proton shuttle of carbonic anhydrase II. *J Am Chem Soc* 113: 9455–9458, 1991.
736. NAKASHIMA S, SUGANUMA A, SATO M, TOHMATSU T, AND NOZAWA Y. Mechanism of arachidonic acid liberation in platelet-activating factor-stimulated human polymorphonuclear neutrophils. *J Immunol* 143: 1295–1302, 1989.
737. NANDA A, CURNUTTE JT, AND GRINSTEIN S. Activation of H^+ conductance in neutrophils requires assembly of components of the respiratory burst oxidase but not its redox function. *J Clin Invest* 93: 1770–1775, 1994.
738. NANDA A AND GRINSTEIN S. Protein kinase C activates an H^+ (equivalent) conductance in the plasma membrane of human neutrophils. *Proc Natl Acad Sci USA* 88: 10816–10820, 1991.
739. NANDA A AND GRINSTEIN S. Chemoattractant-induced activation of vacuolar H^+ pumps and of an H^+-selective conductance in neutrophils. *J Cell Physiol* 165: 588–599, 1995.
740. NANDA A, GRINSTEIN S, AND CURNUTTE JT. Abnormal activation of H^+ conductance in NADPH oxidase-defective neutrophils. *Proc Natl Acad Sci USA* 90: 760–764, 1993.
741. NANDA A, GUKOVSKAYA A, TSENG J, AND GRINSTEIN S. Activation of vacuolar-type proton pumps by protein kinase C. Role in neutrophil pH regulation. *J Biol Chem* 267: 22740–22746, 1992.
742. NANDA A, ROMANEK R, CURNUTTE JT, AND GRINSTEIN S. Assessment of the contribution of the cytochrome *b* moiety of the NADPH oxidase to the transmembrane H^+ conductance of leukocytes. *J Biol Chem* 269: 27280–27285, 1994.
743. NARAHASHI T, DEGUCHI T, URAKAWA N, AND OHKUBO Y. Stabilization and rectification of muscle fiber membrane by tetrodotoxin. *Am J Physiol* 198: 934–938, 1960.
744. NARAHASHI T, FRAZIER T, AND YAMADA M. The site of action and active form of local anesthetics. I. Theory and *pH* experiments with tertiary compounds. *J Pharmacol Exp Ther* 171: 32–44, 1970.
745. NASMITH PE AND GRINSTEIN S. Impairment of Na^+/H^+ exchange underlies inhibitory effects of Na^+-free media on leukocyte function. *FEBS Lett* 202: 79–85, 1986.
746. NAUSEEF WM. Insights into myeloperoxidase biosynthesis from its inherited deficiency. *J Mol Med* 76: 661–668, 1998.
747. NAUSEEF WM, VOLPP BD, MCCORMICK S, LEIDAL KG, AND CLARK RA. Assembly of the neutrophil respiratory burst oxidase. Protein kinase C promotes cytoskeletal and membrane association of cytosolic oxidase components. *J Biol Chem* 266: 5911–5917, 1991.
748. NEHER E, SANDBLOM J, AND EISENMAN G. Ionic selectivity, saturation, and block in gramicidin A channels. II. Saturation behavior of single channel conductances and evidence for the existence of multiple binding sites in the channel. *J Membr Biol* 40: 97–116, 1978.
749. NELSON N, EYTAN E, NOTSANI BE, SIGRIST H, SIGRIST-NELSON K, AND GITLER C. Isolation of a chloroplast *N,N′*-dicyclohexylcarbodiimide-binding proteolipid, active in proton translocation. *Proc Natl Acad Sci USA* 74: 2375–2378, 1977.
750. NÉMETH-CAHALAN KL AND HALL JE. pH and calcium regulate the water permeability of aquaporin 0. *J Biol Chem* 275: 6777–6782, 2000.
751. NERNST W. Zur Kinetik der in Lösung befindlichen Körper. Theorie der Diffusion. *Zeitschrift für Physikalische Chemie* 2: 613–637, 1888.
752. NEYTON J AND MILLER C. Potassium blocks barium permeation through a calcium-activated potassium channel. *J Gen Physiol* 92: 549–567, 1988.
753. NICHOLLS DG. Hamster brown-adipose-tissue mitochondria. The control of respiration and the proton electrochemical potential gradient by possible physiological effectors of the proton conductance of the inner membrane. *Eur J Biochem* 49: 573–583, 1974.
754. NICHOLLS DG AND LOCKE RM. Thermogenic mechanisms in brown fat. *Physiol Rev* 64: 1–64, 1984.
755. NICHOLS JW AND DEAMER DW. Net proton-hydroxyl permeability of large unilamellar liposomes measured by an acid-base titration technique. *Proc Natl Acad Sci USA* 77: 2038–2042, 1980.
756. NIELSON CP, BAYER C, HODSON S, AND HADJOKAS N. Regulation of the respiratory burst by cyclic 3′,5′-AMP, an association with inhibition of arachidonic acid release. *J Immunol* 149: 4036–4040, 1992.
757. NIELSON DW, GOERKE J, AND CLEMENTS JA. Alveolar subphase pH in the lungs of anesthetized rabbits. *Proc Natl Acad Sci USA* 78: 7119–7123, 1981.
758. NIEMTZOW RC. Transmembrane potentials of human lymphocytes. In: *Transmembrane Potentials and Characteristics of Immune and Tumor Cells*, edited by Niemtzow RC. Boca Raton, FL: CRC, 1985, p. 70–85.
759. NOBES CD, BROWN GC, OLIVE PN, AND BRAND MD. Non-ohmic proton conductance of the mitochondrial inner membrane in hepatocytes. *J Biol Chem* 265: 12903–12909, 1990.
760. NOJI H, YASUDA R, YOSHIDA M, AND KINOSITA K JR. Direct observation of the rotation of F_1-ATPase. *Nature* 386: 299–302, 1997.
761. NONNER W, CATACUZZENO L, AND EISENBERG B. Binding and selectivity in L-type calcium channels: a mean spherical approximation. *Biophys J* 79: 1976–1992, 2000.
762. NORDSTRÖM T, ROTSTEIN OD, ROMANEK R, ASOTRA S, HEERSCHE JNM, MANOLSON MF, BRISSEAU GF, AND GRINSTEIN S. Regulation of cytoplasmic pH in osteoclasts. Contribution of proton pumps and a proton-selective conductance. *J Biol Chem* 270: 2203–2212, 1995.
763. NORDSTRÖM T, SHRODE LD, ROTSTEIN OD, ROMANEK R, GOTO T, HEERSCHE JNM, MANOLSON MF, BRISSEAU GF, AND GRINSTEIN S. Chronic extracellular acidosis induces plasmalemmal vacuolar type H^+ ATPase activity in osteoclasts. *J Biol Chem* 272: 6354–6360, 1997.
764. NORRIS FA AND POWELL GL. Characterization of CO_2/carbonic acid mediated proton flux through phosphatidylcholine vesicles as model membranes. *Biochim Biophys Acta* 1111: 17–26, 1992.
765. NOUMI T, BELTRAN C, NELSON H, AND NELSON N. Mutational analysis of yeast vacuolar H^+-ATPase. *Proc Natl Acad Sci USA* 88: 1938–1942, 1991.
766. NOZAKI Y AND TANFORD C. Proton and hydroxide ion permeability of phospholipid vesicles. *Proc Natl Acad Sci USA* 78: 4324–4328, 1981.
767. NÜBE O AND LINDAU M. The dynamics of exocytosis in human neutrophils. *J Cell Biol* 107: 2117–2123, 1988.
768. NUNOGAKI K AND KASAI M. The H^+/OH^- flux localizes around the channel mouth in buffered solution. *J Theor Biol* 134: 403–415, 1988.
769. NUSSBERGER S, STEEL A, TROTTI D, ROMERO MF, BORON WF, AND HEDIGER MA. Symmetry of H^+ binding to the intra- and extracellular side of the H^+-coupled oligopeptide cotransporter PepT1. *J Biol Chem* 272: 7777–7785, 1997.
770. OHLSSON A, CUMMING WA, PAUL A, AND SLY WS. Carbonic anhydrase II deficiency syndrome: recessive osteopetrosis with renal tubular acidosis and cerebral calcification. *Pediatrics* 77: 371–381, 1986.
771. OHMINE I AND SAITO S. Water dynamics: fluctuation, relaxation, and chemical reactions in hydrogen bond network rearrangement. *Acc Chem Res* 32: 741–749, 1999.
772. OHNO YI, HIRAI KI, KANOH T, UCHINO H, AND OGAWA K. Subcellular localization of H_2O_2 production in human neutrophils stimulated with particles and an effect of cytochalasin-B on the cells. *Blood* 60: 253–260, 1982.
773. OHNO YI, HIRAI KI, KANOH T, UCHINO H, AND OGAWA K. Subcellular localization of hydrogen peroxide production in human polymorphonuclear leukocytes stimulated with lectins, phorbol myristate acetate, and digitonin: an electron microscopic study using $CeCl_3$. *Blood* 60: 1195–1202, 1982.
774. OKADA A, MIURA T, AND TAKEUCHI H. Protonation of histidine and histidine-tryptophan interaction in the activation of the M2 ion channel from influenza a virus. *Biochemistry* 40: 6053–6060, 2001.
775. OKAMURA MY, PADDOCK ML, GRAIGE MS, AND FEHER G. Proton and electron transfer in bacterial reaction centers. *Biochim Biophys Acta* 1458: 148–163, 2000.
776. OLIVA C, COHEN IS, AND MATHIAS RT. Calculation of time constants for intracellular diffusion in whole cell patch clamp configuration. *Biophys J* 54: 791–799, 1988.
777. OLIVER AE AND DEAMER DW. α-Helical hydrophobic polypeptides form proton-selective channels in lipid bilayers. *Biophys J* 66: 1364–1379, 1994.
778. ONSAGER L. Ion passages in lipid bilayers. *Science* 156: 541, 1967.
779. ONSAGER L. Thermodynamics and some molecular aspects of bi-

ology. In: *The Neurosciences. A Study Program*, edited by Quarton GC, Melnechuk T, and Schmitt FO. New York: Rockefeller Univ. Press, 1967, p. 75–79.
780. ONSAGER L. The motion of ions: principles and concepts. *Science* 166: 1359–1364, 1969.
781. ONSAGER L. Possible mechanisms of ion transit. In: *Physical Principles of Biological Membranes. Proceedings Coral Gables Conference, 1968*, edited by Snell F, Wolken J, Iverson G, and Lam J. New York: Gordon and Breach, 1970, p. 137–139.
782. ONSAGER L. Introductory lecture. In: *Physics and Chemistry of Ice*, edited by Whalley E, Jones SJ, and Gold LW. Ottawa, Canada: Univ. of Toronto Press, 1973, p. 7–12.
783. ONSAGER L AND DUPUIS M. The electrical properties of ice. In: *Termodinamica dei processi irreversibili, Rendiconti della Scuola Internazionale di Fisica "Enrico Fermi," Corso X, Varenna, 1959*. Bologna: Nicola Zanichelli, 1960, p. 294–315.
784. ORENTLICHER M AND VOGELHUT PO. Structure and properties of liquid water. *J Chem Phys* 45: 4719–4724, 1966.
785. OTSU K, KINSELLA JL, KOH E, AND FROEHLICH JP. Proton dependence of the partial reactions of the sodium-proton exchanger in renal brush border membranes. *J Biol Chem* 267: 8089–8096, 1992.
786. OWEN BB AND SWEETON FH. The conductance of hydrochloric acid in aqueous solutions from 5 to 65°. *J Am Chem Soc* 63: 2811–2817, 1941.
787. PADDOCK ML, ÄDELROTH P, FEHER G, OKAMURA MY, AND BEATTY JT. Determination of proton transfer rates by chemical rescue: application to bacterial reaction centers. *Biochemistry* 41: 14716–14725, 2002.
788. PADDOCK ML, ÄDELROTH P, CHANG C, ABRESCH EC, FEHER G, AND OKAMURA MY. Identification of the proton pathway in bacterial reaction centers: cooperation between Asp-M17 and Asp-L210 facilitates proton transfer to the secondary quinone (Q_B). *Biochemistry* 40: 6893–6902, 2001.
789. PADDOCK ML, FEHER G, AND OKAMURA MY. Identification of the proton pathway in bacterial reaction centers: replacement of Asp-M17 and Asp-L210 with Asn reduces the proton transfer rate in the presence of Cd^{2+}. *Proc Natl Acad Sci USA* 97: 1548–1553, 2000.
790. PADDOCK ML, GRAIGE MS, FEHER G, AND OKAMURA MY. Identification of the proton pathway in bacterial reaction centers: inhibition of proton transfer by binding of Zn^{2+} or Cd^{2+}. *Proc Natl Acad Sci USA* 96: 6183–6188, 1999.
791. PALADE PT AND BARCHI RL. Characteristics of the chloride conductance in muscle fibers of the rat diaphragm. *J Gen Physiol* 69: 325–342, 1977.
792. PAOLETTI P, ASCHER P, AND NEYTON J. High-affinity zinc inhibition of NMDA NR1-NR2A receptors. *J Neurosci* 17: 5711–5725, 1997.
793. PARK JW, HOYAL CR, EL BENNA J, AND BABIOR BM. Kinase-dependent activation of the leukocyte NADPH oxidase in a cell-free system. Phosphorylation of membranes and $p47^{PHOX}$ during oxidase activation. *J Biol Chem* 272: 11035–11043, 1997.
794. PARSEGIAN A. Energy of an ion crossing a low dielectric membrane: solutions to four relevant electrostatic problems. *Nature* 221: 844–846, 1969.
795. PATI S, BRUSILOW WS, DECKERS-HEBESTREIT G, AND ALTENDORF K. Assembly of the F_o proton channel of the *Escherichia coli* F_1F_o ATPase: low proton conductance of reconstituted F_o sectors synthesized and assembled in the absence of F_1. *Biochemistry* 30: 4710–4714, 1991.
796. PATIÑO PJ, RAE J, NOACK D, ERICKSON R, DING J, DE OLARTE DG, AND CURNUTTE JT. Molecular characterization of autosomal recessive chronic granulomatous disease caused by a defect of the nicotinamide adenine dinucleotide phosphate (reduced form) oxidase component p67-*phox*. *Blood* 94: 2505–2514, 1999.
797. PAULA S, VOLKOV AG, VAN HOEK AN, HAINES TH, AND DEAMER DW. Permeation of protons, potassium ions, and small polar molecules through phospholipid bilayers as a function of membrane thickness. *Biophys J* 70: 339–348, 1996.
798. PAULING L. The nature of the chemical bond. Application of results obtained from the quantum mechanics and from a theory of paramagnetic susceptibility to the structure of molecules. *J Am Chem Soc* 53: 1367–1400, 1931.
799. PAULING L. The structure and entropy of ice and of other crystals with some randomness of atomic arrangement. *J Am Chem Soc* 57: 2680–2684, 1935.
800. PAULING L. The hydrogen bond. In: *The Nature of the Chemical Bond and the Structure of Molecules and Crystals; An Introduction to Modern Structural Chemistry*. Ithaca, NY: Cornell Univ. Press, 1939, p. 264–314.
801. PEBAY-PEYROULA E, RUMMEL G, ROSENBUSCH JP, AND LANDAU EM. X-ray structure of bacteriorhodopsin at 2.5 Angstroms from microcrystals grown in lipidic cubic phases. *Science* 277: 1676–1681, 1997.
802. PERAL MJ AND ILUNDÁIN AA. Proton conductance and intracellular pH recovery from an acid load in chicken enterocytes. *J Physiol* 484: 165–172, 1995.
803. PEREIRA MM, GOMES CM, AND TEIXEIRA M. Plasticity of proton pathways in haem-copper oxygen reductases. *FEBS Lett* 522: 14–18, 2002.
804. PERKINS WR AND CAFISO DS. An electrical and structural characterization of H^+/OH^- currents in phospholipid vesicles. *Biochemistry* 25: 2270–2276, 1986.
805. PERRIN DD AND DEMPSEY B. *Buffers for pH and Metal Ion Control*. London: Chapman and Hall, 1974.
806. PESKOFF A AND BERS DM. Electrodiffusion of ions approaching the mouth of a conducting membrane channel. *Biophys J* 53: 863–875, 1988.
807. PETRECCIA DC, NAUSEEF WM, AND CLARK RA. Respiratory burst of normal human eosinophils. *J Leukoc Biol* 41: 283–288, 1987.
808. PETRENKO VF AND WHITWORTH RW. *Physics of Ice*. Oxford, UK: Oxford Univ. Press, 1999.
809. PETRENKO VF, WHITWORTH RW, AND GLEN JW. Effects of proton injection on the electrical properties of ice. *Phil Mag B* 47: 259–278, 1983.
810. PHILLIPS LR, COLE CD, HENDERSHOT RJ, COTTEN M, CROSS TA, AND BUSATH DD. Noncontact dipole effects on channel permeation. III. Anomalous proton conductance effects in gramicidin. *Biophys J* 77: 2492–2501, 1999.
811. PINTO LH, DIECKMANN GR, GANDHI CS, PAPWORTH CG, BRAMAN J, SHAUGHNESSY MA, LEAR JD, LAMB RA, AND DEGRADO WF. A functionally defined model for the M_2 proton channel of influenza A virus suggests a mechanism for its ion selectivity. *Proc Natl Acad Sci USA* 94: 11301–11306, 1997.
812. PINTO LH, HOLSINGER LJ, AND LAMB RA. Influenza virus M_2 protein has ion channel activity. *Cell* 69: 517–528, 1992.
813. PODOLSKY RD. Temperature and water viscosity: physiological versus mechanical effects on suspension feeding. *Science* 265: 100–103, 1994.
814. POMÈS R. Theoretical studies of the Grotthuss mechanism in biological proton wires. *Isr J Chem* 39: 387–395, 1999.
815. POMÈS R, HUMMER G, AND WIKSTRÖM M. Structure and dynamics of a proton shuttle in cytochrome *c* oxidase. *Biochim Biophys Acta* 1365: 255–260, 1998.
816. POMÈS R AND ROUX B. Structure and dynamics of a proton wire: a theoretical study of H^+ translocation along the single-file water chain in the gramicidin A channel. *Biophys J* 71: 19–39, 1996.
817. POMÈS R AND ROUX B. Theoretical study of H^+ translocation along a model proton wire. *J Phys Chem* 100: 2519–2527, 1996.
818. POMÈS R AND ROUX B. Free energy profiles for H^+ conduction along hydrogen-bonded chains of water molecules. *Biophys J* 75: 33–40, 1998.
819. POMÈS R AND ROUX B. Molecular mechanism of H^+ conduction in the single-file water chain of the gramicidin channel. *Biophys J* 82: 2304–2316, 2002.
820. PRATS M, TEISSIE J, AND TOCANNE JF. Lateral proton conduction at lipid-water interfaces and its implications for the chemiosmotic-coupling hypothesis. *Nature* 322: 756–758, 1986.
821. PRATS M, TOCANNE JF, AND TEISSIE J. Lateral proton conduction at a lipid/water interface. Effect of lipid nature and ionic content of the aqueous phase. *Eur J Biochem* 162: 379–385, 1987.
822. PRICE MO, MCPHAIL LC, LAMBETH JD, HAN CH, KNAUS UG, AND DINAUER MC. Creation of a genetic system for analysis of the phagocyte respiratory burst: high-level reconstitution of the NADPH oxidase in a nonhematopoietic system. *Blood* 99: 2653–2661, 2002.
823. PROD'HOM B, PIETROBON D, AND HESS P. Direct measurement of

proton transfer rates to a group controlling the dihydropyridine-sensitive Ca^{2+} channel. *Nature* 329: 243–246, 1987.
824. PUSCH M. Knocking on channel's door. The permeating chloride ion acts as the gating charge in ClC-0. *J Gen Physiol* 108: 233–236, 1996.
825. PUSCH M, LUDEWIG U, AND JENTSCH TJ. Temperature dependence of fast and slow gating relaxations of ClC-0 chloride channels. *J Gen Physiol* 109: 105–116, 1997.
826. PUSCH M, LUDEWIG U, REHFELDT A, AND JENTSCH TJ. Gating of the voltage-dependent chloride channel CIC-0 by the permeant anion. *Nature* 373: 527–531, 1995.
827. PUSCH M AND NEHER E. Rates of diffusional exchange between small cells and a measuring patch pipette. *Pflügers Arch* 411: 204–211, 1988.
828. PUUSTINEN A AND WIKSTRÖM M. Proton exit from the heme-copper oxidase of *Escherichia coli*. *Proc Natl Acad Sci USA* 96: 35–37, 1999.
829. QIAN M, TU C, EARNHARDT JN, LAIPIS PJ, AND SILVERMAN DN. Glutamate and aspartate as proton shuttles in mutants of carbonic anhydrase. *Biochemistry* 36: 15758–15764, 1997.
830. QU AY, NANDA A, CURNUTTE JT, AND GRINSTEIN S. Development of a H^+-selective conductance during granulocytic differentiation of HL-60 cells. *Am J Physiol Cell Physiol* 266: C1263–C1270, 1994.
831. QUIGLEY EP, QUIGLEY P, CRUMRINE DS, AND CUKIERMAN S. The conduction of protons in different stereoisomers of dioxolane-linked gramicidin A channels. *Biophys J* 77: 2479–2491, 1999.
832. QUINN MT, EVANS T, LOETTERLE LR, JESAITIS AJ, AND BOKOCH GM. Translocation of Rac correlates with NADPH oxidase activation. Evidence for equimolar translocation of oxidase components. *J Biol Chem* 268: 20983–20987, 1993.
833. RAKOWSKI RF, GADSBY DC, AND DE WEER P. Stoichiometry and voltage dependence of the sodium pump in voltage-clamped, internally dialyzed squid giant axon. *J Gen Physiol* 93: 903–941, 1989.
834. RANDA HS, FORREST LR, VOTH GA, AND SANSOM MS. Molecular dynamics of synthetic leucine-serine ion channels in a phospholipid membrane. *Biophys J* 77: 2400–2410, 1999.
835. RASTOGI VK AND GIRVIN ME. Structural changes linked to proton translocation by subunit *c* of the ATP synthase. *Nature* 402: 263–268, 1999.
836. REENSTRA WW, WARNOCK DG, YEE VJ, AND FORTE JG. Proton gradients in renal cortex brush-border membrane vesicles. Demonstration of a rheogenic proton flux with acridine orange. *J Biol Chem* 256: 11663–11666, 1981.
837. REEVES EP, LU H, JACOBS HL, MESSINA CG, BOLSOVER S, GABELLA G, POTMA EO, WARLEY A, ROES J, AND SEGAL AW. Killing activity of neutrophils is mediated through activation of proteases by K^+ flux. *Nature* 416: 291–297, 2002.
838. REGIER DS, GREENE DG, SERGEANT S, JESAITIS AJ, AND MCPHAIL LC. Phosphorylation of $p22^{phox}$ is mediated by phospholipase D-dependent and -independent mechanisms. Correlation of NADPH oxidase activity and $p22^{phox}$ phosphorylation. *J Biol Chem* 275: 28406–28412, 2000.
839. REN G, REDDY VS, CHENG A, MELNYK P, AND MITRA AK. Visualization of a water-selective pore by electron crystallography in vitreous ice. *Proc Natl Acad Sci USA* 98: 1398–1403, 2001.
840. RESTREPO D, CHO DS, AND KRON MJ. Essential activation of Na^+-H^+ exchange by $[H^+]_i$ in HL-60 cells. *Am J Physiol Cell Physiol* 259: C490–C502, 1990.
841. RETTINGER J. Characteristics of Na^+/K^+-ATPase mediated proton current in Na^+- and K^+-free extracellular solutions. Indications for kinetic similarities between H^+/K^+-ATPase and Na^+/K^+-ATPase. *Biochim Biophys Acta* 1282: 207–215, 1996.
842. RICH PR, MEUNIER B, MITCHELL R, AND MOODY AJ. Coupling of charge and proton movement in cytochrome *c* oxidase. *Biochim Biophys Acta* 1275: 91–95, 1996.
843. RIISTAMA S, HUMMER G, PUUSTINEN A, DYER RB, WOODRUFF WH, AND WIKSTRÖM M. Bound water in the proton translocation mechanism of the haem-copper oxidases. *FEBS Lett* 414: 275–280, 1997.
844. ROBERTS NK AND NORTHEY HL. Proton and deuteron mobility in normal and heavy water solutions of electrolytes. *J Chem Soc Faraday Trans* 70: 253–262, 1974.
845. ROBINSON RA AND STOKES RH. *Electrolyte Solutions*. London: Butterworths, 1959.
846. RODKEY FL. Oxidation-reduction potentials of the diphosphopyridine nucleotide system. *J Biol Chem* 213: 777–786, 1955.
847. ROKITSKAYA TI, KOTOVA EA, AND ANTONENKO YN. Membrane dipole potential modulates proton conductance through gramicidin channel: movement of negative ionic defects inside the channel. *Biophys J* 82: 865–873, 2002.
848. ROMERO MF, HEDIGER MA, BOULPAEP EL, AND BORON WF. Expression cloning and characterization of a renal electrogenic Na^+/HCO_3^- cotransporter. *Nature* 387: 409–413, 1997.
849. ROOS A AND BORON WF. The buffer value of weak acids and bases: origin of the concept, and first mathematical derivation and application to physico-chemical systems. The work of M. Koppel and K. Spiro (1914). *Respir Physiol* 40: 1–32, 1980.
850. ROOS A AND BORON WF. Intracellular pH. *Physiol Rev* 61: 296–434, 1981.
851. ROOS D, DE BOER M, KURIBAYASHI F, MEISCHL C, WEENING RS, SEGAL AW, ÅHLIN A, NEMET K, HOSSLE JP, BERNATOWSKA-MATUSZKIEWICZ E, AND MIDDLETON-PRICE H. Mutations in the X-linked and autosomal recessive forms of chronic granulomatous disease. *Blood* 87: 1663–1681, 1996.
852. ROSENBERG HF. Eosinophils. In: *Inflammation: Basic Principles and Clinical Correlates*, edited by Gallin JI and Snyderman R. Philadelphia, PA: Lippincott Williams & Wilkins, 1999, p. 61–76.
853. ROSSI F. The O_2^--forming NADPH oxidase of the phagocytes: nature, mechanisms of activation and function. *Biochim Biophys Acta* 853: 65–89, 1986.
854. ROTSTEIN OD, NASMITH PE, AND GRINSTEIN S. The *Bacteroides* byproduct succinic acid inhibits neutrophil respiratory burst by reducing intracellular pH. *Infect Immun* 55: 864–870, 1987.
855. ROTTENBERG H. The generation of proton electrochemical potential gradient by cytochrome *c* oxidase. *Biochim Biophys Acta* 1364: 1–16, 1998.
856. ROUX B AND KARPLUS M. Ion transport in a gramicidin-like channel: dynamics and mobility. *J Phys Chem* 95: 4856–4868, 1991.
857. ROUX B AND KARPLUS M. Ion transport in a model gramicidin channel. Structure and thermodynamics. *Biophys J* 59: 961–981, 1991.
858. ROUX B, NINA M, POMES R, AND SMITH JC. Thermodynamic stability of water molecules in the bacteriorhodopsin proton channel: a molecular dynamics free energy perturbation study. *Biophys J* 71: 670–681, 1996.
859. ROUX B, PROD'HOM B, AND KARPLUS M. Ion transport in the gramicidin channel: molecular dynamics study of single and double occupancy. *Biophys J* 68: 876–892, 1995.
860. ROWLETT RS AND SILVERMAN DN. Kinetics of the protonation of buffer and hydration of CO_2 catalyzed by human carbonic anhydrase II. *J Am Chem Soc* 104: 6737–6741, 1982.
861. RUBINEK T AND LEVY R. Arachidonic acid increases the activity of the assembled NADPH oxidase in cytoplasmic membranes and endosomes. *Biochim Biophys Acta* 1176: 51–58, 1993.
862. RUITENBERG M, KANNT A, BAMBERG E, LUDWIG B, MICHEL H, AND FENDLER K. Single-electron reduction of the oxidized state is coupled to proton uptake via the K pathway in *Paracoccus denitrificans* cytochrome *c* oxidase. *Proc Natl Acad Sci USA* 97: 4632–4636, 2000.
863. RYCHKOV GY, ASTILL DS, BENNETTS B, HUGHES BP, BRETAG AH, AND ROBERTS ML. pH-dependent interactions of Cd^{2+} and a carboxylate blocker with the rat C1C-1 chloride channel and its R304E mutant in the Sf-9 insect cell line. *J Physiol* 501: 355–362, 1997.
864. RYCHKOV GY, PUSCH M, ASTILL DS, ROBERTS ML, JENTSCH TJ, AND BRETAG AH. Concentration and pH dependence of skeletal muscle chloride channel ClC-1. *J Physiol* 497: 423–435, 1996.
865. RYDSTRÖM J, HU X, FJELLSTRÖM O, MEULLER J, ZHANG J, JOHANSSON C, AND BIZOUARN T. Domains, specific residues and conformational states involved in hydride ion transfer and proton pumping by nicotinamide nucleotide transhydrogenase from *Escherichia coli*. *Biochim Biophys Acta* 1365: 10–16, 1998.
866. SABBERT D, ENGELBRECHT S, AND JUNGE W. Intersubunit rotation in active F-ATPase. *Nature* 381: 623–625, 1996.
867. SACKS V, MARANTZ Y, AAGAARD A, CHECOVER S, NACHLIEL E, AND

GUTMAN M. The dynamic feature of the proton collecting antenna of a protein surface. *Biochim Biophys Acta* 1365: 232–240, 1998.
868. SADEGHI RR AND CHENG H-P. The dynamics of proton transfer in a water chain. *J Chem Phys* 111: 2086–2094, 1999.
869. SAGLE L, PADDOCK ML, FEHER G, AND OKAMURA MY. Binding of Cd^{2+} or Ni^{2+} to the reaction center displaces a proton (Abstract). *Biophys J* 82: 196a, 2002.
870. SAGNELLA DE AND VOTH GA. Structure and dynamics of hydronium in the ion channel gramicidin A. *Biophys J* 70: 2043–2051, 1996.
871. SAITO M, HISATOME I, NAKAJIMA S, AND SATO R. Possible mechanism of oxygen radical production by human eosinophils mediated by K^+ channel activation. *Eur J Pharmacol* 291: 217–219, 1995.
872. SAKATA A, IDA E, TOMINAGA M, AND ONOUE K. Arachidonic acid acts as an intracellular activator of NADPH-oxidase in Fcγ receptor-mediated superoxide generation in macrophages. *J Immunol* 138: 4353–4359, 1987.
873. SALOM D, HILL BR, LEAR JD, AND DEGRADO WF. pH-dependent tetramerization and amantadine binding of the transmembrane helix of M2 from the influenza A virus. *Biochemistry* 39: 14160–14170, 2000.
874. SANDBLOM J, EISENMAN G, AND NEHER E. Ionic selectivity, saturation and block in gramicidin A channels. I. Theory for the electrical properties of ion selective channels having two pairs of binding sites and multiple conductance states. *J Membr Biol* 31: 383–47, 1977.
875. SANDERS D, SLAYMAN CL, AND PALL ML. Stoichiometry of H^+/amino acid cotransport in *Neurospora crassa* revealed by current-voltage analysis. *Biochim Biophys Acta* 735: 67–76, 1983.
876. SANDVIG K AND OLSNES S. Diphtheria toxin-induced channels in Vero cells selective for monovalent cations. *J Biol Chem* 263: 12352–12359, 1988.
877. SANSOM MSP, KERR ID, BREED J, AND SANKARARAMAKRISHNAN R. Water in channel-like cavities: structure and dynamics. *Biophys J* 70: 693–702, 1996.
878. SANSOM MSP, KERR ID, SMITH GR, AND SON HS. The influenza A virus M2 channel: a molecular modeling and simulation study. *Virology* 233: 163–173, 1997.
879. SANYAL G AND MAREN TH. Thermodynamics of carbonic anhydrase catalysis. A comparison between human isoenzymes B and C. *J Biol Chem* 256: 608–612, 1981.
880. SATHYAMOORTHY M, DE M, I, ADAMS AG, AND LETO TL. $p40^{phox}$ down-regulates NADPH oxidase activity through interactions with its SH3 domain. *J Biol Chem* 272: 9141–9146, 1997.
881. SBARRA AJ AND KARNOVSKY ML. The biochemical basis of phagocytes. I. Metabolic changes during the ingestion of particles by polymorphonuclear leucocytes. *J Biol Chem* 234: 1355–1362, 1959.
882. SCHEINER S. Proton transfers in hydrogen-bonded systems: cationic oligomers of water. *J Am Chem Soc* 103: 315–320, 1981.
883. SCHEINER S. Proton transfers in hydrogen-bonded systems. 4. Cationic dimers of NH_3 and OH_2. *J Phys Chem* 86: 376–382, 1982.
884. SCHEINER S. Theoretical calculation of energetics of proton translocation through membranes. *Methods Enzymol* 127: 456–465, 1986.
885. SCHEINER S AND NAGLE JF. Ab initio molecular orbital estimates of charge partitioning between Bjerrum and ionic defects in ice. *J Phys Chem* 87: 4267–4272, 1983.
886. SCHILLING T, GRATOPP A, DECOURSEY TE, AND EDER C. Voltage-activated proton currents in human lymphocytes. *J Physiol* 545: 93–105, 2002.
887. SCHINDLER H AND NELSON N. Proteolipid of adenosinetriphosphatase from yeast mitochondria forms proton-selective channels in planar lipid bilayers. *Biochemistry* 21: 5787–5794, 1982.
888. SCHLEGEL A, OMAR A, JENTSCH P, MORELL A, AND KEMPF C. Semliki Forest virus envelope proteins function as proton channels. *Biosci Rep* 11: 243–255, 1991.
889. SCHMID-ANTOMARCHI H, SCHMID-ALLIANA A, ROMEY G, VENTURA MA, BREITTMAYER V, MILLET MA, HUSSON H, MOGHRABI B, LAZDUNSKI M, AND ROSSI B. Extracellular ATP and UTP control the generation of reactive oxygen intermediates in human macrophages through the opening of a charybdotoxin-sensitive Ca^{2+}-dependent K^+ channel. *J Immunol* 159: 6209–6215, 1997.
890. SCHMITT UW AND VOTH GA. The computer simulation of proton transport in water. *J Chem Phys* 111: 9361–9381, 1999.
891. SCHNEIDER E AND ALTENDORF K. Bacterial adenosine 5′-triphosphate synthase (F_1F_o): purification and reconstitution of F_o complexes and biochemical and functional characterization of their subunits. *Microbiol Rev* 51: 477–497, 1987.
892. SCHOENKNECHT G, JUNGE W, LILL H, AND ENGELBRECHT S. Complete tracking of proton flow in thylakoids the unit conductance of CF_o is greater than 10 fS. *FEBS Lett* 203: 289–294, 1986.
893. SCHÖNKNECHT G, ALTHOFF G, APLEY EC, WAGNER R, AND JUNGE W. Cation channels by subunit III of the channel portion of the chloroplast H^+-ATPase. *FEBS Lett* 258: 190–194, 1989.
894. SCHOWEN RL. Solvent isotope effects on enzymic reactions. In: *Isotope Effects on Enzyme-Catalyzed Reactions*, edited by Cleland WW, O'Leary MH, and Northrop DB. Baltimore, MD: University Park Press, 1977, p. 64–99.
895. SCHRENZEL J, LEW DP, AND KRAUSE KH. Proton currents in human eosinophils. *Am J Physiol Cell Physiol* 271: C1861–C1871, 1996.
896. SCHRENZEL J, SERRANDER L, BÁNFI B, NÜSSE O, FOUYOUZI R, LEW DP, DEMAUREX N, AND KRAUSE KH. Electron currents generated by the human phagocyte NADPH oxidase. *Nature* 392: 734–737, 1998.
897. SCHREUDER HA, MATTEVI A, OBMOLOVA G, KALK KH, HOL WG, VAN DER BOLT FJ, AND VAN BERKEL WJ. Crystal structures of wild-type *p*-hydroxybenzoate hydroxylase complexed with 4-aminobenzoate, 2,4-dihydroxybenzoate, and 2-hydroxy-4-aminobenzoate and of the Tyr222Ala mutant complexed with 2-hydroxy-4-aminobenzoate. Evidence for a proton channel and a new binding mode of the flavin ring. *Biochemistry* 33: 10161–10170, 1994.
898. SCHROEDER C, FORD CM, WHARTON SA, AND HAY AJ. Functional reconstitution in lipid vesicles of influenza virus M2 protein expressed by baculovirus: evidence for proton transfer activity. *J Gen Virol* 75: 3477–3484, 1994.
899. SCHULTE U, HAHN H, KONRAD M, JECK N, DERST C, WILD K, WEIDEMANN S, RUPPERSBERG JP, FAKLER B, AND LUDWIG J. pH gating of ROMK ($K_{ir}1.1$) channels: control by an Arg-Lys-Arg triad disrupted in antenatal Bartter syndrome. *Proc Natl Acad Sci USA* 96: 15298–15303, 1999.
900. SCHULTEN Z AND SCHULTEN K. A model for the resistance of the proton channel formed by the proteolipid of ATPase. *Eur Biophys J* 11: 149–155, 1985.
901. SCHUMAKER MF, POMÈS R, AND ROUX B. A combined molecular dynamics and diffusion model of single proton conduction through gramicidin. *Biophys J* 79: 2840–2857, 2000.
902. SCHUMANN MA, GARDNER P, AND RAFFIN TA. Recombinant human tumor necrosis factor alpha induces calcium oscillation and calcium-activated chloride current in human neutrophils. The role of calcium/calmodulin-dependent protein kinase. *J Biol Chem* 268: 2134–2140, 1993.
903. SCHUMANN MA, LEUNG CC, AND RAFFIN TA. Activation of NADPH-oxidase and its associated whole-cell H^+ current in human neutrophils by recombinant human tumor necrosis factor alpha and formyl-methionyl-leucyl-phenylalanine. *J Biol Chem* 270: 13124–13132, 1995.
904. SCHUMANN MA AND RAFFIN TA. Activation of a voltage-dependent chloride current in human neutrophils by phorbol 12-myristate 13-acetate and formyl-methionyl-leucyl-phenylalanine. The role of protein kinase C. *J Biol Chem* 269: 2389–2398, 1994.
905. SCHUMANN MA, TANIGAKI T, HELLER DN, AND RAFFIN TA. Ca^{2+}-dependent and Ca^{2+}-independent mechanisms modulate whole-cell cationic currents in human neutrophils. *Biochem Biophys Res Commun* 185: 531–538, 1992.
906. SCHWEIGHOFER KJ AND POHORILLE A. Computer simulation of ion channel gating: the M_2 channel of influenza A virus in a lipid bilayer. *Biophys J* 78: 150–163, 2000.
907. SCHWIENING CJ, KENNEDY HJ, AND THOMAS RC. Calcium-hydrogen exchange by the plasma membrane Ca-ATPase of voltage-clamped snail neurons. *Proc Roy Soc Lond B Biol Sci* 253: 285–289, 1993.
908. SCHWIENING CJ AND WILLOUGHBY D. Depolarization-induced pH microdomains and their relationship to calcium transients in isolated snail neurones. *J Physiol* 538: 371–382, 2002.
909. SCHWINGSHACKL A, MOQBEL R, AND DUSZYK M. Involvement of ion channels in human eosinophil respiratory burst. *J Allergy Clin Immunol* 106: 272–279, 2000.
910. SCOTT WA, ZRIKE JM, HAMILL AL, KEMPE J, AND COHN ZA. Regulation

of arachidonic acid metabolites in macrophages. *J Exp Med* 152: 324–335, 1980.
911. SEEDS MC, PARCE JW, SZEJDA P, AND BASS DA. Independent stimulation of membrane potential changes and the oxidative metabolic burst in polymorphonuclear leukocytes. *Blood* 65: 233–240, 1985.
912. SEGAL AW AND COADE SB. Kinetics of oxygen consumption by phagocytosing human neutrophils. *Biochem Biophys Res Commun* 84: 611–617, 1978.
913. SEGAL AW, GARCIA R, GOLDSTONE H, CROSS AR, AND JONES OT. Cytochrome b_{-245} of neutrophils is also present in human monocytes, macrophages and eosinophils. *Biochem J* 196: 363–367, 1981.
914. SEGAL AW, GEISOW M, GARCIA R, HARPER A, AND MILLER R. The respiratory burst of phagocytic cells is associated with a rise in vacuolar pH. *Nature* 290: 406–409, 1981.
915. SEGAL AW, HEYWORTH PG, COCKCROFT S, AND BARROWMAN MM. Stimulated neutrophils from patients with autosomal recessive chronic granulomatous disease fail to phosphorylate a M_r-44,000 protein. *Nature* 316: 547–549, 1985.
916. SEGAL AW AND JONES OT. Novel cytochrome *b* system in phagocytic vacuoles of human granulocytes. *Nature* 276: 515–517, 1978.
917. SELIGMANN BE AND GALLIN JI. Use of lipophilic probes of membrane potential to assess human neutrophil activation. Abnormality in chronic granulomatous disease. *J Clin Invest* 66: 493–503, 1980.
918. SELIGMANN BE AND GALLIN JI. Comparison of indirect probes of membrane potential utilized in studies of human neutrophils. *J Cell Physiol* 115: 105–115, 1983.
919. SHA'AFI RI, MOLSKI TF, AND NACCACHE PH. Chemotactic factors activate differentiable permeation pathways for sodium and calcium in rabbit neutrophils. Effect of amiloride. *Biochem Biophys Res Commun* 99: 1271–1276, 1981.
920. SHARP LL, ZHOU J, AND BLAIR DF. Features of MotA proton channel structure revealed by tryptophan-scanning mutagenesis. *Proc Natl Acad Sci USA* 92: 7946–7950, 1995.
921. SHEDLOVSKY T. The electrolytic conductivity of some uni-univalent electrolytes in water at 25°. *J Am Chem Soc* 54: 1411–1429, 1932.
922. SHIMBO K, BRASSARD DL, LAMB RA, AND PINTO LH. Viral and cellular small integral membrane proteins can modify ion channels endogenous to *Xenopus* oocytes. *Biophys J* 69: 1819–1829, 1995.
923. SHIMBO K, BRASSARD DL, LAMB RA, AND PINTO LH. Ion selectivity and activation of the M_2 ion channel of influenza virus. *Biophys J* 70: 1335–1346, 1996.
924. SHIOSE A AND SUMIMOTO H. Arachidonic acid and phosphorylation synergistically induce a conformational change of $p47^{phox}$ to activate the phagocyte NADPH oxidase. *J Biol Chem* 275: 13793–13801, 2000.
925. SHUCK K, LAMB RA, AND PINTO LH. Analysis of the pore structure of the influenza A virus M_2 ion channel by the substituted-cysteine accessibility method. *J Virol* 74: 7755–7761, 2000.
926. SHULT PA, GRAZIANO FM, WALLOW IH, AND BUSSE WW. Comparison of superoxide generation and luminol-dependent chemiluminescence with eosinophils and neutrophils from normal individuals. *J Lab Clin Med* 106: 638–645, 1985.
927. SICZKOWSKI M, DAVIES JE, AND NG LL. Activity and density of the Na^+-H^+ antiporter in normal and transformed human lymphocytes and fibroblasts. *Am J Physiol Cell Physiol* 267: C745–C752, 1994.
928. SIGRIST-NELSON K AND AZZI A. The proteolipid subunit of the chloroplast adenosine triphosphatase complex. Reconstitution and demonstration of proton-conductive properties. *J Biol Chem* 255: 10638–10643, 1980.
929. SIGURDSON H, BRÄNDÉN M, NAMSLAUER A, AND BRZEZINSKI P. Ligand binding reveals protonation events at the active site of cytochrome *c* oxidase; is the K-pathway used for the transfer of H^+ or OH^-? *J Inorg Biochem* 88: 335–342, 2002.
930. SIGWORTH FJ. Charge movement in the sodium channel. *J Gen Physiol* 106: 1047–1051, 1995.
931. SILVERMAN DN. Marcus rate theory applied to enzymatic proton transfer. *Biochim Biophys Acta* 1458: 88–103, 2000.
932. SILVERMAN DN AND LINDSKOG S. The catalytic mechanism of carbonic anhydrase: implications of a rate-limiting protolysis of water. *Acc Chem Res* 21: 30–36, 1988.
933. SILVERMAN DN AND TU CK. Buffer dependence of carbonic anhydrase catalyzed oxygen-18 exchange at equilibrium. *J Am Chem Soc* 97: 2263–2269, 1975.
934. SILVERMAN DN AND VINCENT SH. Proton transfer in the catalytic mechanism of carbonic anhydrase. *CRC Crit Rev Biochem* 14: 207–255, 1983.
935. SIMCHOWITZ L. Chemotactic factor-induced activation of Na^+/H^+ exchange in human neutrophils. I. Sodium fluxes. *J Biol Chem* 260: 13237–13247, 1985.
936. SIMCHOWITZ L. Chemotactic factor-induced activation of Na^+/H^+ exchange in human neutrophils. II. Intracellular pH changes. *J Biol Chem* 260: 13248–13255, 1985.
937. SIMCHOWITZ L. Intracellular pH modulates the generation of superoxide radicals by human neutrophils. *J Clin Invest* 76: 1079–1089, 1985.
938. SIMCHOWITZ L AND CRAGOE EJ JR. Intracellular acidification-induced alkali metal cation/H^+ exchange in human neutrophils. *J Gen Physiol* 90: 737–762, 1987.
939. SIMCHOWITZ L, FOY MA, AND CRAGOE EJ JR. A role for Na^+/Ca^{2+} exchange in the generation of superoxide radicals by human neutrophils. *J Biol Chem* 265: 13449–13456, 1990.
940. SIMCHOWITZ L AND ROOS A. Regulation of intracellular pH in human neutrophils. *J Gen Physiol* 85: 443–470, 1985.
941. SIMCHOWITZ L, SPILBERG I, AND DE WEER P. Sodium and potassium fluxes and membrane potential of human neutrophils: evidence for an electrogenic sodium pump. *J Gen Physiol* 79: 453–479, 1982.
942. SIMMEN HP AND BLASER J. Analysis of pH and pO_2 in abscesses, peritoneal fluid, and drainage fluid in the presence or absence of bacterial infection during and after abdominal surgery. *Am J Surg* 166: 24–27, 1993.
943. SIVERTZ V, REITMEIER RE, AND TARTAR HV. The ionization constant of monoethanolammonium hydroxide at 25° from electrical conductance measurements. *J Am Chem Soc* 62: 1379–1382, 1940.
944. SKERRA A AND BRICKMANN J. Structure and dynamics of one-dimensional ionic solutions in biological transmembrane channels. *Biophys J* 51: 969–976, 1987.
945. SKLAR LA, JESAITIS AJ, PAINTER RG, AND COCHRANE CG. The kinetics of neutrophil activation. The response to chemotactic peptides depends upon whether ligand-receptor interaction is rate-limiting. *J Biol Chem* 256: 9909–9914, 1981.
946. SKULACHEV VP. Fatty acid circuit as a physiological mechanism of uncoupling of oxidative phosphorylation. *FEBS Lett* 294: 158–162, 1991.
947. SLAYMAN CL AND SLAYMAN CW. Depolarization of the plasma membrane of *Neurospora* during active transport of glucose: evidence for a proton-dependent cotransport system. *Proc Natl Acad Sci USA* 71: 1935–1939, 1974.
948. SMEDARCHINA Z, SIEBRAND W, FERNÁNDEZ-RAMOS A, GORB L, AND LESZCZYNSKI J. A direct-dynamics study of proton transfer through water bridges in guanine and 7-azaindole. *J Chem Phys* 112: 566–573, 2000.
949. SMIRNOVA IA, ÄDELROTH P, GENNIS RB, AND BRZEZINSKI P. Aspartate-132 in cytochrome *c* oxidase from *Rhodobacter sphaeroides* is involved in a two-step proton transfer during oxo-ferryl formation. *Biochemistry* 38: 6826–6833, 1999.
950. SMITH GD, DAI L, MIURA RM, AND SHERMAN A. Asymptotic analysis of buffered calcium diffusion near a point source. *SIAM J Appl Math* 61: 1816–1838, 2001.
951. SMITH RJ, SAM LM, JUSTEN JM, LEACH KL, AND EPPS DE. Human polymorphonuclear neutrophil activation with arachidonic acid. *Br J Pharmacol* 91: 641–649, 1987.
952. SMOLEN JE AND WEISSMANN G. Effects of indomethacin, 5,8,11,14-eicosatetraynoic acid, and *p*-bromophenacyl bromide on lysosomal enzyme release and superoxide anion generation by human polymorphonuclear leukocytes. *Biochem Pharmacol* 29: 533–538, 1980.
953. SMONDYREV AM AND VOTH GA. Molecular dynamics simulation of proton transport near the surface of a phospholipid membrane. *Biophys J* 82: 1460–1468, 2002.
954. SOHN HY, KELLER M, GLOE T, MORAWIETZ H, RUECKSCHLOSS U, AND POHL U. The small G-protein Rac mediates depolarization-induced superoxide formation in human endothelial cells. *J Biol Chem* 275: 18745–18750, 2000.

955. Sokolov VS, Cherny VV, Simonova MV, and Markin VS. Electrical potential distribution over the bilayer lipid membrane due to amphiphilic ion adsorption. *Bioelectrochem Bioenerget* 23: 27–44, 1990.
956. Someya A, Nishijima K, Nunoi H, Irie S, and Nagaoka I. Study on the superoxide-producing enzyme of eosinophils and neutrophils: comparison of the NADPH oxidase components. *Arch Biochem Biophys* 345: 207–213, 1997.
957. Spitzer KW, Ershler PR, Skolnick RL, and Vaughan-Jones RD. Generation of intracellular pH gradients in single cardiac myocytes with a microperfusion system. *Am J Physiol Heart Circ Physiol* 278: H1371–H1382, 2000.
958. Stahlberg H, Muller DJ, Suda K, Fotiadis D, Engel A, Meier T, Matthey U, and Dimroth P. Bacterial Na^+-ATP synthase has an undecameric rotor. *EMBO Rep* 2: 229–233, 2001.
959. Stankovic CJ, Heinemann SH, and Schreiber SL. Immobilizing the gate of a tartaric acid-gramicidin A hybrid channel molecule by rational design. *J Am Chem Soc* 112: 3702–3704, 1990.
960. Starace DM and Bezanilla F. Histidine scanning mutagenesis of basic residues of the S4 segment of the *Shaker* K^+ channel. *J Gen Physiol* 117: 469–490, 2001.
961. Starace DM, Stefani E, and Bezanilla F. Voltage-dependent proton transport by the voltage sensor of the *Shaker* K^+ channel. *Neuron* 19: 1319–1327, 1997.
962. Steinbeck MJ, Hegg GG, and Karnovsky MJ. Arachidonate activation of the neutrophil NADPH-oxidase. Synergistic effects of protein phosphatase inhibitors compared with protein kinase activators. *J Biol Chem* 266: 16336–16342, 1991.
963. Steiner H, Jonsson BH, and Lindskog S. The catalytic mechanism of carbonic anhydrase. Hydrogen-isotope effects on the kinetic parameters of the human C isoenzyme. *Eur J Biochem* 59: 253–259, 1975.
964. Stern MD. Buffering of calcium in the vicinity of a channel pore. *Cell Calcium* 13: 183–192, 1992.
965. Stewart AK, Boyd CA, and Vaughan-Jones RD. A novel role for carbonic anhydrase: cytoplasmic pH gradient dissipation in mouse small intestinal enterocytes. *J Physiol* 516: 209–217, 1999.
966. Stewart AK, Chernova MN, Kunes YZ, and Alper SL. Regulation of AE2 anion exchanger by intracellular pH: critical regions of the NH_2-terminal cytoplasmic domain. *Am J Physiol Cell Physiol* 281: C1344–C1354, 2001.
967. Stillinger FH. Water revisited. *Science* 209: 451–457, 1980.
968. Stoddard JS, Steinbach JH, and Simchowitz L. Whole cell Cl^- currents in human neutrophils induced by cell swelling. *Am J Physiol Cell Physiol* 265: C156–C165, 1993.
969. Stoeckenius W, Lozier RH, and Bogomolni RA. Bacteriorhodopsin and the purple membrane of halobacteria. *Biochim Biophys Acta* 505: 215–278, 1979.
970. Stolz B and Berg HC. Evidence for interactions between MotA and MotB, torque-generating elements of the flagellar motor of *Escherichia coli*. *J Bacteriol* 173: 7033–7037, 1991.
971. Subramaniam S and Henderson R. Molecular mechanism of vectorial proton translocation by bacteriorhodopsin. *Nature* 406: 653–657, 2000.
972. Sugai N, Ninomiya Y, and Oosaki T. Localization of carbonic anhydrase in the rat lung. *Histochemistry* 72: 415–424, 1981.
973. Suh YA, Arnold RS, Lassegue B, Shi J, Xu X, Sorescu D, Chung AB, Griendling KK, and Lambeth JD. Cell transformation by the superoxide-generating oxidase Mox1. *Nature* 401: 79–82, 1999.
974. Sullivan R, Melnick DA, Malech HL, Meshulam T, Simons ER, Lazzari KG, Proto PJ, Gadenne AS, Leavitt JL, and Griffin JD. The effects of phorbol myristate acetate and chemotactic peptide on transmembrane potentials and cytosolic free calcium in mature granulocytes evolve sequentially as the cells differentiate. *J Biol Chem* 262: 1274–1281, 1987.
975. Sun B, Leem CH, and Vaughan-Jones RD. Novel chloride-dependent acid loader in the guinea-pig ventricular myocyte: part of a dual acid-loading mechanism. *J Physiol* 495: 65–82, 1996.
976. Suszták K, Káldi K, Kapus A, and Ligeti E. Ligands of purinergic receptors stimulate electrogenic H^+-transport of neutrophils. *FEBS Lett* 375: 79–82, 1995.
977. Suszták K, Mócsai A, Ligeti E, and Kapus A. Electrogenic H^+ pathway contributes to stimulus-induced changes of internal pH and membrane potential in intact neutrophils: role of cytoplasmic phospholipase A_2. *Biochem J* 325: 501–510, 1997.
978. Suzuki T, Ueno H, Mitome N, Suzuki J, and Yoshida M. F_o of ATP synthase is a rotary proton channel. Obligatory coupling of proton translocation with rotation of *c*-subunit ring. *J Biol Chem* 277: 13281–13285, 2002.
979. Svensson-Ek M, Abramson J, Larsson G, Törnroth S, Brzezinski P, and Iwata S. The X-ray crystal structures of wild-type and EQ(I-286) mutant cytochrome *c* oxidases from *Rhodobacter sphaeroides*. *J Mol Biol* 321: 329–339, 2002.
980. Swain SD, Helgerson SL, Davis AR, Nelson LK, and Quinn MT. Analysis of activation-induced conformational changes in $p47^{phox}$ using tryptophan fluorescence spectroscopy. *J Biol Chem* 272: 29502–29510, 1997.
981. Swallow CJ, Grinstein S, and Rotstein OD. Regulation of cytoplasmic pH in resident and activated peritoneal macrophages. *Biochim Biophys Acta* 1022: 203–210, 1990.
982. Swallow CJ, Grinstein S, Sudsbury RA, and Rotstein OD. Modulation of the macrophage respiratory burst by an acidic environment: the critical role of cytoplasmic pH regulation by proton extrusion pumps. *Surgery* 108: 363–368, 1990.
983. Swenson ER, Deem S, Kerr ME, and Bidani A. Inhibition of aquaporin-mediated CO_2 diffusion and voltage-gated H^+ channels by zinc does not alter rabbit lung CO_2 and NO excretion. *Clin Sci* 103: 567–575, 2002.
984. Swenson ER, Graham MM, and Hlastala MP. Acetazolamide slows V_A/Q matching after changes in regional blood flow. *J Appl Physiol* 78: 1312–1318, 1995.
985. Swenson ER and Maren TH. Roles of gill and red cell carbonic anhydrase in elasmobranch HCO_3^- and CO_2 excretion. *Am J Physiol Regul Integr Comp Physiol* 253: R450–R458, 1987.
986. Swenson ER, Robertson HT, and Hlastala MP. Effects of carbonic anhydrase inhibition on ventilation-perfusion matching in the dog lung. *J Clin Invest* 92: 702–709, 1993.
987. Szundi I and Stoeckenius W. Effect of lipid surface charges on the purple-to-blue transition of bacteriorhodopsin. *Proc Natl Acad Sci USA* 84: 3681–3684, 1987.
988. Szundi I and Stoeckenius W. Surface pH controls purple-to-blue transition of bacteriorhodopsin. A theoretical model of purple membrane surface. *Biophys J* 56: 369–383, 1989.
989. Tajkhorshid E, Nollert P, Jensen MØ, Miercke LJW, O'Connell J, Stroud RM, and Schulten K. Control of the selectivity of the aquaporin water channel family by global orientational tuning. *Science* 296: 525–530, 2002.
990. Takahashi E and Wraight CA. Small weak acids stimulate proton transfer events in site-directed mutants of the two ionizable residues, Glu^{L212} and Asp^{L213}, in the Q_B-binding site of *Rhodobacter sphaeroides* reaction center. *FEBS Lett* 283: 140–144, 1991.
991. Takanaka K and O'Brien PJ. Proton release associated with respiratory burst of polymorphonuclear leukocytes. *J Biochem (Tokyo)* 103: 656–660, 1988.
992. Takeda M, Pekosz A, Shuck K, Pinto LH, and Lamb RA. Influenza a virus M_2 ion channel activity is essential for efficient replication in tissue culture. *J Virol* 76: 1391–1399, 2002.
993. Taki K, Kato H, and Yoshida I. Elimination of CO_2 in patients with carbonic anhydrase II deficiency, with studies of respiratory function at rest. *Respir Med* 93: 536–539, 1999.
994. Taliaferro WH and Sarles MP. The cellular reactions in the skin, lungs, and intestine of normal and immune rats after infection with *Nippostrongylus brasiliensis*. *J Infect Dis* 64: 157–192, 1939.
995. Tang Y, Zaitseva F, Lamb RA, and Pinto LH. The gate of the influenza virus M_2 proton channel is formed by a single tryptophan residue. *J Biol Chem* 277: 39880–39886, 2002.
996. Tannock IF and Rotin D. Acid pH in tumors and its potential for therapeutic exploitation. *Cancer Res* 49: 4373–4384, 1989.
997. Tao W, Molski TF, and Sha'afi RI. Arachidonic acid release in rabbit neutrophils. *Biochem J* 257: 633–637, 1989.
998. Tare M, Prestwich SA, Gordienko DV, Parveen S, Carver JE, Robinson C, and Bolton TB. Inwardly rectifying whole cell potassium current in human blood eosinophils. *J Physiol* 506: 303–318, 1998.
999. Tarsi-Tsuk D and Levy R. Stimulation of the respiratory burst in peripheral blood monocytes by lipoteichoic acid. The involvement

of calcium ions and phospholipase A_2. *J Immunol* 144: 2665–2670, 1990.
1000. TATHAM PE, DELVES PJ, SHEN L, AND ROITT IM. Chemotactic factor-induced membrane potential changes in rabbit neutrophils monitored by the fluorescent dye 3,3′- dipropylthiadicarbocyanine iodide. *Biochim Biophys Acta* 602: 285–298, 1980.
1001. TAYLOR BN. *The International System of Units (SI)*. Washington, DC: United States Government Printing Office, 1991. (National Institute of Standards and Technology Spec Publ 330).
1002. TEISSIÉ J, PRATS M, LEMASSU A, STEWART LC, AND KATES M. Lateral proton conduction in monolayers of phospholipids from extreme halophiles. *Biochemistry* 29: 59–65, 1990.
1003. THOMAS HM, CARSON RC, FRIED ED, AND NOVITCH RS. Inhibition of hypoxic pulmonary vasoconstriction by diphenyleneiodonium. *Biochem Pharmacol* 42: R9–12, 1991.
1004. THOMAS JW, PUUSTINEN A, ALBEN JO, GENNIS RB, AND WIKSTRÖM M. Substitution of asparagine for aspartate-135 in subunit I of the cytochrome *bo* ubiquinol oxidase of *Escherichia coli* eliminates proton-pumping activity. *Biochemistry* 32: 10923–10928, 1993.
1005. THOMAS RC. Recovery of pH_i in snail neurones exposed to high external potassium (Abstract). *J Physiol* 296: 77P, 1979.
1006. THOMAS RC. Changes in the surface pH of voltage-clamped snail neurones apparently caused by H^+ fluxes through a channel. *J Physiol* 398: 313–327, 1988.
1007. THOMAS RC. Proton channels in snail neurones. Does calcium entry mimic the effects of proton influx? *Ann NY Acad Sci* 574: 287–293, 1989.
1008. THOMAS RC AND MEECH RW. Hydrogen ion currents and intracellular pH in depolarized voltage-clamped snail neurones. *Nature* 299: 826–828, 1982.
1009. THORGEIRSSON TE, XIAO W, BROWN LS, NEEDLEMAN R, LANYI JK, AND SHIN YK. Transient channel-opening in bacteriorhodopsin: an EPR study. *J Mol Biol* 273: 951–957, 1997.
1010. TIELEMAN DP, BERENDSEN HJC, AND SANSOM MSP. Voltage-dependent insertion of alamethicin at phospholipid/water and octane/water interfaces. *Biophys J* 80: 331–346, 2001.
1011. TITTOR J, SOELL C, OESTERHELT D, BUTT HJ, AND BAMBERG E. A defective proton pump, point-mutated bacteriorhodopsin Asp96 → Asn is fully reactivated by azide. *EMBO J* 8: 3477–3482, 1989.
1012. TKALCEVIC J, NOVELLI M, PHYLACTIDES M, IREDALE JP, SEGAL AW, AND ROES J. Impaired immunity and enhanced resistance to endotoxin in the absence of neutrophil elastase and cathepsin G. *Immunity* 12: 201–210, 2000.
1013. TOBLER K, KELLY ML, PINTO LH, AND LAMB RA. Effect of cytoplasmic tail truncations on the activity of the M_2 ion channel of influenza A virus. *J Virol* 73: 9695–9701, 1999.
1014. TOMMOS C AND BABCOCK GT. Proton and hydrogen currents in photosynthetic water oxidation. *Biochim Biophys Acta* 1458: 199–219, 2000.
1015. TONEY MD AND KIRSCH JF. Direct Brønsted analysis of the restoration of activity to a mutant enzyme by exogenous amines. *Science* 243: 1485–1488, 1989.
1016. TOSTESON MT, PINTO LH, HOLSINGER LJ, AND LAMB RA. Reconstitution of the influenza virus M_2 ion channel in lipid bilayers. *J Membr Biol* 142: 117–126, 1994.
1017. TRIPP BC AND FERRY JG. A structure-function study of a proton transport pathway in the gamma-class carbonic anhydrase from *Methanosarcina thermophila*. *Biochemistry* 39: 9232–9240, 2000.
1018. TSUKIHARA T, AOYAMA H, YAMASHITA E, TOMIZAKI T, YAMAGUCHI H, SHINZAWA-ITOH K, NAKASHIMA R, YAONO R, AND YOSHIKAWA S. The whole structure of the 13-subunit oxidized cytochrome *c* oxidase at 2.8 Å. *Science* 272: 1136–1144, 1996.
1019. TSUNAWAKI S AND NATHAN CF. Release of arachidonate and reduction of oxygen. Independent metabolic bursts of the mouse peritoneal macrophage. *J Biol Chem* 261: 11563–11570, 1986.
1020. TU C, QIAN M, EARNHARDT JN, LAIPIS PJ, AND SILVERMAN DN. Properties of intramolecular proton transfer in carbonic anhydrase III. *Biophys J* 74: 3182–3189, 1998.
1021. TU C, WYNNS GC, AND SILVERMAN DN. Inhibition by cupric ions of ^{18}O exchange catalyzed by human carbonic anhydrase II. Relation to the interaction between carbonic anhydrase and hemoglobin. *J Biol Chem* 256: 9466–9470, 1981.
1022. TU CK AND SILVERMAN DN. The mechanism of carbonic anhydrase studied by ^{13}C and ^{18}O labeling of carbon dioxide. *J Am Chem Soc* 97: 5935–5936, 1975.
1023. TU CK, SILVERMAN DN, FORSMAN C, JONSSON BH, AND LINDSKOG S. Role of histidine 64 in the catalytic mechanism of human carbonic anhydrase II studied with a site-specific mutant. *Biochemistry* 28: 7913–7918, 1989.
1024. TUCKERMAN M, LAASONEN K, SPRIK M, AND PARRINELLO M. *Ab initio* molecular dynamics simulation of the solvation and transport of hydronium and hydroxyl ions in water. *J Chem Phys* 103: 150–161, 1995.
1025. TUCKERMAN M, LAASONEN K, SPRIK M, AND PARRINELLO M. *Ab initio* molecular dynamics simulation of the solvation and transport of H_3O^+ and OH^- ions in water. *J Phys Chem* 99: 5749–5752, 1995.
1026. TUCKERMAN ME, MARX D, AND PARRINELLO M. The nature and transport mechanism of hydrated hydroxide ions in aqueous solution. *Nature* 417: 925–929, 2002.
1027. UHLINGER DJ, TYAGI SR, INGE KL, AND LAMBETH JD. The respiratory burst oxidase of human neutrophils. Guanine nucleotides and arachidonate regulate the assembly of a multicomponent complex in a semirecombinant cell-free system. *J Biol Chem* 268: 8624–8631, 1993.
1028. URAS-AYTEMIZ N, JOYCE C, AND DEVLIN JP. Protonic and Bjerrum defect activity near the surface of ice at T <145 K. *J Chem Phys* 115: 9835–9842, 2001.
1029. URRY DW. The gramicidin A transmembrane channel: a proposed $\pi_{(L,D)}$ helix. *Proc Natl Acad Sci USA* 68: 672–676, 1971.
1030. VAISSIERE C, LE CV, AND MARIDONNEAU-PARINI I. NADPH oxidase is functionally assembled in specific granules during activation of human neutrophils. *J Leukoc Biol* 65: 629–634, 1999.
1031. VALLEE BL AND AULD DS. Zinc coordination, function, and structure of zinc enzymes and other proteins. *Biochemistry* 29: 5647–5659, 1990.
1032. VALLEE BL AND AULD DS. Cocatalytic zinc motifs in enzyme catalysis. *Proc Natl Acad Sci USA* 90: 2715–2718, 1993.
1033. VAN DE VOSSENBERG JLCM, DRIESSEN AJM, DA COSTA MS, AND KONINGS WN. Homeostasis of the membrane proton permeability in *Bacillus subtilis* grown at different temperatures. *Biochim Biophys Acta* 1419: 97–104, 1999.
1034. VAN KLAVEREN RJ, ROELANT C, BOOGAERTS M, DEMEDTS M, AND NEMERY B. Involvement of an NAD(P)H oxidase-like enzyme in superoxide anion and hydrogen peroxide generation by rat type II cells. *Thorax* 52: 465–471, 1997.
1035. VAN REYK DM, KING NJ, DINAUER MC, AND HUNT NH. The intracellular oxidation of 2′,7′-dichlorofluorescin in murine T lymphocytes. *Free Radic Biol Med* 30: 82–88, 2001.
1036. VAN SLYKE DD. On the measurement of buffer values and on the relationship of buffer value to the dissociation constant of the buffer and the concentration and reaction of the buffer solution. *J Biol Chem* 52: 525–570, 1922.
1037. VAN ZWIETEN R, WEVER R, HAMERS MN, WEENING RS, AND ROOS D. Extracellular proton release by stimulated neutrophils. *J Clin Invest* 68: 310–313, 1981.
1038. VENABLE RM AND PASTOR RW. Molecular dynamics simulations of water wires in a lipid bilayer and water/octane model systems. *J Chem Phys* 116: 2663–2664, 2002.
1039. VERHEUGEN JAH, VIJVERBERG HP, OORTGIESEN M, AND CAHALAN MD. Voltage-gated and Ca^{2+}-activated K^+ channels in intact human T lymphocytes. Noninvasive measurements of membrane currents, membrane potential, and intracellular calcium. *J Gen Physiol* 105: 765–794, 1995.
1040. VERKHOVSKAYA ML, GARCÌA-HORSMAN A, PUUSTINEN A, RIGAUD JL, MORGAN JE, VERKHOVSKY MI, AND WIKSTRÖM M. Glutamic acid 286 in subunit I of cytochrome bo_3 is involved in proton translocation. *Proc Natl Acad Sci USA* 94: 10128–10131, 1997.
1041. VERKHOVSKY MI, JASAITIS A, VERKHOVSKAYA ML, MORGAN JE, AND WIKSTRÖM M. Proton translocation by cytochrome *c* oxidase. *Nature* 400: 480–483, 1999.
1042. VIDAL-PUIG A, SOLANES G, GRUJIC D, FLIER JS, AND LOWELL BB. UCP3: an uncoupling protein homologue expressed preferentially and abundantly in skeletal muscle and brown adipose tissue. *Biochem Biophys Res Commun* 235: 79–82, 1997.
1043. VIDAL-PUIG AJ, GRUJIC D, ZHANG CY, HAGEN T, BOSS O, IDO Y, SZCZEPANIK A, WADE J, MOOTHA V, CORTRIGHT R, MUOIO DM, AND

LOWELL BB. Energy metabolism in uncoupling protein 3 gene knockout mice. *J Biol Chem* 275: 16258–16266, 2000.
1044. VIEIRA L, LAVAN A, DAGGER F, AND CABANTCHIK ZI. The role of anions in pH regulation of *Leishmania major promastigotes*. *J Biol Chem* 269: 16254–16259, 1994.
1045. VIGNE P, FRELIN C, AND LAZDUNSKI M. Intracellular pH measurements using the fluorescence of 9-aminoacridine. *FEBS Lett* 172: 275–278, 1984.
1046. VIK SB, PATTERSON AR, AND ANTONIO BJ. Insertion scanning mutagenesis of subunit a of the F_1F_o ATP synthase near His^{245} and implications on gating of the proton channel. *J Biol Chem* 273: 16229–16234, 1998.
1047. VISENTIN S, AGRESTI C, PATRIZIO M, AND LEVI G. Ion channels in rat microglia and their different sensitivity to lipopolysaccharide and interferon-γ. *J Neurosci Res* 42: 439–451, 1995.
1048. VOLKMAN DJ, BUESCHER ES, GALLIN JI, AND FAUCI AS. B cell lines as models for inherited phagocytic diseases: abnormal superoxide generation in chronic granulomatous disease and giant granules in Chediak-Higashi syndrome. *J Immunol* 133: 3006–3009, 1984.
1049. VUILLEUMIER R AND BORGIS D. Molecular dynamics of an excess proton in water using a non-additive valence bond force field. *J Mol Struct* 436–437: 555–565, 1997.
1050. VUILLEUMIER R AND BORGIS D. Transport and spectroscopy of the hydrated proton: a molecular dynamics study. *J Chem Phys* 111: 4251–4266, 1999.
1051. VYGODINA TV, PECORARO C, MITCHELL D, GENNIS R, AND KONSTANTINOV AA. Mechanism of inhibition of electron transfer by amino acid replacement K362M in a proton channel of *Rhodobacter sphaeroides* cytochrome *c* oxidase. *Biochemistry* 37: 3053–3061, 1998.
1052. WAGNER PD AND WEST JB. Effects of diffusion impairment on O_2 and CO_2 time courses in pulmonary capillaries. *J Appl Physiol* 33: 62–71, 1972.
1053. WAGNER R, APLEY EC, AND HANKE W. Single channel H^+ currents through reconstituted chloroplast ATP synthase CF_o-CF_1. *EMBO J* 8: 2827–2834, 1989.
1054. WAISBREN SJ, GEIBEL JP, MODLIN IM, AND BORON WF. Unusual permeability properties of gastric gland cells. *Nature* 368: 332–335, 1994.
1055. WALDMANN R, CHAMPIGNY G, LINGUEGLIA E, DE WEILLE JR, HEURTEAUX C, AND LAZDUNSKI M. H^+-gated cation channels. *Ann NY Acad Sci* 868: 67–76, 1999.
1056. WALRAFEN GE, YANG W-H, CHU YC, AND HOKMABADI MS. Raman OD-stretching overtone spectra from liquid D_2O between 22 and 152°C. *J Phys Chem* 100: 1381–1391, 1996.
1057. WALSH CE, WAITE BM, THOMAS MJ, AND DECHATELET LR. Release and metabolism of arachidonic acid in human neutrophils. *J Biol Chem* 256: 7228–7234, 1981.
1058. WANG C, LAMB RA, AND PINTO LH. Direct measurement of the influenza A virus M_2 protein ion channel activity in mammalian cells. *Virology* 205: 133–140, 1994.
1059. WANG C, LAMB RA, AND PINTO LH. Activation of the M_2 ion channel of influenza virus: a role for the transmembrane domain histidine residue. *Biophys J* 69: 1363–1371, 1995.
1060. WANG X AND HORISBERGER JD. A conformation of Na^+-K^+ pump is permeable to proton. *Am J Physiol Cell Physiol* 268: C590–C595, 1995.
1061. WARD TT AND STEIGBIGEL RT. Acidosis of synovial fluid correlates with synovial fluid leukocytosis. *Am J Med* 64: 933–936, 1978.
1062. WARD WJ AND ROBB WL. Carbon dioxide-oxygen separation: facilitated transport of carbon dioxide across a liquid film. *Science* 156: 1481–1484, 1967.
1063. WARNER AE. Kinetic properties of the chloride conductance of frog muscle. *J Physiol* 227: 291–312, 1972.
1064. WASHBURN EW. The theory and practice of the iodometric determination of asenious acid. *J Am Chem Soc* 30: 31–46, 1908.
1065. WATANABE T, WATANABE S, ITO H, KIDA H, AND KAWAOKA Y. Influenza A virus can undergo multiple cycles of replication without M2 ion channel activity. *J Virol* 75: 5656–5662, 2001.
1066. WEIDEMA AF. *Ion Channels and Ion Transport in Chicken Osteoclasts* (PhD thesis). The Netherlands: Rijksuniversiteit te Leiden, 1995.
1067. WENZL E AND MACHEN TE. Intracellular pH dependence of buffer capacity and anion exchange in the parietal cell. *Am J Physiol Gastrointest Liver Physiol* 257: G741–G747, 1989.
1068. WHEELER M, STACHLEWITZ RF, YAMASHINA S, IKEJIMA K, MORROW AL, AND THURMAN RG. Glycine-gated chloride channels in neutrophils attenuate calcium influx and superoxide production. *FASEB J* 14: 476–484, 2000.
1069. WHITIN JC, CHAPMAN CE, SIMONS ER, CHOVANIEC ME, AND COHEN HJ. Correlation between membrane potential changes and superoxide production in human granulocytes stimulated by phorbol myristate acetate. Evidence for defective activation in chronic granulomatous disease. *J Biol Chem* 255: 1874–1878, 1980.
1070. WICKE E, EIGEN M, AND ACKERMANN T. Über den Zustand des Protons (Hydroniumions) in wäßriger Lösung. *Zeitschrift für Physikalische Chemie* 1: 340–364, 1954.
1071. WIENTJES FB, HSUAN JJ, TOTTY NF, AND SEGAL AW. $p40^{phox}$, a third cytosolic component of the activation complex of the NADPH oxidase to contain *src* homology 3 domains. *Biochem J* 296: 557–561, 1993.
1072. WIKSTRÖM M. Proton pump coupled to cytochrome *c* oxidase in mitochondria. *Nature* 266: 271–273, 1977.
1073. WIKSTRÖM M. Identification of the electron transfers in cytochrome oxidase that are coupled to proton-pumping. *Nature* 338: 776–778, 1989.
1074. WIKSTRÖM M. Proton translocation by bacteriorhodopsin and heme-copper oxidases. *Curr Opin Struct Biol* 8: 480–488, 1998.
1075. WIKSTRÖM M. Mechanism of proton translocation by cytochrome *c* oxidase: a new four-stroke histidine cycle. *Biochim Biophys Acta* 1458: 188–198, 2000.
1076. WIKSTRÖM M. Proton translocation by cytochrome *c* oxidase: a rejoinder to recent criticism. *Biochemistry* 39: 3515–3519, 2000.
1077. WIKSTRÖM M, JASAITIS A, BACKGREN C, PUUSTINEN A, AND VERKHOVSKY MI. The role of the D- and K-pathways of proton transfer in the function of the haem-copper oxidases. *Biochim Biophys Acta* 1459: 514–520, 2000.
1078. WILKES JM AND HIRST BH. Amiloride sensitivity of proton-conductive pathways in gastric and intestinal apical membrane vesicles. *J Membr Biol* 126: 115–122, 1992.
1079. WILLIAMS RJP. The multifarious couplings of energy transduction. *Biochim Biophys Acta* 505: 1–44, 1978.
1080. WILMSEN HU, FAULSTICH H, EIBL H, AND BOHEIM G. Phallolysin. A mushroom toxin, forms proton and voltage gated membrane channels. *Eur Biophys J* 12: 199–209, 1985.
1081. WOOD PM. The redox potential of the system oxygen-superoxide. *FEBS Lett* 44: 22–24, 1974.
1082. WOODHULL AM. Ionic blockage of sodium channels in nerve. *J Gen Physiol* 61: 687–708, 1973.
1083. WOOLDRIDGE PJ AND DEVLIN JP. Proton trapping and defect energetics in ice from FT-IR monitoring of photoinduced isotopic exchange of isolated D_2O. *J Chem Phys* 88: 3086–3091, 1988.
1084. WOOLLEY GA AND WALLACE BA. Model ion channels: gramicidin and alamethicin. *J Membr Biol* 129: 109–136, 1992.
1085. WOOLLEY GA, ZUNIC V, KARANICOLAS J, JAIKARAN AS, AND STAROSTIN AV. Voltage-dependent behavior of a "ball-and-chain" gramicidin channel. *Biophys J* 73: 2465–2475, 1997.
1086. YAGISAWA M, YUO A, YONEMARU M, IMAJOH-OHMI S, KANEGASAKI S, YAZAKI Y, AND TAKAKU F. Superoxide release and NADPH oxidase components in mature human phagocytes: correlation between functional capacity and amount of functional proteins. *Biochem Biophys Res Commun* 228: 510–516, 1996.
1087. YAMASHITA T, SOMEYA A, AND HARA E. Response of superoxide anion production by guinea pig eosinophils to various soluble stimuli: comparison to neutrophils. *Arch Biochem Biophys* 241: 447–452, 1985.
1088. YANG S, MADYASTHA P, BINGEL S, RIES W, AND KEY L. A new superoxide-generating oxidase in murine osteoclasts. *J Biol Chem* 276: 5452–5458, 2001.
1089. YASUDA R, NOJI H, YOSHIDA M, KINOSITA K, AND ITOH H. Resolution of distinct rotational substeps by submillisecond kinetic analysis of F_1-ATPase. *Nature* 410: 898–904, 2001.
1090. YAZDANBAKHSH M, ECKMANN CM, DE BOER M, AND ROOS D. Purification of eosinophils from normal human blood, preparation of eosinoplasts and characterization of their functional response to various stimuli. *Immunology* 60: 123–129, 1987.

1091. YOSHIDA M, ALLISON WS, ESCH FS, AND FUTAI M. The specificity of carboxyl group modification during the inactivation of the *Escherichia coli* F_1-ATPase with dicyclohexyl[^{14}C]carbodiimide. *J Biol Chem* 257: 10033–10037, 1982.
1092. YOSHIDA M, OKAMOTO H, SONE N, HIRATA H, AND KAGAWA Y. Reconstitution of thermostable ATPase capable of energy coupling from its purified subunits. *Proc Natl Acad Sci USA* 74: 936–940, 1977.
1093. YOSHIKAWA S, SHINZAWA-ITOH K, NAKASHIMA R, YAONO R, YAMASHITA E, INOUE N, YAO M, FEI MJ, LIBEU CP, MIZUSHIMA T, YAMAGUCHI H, TOMIZAKI T, AND TSUKIHARA T. Redox-coupled crystal structural changes in bovine heart cytochrome *c* oxidase. *Science* 280: 1723–1729, 1998.
1094. YU L, QUINN MT, CROSS AR, AND DINAUER MC. Gp91^{phox} is the heme binding subunit of the superoxide-generating NADPH oxidase. *Proc Natl Acad Sci USA* 95: 7993–7998, 1998.
1095. ZAHN D AND BRICKMAN J. Quantum-classical simulation of proton migration in water. *Isr J Chem* 39: 469–482, 1999.
1096. ZEIDEL ML, AMBUDKAR SV, SMITH BL, AND AGRE P. Reconstitution of functional water channels in liposomes containing purified red cell CHIP28 protein. *Biochemistry* 31: 7436–7440, 1992.
1097. ZHANG J, FENG Y, AND FORGAC M. Proton conduction and bafilomycin binding by the V_0 domain of the coated vesicle V-ATPase. *J Biol Chem* 269: 23518–23523, 1994.
1098. ZHANG J, MYERS M, AND FORGAC M. Characterization of the V_0 domain of the coated vesicle (H^+)-ATPase. *J Biol Chem* 267: 9773–9778, 1992.
1099. ZHEN L, KING AA, XIAO Y, CHANOCK SJ, ORKIN SH, AND DINAUER MC. Gene targeting of X chromosome-linked chronic granulomatous disease locus in a human myeloid leukemia cell line and rescue by expression of recombinant gp91^{phox}. Proc Natl Acad Sci USA 90: 9832–9836, 1993.
1100. ZHOU J, SHARP LL, TANG HL, LLOYD SA, BILLINGS S, BRAUN TF, AND BLAIR DF. Function of protonatable residues in the flagellar motor of *Escherichia coli:* a critical role for Asp 32 of MotB. *J Bacteriol* 180: 2729–2735, 1998.
1101. ZUNDEL G. Proton polarizability and proton transfer processes in hydrogen bonds and cation polarizabilities of other cation bonds: their importance to understand molecular processes in electrochemistry and biology. *Trends Phys Chem* 3: 129–156, 1992.
1102. ZUNDEL G. *Proton Polarizability of Hydrogen Bonds and Proton Transfer Processes, Their Role in Electrochemistry and Biology.* München, Germany: Institut für Physikalische Chemie der Universität München, 1997.
1103. ZUNDEL G. Hydrogen bonds with large proton polarizability and proton transfer processes in electrochemistry and biology. *Adv Chem Phys* 111: 1–217, 2000.